Alma Mater Studiorum – Università di Bologna

DOTTORATO DI RICERCA IN

Oncologia e Patologia Sperimentale

Ciclo XXVII

Settore Concorsuale di afferenza: 06/A2

Settore Scientifico disciplinare: MED/04

Mitochondrial DNA rearrangements during human aging: a study on liver, muscle and adipose tissue

Presentata da: **Dott.ssa Fiammetta Biondi**

Relatore
Prof. Stefano Salvioli

Coordinatore Dottorato
Prof. Pierluigi Lollini

Co-relatore
Prof. Claudio Franceschi

Esame finale anno 2015

Al mio dono più grande, la mia famiglia.
A Maria Grazia, a Marco ed a Eleonora.
Alla loro forza e al loro coraggio.

1 Introduction

1.1 Human aging

Aging is an essential, inevitable, physiological complex phenomenon characterized by a progressive decline in the functional maintenance of tissue homeostasis and an expanding propensity to degenerative diseases and death (Cui et al., 2012). Even if this process is still not completely understood (Vitale et al., 2013), there is a large agreement on fact that the aging is: (1) universal; (2) intrinsic (i.e., "built-in"); (3) deleterious and (4) irreversible (Shokolenko et al., 2014). Over time, different aging theories proposed a variety of such basic mechanisms in order to explain it (Shokolenko et al., 2014), even if, at the molecular level, many evidences suggest that damages to macromolecules are at the base of several of the most important mechanisms (Kirkwood, 2005). In particular, as summarized by López-Otín and colleagues in figure 1, the main phenomena thought to be among the causes of aging are: genomic damages due to both endogenous and environmental factors, which lead to genomic instability; epigenetic alterations that involve changes in DNA methylation patterns, post-translational modification of histones and chromatin remodelling; decline of stem cell regenerative potential; deregulation of nutrient sensing mediated by insulin and IGF-1 signalling pathway, mTOR, AMPK and sirtuins; decline in protein quality control and degradation systems (autophagy-lysosomal and ubiquitin-proteasome systems) and accumulation of oxidised cell components and indigested garbage; cellular senescence; telomere shortening; mitochondria dysfunction; altered intercellular communication particularly in relation to inflammation (López-Otínet al., 2013).

Figure 1: The 9 hallmarks of aging (Lopez-Otin et al., 2013).

These hallmarks of aging can be modulated by circulatory factors (Kennedy et al., 2014), between which, there are IL-6, IL-18 and C-reactive protein, that are pro-inflammatory molecules whose levels increase with age in both women and men (Howcroft et al., 2013). Elevated levels of inflammatory biomarkers, such as the above mentioned, are predictive and associated with the age-related phenotype, diseases and mortality (Franceschi and Campisi, 2014). In particular, Franceschi and colleagues found that a low-grade, chronic, systemic inflammatory status exists in absence of overt infection and characterizes the aging process. They named this status "Inflamm-aging" (Franceschi et al., 2000), it is provoked by continuous antigenic load and stress, with the persistence of inflammatory stimuli over time (Morrisette-Thomas et al., 2014) and in particular by an impairment of the balance between pro-inflammatory and anti-inflammatory agents (Cevenini et al., 2013), as well as the activation of macrophages and the expansion of specific clones of T lymphocytes directed toward common antigens (Franceschi et al., 2000). However, the identification of pathways involved in the control of age-related inflammation across multiple system is very important, above all because several mechanisms of chronic inflammation could be implicated. Among others, it can be recognized: (i) constant production of reactive molecules by infiltrating leukocytes, that at the end damages the structural and cellular components of tissues; (ii) amplification of inflammatory response due to damaged non-immune cells and activated immune cells and (iii) interference with "anabolic signalling" (Franceschi and Campisi, 2014). Moreover, from the fields of genetics, epigenetics, proteomics and other "omics" platforms, new experimental data come to demonstrate that others cellular processes are involved, also of non-immunological nature, such as microRNAs (miRs), agalactosylated N-glycans, gut microbiota-related products and metabolites, cellular senescence, mitochondrial function and reactive species production (Santoro et al., 2014).

These latter processes are also the principal actors of two of the most important aging theories proposed and for this reason, will be discussed in more detail below (see section 1.2 and 1.3).

On the whole, the aging of human body could be considered as a mosaic (Cevenini et al., 2008) because the different tissues could age at different rates and likely with slightly different mechanisms thus differently contributing to inflammaging. Hereafter it is summarized the knowledge of the aging process in liver, muscle and adipose tissues, which are the object of the study in this thesis, with particular attention to mitochondria and telomeres.

1.1.1 Human liver aging

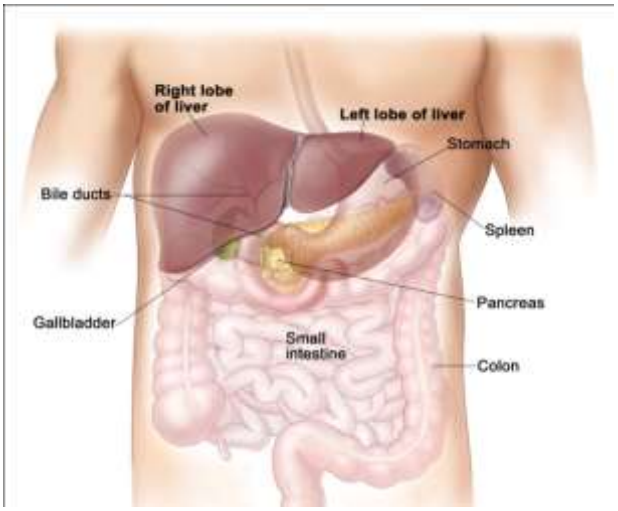

Figure 2: Liver in human body (http://www.ncbi.nlm.nih.gov/pubmedhealth/PMHT0018957/).

Liver is a vital organ supporting a multitude of different functions and playing a central role in human physiology. In particular, among other functions, the liver represents the main reservoir of blood in the body and hepatocytes are assigned to the synthesis of bile, as well as to the control of levels of circulating lipids, carbohydrates and amino acids, to the removal of toxins from the blood and to the assimilation of nutrients and liposoluble vitamins (A, D, K and E), that can be also stored in the liver (Martini et al., 2008).

Besides, one of the most important liver characteristic is that it is able to regenerate itself after suffering several injuries, but during aging the ability to withstand a hepatic insult is reduced (Hoare et al., 2010). Indeed, studies in rodents and humans show as some structural changes in liver morphology occur (Schmucker and Sanchez, 2011): (a) the volume of hepatocytes declines with senescence and also the relative volumes of hepatocyte organelles change during ageing (Hoare et al., 2010), (b) the smooth surfaced of endoplasmic reticulum is progressively lost, (c) the volume of the dense body compartment, for example, secondary lysosomes, residual bodies, or lipofuscin increases, as well as (d) the hepatocyte polyploidy increases (Schmucker, 1990). In spite of this, liver function tests failed to identify significant age-related deficits (Schmucker and Sanchez, 2011).

Additionally, in the last years it is notably increased the number of orthotopic liver transplants where the age of the donor is considerably higher than that of the recipient. Clinical data, in fact, point out how, in some conditions, function and duration of liver graft from aged subjects are comparable to those achievable with liver grafts from young donors (Cescon et al., 2003, 2008;). Therefore a peculiar aging pattern for liver seems to emerge from this evidence

(Conboy et al., 2005; Bellavista et al., 2014), but the molecular mechanisms involved are still largely unknown (Bellavista et al., 2014).

One hypothesis is that mitochondrial dysfunction might play a pivotal role. It was seen, indeed, that in liver, as well as in some other tissues, the activities of the electron transport chain protein complex are decreased with age and in liver this is particularly true for complex I and IV (Castro et al., 2012). Moreover, Navarro and colleagues suggest that the activities of complex I and IV are inversely correlated with the accumulation of oxidative damaged lipid, proteins and DNA (Navarro et al, 2002), that leads to a vicious circle and to more accumulation of mitochondrial dysfunction (Castro et al., 2012).

As Muller-Hocker and colleagues suggested, also in liver the expression either of mitochondrial and nuclear encoded electron transporter chain complexes or the respiration rates are reduced during aging (Muller-Hocker et al., 1997) and these deficits probably are due to the oxidative mtDNA lesions occurring in aged liver, that if not repaired, may result in mtDNA deletion (Gredilla et al., 2010).

The elevated mtDNA damage levels are consistent with the age-dependent rises in lipid peroxidation and thus in agreement with the age-associated accumulation of lipofuscin in the liver (Brunk and Terman, 2002), that reflects an inability to eliminate cellular waste products and compromised normal cell activities (Schmucker and Sachs, 2002).

1.1.2 Human skeletal muscle aging

In human body, skeletal muscle is the most abundant tissue, accounting for almost 40% of the total body mass. It is also a major site of metabolic activity and, in healthy conditions, carries out an important role in the prevention of metabolic disorders, such as obesity, diabetes and hypertension, among others (Romanello and Sandri, 2010). Changes in exercise, loading, nutrition and hormones are factors able to induce a muscle answer, since skeletal muscle is a plastic tissue able to respond and, above all, adapt to them (Sandri, 2008). This ability is attributable to contractile proteins located inside the muscle cells (myocytes), which determine the cellular size, morphology (Masiero and Sandri, 2010), but also different type of contraction and of movement abilities. Since ATP is required for muscle contraction, in muscle cells there are many mitochondria (Cogswell et al., 1993; Manneschi and Federico, 1995; Bizeau et al., 1998; Picard et al., 2013), that carry out vital functions in the maintenance of myocite viability, in particular in the context of energy provision, redox homeostasis and regulation of several catabolic pathways (Marzetti et al., 2013). Since the importance of these

organelles, it is possible that their dysfunction is implicated in the age-dependent muscle degeneration.

In particular, the age-associated decline in skeletal muscle mass, strength and function is named “sarcopenia” (Roseberg, 1989) and it is referred to a complex medical condition that predicts a deficiency in mobility, disability, leading in turn to loss of independence, a higher risk of falls, reduced quality of life, increased health care costs and eventually an increased risk of mortality (Montero-Fernandez and Serra-Rexach, 2013). The reduction in size of type II fibers seems to be the main cause of sarcopenia (Nilwiket al., 2013), together with a decreased capacity of proliferation and differentiation of the muscle stem cells (satellite cells) that lead to diminished generation of myogenic fibers and a replacement of them with fibrous tissue (Verdijk et al., 2007; Gopinath and Rando, 2008; Sahin and De Pinho, 2010;).

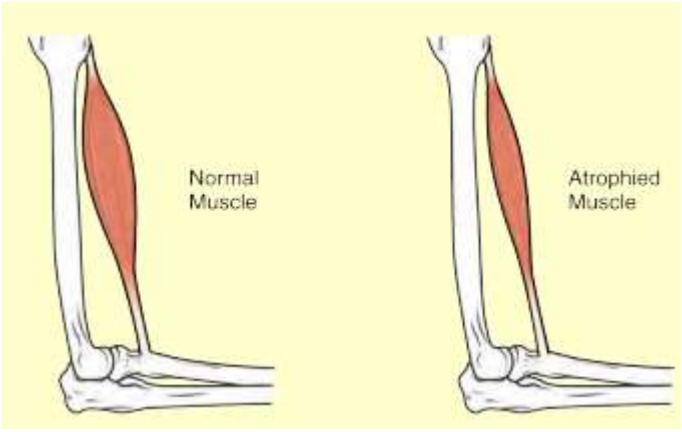

Figure 3: Sarcopenia is the age associated decline in muscle mass, strength and function, with an increment of muscle atrophy. (OpenStax College. Anatomy & Physiology. Connexions, June 19, 2013. http://cnx.org/content/col11496/1.6/)

As previous anticipated, an increasing number of evidences suggest that mitochondrial dysfunction is the main responsible of age-related skeletal muscle decline (Johnson et al., 2013), but the interpretation of the consequences is complicated by the presence of two population of mitochondria inside myocites: sub-sarcolemmal and inter-myofibrillar mitochondria (Johnson et al., 2013), with different specific biochemical and functional proprieties and, above all, a distinct behaviour during aging (Marzetti et al., 2013).

Besides, in last years, increasing literature reports an accumulation with aging of fat between the fibres. This type of fat, named inter-muscular adipose tissue (IMAT), has been identified as a potential contributor to sarcopenia and to reduced mobility of the elderly. According to Marcus and colleagues, IMAT may also be metabolically active secreting, like inflammatory cytokines that contribute to systemic inflammation (Marcus et al., 2012).

1.1.3 Human white adipose tissue aging

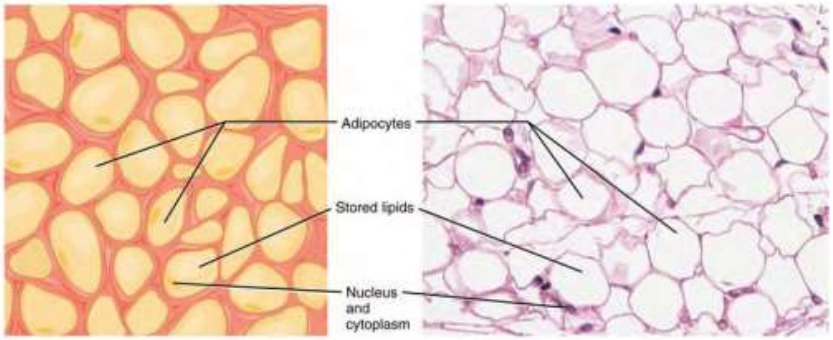

Figure 4: Adipose tissue is a connective tissue, consisting of fat cell with little extracellular matrix. (OpenStax College. Anatomy & Physiology. Connexions, June 19, 2013. http://cnx.org/content/col11496/1.6/)

Two types of adipose tissue could be distinguished: brown adipose tissue, whose main role is thermogenesis, particularly in small mammals and human neonates, and white adipose tissue (WAT). The latter is composed by adipocytes, that are the most prevalent cell type, and many others, like the stromovascular fraction, which in turn is constituted from approximately 10% of $CD14^{+}CD31^{+}$ macrophages (Fantuzzi, 2005). In mammals and birds, WAT is the main site of energy storage, since substrate being deposited as triacylglycerols at a high energy density. Initially it was thought that this was the principal function of white adipose tissue, together with thermal and mechanical insulation, but now this tissue is seen as a highly dynamic organ, involved in several physiological and metabolic processes (Trayhurn and Wood, 2004). Indeed, WAT is an important source of cytokines, chemokines and adipocyte-specific factors, known as adipokines, that are used by WAT to regulate several biologic activities, like, among others, appetite, energy expenditure, insulin sensitivity, bone metabolism and the endocrine and reproductive system (Fantuzzi, 2005). In particular, WAT produces as much as 30% of circulating IL-6 and tumor necrosis factor, that increase its release in people with obesity (Vitale et al., 2013). In this way, WAT affects inflammation and immunity, as seen by Ostan and colleagues in a study on centenarians, where the healthy status of old people it is argued to be due by levels of adipokines (Ostan et al.,2008). Specifically, the production of inflammatory mediators is linked to oxidative stress and generation of reactive oxygen species, that are increased during hypoxia and that lead to a deregulated expression of adipokines and to induction of adipogenesis (Vitale et al., 2013). In fact, white adipose tissue in adults is increased, as result of adipocytes hypertrophy and hyperplasia. This is the reason why WAT is the only endocrine tissue that increase with age (Jackson et al., 2012). Moreover, the increment of adipose tissue is preferentially in its visceral component, but, above all, it is invaded by activated macrophages and T-cells, able in turn to induce the activation of multiple

signalling networks and the generation of inflammatory compounds. These are the principal responsible of a low-grade, chronic inflammation, orchestrated by metabolic cells in response to excess nutrients and energy, referred as “metaflammation” (Gregor and Hotamisligil, 2011). Classically it is thought that metaflammation occurs in young and adult (obese) people, while inflammaging occurs later in life even in non obese and lean people, but a possible overlapping of the two phenomena in the same individual cannot be excluded and it is an interesting perspective to purse (Cevenini et al., 2013), also because little is known about modifications of this peculiar endocrine tissue, as white adipose tissue is yet (Vitale et al., 2013).

1.2 Mitochondria

1.2.1 Mitochondria structure and function

Mitochondria – from the Greek *mitos* (thread-like) and *khondros* (grain or granule) – are intracellular, bacteria-sized organelles present in all eukaryotic cells (Schon et al., 2012). They are bound by two lipid bilayer membranes (Okamoto and Kondo-Okamoto, 2012), with specific and different characteristics and functions. The outer mitochondrial membrane (OMM) is highly permeable, regulates the mitochondrial shape and contains enzymes involved in amino acids’ oxidation, fatty acids’ elongation, phospholipids biosynthesis and hydroxylases. Instead, the inner mitochondrial membrane (IMM) is characterised by some peculiar structures, called cristae. Cristae contain the electron transport proteins and in particular, the cytochromes that form the electron transport chain, and are associated to the five respiration complexes located in the mitochondrial matrix. Thus, each mitochondrion results divided in four distinct section: OMM, the inter-membrane space, IMM and the mitochondrial matrix, as shown in figure 5.

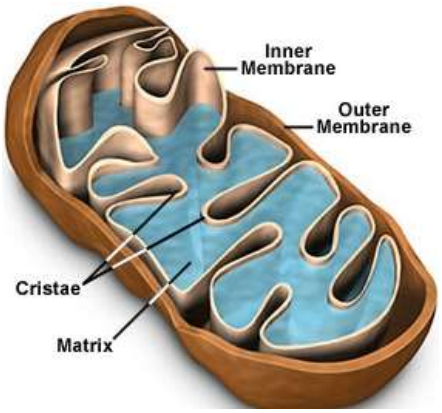

Figure 5: Mitochondrial structure(http://mjlightfoot.edublogs.org/).

Inside the cells, mitochondria carry out many functions as iron/sulfur cluster biosynthesis, the synthesis of amino acids, lipid metabolism, copper homeostasis, signal transduction, thermogenesis and the control of apoptosis, among others (Peterson et al., 2012; Osiewacz and Bernhardt, 2013). Nevertheless, the main mitochondrial function is to produce energy, generating more than 90% of a typical cell adenosine triphosphate (ATP), which is used to drive all cellular energy-consuming processes (Schon et al., 2012, Osiewacz and Bernhardt, 2013).

Mitochondrial energy production is the result of two coordinated processes: the tricarboxylic acid (TCA) cycle, also known as the Kreb's or the citric acid cycle, and the electron transport chain (ETC). The former produces only a small amount of ATP from carbohydrates and fats, since its main aim is to provide, from pyruvate generated by glycolysis, not ATP but coenzymes NADH and FADH for ETC. More specifically, the Kreb's cycle consists of nine steps leading to the production of three molecules of NADH and two molecules of FADH, for a total of six molecules of NADH and four molecules of FADH per molecule of pyruvate. Furthermore, two molecules of ATP are generated during acetyl-CoA oxidation with two additional molecules of CO_2 (Lehninger, 2004).

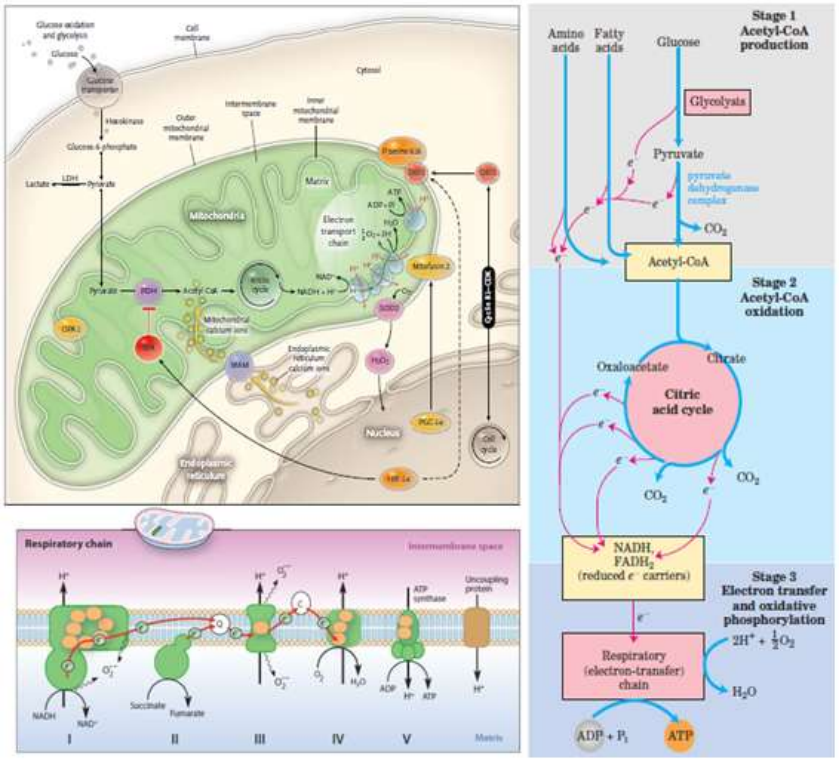

Figure 6: Mitochondrial structure and energy production processes (Adapted from Lehninger, 2004 and Larsson, 2010).

The role of NADH and FADH is to carry electrons to the electron transport chain, whose reactions create a reduction potential that increases along the chain. In this way, the

generated energy is sufficient to drive the protons translocation across the IMM, creating a proton gradient and a membrane potential, collectively called the proton motive force, which drives the synthesis of ATP. This process, named also oxidative phosphorylation (OXPHOS), is not a perfect system since proton leakages occurs reducing the yields of ATP production (Mathews et al., 2004).

1.2.2 Mitochondrial genome (mtDNA)

A fundamental characteristic of mitochondria is that, as evolutionary relics of aerobic bacteria that invaded the proto-eukaryotic cell a billion of years ago, they have a separate genome (Green et al., 2011), that is maternally inherited (figure 7). The human mtDNA is a circular double strand DNA molecule of 16569bp (Anderson et al., 1981), present in multiple copies in each cell. They are organised in protein-DNA complexes (mitochondrial nucleoids) often associated to the inner mitochondrial membrane and that look like globular foci. Each mtDNA molecule can be divided in two regions. The former is a regulatory region (16024-576bp), named displacement loop (D-loop) and involved in the replication and transcription processes, since it contains transcriptional promoters and replication origins. The second one is the coding region (577-16023bp), containing only 37 genes, 13 of which encoding for proteins which are part of the core subunits of the respiratory complexes I, III, IV and V, the others encoding for 2 rRNAs (12S and 16S) and 22 tRNAs necessary for mtDNA translation (Ylikallio et al., 2010). Moreover, the strands of the duplex DNA can be distinguished on the basis of G+C content in heavy (H, G-rich) and light (L, C-rich) strands (Kasamatsu et al., 1974). Most of the information is encoded on the H strand, that includes 2 rRNAs, 14 tRNAs and 12 polypeptides, while the L strand codes for only 8 tRNAs and one polypeptide.

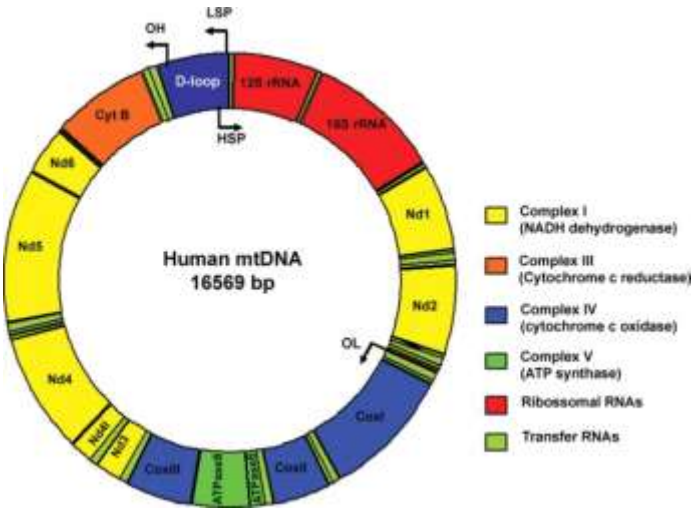

Figure 7: Mitochondrial genome (St John, 2012)

1.2.2.1 Replication models of mtDNA

It is known that each cell contains numerous mitochondria and that each of them contains several hundreds to thousands copies of mtDNA, probably due to the faster evolution of mtDNA in respect to nuclear DNA (Kato, 2001). Therefore, replication of mtDNA is essential to the maintenance of the mtDNA copy number per cell, but there is any agreement about how mitochondrial DNA replicates itself. For this reason, three main models have been proposed (figure 8). The strand-displacement model is the first, proposing that the synthesis of H strand initiates at the O_H origin within the D-loop and proceeds continuously. Continuing the H strand synthesis, replication intermediates progressively distance from the parental H stand maintained in a single stranded form, while the L strand synthesis begins at about two thirds of the distance around the genome, when the O_L get exposed, and proceeds continuously (Kasamatsu and Vinograd, 1973). The second model is the strand-coupled model and it is based on what happen during DNA replication in bacteria, with the presence of fully double-stranded DNA theta-like replication intermediates which are indicative of coupled H and L strand synthesis and of a bidirectionally progression of the replication. The progression ends within the D-loop region (Holt et al.,2000). Finally, the third model proposed is that referred to as RITOLS (RNA Incorporated Through Out the Lagging Strand) (Yasukawa et al., 2006). It suggests that during mtDNA replication, RNA is incorporated throughout the H strand and implies strand-coupled replication proceeding unidirectionally from the D-loop region, with the RNA replication intermediates subsequently being maturated into DNA (Holt and Reyes, 2012; McKinney and Oliveira, 2013).

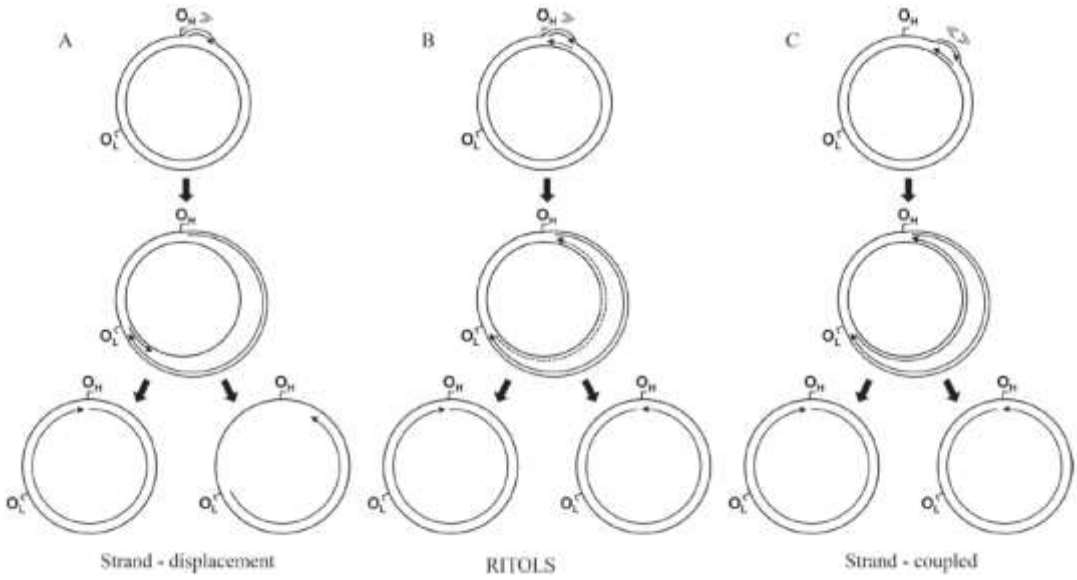

Figure 8: mtDNA replication models (McKinney and Oliveira, 2013).

1.2.3 Mitochondrial Theory of Aging and mtDNA rearrangements

Among the proposed theories of aging, one of the most popular is the Free Radical/Mitochondrial Theory of Aging (MTA), proposed by Harman in 1956. At the beginning, this theory postulated that the increase of reactive species of oxygen (ROS), that are generated in mitochondria as a "waste" of aerobic respiration and several other catabolic and anabolic processes, lead to damage of the cellular components, including nucleic acids on the genome and in this way to cellular senescence (Harman, 1956; Halliwell, 1991). Hereafter, the theory was redefined since mitochondria were identified as both the source and the target of ROS, and in particular mtDNA is the main keeper of damage. In fact, the proximity of the mtDNA to the ROS source makes it more susceptible to injury, which can be converted to point mutation and deletions and the latter can be transmitted and accumulated to daughter molecules throughout replication process, changing the hereditary information over time (Shokolenko et al., 2014). In this way, the accumulation of mutations in mtDNA may arrive to a critical threshold causing adverse effects especially in those mitochondria where components of the respiratory chain improperly function or are damaged and need to be replaced (Chistiakov et al., 2014). However, inefficient transfer of electrons across the electron transport chain generates more ROS, that in turn can damage mitochondria and further decrease the efficiency of ETC, constituting a "vicious cycle" that lead to more mitochondrial ROS generation and oxidative damage (Ziegler et al., 2014), as well as more mtDNA modifications. Indeed, mtDNA shows a high mutation rate, due to its vicinity with ROS source and to the occurrence of spontaneous errors generated through DNA replication or unrepaired damage to mtDNA that introduces mis-coding lesions (Santoro et al., 2006; Copeland and Longley, 2014). The random distribution of mtDNA molecules during cell division can generate two different situation: the former is named heteroplasmy and indicates the coexistence of mutated and wild-type mtDNA molecules in the same cell, tissue or organ, while the second one is named homoplasmy and indicates cells containing only one type of mtDNA molecules, mutated or wild-type (Santoro et al., 2006). As suggests by Trifunovic's experiment on mtDNA mutator mice, these random distributed mtDNA mutations are associated with age. In fact, these engineered mice accumulated mtDNA mutations during the process of mitochondrial biogenesis, due to a defect in the proofreading function of mitochondrial DNA polymerase, developing a premature onset of age-related phenotypes, like weight loss, reduces subcutaneous fat, alopecia, anemia, reduced fertility, kyphosis, progressive hearing loss, heart disease, decreased spontaneous activity and sarcopenia (Trifunovic e al., 2004).

Nevertheless, even if it is well known that age-associated mtDNA mutations occur and are distributed randomly in the mitochondrial genome, differential pattern of mtDNA point mutations accumulation and some differences between in mitotic and post-mitotic tissues appear. In particular, base substitutions are the most common type of mtDNA mutations in mitotic tissue, while in post-mitotic tissues, large-scale deletions occur more commonly (Shokolenko et al., 2014).

mtDNA deletions refer to mtDNA molecules that have lost large section of the mitochondrial genome (Krishnan et al., 2008; fig. 9) and originate as an interplay of large number of base-pair direct repeats contained in mtDNA with the asynchronous replication of the heavy and light strands (Kovalenko et al., 1998). Recent studies also suggest that mtDNA deletions arise not only by defective replication, but also during repair of damaged mtDNA, since during aging, oxidative damage leads to generation of double strands breaks that, when are processed, generate single-strand regions free to anneal with microhomologous sequences on other single-stranded mtDNA or with non coding region. The resulting formation of an intact mitochondrial genome carrying a deletion is due to the processes of repair, ligation and degradation of the single strands that remain exposed (Cui et al., 2012). Most mtDNA deletions share that they are located between the two origins of replication (O_H and O_L), also known as major arc of mtDNA (Krishnan et al., 2008), but a clear pattern of mtDNA deletions show how accumulation intervene with age (Kazachkova et al., 2013). Between these, the most studied in human is a 4977bp deletion, also named “common deletion”, that generate a mtDNA molecule lacking of the genes for NADH dehydrogenase subunits 3, 4, 4L and 5, cytochrome c oxidase subunit III and ATP synthase subunits 6 and 8 (Hebert et al., 2010). In 1992, Cortopassi and colleagues demonstrated that dissimilar levels of this deletion appeared in different tissues of older individuals, and in particular brain stem and brain cortex, heart, psoas and diaphragm muscles have higher levels of the common deletion than skin, lung, spleen, kidney and liver. They therefore suggested that tissues with elevated oxygen consumption, as muscle and brain are, have higher levels of oxidative damage to mtDNA, causing also increased deletion frequency (Cortopassi et al., 1992). Later, in 1997, also Zhang and colleagues corroborated this study also in animal model, demonstrated that in rats the mtDNA deletions differently accumulate in different tissues (Zhang et al., 1997). Therefore, as mtDNA deletions are tissue-specific, it is likely that mitochondrial dysfunction with different grade of severity are caused by different levels of mtDNA deletions (Frahm et al., 2005).

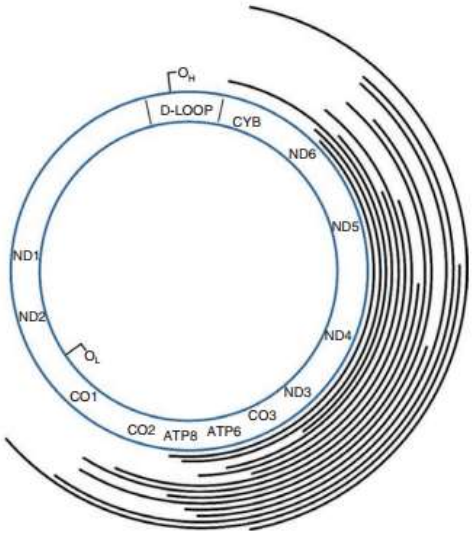

Figure 9: Schematic representation of mtDNA deletions in which each line represents a possible deleted region of mtDNA (Payne et al., 2011)

Furthermore, in addition to qualitative changes in mtDNA, also quantitative alterations in mtDNA amount (mtDNA copy number) have been associated with mitochondrial disease and ageing (Masuyama et al., 2005). Several studies, both in rodents and in humans, were conducted but contrasting data emerged about the age-related changes in mtDNA coy number (Santoro et al., 2006). Barazzoni and colleagues analyzed mtDNA copy number in rats, founding that it was significantly decreased in almost all tissue from old animals even if also this reduction showed a tissue-specificity: mtDNA decline was similar in the red and white portions of the skeletal muscle gastrocnemius, while it was higher in soleus muscle and highest in the liver. Instead, mtDNA copy number did not change with age in rat's hearts (Barazzoni et al., 2000). Also in humans, different tissues show different changes of the amount of mtDNA with age. In particular, in human lung there is an age-dependent increase in mtDNA copies (Lee et al., 1998), while in blood there is a significant decrease (Bai et al., 2004). A different situation appears for skeletal muscle, for which there are any consensus data yet: Pesce analyzed mtDNA copy number in *vastus lateralis* and *rectus abdominalis*, finding that in both the mtDNA content increased about 2-folder in elderly individuals (Pesce et al., 2001). However, in 2003 Welle found that in human *vastus lateralis*, the mtDNA amount diminished with age (Welle et al., 2003). Still different data come from the study of Frahm, which, analysing mtDNA copy number in five diverse tissues (caudate nucleus, the frontal lobe brain, cerebellar cortex, *ilipsoas* muscle and heart), did not find any significative age-related changes (Frahm et al., 2005). These reported discrepancies in mtDNA abundance may be due to the different methods utilized to quantify the mtDNA content and also to the region analyzed for estimation of mtDNA copy number, especially if this corresponds to the mtDNA region

frequently deleted. However, these data also show a marked tissue specificity (Santoro et al., 2006; Hebert et al., 2010; Kazachkova et al., 2014) that can be attributable to the tissue specific need of oxidative metabolism and to its oxidative capacities (Santoro et al., 2006) as well as to the developmental stage.

Therefore, loss of mtDNA copy number control affect human aging (Clay Montier et al., 2009), together with respiratory chain deficiency due to high levels of mtDNA rearrangements, like clonally expanded deletions (Trifunovic and Larsson, 2008).

1.2.4 Nuclear-mitochondrial interconnections

Inside the cells, mitochondria are not self-supporting entities, since the preservation of their function are governed by genes present in mitochondrial DNA but also by genes located in chromosomal DNA (Taanman JW, 1999; Zhang and Singh, 2014). Moreover nuclear-encoded proteins are fundamental for the maintenance and the expression of mtDNA (Trifunovic and Larsson, 2008). This is probably due to the fact that during evolution there is a great translocation of the original information encoded by mitochondrial genome into the nuclear genome, which now coded structural mitochondrial proteins. Thus, nucleus has to be constantly informed about the functional status of mitochondria, in order to regulate mitochondrial activity, in both physiological and pathological conditions (Santoro et al., 2006; Dato et al., 2013). Therefore the cross-talk between nuclear and mitochondrial genome has to be intact to ensure normal mitochondrial biogenesis, dynamics, mitophagy, quality of the mitochondrial proteins and finally scavenging of ROS (Michel et al., 2012).

1.2.4.1 Mitochondrial biogenesis

Mitochondrial biogenesis refers to either the formation of mitochondria during cell cycle, the genesis of organelles for normal turnover and the phylogenesis and ontogenesis of mitochondria (Attardi and Schatz, 1988; Shepard et al, 1998). As for many processes that happening in mitochondria, also mitochondrial biogenesis is dependent of the import of a large number of proteins encoded by nuclear genes and then transferred by the translocase of the outer mitochondrial membrane (TOMM) complex in the mitochondrial sub-compartments. Mutations on these translocases, like for instance TOMM40, lead mice to death in 4-6 weeks for abnormal heart, pulmonary vascular congestion and hypertension (Desler and Rasmussen, 2014).

Anyway, the formation of new mitochondria depends also by others players, like Pgc-1α, that is the main regulator of mitobiogenesis. It is regulated by several external stimuli, such as cold exposure, energy deprivation, caloric restriction or physical activity (Michel et al., 2012). In

particular physical activity or nutrition stress cause post-translational modification of Pgc-1α through the deacetylation mediated by sirtuins (SIRT1 and SIRT3), that are able to activate PGC-1α and its mitochondriogenesis pathway (López-Llunch et al., 2008; Gurd, 2011; Johnson et al., 2013). In turn, Pgc-1α activates nuclear respiratory factors 1 and 2 (Nrf1/2), which are, above all NRF1, potent stimulators of the expression of mitochondrial transcription factor A, TFAM (Viña et al., 2009). TFAM, together with DNA polymerase γ (POLγ), twinkle and mitochondrial single strand binding protein (mtSSB) are responsible to carry out mtDNA replication and repair, through mtDNA helix destabilization and replication, which is an essential component of mitochondrial biogenesis (Michel et al., 2012).

1.2.4.2 Mitochondrial dynamics

Mitochondria are not isolated organelles, but rather they exist in a dynamic network adapting to cellular needs constantly through fusion and fission processes. Moreover, these processes are fundamental also to regulate mitochondrial morphology and number (Romanello and Sandri, 2010), in an opposing way (Mishra and Chan, 2014). The former generates an extended interconnected network, starting from isolated mitochondria which can thus mix their contents and redistribute metabolites, proteins and mitochondrial DNA, preventing the accumulation of defective or abnormal mitochondria. Instead the latter allows the segregation of dysfunctional mitochondria from the network components, resulting in the activation of autophagy (Romanello and Sandri, 2010).

In humans, the key factors of the fusion machinery are GTP-hydrolysing enzymes located either in the outer and in the inner membranes: the OMM fusion is driven by mitofusin 1 and 2 (Mfn1/2), whereas the IMM are fused by dynamin-related protein optic atrophy 1 (OPA1) (Zorzano et al., 2010). For the opposite mechanism of fission, dynamin-related protein 1 (DRP1) and mitochondrial fission 1 (Fis1) are required, leading before to the constriction and after to the fission of the mitochondrion (fig. 10; Mishra and Chan, 2014).

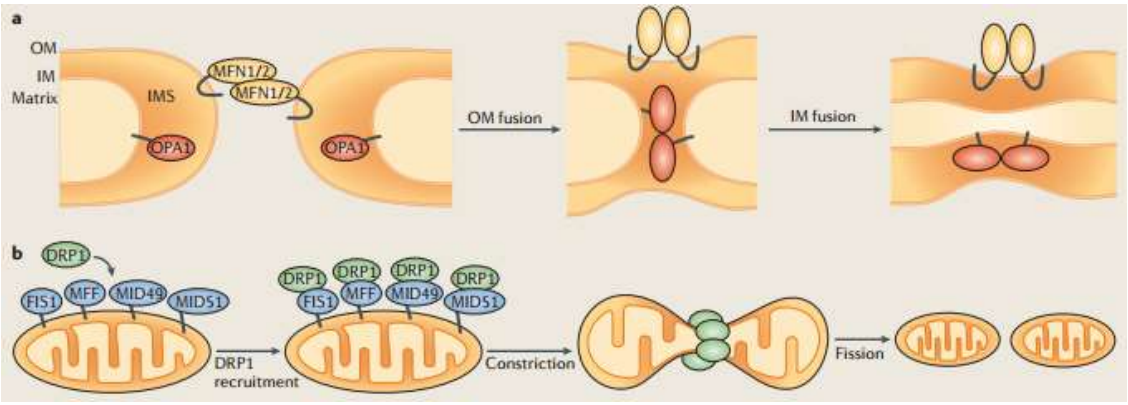

Figure 10: Fusion (a) and fission (b) processes in mitochondria (Mishra and Chan, 2014)

1.2.4.3 Mitophagy

Autophagy is the process by which organelles are surrounded by double membrane that fuses with lysosomes, allowing the hydrolytic digestions and recycling (Klionsky, 2007). Mitophagy is simply a selective type of autophagy targeted to mitochondria (Okamoto and Kondo-Okamoto, 2012). Indeed, digestion of the entire organelles by mitophagy allows the control of the abundance of mitochondrial population through the right level of turnover (Michel et al., 2012), but above all mitophagy is the key mechanism of the mitochondrial quality control system, which is evolved to avoid cell damage and maintain the overall fitness of the cell (Gomes and Scorrano, 2013). Fission is strictly linked to mitophagy, since it generates unequal daughter mitochondria, that differ in membrane potential, and in particular, the dissipation of the membrane potential lead to proteolytic processing of OPA1, causing the inhibition of mitochondrial fusion and ensuring effective mitophagy (Okamoto and Kondo-Okamoto, 2012).

E3-ubiquitin ligase Parkin (Parkin) and the PTEN-induced putative kinase 1 (PINK1) are the main factors that cause the collapse of membrane potential, following by the action of Beclin and AMBRA1 (activating molecule in beclin 1-regulated autophagy) that localize on endoplasmic reticulum and mitochondrial surface respectively to stimulate autophagy (Michel et al., 2012; Okamoto and Kondo-Okamoto, 2012).

Interestingly, cells lacking mtDNA are autophagic-deficient, but also a controlled degradation of the organelle represents a crucial steps for proper mitochondrial and cell function (Michel., 2012).

1.2.4.4 Protein Quality Control System

Mitochondrial proteins, such as the others proteins present inside the cells, have to be kept properly folded, while damage or aggregated proteins have to be rapidly degraded by proteases (Michel et al., 2012). In particular, oxidized proteins have to be eliminated in order to maintain mitochondrial homeostasis (Bulteau el al., 2006). For this reason, inside mitochondria there are three known proteases, all of which are able to degrade short-lived, misfolded or damaged proteins (Bota et al., 2005). One of these, AAA protease, is localized in IMM, whereas Clp and Lon proteases are immersed in the mitochondrial matrix. In particular, Lon Protease (LonP) is the most studied, since it is the main protease for degradation of oxidized proteins, even if does not recognize a specific consensus peptide sequence (Ngo et al., 2013).

LonP is age-modulated, as demonstrated in old rats by Bakala and colleagues. The Lon activity in these animals, in fact, was found decreased by 2.5 fold in liver, even if the level of protein in

the mitochondrial matrix remained the same, as to indicate Lon inactivation. In heart, instead, the activity is similar between young and old rats, but the protein level was 5-fold increased, suggesting a sort of compensation for the loss of activity (Bakala et al., 2003).

1.2.4.5 Super oxide product scavenging

Inside cells, ROS carry out multiple functions, such as cell migration, proliferation, differentiation and they are also essential for signalling cascades. However, when the redox equilibrium is lost, ROS abundance causes a state of oxidative stress that is linked also to the aging process (Scheurmann et al., 2014). For this reason, during evolution, a variety of defense mechanisms have been developed to remove ROS from cells (Trifunovic and Larsson, 2008), since they are a well-known cause of oxidative damage, which in turn has long been suggested as a possible cause of mtDNA mutations and deletions (Wanagat et al., 2015).

In mammalian cells sophisticated antioxidant defenses are present in order to scavenge ROS in non-toxic forms. These include catalase, glutathione peroxidase and superoxide dismutase, SOD (Cui et al., 2012). Superoxide dismutases are responsible to catalyze the conversion of superoxide radicals ($O_2^{\bullet-}$) to hydrogen peroxide (H_2O_2) and O_2; inside the cells there are three isoforms of SOD that are noticeable by the intercellular localization: SOD1, or CuZn-SOD, is present in cytoplasm, SOD2, or MnSOD, is the prevalent mitochondrial isoform, being distributed in the mitochondrial matrix, and finally SOD3, or extracellular SOD, that it can be found in lymph, synovial fluid, plasma and all the other extracellular fluids (Watanabe et al., 2014).

Different *sod*-null mutant mice were generated in order to understand the role of the different SODs: Reaume and colleagues described a shortened lifespan in mice $sod1^{-/-}$ mice (Reaume et al., 1996), Li and colleagues studied $sod2^{-/-}$ mice, that showed neonatal lethality (Li et al., 1995) and finally Carlsson et al. generated $sod3^{-/-}$ mice which, conversely from the others, exhibited a shorter survival time under hyperoxic condition, with no apparent abnormalities until late in life (Carlsson et al., 1995).

1.3 Telomeres

1.3.1 Telomeres and aging

Telomeres are long sequences of non-coding DNA, located at the end of chromosomes, where the specific TTAGGG hexanucleotide sequence is repeated thousands time in tandem and is associated with protein complexes. Shelterin is the name of the specialized multi-protein

complex, composed by six proteins: TRF1 and TRF2, binding telomeric double strand DNA, RAP1 that interacts with TRF2, TIN2 and TPP1, which are linker proteins that stabilize and hold the complex together and POT1, that instead binds telomeric single strand DNA. In fact, telomeres contain a region of double-stranded (ds) and a region of single-stranded (ss) DNA, that is an extension at the 3' end of the G-rich strand and consists in about 100 nucleotides. It can form a telomere-loop (t-loop) structure, in order to mask the chromosomal ends by strand-invading into the ds DNA thus forming a displacement loop (D-loop) (Sahin and DePinho, 2012). This peculiar structure allows performing two protective functions: telomere prevent chromosomal end-end fusion and non reciprocal translocation (Hoare et al., 2010).

Indeed, at each cellular division a telomeric fragment of 50-200bp is lost, causing progressive shortening of telomeres that, in fibroblast, is related to progressive loss of the proliferation capacity after a limited number of cell divisions, a phenomenon called by Hayflick limit or cellular replicative senescence (Hayflick and Moorhead, 1961).

Senescence is now known to be triggered by telomeres shortening or disruption, but it is largely heterogeneous, probably because several factors participate, such as telomere structure and composition, telomerase availability and activation state, interplay between proteins, telomerase and DNA replication machinery (Stewart et al., 2012). Also environmental factors like stress, pathologies and ROS can increase telomere shortening by increasing telomeric DNA damage and telomere shortening rate (Saretzki and von Zglinicki, 2002).

However, telomere length is regulated by telomerase, i.e. a reverse transcriptase consisting of a complex of several proteins and RNA template (Cong et al., 2002), that increases telomere length adding TTAGGG repeats, in order to maintain the telomeric length in embryonic cells, in adult stem cells and finally in cancer cells (Hoare et al., 2010). Conversely, in most somatic cells telomerase is suppressed within few weeks after birth (Oeseburg et al., 2010). Moreover, it was seen that in some human premature diseases telomerase complex is mutated, resulting in decreased telomerase stability and shorter telomeres (Mitchell et al., 1999), proving a plausible involvement in aging process.

1.3.2 Telomere and mitochondria, a connection in aging

Since mitochondria are the most important source of ROS in the cells, a possible role of mitochondria and oxidative stress in telomere-driven replicative senescence has been proposed. Knowing that ROS production and mitochondrial dysfunction are involved in aging and that mitochondrial dysfunction induces a retrograde response to signal the disruption of the ETC to the nucleus, it is possible that nucleus implement an adaption response. Likely, this

retrograde signalling of adaption response corresponds to the up-regulation of mitochondrial biogenesis induced by PGC-1α and PPARγ and increases mitochondrial uncoupling, causing a reduction in ROS production by the mitochondria, with less oxidative stress impacting on telomeres (Passos et al., 2007).

Supporting the connection between telomeres and mitochondria during aging there is the fact that chronic or mild long lasting oxidative stress causes exportation of telomerase from the nucleus to the mitochondria, avoiding its activity on telomeres. However, it has been shown that the catalytic subunit of telomerase (TERT) may have a telomere-independent function in mitochondria, carrying out the protection of mitochondria and mtDNA from ROS-induced damage as a result of improved mitochondrial function, decreased ROS production, increased mitochondrial coupling and suppressed retrograde response (Ahmed et al., 2008).

Basing on the fact that telomere maintenance is controlled also by some proteins involved in the repair pathways, it is clear that active genome maintenance and repair systems are fundamental to avoid premature aging. Thus, a constitutive activation of repair pathways with sustained p53 induction could be due to shortened of disrupted telomeres, as signal of DNA damages. In turn, p53 activation can lead to cell growth arrest, stimulation of repair, apoptosis or senescence pathways depending on its degree of activation, in addition to mitochondrial changes, due to its binding with the promoter of the mitochondrial transcriptional co-activators family of PGC-1α, master regulators of mitochondrial biogenesis, as shown in figure 11 (von Zglinicki et al., 2001; Sahin and De Pinho, 2012;).

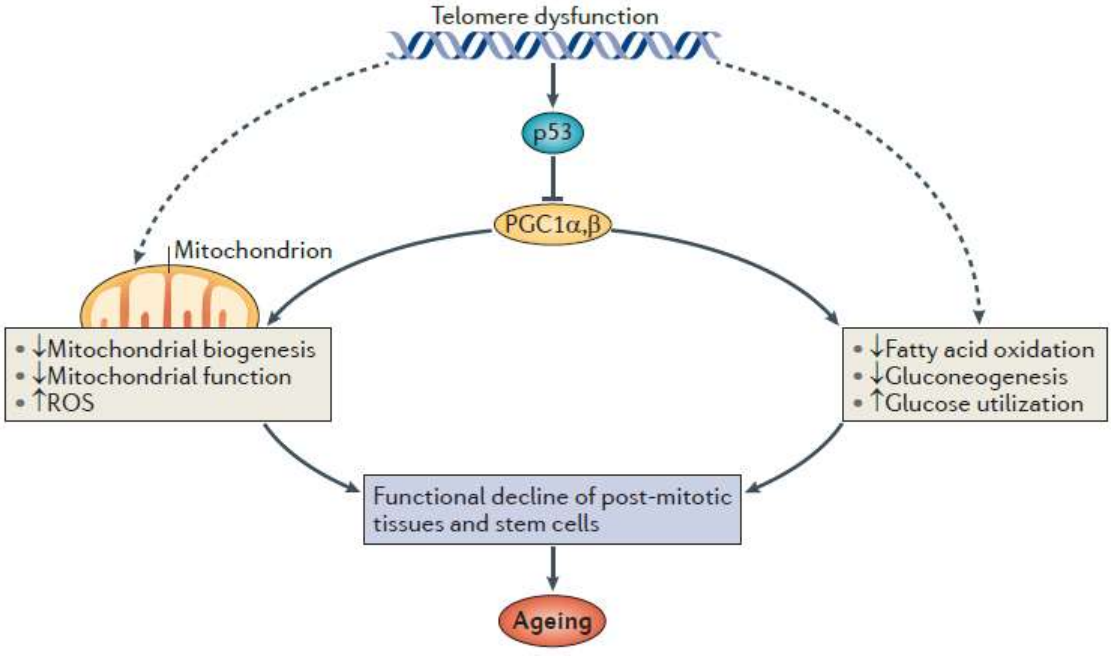

Figure 11: Telomeres-p53-PGC aging pathway (Sahin and De Pinho, 2012).

2 Aim of the thesis

Aging is characterized by an increasing propensity to degenerative diseases and death due to the progressive decline in the functional maintenance of tissue homeostasis (Hayflick, 1998), caused by the accumulation of unrepaired and deleterious changes of molecules and cells. Thus, in order to compensate and neutralize the adverse effects of such damages, each tissue acts out a series of adaptive mechanisms resulting in the tissue-specificity of the aging process (Meissner et al., 2006; Ostan et al., 2008).

However it is well known that age-related declines in mitochondrial function underlie several of those biological changes that cause an incremented vulnerability to multiple disease states, functional and cognitive decline and, at the end, mortality (Ashar et al., 2014). Mitochondrial dysfunction includes decreased oxidative capacity and increased oxidative damage to biomolecules (DNA, proteins and lipids) due to the excessive production of reactive oxygen species, which are highly toxic (Chistiakov et al., 2014). In particular, ROS can damage mitochondrial component like mitochondrial DNA (mtDNA), causing mtDNA point mutations, varying its copy number or inducing mtDNA deletion. Thus, mtDNA rearrangements, intended as mtDNA copy number, deletion level and integrity, are likely to play an important role in the aging process. Several studies investigate mtDNA copy number or mtDNA deletion in different tissue from either human and animal models but data on mtDNA rearrangements are still controversial.

Thus, in order to understand the involvement of mtDNA rearrangements during human aging, the primary aim of this thesis is the analysis of mtDNA copy number, deletion level and integrity, in human biopsies from liver, *vastus lateralis* skeletal muscle from healthy subjects and patients with limited mobility of lower limbs (LMLL) undergone hip replacement surgery, and adipose tissue. The biopsies were recruited in the framework of the project MIUR-PRIN 2008, for what concern liver, whereas all muscle and adipose tissue biopsies were recruited in the framework of the European project MYOAGE (Understanding and Combating age related muscle weakness; FP7-223576; 2008-2012), and all of them are from subjects at different ages.

Moreover, the telomere length was also investigated, considering its possible relationship with mitochondrial function (Sahin et al., 2011) and its role as marker of cellular aging.

To further characterise the involvement of mtDNA rearrangements in the aging of human liver, skeletal muscle and adipose tissue, the expression of nuclear genes related to mitochondrial biogenesis (*pgc-1α*, *polγ*, *nrf1*, *tfam*, *twinkle*, *sirt1*, *sirt3*, *tomm40* and *ppard*), mitochondrial dynamics, i.e. fusion and fission processes (*mfn2*, *fis1* and *opa1*), mitophagy (*ambra1*, *beclin*,

pink1, *parkin*, *atg16l* and *pik3cd*), mitochondrial protein quality control system (*lonp*), production of ROS (*nos3*), protection from ROS (*sod1* and *sod2*) and hypoxia (*hif-1*α) were also evaluated in the same samples.

Finally, a comparison among the considered tissues was realized, in order to understand the tissue specificity of mtDNA rearrangements and to extend the comprehensive and age-independent vision of tissue-related variability in mtDNA rearrangements and of the nuclear genes expression involved in mitochondrial pathways, which is still poor of evidences.

3 Materials and methods

3.1 Tissues samples

For the present work, biopsies from three different human tissues have been collected.

For human liver, 82 biopsies have been obtained from organ donors at different ages (13-84 years) in collaboration with the Unit of Surgery of liver and multi-organ transplants of the S. Orsola-Malpighi Hospital in Bologna, in the framework of the project MIUR-PRIN 2008 coordinated by Dr. Gianluca Grazi (Transplantation Unit) and Dr. Miriam Capri (Lab of Immunology of Prof. Franceschi). The biopsies have been recovered during the explants of the liver, which were performed at beating heart.

For skeletal muscle, biopsies of *vastus lateralis* were taken from two group of subjects recruited in the framework of the European Project MYOAGE. The former was the patients group, i.e. 50 biopsies from subjects with lower limb mobility impairment (LLMI) who underwent hip replacement surgery, recruited in Bologna, Italy (Prof. Ermanno Martucci, Istituto Ortopedico Rizzoli, Bologna). The latter enclosed 109 biopsies from healthy subjects of two different age groups, subjects under 40 years and subjects that are more than 65 years old, coming from Tartu, Estonia (Prof Enn Seppet, Centre of Molecular and Clinical Medicine, University of Tartu) and Leiden, the Netherlands (Prof. Andrea Mayer, Department of Gerontology and Geriatrics, Leiden University).

From LLMI patients were also picked up 20 biopsies of adipose tissue in order to obtain two different tissues from the same subjects. For this reason, the range of age of adipose tissue is the same of LLMI patients group (24-89 years).

Table 1 shows the number of samples studied in this thesis grouped by tissue, age and gender.

	Liver			**LLMI muscle**			**Adipose Tissue**			**Healthy muscle**			
Age Group (age range)	Gender		Total	Gender		Total	Gender		Total	Age Group (age range)	Gender		Total
	M	F		M	F		M	F			M	F	
1: ≤30	10	5	15	10	5	15	2	1	3	1: ≤40	15	21	36
2: 31-50	10	4	14	7	4	11	3	1	4	2: ≥65	38	35	73
3: 51-70	11	15	26	5	7	12	2	3	5				
4: ≥71	14	13	27	6	6	12	4	4	8				

Table 1: Biopsy samples of different tissue divided by age and gender.

3.2 Nucleic acid isolation and purification

3.2.1 DNA isolation

3.2.1.1 Liver and skeletal muscle biopsies

Quick-gDNA™ MiniPrep kit from Zymoresearch (USA) was used to isolate total DNA from liver and *vastus lateralis* muscle biopsies, since it allowed the isolation of total DNA from various biological sample sources, including different solid tissues, as in this case.

To obtain total DNA is not require the use of organic denaturants or Proteinase K digestion, but just columns with high DNA affinity. Following the provided data sheet:

1. Homogenize about 25mg of frozen biopsy in 500µl of Genomic Lysis Buffer by an automatic homogenizator
2. Centrifuge the lysate at 10000 x g for 5 minutes
3. Transfer the supernatant to a Zymo-Spin™ Column in a Collection Tube, without disturb the pellet debris
4. Centrifuge at top speed for one minute and discard the Collection Tube with the flow trough and transfer the Zymo-Spin™ Column to a new Collection Tube
5. Add 200µl of DNA Pre-Wash Buffer to the spin column and centrifuge at 10000 x g for one minute
6. Discard the flow trough, add 500µl of g-DNA Wash Buffer to the spin column and centrifuge at 10000 x g for one minute
7. Transfer the Zymo-Spin™ Column in a new and clean eppendorf tube and add 70µl of Elution Buffer
8. Incubate for 5 minutes at room temperature
9. Centrifuge at 10000 x g for 30 seconds to elute DNA

Purified DNA is suitable for many experiments, like quantitative Real Time PCR, but before its use, all samples were quantified by Nanodrop spectrophotometer (see paragraph 3.2.4) and normalized to a working concentration of 0,4ng/µl.

3.2.1.2 Adipose tissue biopsies

To isolate total DNA from adipose tissue biopsies ZR Genomic DNA™ –Tissue MiniPrep kit from Zymoresearch (USA) was utilized since it allowed the isolation of total DNA from specific solid tissues, as adipose tissue.

Following the provided data sheet:

1. Put a sample of about 25mg of frozen biopsy in a microcentrifuge tube and add, mixing, 95µl of H_2O, 95µl of 2X Digestion Buffer and 10µl of Proteinase K. Incubate the eppendorf at 55°C for 3hours
2. Add 700µl of Genomic Lysis Buffer to the tube and vortex
3. Centrifuge at 10000 x g for 1 minute to see insoluble debris
4. Without disturb the pellet, transfer the supernatant to a Zymo-Spin™ Column in a Collection Tube and centrifuge at 10000 x g for 1 minute
5. Change the Collection Tube and add 200µl of DNA Pre-Wash Buffer to the spin column. Centrifuge at 10000 x g for one minute
6. Discard the flow trough, add 400µl of g-DNA Wash Buffer to the spin column and centrifuge at 10000 x g for one minute
7. Transfer the Zymo-Spin™ Column in a new and clean eppendorf tube and add 70µl of water and incubate for 5 minutes at room temperature
8. Centrifuge at 10000 x g for 30 seconds to elute DNA

After purification, all DNA samples were quantified by Nanodrop spectrophotometer (see paragraph 3.2.4) and normalized to the working concentration of 0,4ng/µl.

3.2.2 RNA isolation

RNA was extracted by mirVana Isolation Kit (Life Technologies, California, USA), from about 25mg of frozen biopsies from each tissue.

The whole procedure was performed on ice, and the following protocol has been used:

1. Mechanically homogenize the biopsies in 10 volumes per tissue mass of lysis buffer (Lysis\Binding Buffer)
2. Add 1/10 volume of *miRNA Homogenate Additive* to the homogenate and incubate for 10minutes
3. Add a volume of acid-phenol:chloroform equal to the initial volume of lysate and mix by vortex for 60 seconds
4. Centrifuge at 10000 x g for 10 minutes to separate aqueous and organic phase
5. Transfer carefully the aqueous upper phase, containing the RNA, in a new eppendorf and add 1.25 volumes of room temperature 100% ethanol, mixing with pipette
6. Transfer up to 700 µl of solution to a spin-column (*Filter Catridge* with *Collection Tube*) and centrifuge at 10000 x g for 30 seconds. Discard the flow through and repeat until all solution pass to the filter

7. Add 700 µl of *Wash Solution 1* and centrifuge at 10000 x g for 30 seconds, discarding the flow through
8. Wash two time the filter through adding 500 µl of *Wash Solution 2/3*, and centrifuging at 10000 x g for 30 seconds
9. Transfer the filter to a new eppendorf and add 70 µl of pre-heated 95°C RNase-free sterile H_2O. Centrifuge at 10000 x g for 30 seconds to elute RNA

Isolated RNA was tested with electrophoresis on 1% agarose gel to evaluate the quality and integrity. Each sample was prepared with 3 µl extracted RNA, 2 µl H_2O and 1 µl Bromophenol 6X, loaded on the gel and run at 60-80 V for 30-45 minutes, monitoring voltage and run time to avoid excessive heating and RNA degradation. A positive control RNA has been also loaded on the gel. Extracted RNA was stored at -80°C.

3.2.3 RNA treatment with DNAse

To eliminate possible DNA traces, RNA extracted with mirVANA Isolation Kit was treated with DNase of Turbo DNA-free kit (Life Technologies, California, USA). Following the company indications, 2 µl of Turbo DNase Buffer and 1 µl of Turbo DNaseI enzyme were added to 17 µl of RNA and incubated at 55°C for 25 minutes. After this incubation time, 2 µl of DNase Inactivation Reagent were added to the mixture that was incubated for 5 minutes at room temperature and then centrifuged at 10000 x g for 90 seconds. Later than centrifugation, the supernatant was recovered avoiding removal or touching of the pellet with pipette tip and 3 µl of treated RNA were transferred in a new eppendorf to quantify them by Nanodrop spectrophotometer (see paragraph 3.2.4).

3.2.4 Nucleic acid quantification

NanoDrop 1000 spectrophomometer (Thermo Scientific, Wilmington, USA) was used to quantify isolated DNA and DNase treated RNA in order to later normalize samples in the working solutions.

Measurements for both DNA and RNA were expressed as ng/µl and taken in triplicate, utilizing each time 1 µl of sample. The mean value was used as final concentration. Also other two parameters (260/280 and 260/230 ratio) were taken into account to assess samples purity and identify potential contaminations. In particular, for the 260/280 ratio values should be around 1.8 for pure DNA and around 2.0 for pure RNA, while for the ratio 260/230 around 2.0-2.2. Lower values may indicate presence of contaminants and residues of reagent used in the extraction protocol (for example phenol).

3.3 cDNA synthesis

SuperScript® III First Strand Synthesis System for RT-PCR (Life Technologies, California, USA) was used to convert DNase treated RNA in cDNA.

Following the provided protocol, the quantified RNA was used to start with 750ng, 250 ng and 150 ng of RNA for liver, muscle and adipose tissue respectively for a maximum of 12,5 µl. To this first solution of RNA and water, 0,5 µl of Random Primer 3 µg/µl and 1 µl of dNTPs 2.5 mM were added and incubated for 5 minutes at 65°C on ice for 2 minutes. Then, before continuing the RT-PCR program, 4 µl of Buffer FS 5X, 1 µl of DTT 0.1M and 0,5 µl of SuperScript III 200 U/ µl were added to each starting solution.

All the reagents used for the cDNA synthesis reaction and the overall RT-PCR program are summarized in the tables 2 and 3:

Reagent	Volume	Step
DNAseI treated RNA	750/250/150 ng	
Random primer 3 µg/ µl	0.5 µl	**Addition 1**
dNTPs 2.5 mM	1 µl	
Buffer FS 5X	4 µl	
DTT 0.1 M	0.5 µl	**Addition 2**
SuperScript III 200 U/ µl	0.5 µl	

Table 2: RT-PCR reagents for cDNA synthesis.

Steps
5’ at 65°C
2’ on ice
Addition 2
5’ at 25°C
50’ at 50°C
15’ at 72°C

Table 3: RT-PCR program for cDNA synthesis.

cDNA was then diluted 1 to 10 to use it for qPCR assays and then stored at -80°C.

3.4 Quantitative Real Time PCR SYBR® Green assay

Quantitative Real Time polymerase chain reaction (qPCR) assay allows the simultaneous amplification and quantification of target nucleic acid after every reaction cycle, detecting the amplification product through the use of a fluorophore. In this case, the used fluorophore is

SYBR® Green I, enclosed in the two utilized master mixes, MesaGreen qPCR MasterMix for SYBR® Assay No Rox (Eurogentec, Belgium) and iTaq™ Universal SYBR® Green Supermix (Bio-Rad, USA). Both master mixes contain also the other necessary components for the amplification reaction, like dNTPs, $MgCl_2$, and stabilizers but they differ for the polymerase enzyme (Meteor*Taq* DNA polymerase and antibody-mediated hot-start iTaq DNA polymerase, respectively) and thus for the thermal profile that has to be used. The fluorophore is important because it binds aspecifically double-strand DNA (dsDNA) and the complex fluorophore-DNA absorbs blue light at wavelength λ_{max} = 494 nm and emits green light with λ_{max} = 520 nm, in order to monitor the reaction progression. The melting curve analysis, instead, consent to evaluate the specificity of the amplification, which relies mainly on the primers, since it is built at the end of the amplification reaction by a gradual and regular increase in temperature that gradually denature the dsDNA. When the dsDNA is denaturated, the intensity of the fluorescence dramatically decreases, as shows the melting curve graph. The trend illustrates a pick which represents the temperature at which the 50% of DNA duplex are disrupted (melting temperature, Tm). The Tm is specific for each amplicon. Real time PCR was performed on a *Rotor-Gene Q 6000* (*Qiagen, USA*) thermalcycler, that has a Rotor Gene Q Series Software being able to analyze qPCR data with a comparative method, since it compare the C_t values of the samples of interest with that of a sample used as calibrator which will be run with all samples, without using a standard curve as a reference. The C_t values represent the number of cycle required for the fluorescent signal to cross the threshold and is inversely proportional to the amount of target nucleic acid in the sample. The quantification of the samples were then obtained with the delta delta C_t ($\Delta\Delta C_t$) method (Pfaffl, 2001), since the final value is gained from the subtraction of the delta C_t of the gene of interest and the delta C_t of the gene used as reference.

This method has been used to assess in each tissue:

- mtDNA rearrangements (mtDNA copy number, deletion level and integrity) on extracted DNA
- telomere length on extracted DNA
- gene expression on cDNA synthetised from isolated RNA

The details of each assay are described below.

3.4.1 mtDNA rearrangements analysis

As written above, real time qPCR SYBR® Green assay has been used to determine copy number, deletion level and integrity of mtDNA.

To quantify mtDNA copy number a primers pair to amplify the mitochondrial gene *nd1*, located in a portion of the mtDNA rarely deleted and a primers pair to amplify a nuclear gene, β-*actin*, which is necessary to normalize mtDNA were chosen.

Instead to quantify mtDNA deletion level, primers for the gene *nd4*, which is located in the major arch of the mtDNA where deletion frequently occurs, where used in combination with those for *nd1*.

The ratio between mtDNA deletion level and mtDNA copy number represents the mtDNA integrity, intended as the number of deleted molecules on the total number of mtDNA molecules.

The sequences of utilized primers are described in table 4:

Gene	Primers sequence	Product size
ND1	FOR: CCCTAAAACCCGCCACATCT REV: GAGCGATGGTGAGAGCTAAGGT	94
ND4	CCATTCTCCTCCTATCCCTCAAC REV: CACAATCTGATGTTTTGGTTAAACTATATTT	98
ACTB	FOR: ACCCACACTGTGCCCATCTAC REV: TCGGTGAGGATCTTCATGAGGTA	107

Table 4: Pairs of primers for mtDNA deletion level and copy number.

The qPCR assays were conducted on Rotor gene Q 6000 system (Qiagen, USA). The assays for *nd1*, *nd4* and *actin* were run together on the same samples in different tube in duplicate. To obtain compelling results and to perform significant statistical analysis, qPCR reaction was run three times.

Each mix was prepared by following the directions supplied with the Eurogentec MasterMix (Eurogentec, Belgium) protocol in a final reaction volume of 10µl, as described in table 5. In table 6, instead, is described the thermal profile used for qPCR assays, as indicate in the protocol provided with MasterMix by Eurogentec.

Component	Volume per 1 reaction
Mesa Green qPCR MasterMix for SYBR Assay No Rox (Eurogentec) (2X)	5 µl
Primer forward (10 µM)	0.15 µl
Primer revers (10 µM)	0.15 µl
DNA (0.4 ng/µl)	3 µl
H_2O	1.7 µl
Final volume	10 µl

Table 5: Reagents mix used for the real time assays.

Condition	Cycles	Step
95°C for 5 min		Initialization
95°C for 15 sec		Template denaturation
60°C for 60 sec	**40 cycles**	Primers annealing
72°C for 20 sec		DNA synthesis
From 55°C to 99°C		Melt

Table 6: Thermal profile of qPCR assays for Eurogentec MasterMix.

3.4.2 Telomere length analysis

To assess telomere length with a relative quantification method a pool of six different DNAs from young subjects was used as calibrator sample in qPCR assays. The primers chosen for telomere and for the reference gene are taken from Cawthon et al., 2002 and are listed in table 7. 36B4 is the reference gene and encodes for the acidic ribosomal phosphoprotein P0. The ratio between the amounts of telomeres and 36B4 was used to calculate the telomere length.

Primers	Sequences
Telomere	For: 5'-GGTTTT-TGAGGGTGAGGGTGAGGGTGAGGGTGAGGGT-3' Rev: 3'-TCCCGACTATCCCTATCCCTATCCCTATCCCTATCCCTA-5'
36B4	D: 5'-CCCATTCTATCATCAACGGGTACAA-3' U: 5'- CAGCAAGTGGGAAGGTGTAATCC-3'

Table 7: Primers pair for telomere and 36B4.

As previous, the reaction and the thermal profile were set up following the protocol provided with MesaGreen qPCR MasterMix as shown in table 8 and 9.

Reagent	Volume per 1 reaction
Mesa Green qPCR MasterMix for SYBR Assay No Rox (Eurogentec) (2X)	5 µl
Primer forward (10 µM)	0.15 µl
Primer revers (10 µM)	0.15 µl
DNA (0.4 ng/µl)	3 µl
H_2O	1.7 µl
Finale volume	10 µl

Table 8: Mix used during the assay to determine the telomere length.

Condition	Cycles	Step
95°C for 5 min		Initialization/activation
95°C for 15 sec		Template denaturation
60°C for 60 sec	**40 cycles**	Primers annealing
72°C for 20 sec		DNA synthesis
From 65°C to 90°C		Melt

Table 9: Thermal profile of the qPCR assay.

To obtain compelling results and to perform significant statistical analysis, qPCR reaction was performed in duplicate and each run was repeated three times. Telomere length was calculated as the ratio between the amounts of telomeres with reference to 36B4 gene.

3.4.3 Gene expression analysis

Purified RNA converted in cDNA was used in qPCR to evaluate the gene expression level of different nuclear genes, involved in several mitochondrial pathways.

For mitobiogenesis, the analyzed genes are *pgc-1α*, *polγ*, *nrf1*, *tfam*, *twinkle*, *sirt1*, *sirt3*, *tomm40* and *ppard*. In the table below are reported the primers used.

Gene	Primers	Product size
pgc-1α	FOR: AGACACCGCACGCACCGAAA REV: GCCGACGGCTGTAGGGCGAT	70 bp
polγ	FOR: TGTCAACCAGAACTGGGAGCGTTA REV: TGGCCAGATCCATCAACGACTTCT	95 bp
nrf1	FOR: TGTAGAACTTCATGGAGGAACAC REV: CACATGGACCTGCTGCACTT	98 bp
tfam	FOR: GAAGCATGTGGGGCGTGCTGA REV: GGGAGCGCAGTCGACTTCCAC	81 bp
twinkle	FOR: GTGGGCCAACAGGCAGTGGAA REV:CCGCCCCTCGGCAAACTGTG	147 bp
sirt1	FOR: TCCTGGACAATTCCAGCCATCTCT REV: TTCCAGCGTGTCTATGTTCTGGGT	103 bp
sirt3	FOR: GCCGCACTTCTAGCATGTTG REV: CCTGCAGTCCCTTTGAGGAG	107 bp
tomm40	FOR: CCGGAATTGAGGGGCACGCA REV: TGGAGGATGGGGACGCCAGG	92 bp
ppard	FOR: AGCTGGAGTACGAGAAGTGTGAGC REV: GATAGCGTTGTGTGACATGCCCAG	116 bp

Table 10: Primers pair for genes involved in mitobiogenesis.

As shown in table 11, for the processes of fusion and fission, the genes considered are *mfn2* for fusion and *fis1* and *opa1*, for fission.

Gene	Primers	Product size
mfn2	FOR: GACCAAGTTTGAGCAGGCACACG REV: TTCAGCCATTTCCTCGCAGTAA	121 bp
fis1	FOR: CCAAGAGCACGCAGTTTGAG REV: GAGCAGCACGATGCCTTTAC	83 bp
opa1	FOR: GCTGCCCGCCTAGAAAGGGTG REV: CCCTCCCAATGGCGCATGGA	97 bp

Table 11: Primers pair for genes involved in fusion and fission processes.

From literature is known that *ambra1*, *beclin*, *pink1*, *parkin*, *atg16l* and *pik3cd* are involved in mitophagy process, thus these are the genes chosen to evaluate this pathway.

Gene	Primers	Product size
ambra	FOR: CAGGCCTCGTCAACGCAGCA REV: CGGCGGGTAGGACCCAGACT	119 bp
beclin	FOR: ACAGTGCCTCCGCGGTAGACC REV: ACGAAGCTCACCTGCATGGTGC	116 bp
pink1	FOR: TGGGGAGTATGGAGCAGTCA REV: CGGAGAACCCGGATGATGTT	87 bp
parkin	FOR: AGCCGGGAAAACTCAGGGTA REV: TGGCATTCACCACTCATCCG	118 bp
atg16l	FOR: TGCCGGCATTCCCGCTTCTG REV: GGCACCTCAGCGCCACCAAT	85 bp
pik3cd	FOR: ACCAAGGAGGAGAATCAGAGCGTT FOR: ACCAAGGAGGAGAATCAGAGCGTT	101 bp

Table 12: Primers pair for genes involved in mitophagy.

Also the expression level of the genes for superoxide dismutases 1 and 2 (*sod1* and *sod2*) were considered, together with the expression level of *nos3*, which is, instead, involved in the production of reactive oxygen species.

Gene	Primers	Product size
sod1	FOR: GGAGACGGGGTGCTGGTTTGC REV: TAACTCGCTAGGCCACGCCG	97 bp
sod2	FOR: TGGGGACTTGTAGGGATGCCTTT REV: AGAAAGCCGAGTGTTTCCCTTGG	123 bp
nos3	FOR: GACGTGGTGTCCCTCGAACACG REV: CTCCATCAGGGCAGCTGCAAAGC	108 bp

Table 13: Primers pair for genes involved in protection from and production of ROS.

Finally, the expression level of *lonp* and *hif-1α* were assessed as indicative of the protein system quality control and the level of hypoxia, respectively.

Gene	Primers	Product size
lonp	FOR: AAACGCATCCTGGAGTTCATTGCC REV: ATGGAGCGAGCAATGCTGGTCTTA	113 bp
hif-1α	FOR: ACCTATGACCTGCTTGGTGC REV: GGCTGTGTCGACTGAGGAAA	98 bp

Table 14: Primers pair for genes encoding LONP and HIF1α.

The gene chosen as house-keeping was β-*actin*. Each cDNA sample was run in duplicate and each run was performed twice. The reaction and the thermal profile were set up as indicated in the protocol:

Component	Volume per 1 reaction
iTaq™ Universal SYBR® Green Supermix (Bio-Rad) (2X)	5 µl
Primer forward (10 µM)	0.15 µl
Primer revers (10 µM)	0.15 µl
cDNA dil. 1:10	2 µl
H_2O	2.7 µl
Final volume	10 µl

Table 15: Mix used during the assay to evaluate genes expression levels.

Condition	Cycles	Step
95°C for 30 sec		Polymerase Activation
95°C for 5 sec		Denaturation
60°C for 30 sec	**40 cycles**	Annealing/ Extension and Plate Read at 60°C
From 65°C to 90°C		Melt-Curve Analysis

Table 16: Thermal profile of the qPCR assay with iTaq™ Universal SYBR® Green Supermix (Bio-Rad) (2X).

3.5 Statistical Analysis

All the analyses were performed by the software STATA v.9.0. (Stata Corp. Texas, USA) and p-values < 0.05 were considered as significant. Values, which deviate from the average more than three times the variance, were considered outliers and excluded from the analysis.

Regression analysis has been used to correlate age, as a continuous variable, with the levels of, mtDNA relative copy number, mtDNA relative deletion level, mtDNA integrity, and telomere length as well as the expression levels of the considered genes.

Data were analyzed by Analysis of Variance (ANOVA) test when age was considered as a discrete variable (age-group) and to compare mtDNA rearrangements and gene expression level among the different tissues.

Shapiro-Wilk, Shapiro-Francia and Skewness/Kurtosis tests were employed to verify if variables follow a normal distribution and are homoscedastic (that is with finite variance). When these criteria were not satisfied, Mann-Whitney or Kruskal-Wallis tests were applied to compare two groups or four groups of variables, respectively. Bonferroni's correction was applied for multiple comparisons and the level of significance was set at $p<0,0083$.

4 Results

In order to understand the role of mtDNA rearrangements in the aging of human liver, skeletal muscle and adipose tissue, mtDNA relative deletion level, copy number and mtDNA integrity were evaluated using DNA isolated from biopsies of these different tissues, as reported in table 1 of materials and methods. In each tissue, the above mentioned variables were analyzed in relation to age and then in females and males separately in order to observe any possible gender differences.

Telomere length was also measured on the same DNA samples to assess its association with age, gender and mtDNA rearrangements.

Furthermore, the expression level of nuclear genes involved in several mitochondrial pathways, responsible for impacting on mtDNA rearrangements, was evaluated:

- *pgc-1α*, *polγ*, *nrf1*, *tfam*, *twinkle*, *sirt1*, *sirt3*, *tomm40*, *ppard* for mitobiogenesis
- *mfn2*, *fis1* and *opa1* for fusion and fission processes
- *ambra1*, *beclin*, *pink1*, *parkin*, *atg16l* and *pik3cd* for mitophagy
- *nos3* for production of ROS
- *sod1* and *sod2* for protection from ROS
- *lonp* for the protein quality control system
- *hif-1α* for hypoxia

All these genes were evaluated in relation to age, gender, mtDNA rearrangements and telomere length to understand which of these genes regulating mitochondrial function is expressed or not during human aging process.

Data are presented in four sections: one for liver, one for skeletal muscle, one for adipose tissue and one comparing the results of the three different tissues in order to unravel the tissue-specific role of mtDNA rearrangements during aging.

4.1 Human Liver

4.1.1 mtDNA copy number

mtDNA copy number was quantified by measuring the amount of mitochondrial gene *nd1* located in the rarely deleted mtDNA portion compared to the reference gene *β–actin*, that is nuclear.

mtDNA copy number was found to significantly increase with age in the total number of subjects (p=0.0422, R^2=0.0506; figure 12a); a gender difference also appeared when analysis was conducted separately: in females there was any significative difference (p=0.4044, R^2=0.1392), while in males a significant increase in mtDNA copy number with age was found (p=0.0318, R^2=0.3242; figures 12b and 12c).

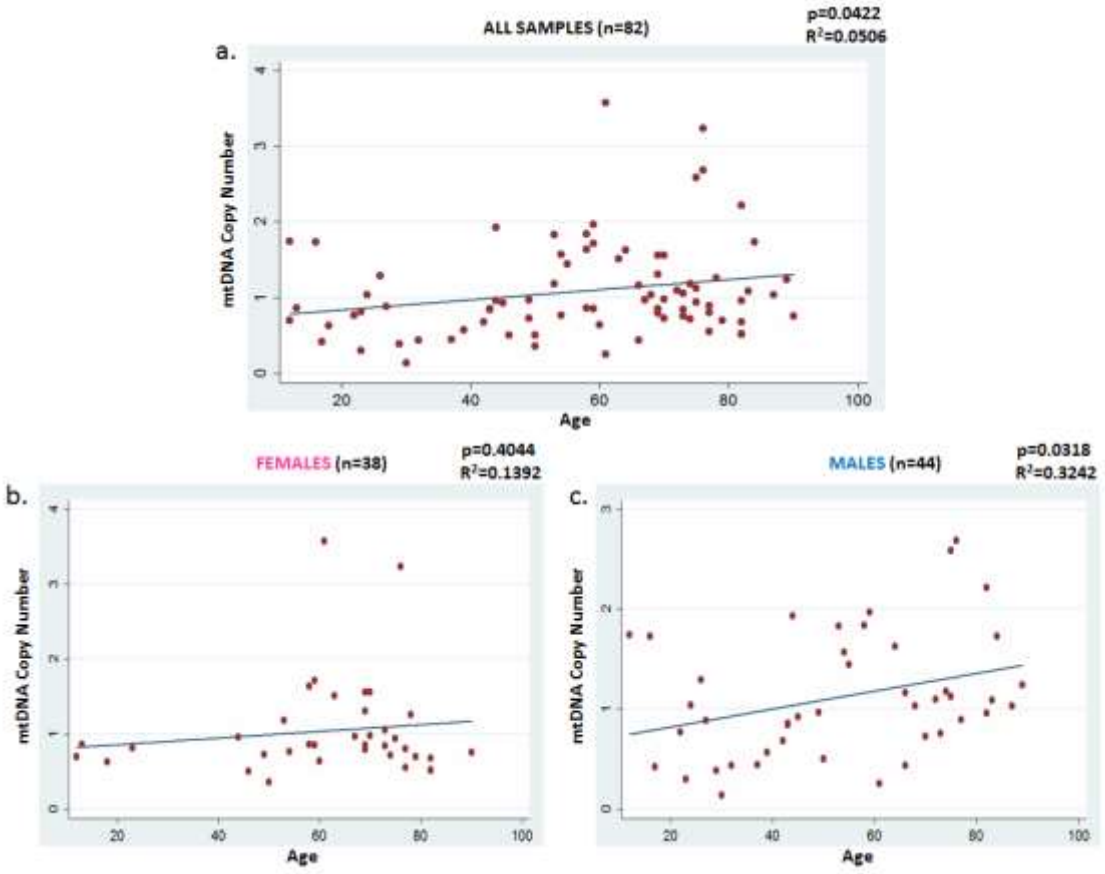

Figure 12: Regression analysis of mtDNA copy number as a function of age was performed in 82 DNA samples from liver biopsies. a.) In the total number of samples (N=82), mtDNA copy number significantly increases with age (p=0.0422; R^2=0.0506). b.) In females (N=38) mtDNA copy number does not change significantly with age (p=0.4044; R^2=0.1392). c.) In males (N=44) mtDNA copy number significantly increases with age (p=0.0318; R^2=0.3242).

4.1.2 mtDNA deletion level

mtDNA deletion level was analyzed with qPCR, quantifying the amount of the mitochondrial gene *nd1*, located in the mtDNA arch rarely deleted, compared with the mitochondrial gene *nd4*, located in the major arch of mtDNA frequently deleted.

As shown in fig. 13a, in the total of samples, mtDNA deletion level did not significantly change with age (p=0.3802, R^2=0.0096). Even when regression analysis was performed on female and male subjects separately (figures 13b and 13c), no gender difference emerged (p=0.1926 and R^2=0.0467, p=0.9477 and R^2=0.0001, respectively).

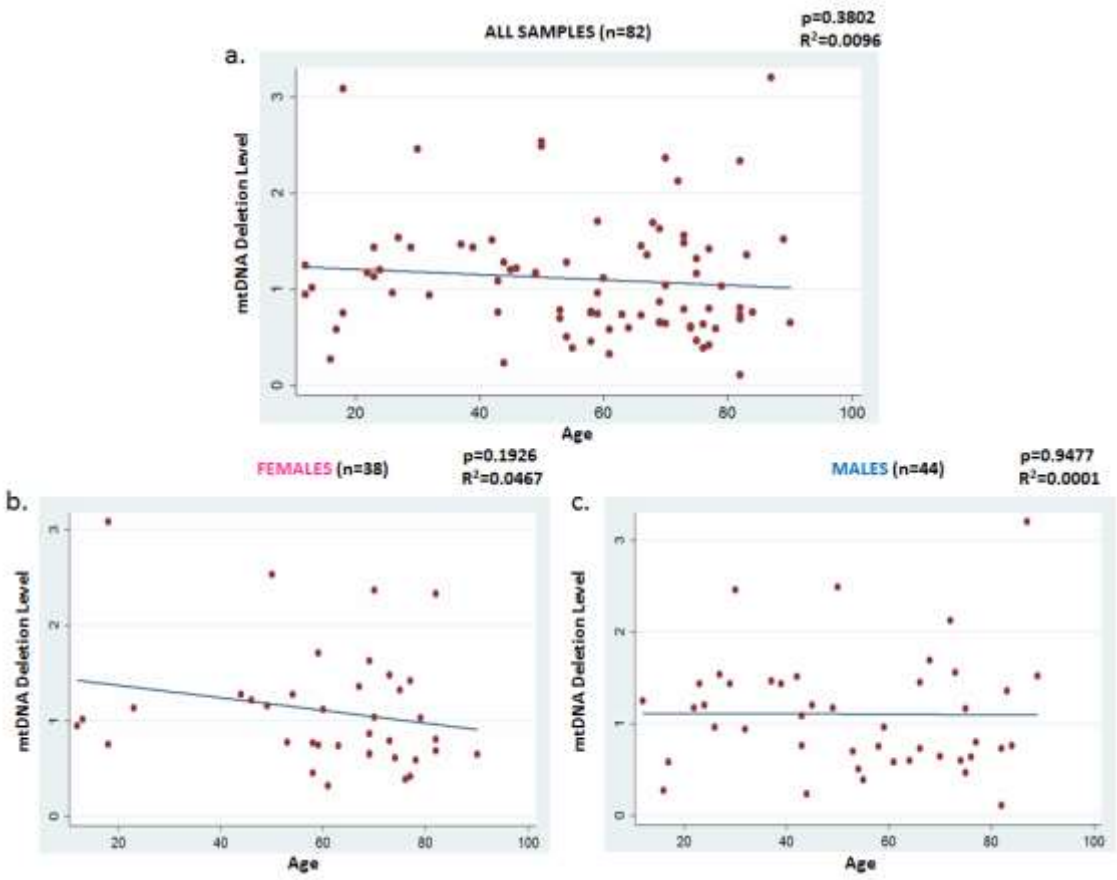

Figure 13: Regression analysis of mtDNA deletion level as a function of age was performed in 82 DNA samples from liver biopsies. a.) In the total number of samples (N=82), mtDNA deletion level does not change significantly with age (p=0.3802; R^2=0.0096). b.) In females (N=38) mtDNA deletion level does not change significantly with age (p=0.1926; R^2=0.0467). c.) In males (N=44) mtDNA deletion level does not change significantly with age (p=0.9477; R^2=0.0001).

4.1.3 mtDNA integrity

Deeper analyzing the relationship between mtDNA deletion level and copy number, a strong correlation was found between these two parameters (p=0.0000, R^2=0.1907), as shown in figure 14a. This strong correlation was maintained also when samples were analyzed by gender: both females and males displayed a significant decrease of mtDNA deletion level as copy number increase (female: p=0.0211,R^2=0.1391, fig. 14b; males: p=0.0006, R^2=0.2464, fig. 14c).

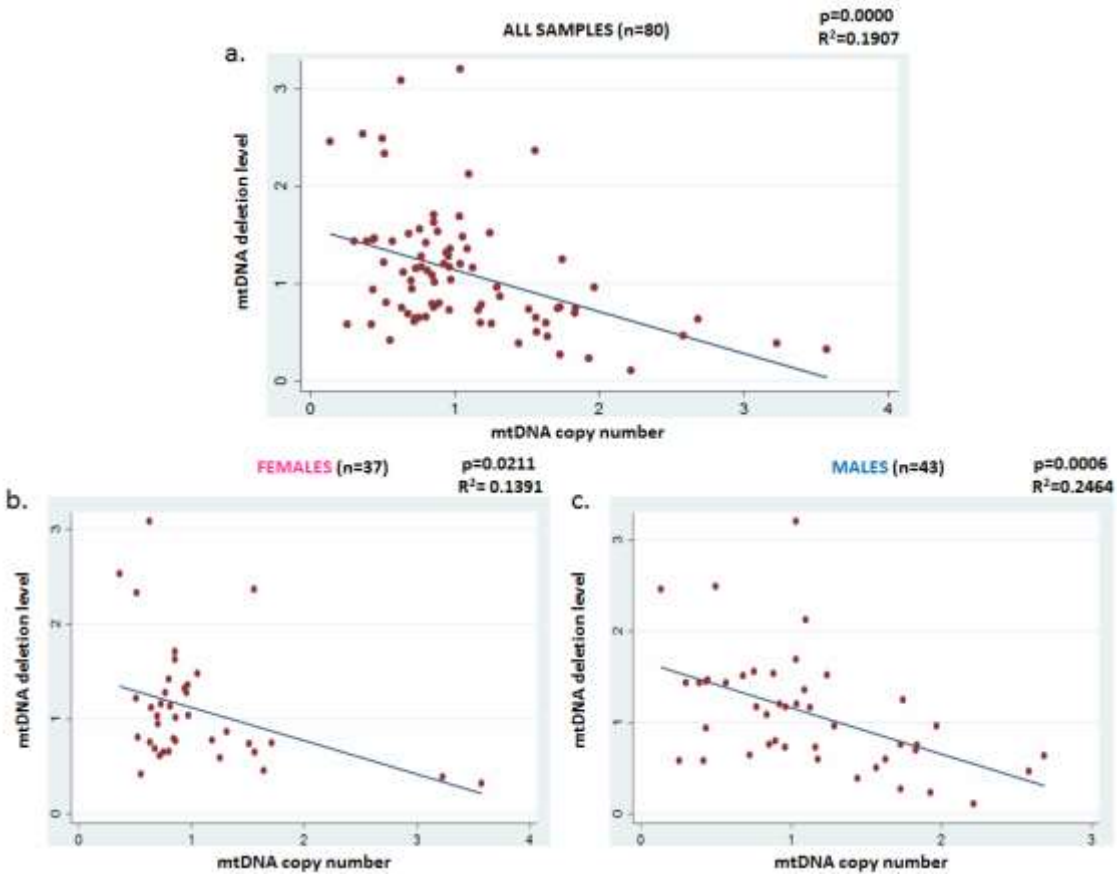

Figure 14: Regression analysis of mtDNA deletion level as a function of mtDNA copy number in 80 DNA samples from liver biopsies. a.) In the total number of samples (N=80), mtDNA deletion level significantly decreases with the increase of mtDNA copy number (p=0.0000; R^2=0.1907). b.) In females (N=37) mtDNA deletion level significantly decreases with the increase of mtDNA copy number (p=0.0211; R^2=0.1391). c.) In males (N=43) mtDNA deletion level significantly decreases with the increase of mtDNA copy number (p=0.0006; R^2=0.2464).

In all samples was then investigated the mtDNA integrity, intended as the number of intact molecules over the total number of mtDNA molecules per subject. This parameter was examined in relation with age, but only a barely significative decrease appeared in the total number of subjects (p=0.0477, R^2=0.0493, fig. 15a). This significative change, indeed, was completely lost when data were analyzed by gender: both females and males did not reveal any significant variation in mtDNA integrity with age (p=0.1972, R^2=0.0493 and p=0.1563, R^2=0.0484, respectively).

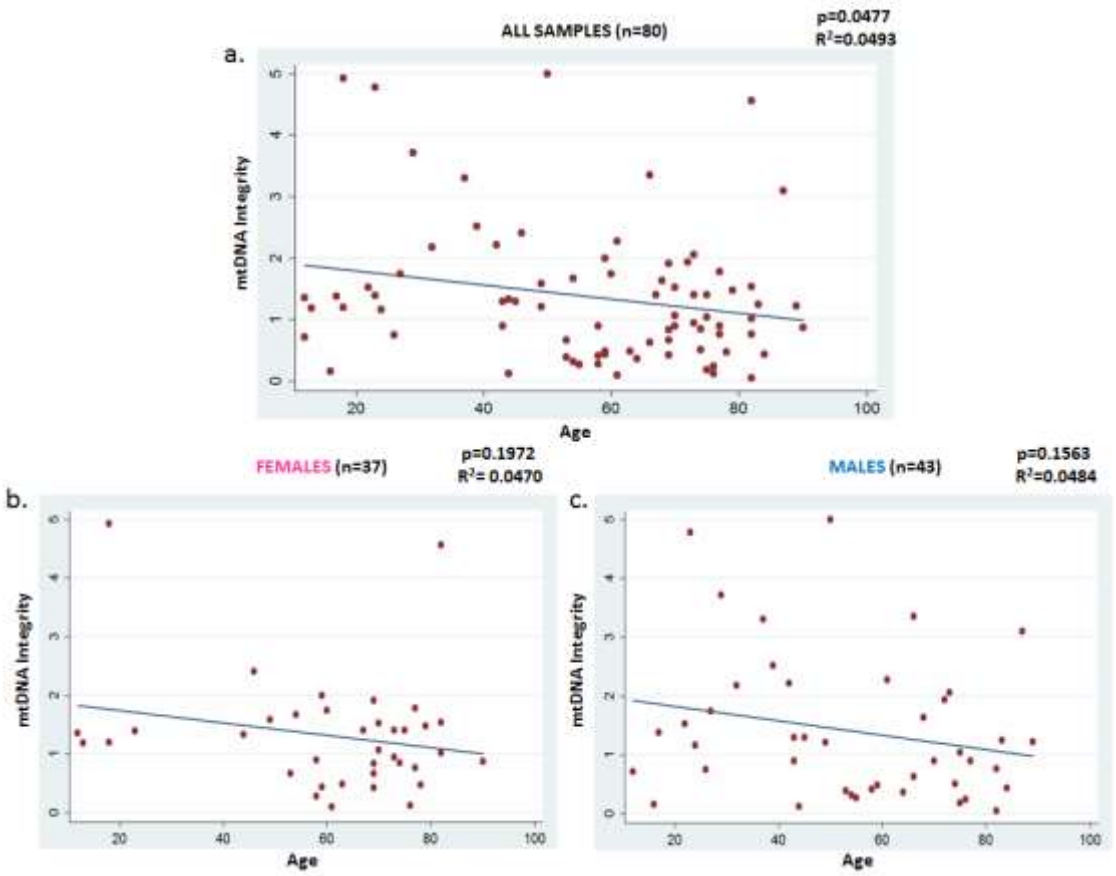

Figure 15: Regression analysis of mtDNA integrity as a function of age was performed in 80 DNA samples from liver biopsies. a.) In the total number of samples (N=80), mtDNA integrity significantly decreases with age (p=0.0477; R^2=0.0493). b.) In females (N=37) mtDNA integrity level does not change significantly with age (p=0.1972; R^2=0.0470). c.) In males (N=43) mtDNA integrity does not change significantly with age (p=0.1563; R^2=0.0484).

4.1.4 Telomere length

Telomere length was examined since telomeres shortening is a well-recognized marker of aging.

As expected, telomere length significantly decreased during human liver aging (p=0.0000, R^2=0.2415), also when genders were considered separately (females: p=0.0022, R^2=0.2648 and males: p=0.0015, R^2=0.2742), as shown in figure 16.

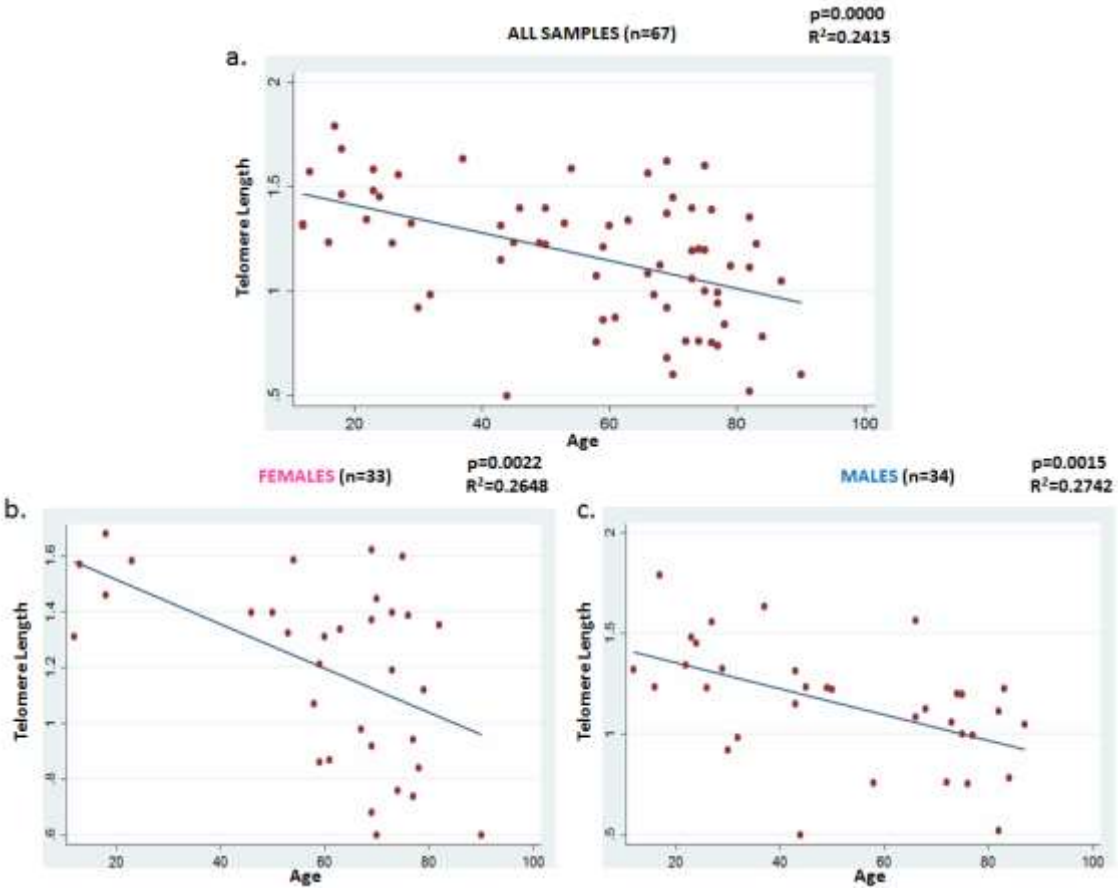

Figure 16: Regression analysis of telomere length as a function of age was performed in 67 DNA samples from liver biopsies. a.) In the total number of samples (N=67), telomere length significantly decreases with age (p=0.0000; R^2=0.2415). b.) In females (N=33) telomere length significantly decreases with age (p=0.0022; R^2=0.2648). c.) In males (N=34) telomere length significantly decreases with age (p=0.0015; R^2=0.2742).

As in 2011 Sahin and colleagues reported an interaction between telomeres shortening and mitobiogenesis (Sahin et al., 2011), the possible relationship between telomere length and mtDNA deletion level, copy number and integrity were studied.

The regression analysis of telomere length and mtDNA copy number revealed a significant relationship in the total number of subjects (fig. 17a; p=0.0030, R^2=0.1277): as copy number increases, telomeres become shorter. When analysis was performed by gender, this relationship was conserved in males (fig. 17b; p=0.0002, R^2=0.3597), but not in females (fig. 17c; p=0.4082, R^2=0.0222).

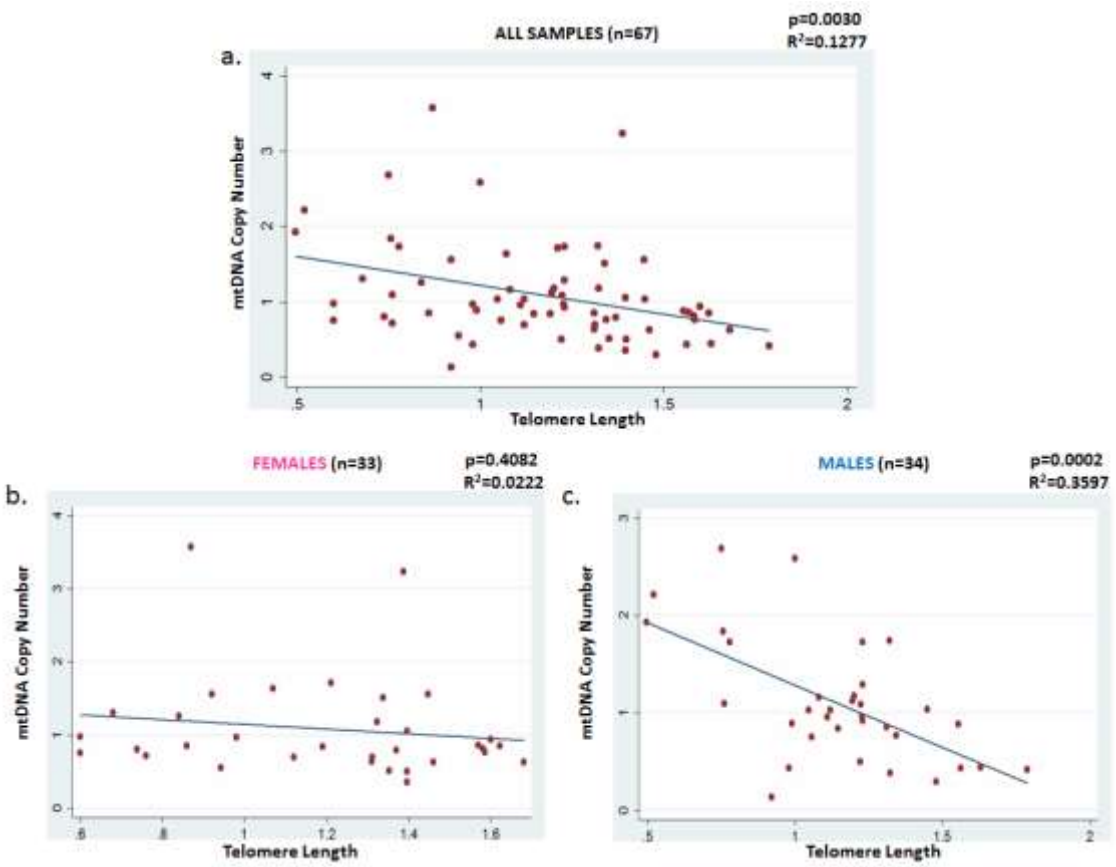

Figure 17: Regression analysis of mtDNA copy number as a function of telomere length was performed in 67 DNA samples from liver biopsies. a.) In the total number of samples (N=67), mtDNA copy number significantly decreases with telomere length (p=0.0030; R^2=0.1277). b.) In females (N=33) mtDNA copy number does not change significantly with telomere length (p=0.4082; R^2=0.0222). c.) In males (N=34) mtDNA DNA copy number significantly decreases with telomere length (p=0.0002; R^2=0.3597).

Looking at mtDNA deletion level, the regression analysis showed a significant direct association between the two parameters (figure 18): as telomere length increases, mtDNA deletion level increases as well all the samples (p=0.0305, R^2=0.0700). Considering gender separately, either females and males lost the significative relationship (p=0.0506, R^2=0.1177 and p=0.2825, R^2=0.0360, respectively), as figures 18b and 18c show.

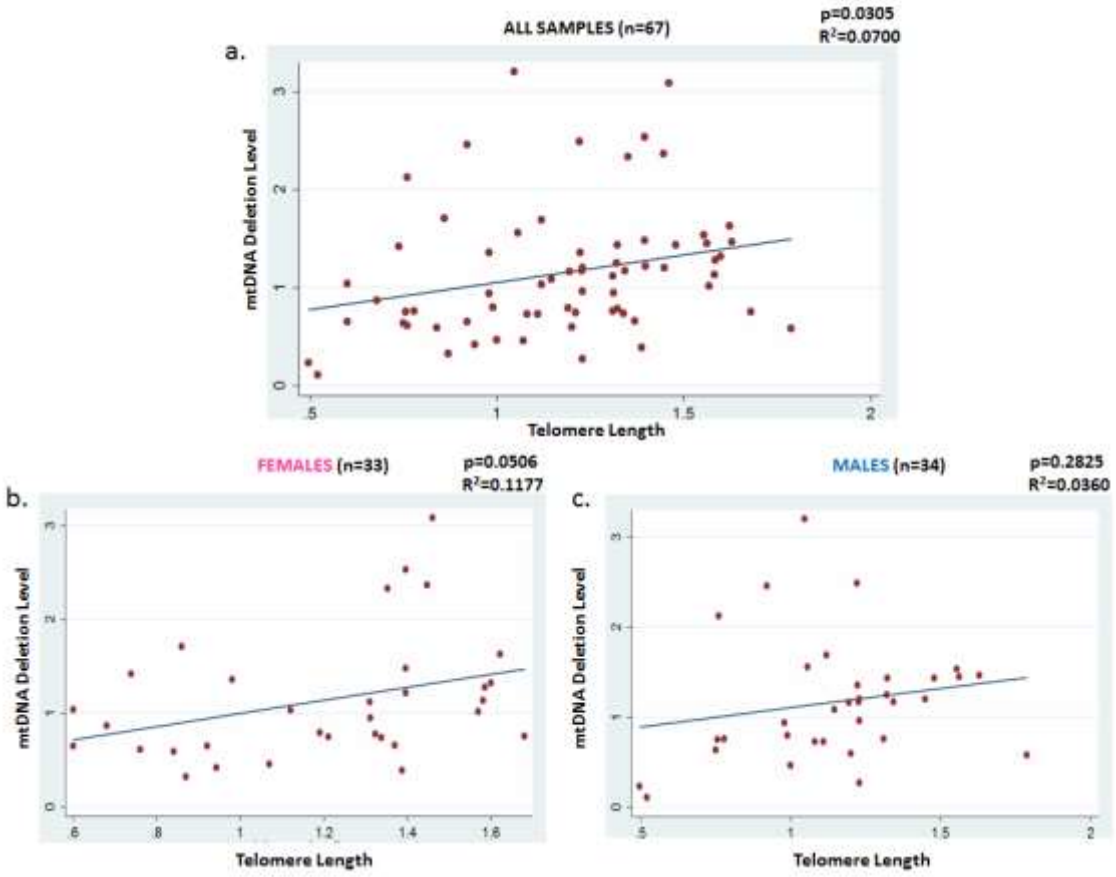

Figure 18: Regression analysis of mtDNA deletion level as a function of telomere length was performed in 67 DNA samples from liver biopsies. a.) In the total number of samples (N=67), mtDNA deletion level significantly increases with telomere length (p=0.0305; R^2=0.1277). b.) In females (N=33) mtDNA deletion level does not change significantly with telomere length (p=0.0506; R^2=0.1177). c.) In males (N=34) mtDNA DNA deletion level does not change significantly with telomere length (p=0.2825; R^2=0.0360).

Finally also the possible connection among telomere length and mtDNA integrity was taken into account. In all samples and in particular in males, but not in females, there was a strong direct connection (p=0.0018, R^2=0.1444; p=0.0069, R^2=0.2128; p=0.0856, R^2=0.0953, respectively): as telomere length increases, mtDNA integrity also increases (fig. 19).

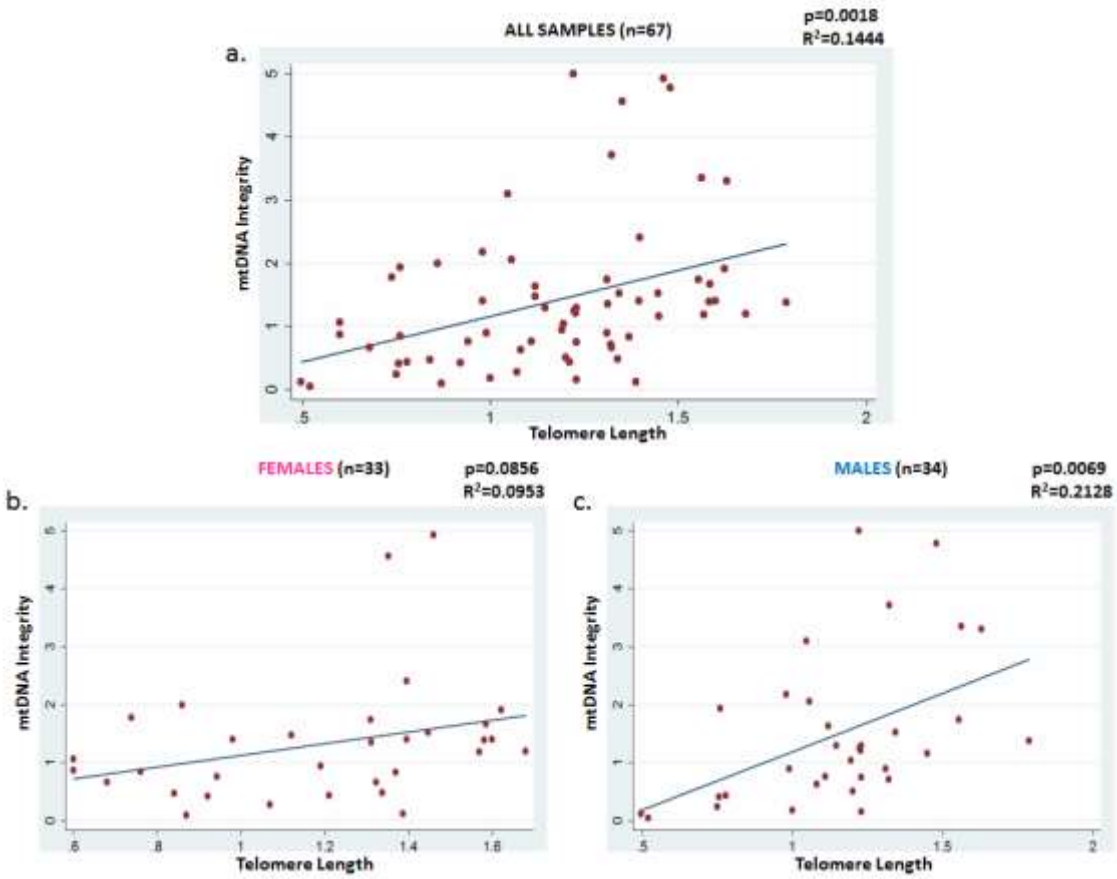

Figure 19: Regression analysis of mtDNA integrity as a function of telomere length was performed in 67 DNA samples from liver biopsies. a.) In the total number of samples (N=67), mtDNA integrity significantly increases with telomere length (p=0.0018; R^2=0.1444). b.) In females (N=33) mtDNA integrity does not change significantly with telomere length (p=0.0856; R^2=0.0953). c.) In males (N=34) mtDNA integrity significantly increases with telomere length (p=0.0069; R^2=0.2128).

4.1.5 Gene expression analysis

To further characterise the involvement of mtDNA rearrangements during the aging of human liver, the relative expression of some key genes involved in several mitochondrial pathways was evaluated in a subgroup of liver biopsies.

The relative expression of each gene, determined by qPCR assays, was considered as function of age and to evaluate a possible gender difference, all analyses were conducted first in the total number of samples and then on females and males separately.

From the regression analysis, shown in figure 20, emerged that among genes involved in mitochondrial biogenesis (*pgc-1α*, *polγ*, *nrf1*, *tfam*, *twinkle*, *sirt1*, *sirt3*, *tomm40*, *ppard*), only *nrf1* showed significative changes in its expression level, either when samples were considered all together (p=0.0013, R^2=0.3555) or when gender was taken into account (p=0.0387, R^2=0.2711 and p=0.0107, R^2=0.5776, for females and males, respectively).

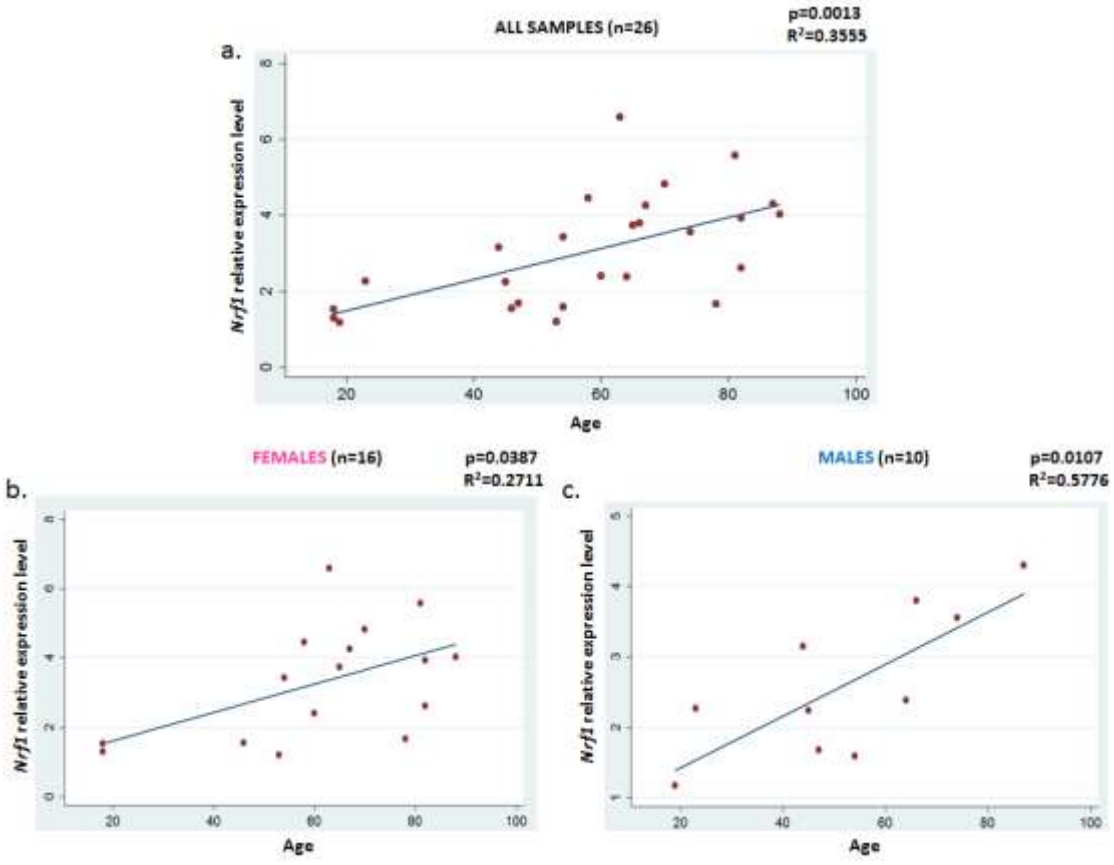

Figure 20: Regression analysis of expression level of *nrf1* as a function of age was performed in 26 cDNA samples from liver biopsies. a.) In the total number of samples (N=26), expression level of *nrf1* significantly increases with age (p=0.0013; R^2=0.3555). b.) In females (N=16) expression level of *nrf1* significantly increases with age (p=0.0387; R^2=0.2711). c.) In males (N=10) expression level of *nrf1* significantly increases with age (p=0.0107; R^2=0.5776).

Regarding mitochondrial dynamics (*mfn2*, *fis1* and *opa1*), there were significant changes in relative expression levels. In particular, for *mfn2* there was a significant increase in the total number of subjects (p=0.0104, R^2=0.2349), that was completely lost both in females (p=0.0508, R^2=0.2458) and males (p=0.1883, R^2=0.1838) considered separately, as shown in figure 21.

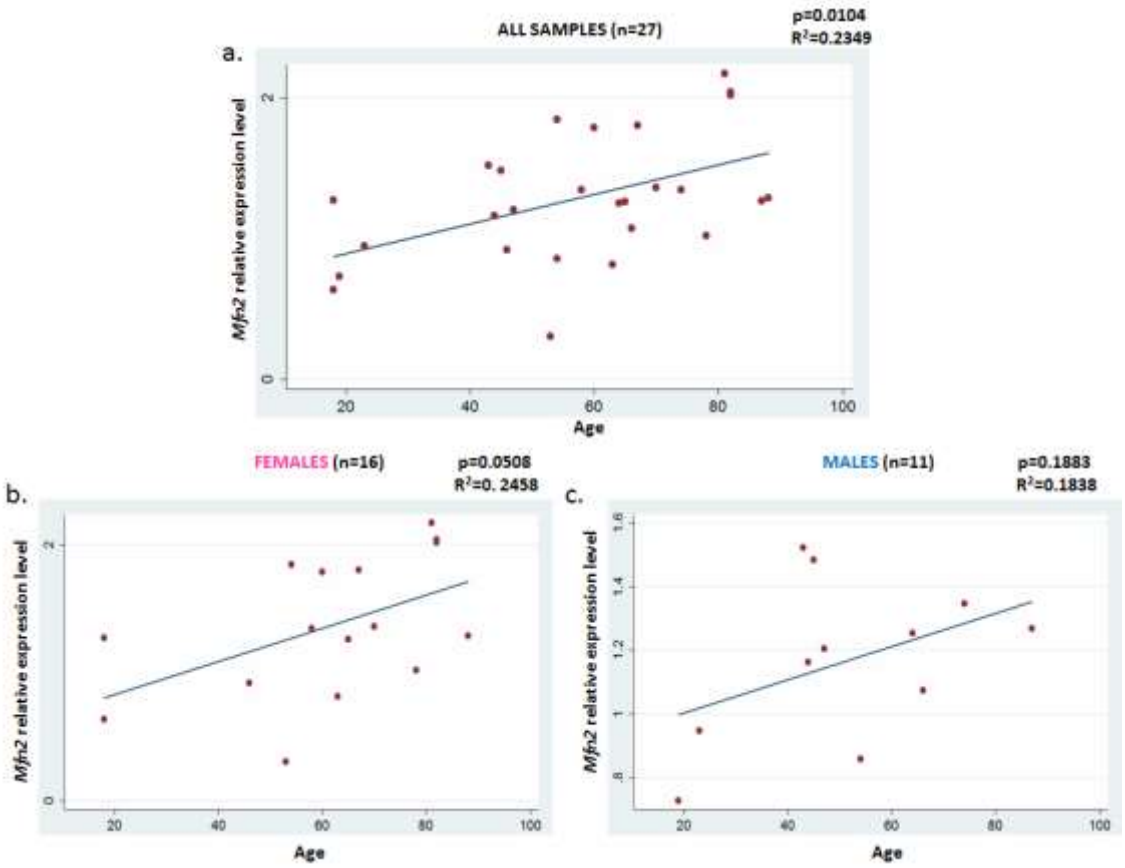

Figure 21: Regression analysis of expression level of *mnf2* as a function of age was performed in 27 cDNA samples from liver biopsies. a.) In the total number of samples (N=27), expression level of *mnf2* significantly increases with age (p=0.0104; R^2=0.2349). b.) In females (N=16) does not change with age (p=0.0508; R^2=0.2458). c.) In males (N=10) expression level of *mnf2* does not change with age (p=0.1883; R^2=0.1838).

The same result came from *fis1* expression level. Indeed the expression level of *fis1* significantly increased with age in the total number of samples (p=0.0088, R^2=0.2440; figure 22a), but a gender difference appeared when data were analyzed by gender. The regression analysis in females revealed a significant increase in the expression level of *fis1* (p=0.0132, R^2=0.3649; figure 22b), while no significative difference emerged in males (p=0.2836, R^2=0.1262; figure 22c).

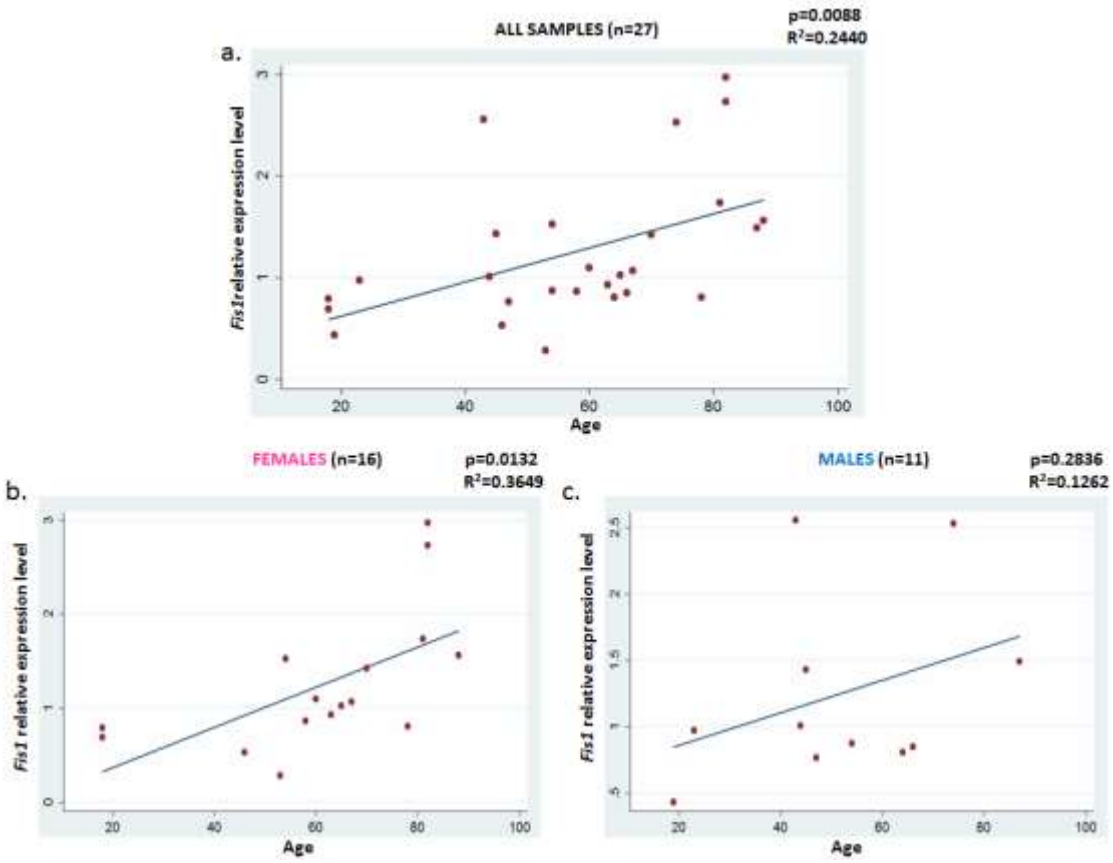

Figure 22: Regression analysis of expression level of *fis1* as a function of age was performed in 27 cDNA samples from liver biopsies. a.) In the total number of samples (N=27), expression level of *fis1* significantly increases with age (p=0.0088; R^2=0.2440). b.) In females (N=16) expression level of *fis1* significantly increases with age (p=0.0132; R^2=0.3649). c.) In males (N=10) expression level of *fis1* does not change with age (p=0.2836; R^2=0.1262).

Finally, in the case of nuclear proteins that are involved in mitochondrial proteins quality control system, a significant increase in *lonp* expression level was found in the total number of subjects (p=0.0009, R^2=0.3638). This increment was also maintained when analysis was conducted by gender, as figure 23 displays (p=0.0272, R^2=0.3027 and p=0.0139, R^2=0.5075, females and males respectively).

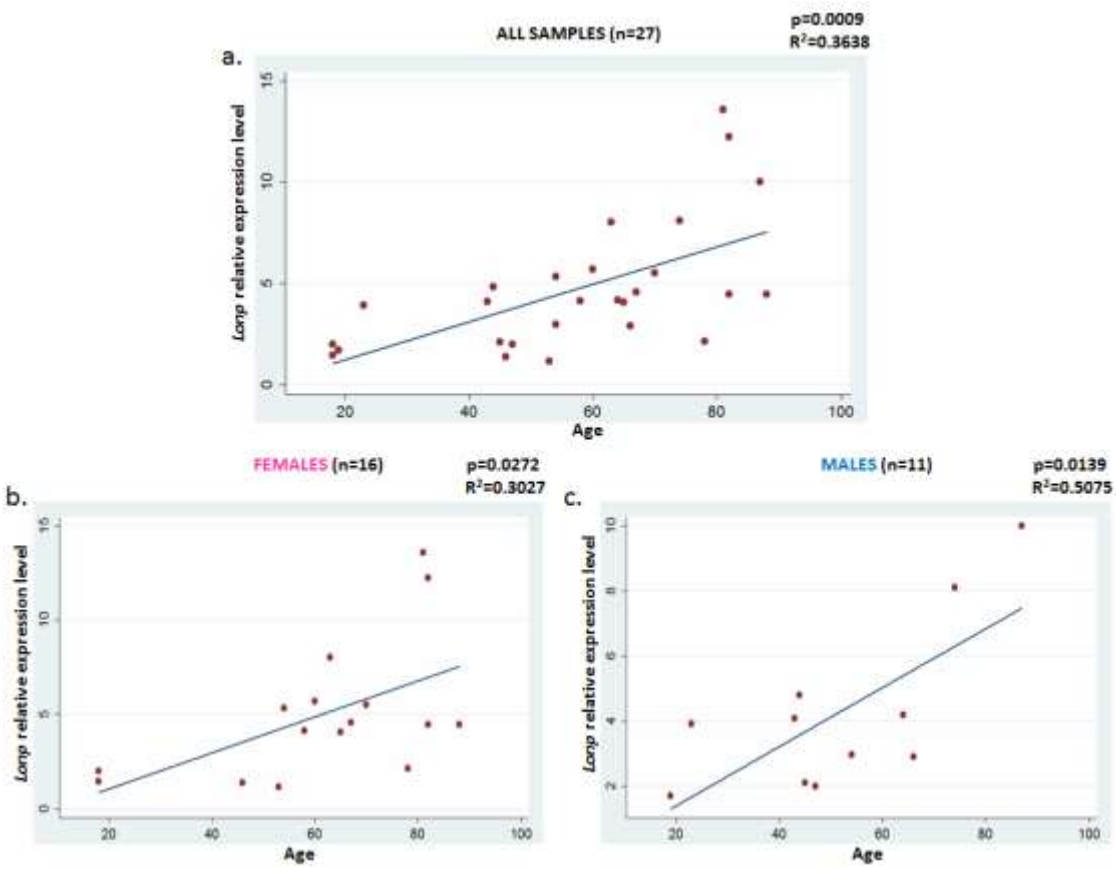

Figure 23: Regression analysis of expression level of *lonp* as a function of age was performed in 27 cDNA samples from liver biopsies. a.) In the total number of samples (N=27), expression level of *lonp* significantly increases with age (p=0.0009; R^2=0.3638). b.) In females (N=16) expression level of *lonp* significantly increases with age (p=0.0272; R^2=0.3027). c.) In males (N=10) expression level of *fis1* expression level of *lonp* significantly increases with age (p=0.0139; R^2=0.5075).

No significant changes with age emerged when analysing the relative gene expression of mitophagy (*ambra1*, *beclin*, *pink1*, *parkin*, *atg16l* and *pik3cd*), production of ROS (*nos3*), protection from ROS (*sod1* and *sod2*) and hypoxia (*hif-1*α), neither in the total number of patients, nor in females, nor in males (data not shown).

4.2 Human Skeletal Muscle

To study the role of mtDNA rearrangements in the aging of human skeletal muscle, mtDNA copy number, mtDNA deletion level, mtDNA integrity, telomere length and gene expression levels were evaluated using DNA and RNA isolated from *Vastus lateralis* muscle biopsies of two groups of subjects: healthy young (<40 years) and old (>65 years) subjects and patients with lower limbs mobility impairment (LMLL) underwent hip replacement surgery aged from 24 to 96 years. These variables were analyzed in relation to age in each group of subjects and then in females and males separately to evaluate possible gender differences.

4.2.1 Healthy subjects

4.2.1.1 mtDNA copy number

mtDNA copy number was measured in healthy subjects' *Vastus lateralis* muscle biopsies. Figure 24 shows that there was a barely significative decrease in mtDNA copy number in healthy elderly subjects with respect to young ones (p=0.0448, X^2=2.007). However, this difference in mtDNA copy number was not maintained when analysis was conducted by gender (p=0.1136, X^2=1.582 and p=0.3139, X^2=1.007, for females and males respectively).

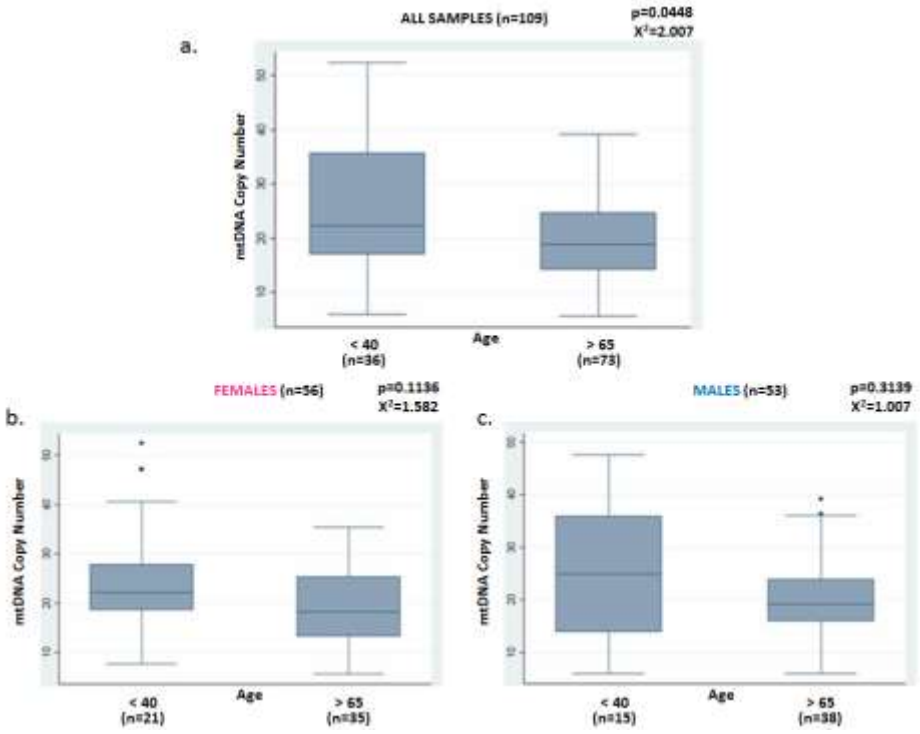

Figure 24: Analysis of mtDNA copy number in relation to age. To compare young (<40 years) and old (>65 years) subjects, Mann-Whitney test was applied. a.) In the total number of subjects (N=109) mtDNA relative copy number is barely significantly higher (p=0.0488; X^2=2.007) in young subjects (N=36) than in old subjects (N=73). b.) In healthy females (N=56), any significant change is mtDNA relative copy number (p=0.1136; X^2=1.582) between young (N=21) and old (N=32) subjects was observed. c.) In healthy males (N=53), mtDNA content does not significantly vary (p=0.3139; X^2=1.007) between young (N=15) and old (N=38) subjects.

4.2.1.2 mtDNA deletion level

No significative changes were found in mtDNA deletion level in total number of subjects (p=0.1758, X^2=-1.252) and in males (p=0.5508, X^2=0.597), while in females, a marginally significative increase in deletion level was found (p=0.0414, X^2=-1.920, fig. 25b).

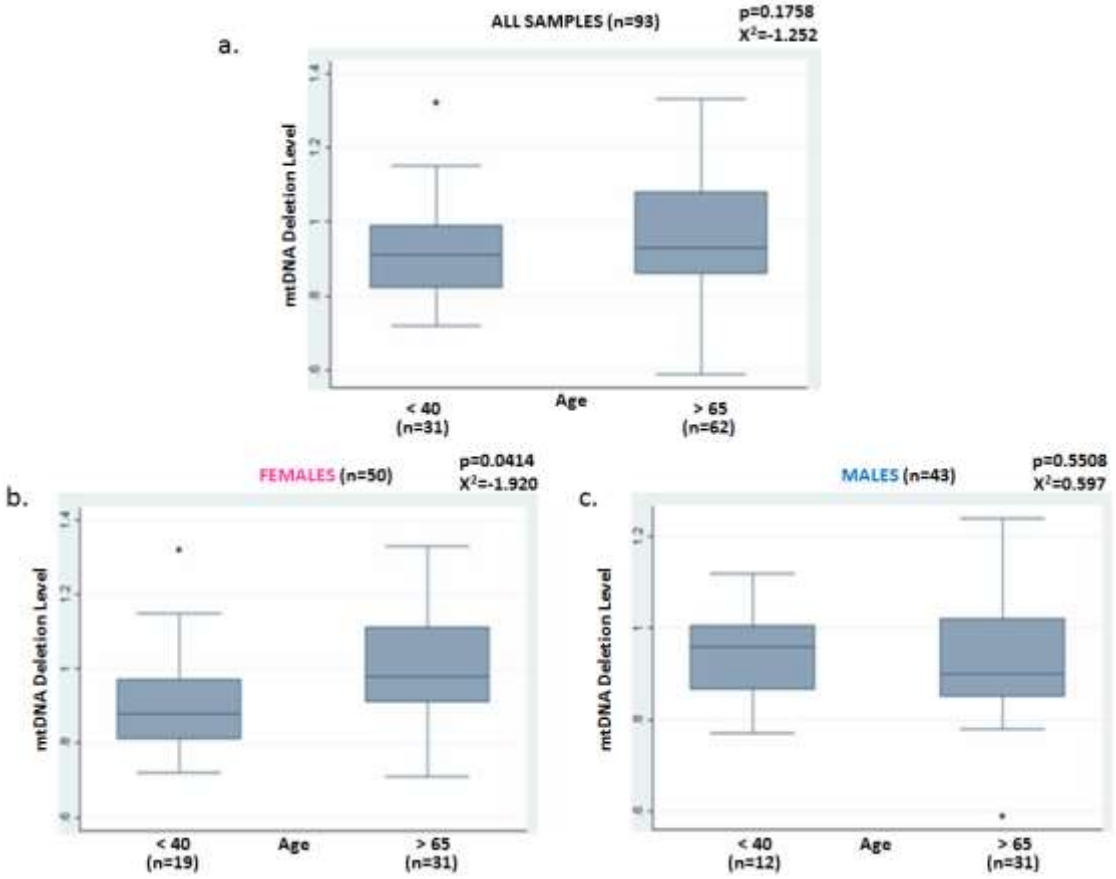

Figure 25: Analysis of mtDNA deletion level in relation to age. To compare young (<40 years) and old (>65 years) subjects, Mann-Whitney test was applied. a.) In the total number of subjects (N=93) mtDNA deletion level is not significantly different (p=0.1758; X^2=-1.252) between young (N=31) and old subjects (N=63). b.) In healthy females (N=50), mtDNA deletion level is significantly lower (p=0.0414; X^2=-1.920) in young (N=19) with respect to old (N=31) subjects. c.) In healthy males (N=43), mtDNA deletion level does not significantly vary (p=0.5508; X^2=0.597) between young (N=12) and old (N=31) subjects.

4.2.1.3 mtDNA integrity

mtDNA integrity was found higher in healthy young than in elderly subjects (p=0.0012, X^2=3.046). Also when samples were sorted by gender, mtDNA integrity was found still statistically different among young and elderly subjects, both in females (p=0.0265, X^2=2.210) and males (p=0.0285, X^2=2.120). Data are shown in figure 26.

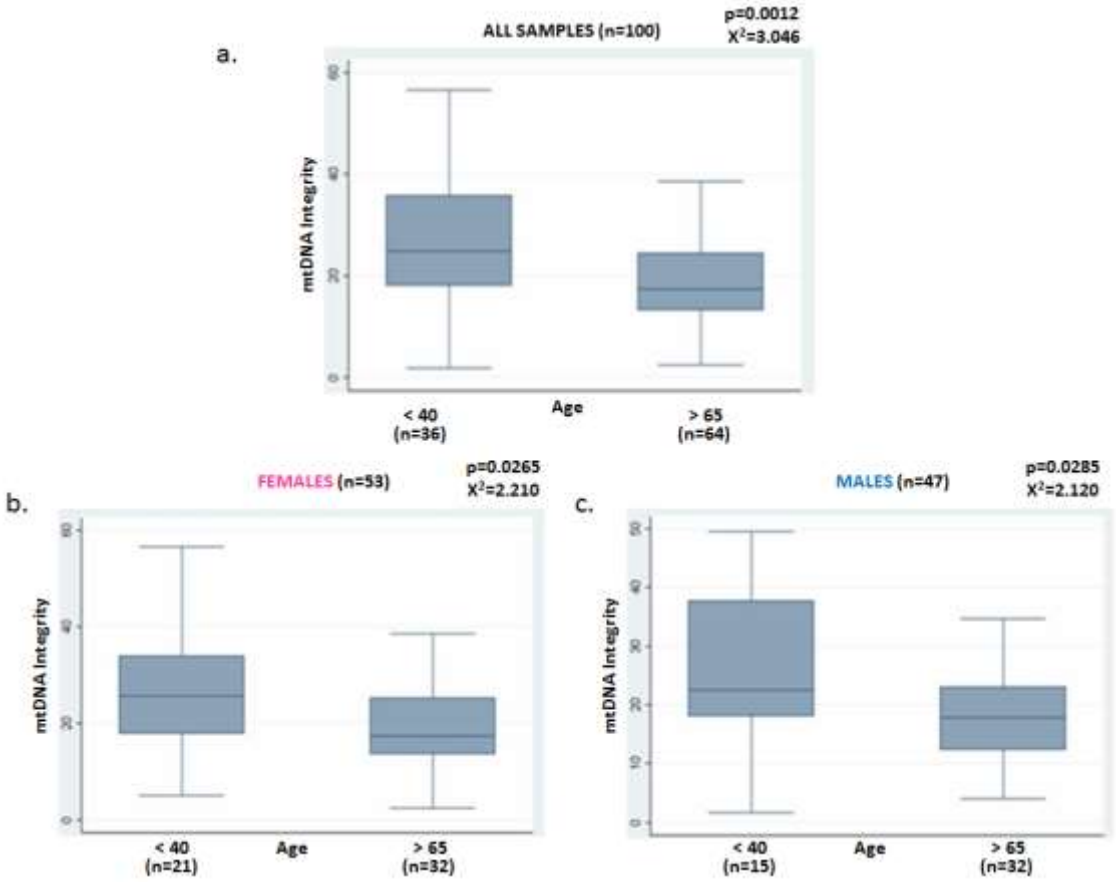

Figure 26: Analysis of mtDNA integrity in relation to age. To compare young (<40 years) and old (>65 years) subjects, Mann-Whitney test was applied. a.) In the total number of subjects (N=100) mtDNA integrity is significantly lower (p=0.0012; X^2=3.046) in young (N=36) with respect to old subjects (N=64). b.) In healthy females (N=53), mtDNA integrity is significantly lower (p=0.0265; X^2=2.210) in young (N=21) with respect to old (N=32) subjects. c.) In healthy males (N=47), mtDNA integrity is significantly lower (p=0.0285; X^2=2.120) in young (N=15) with respect to old (N=32) subjects.

4.2.1.4 Telomere length

Any significative differences emerged in telomere length between young and old healthy subjects, both in all samples (p=0.8570, X^2=0.17; fig. 27a) and by gender (p=0.8078, X^2=0.01 and p=0.5034, X^2=0.25, for females and males respectively; fig.27b and 27c).

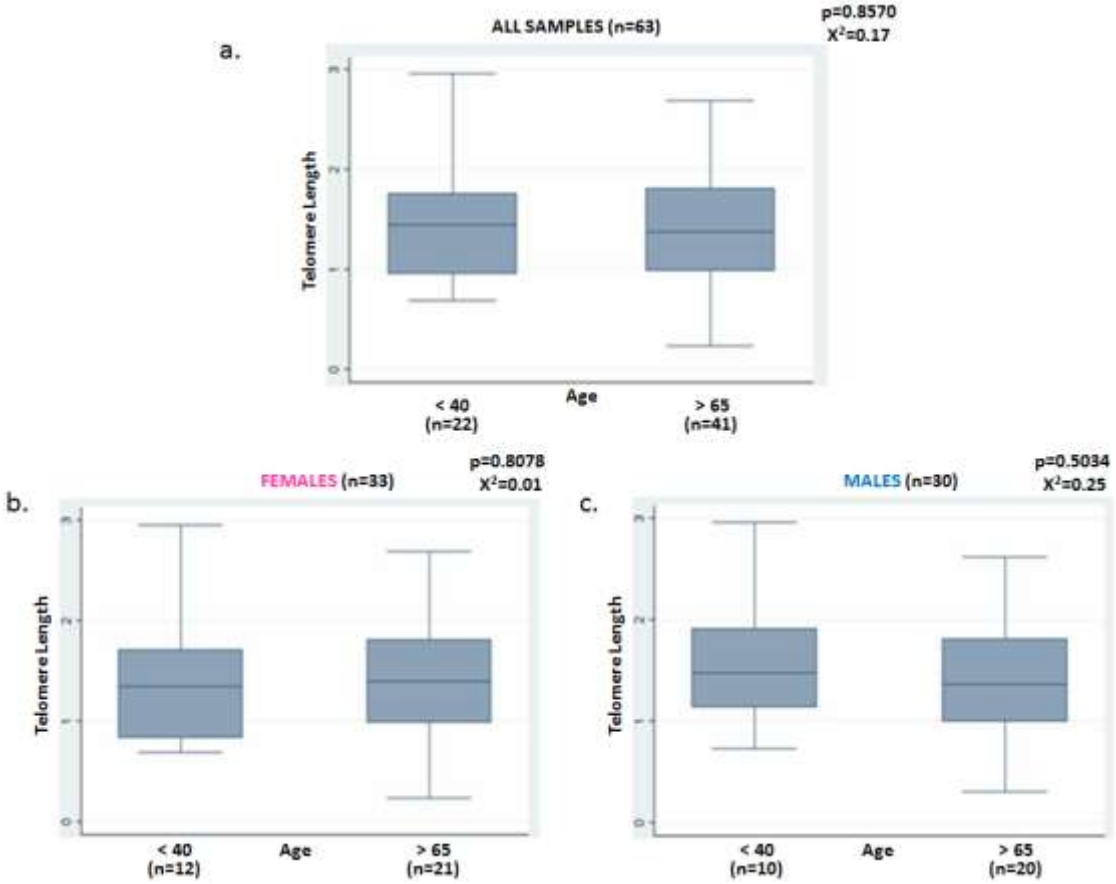

Figure 27: Analysis of telomere length in relation to age. To compare young (<40 years) and old (>65 years) subjects, Mann-Whitney test was applied. a.) In the total number of subjects (N=63) telomere length is not significantly different (p=0.8570; X^2=0.17) between young (N=22) and old subjects (N=41). B.) In healthy females (N=33) telomere length is not significantly different (p=0.8078; X^2=0.01) between young (N=12) and old subjects (N=21). c.) Also in healthy males (N=30), telomere length does not differ (p=0.5034; X^2=0.25) between young (N=10) and old (N=20) subjects.

Moreover, also studying possible relations between telomere shortening and mtDNA dysfunction, no significative association with telomere length emerged, neither for mtDNA copy number, nor for mtDNA deletion level and mtDNA integrity (data not shown).

4.2.1.5 Gene expression analysis

A subgroup of healthy subjects biopsies was chosen to analyse the gene expression level of the same genes analyzed in liver samples (*pgc-1α*, *polγ*, *nrf1*, *tfam*, *twinkle*, *sirt1*, *sirt3*, *tomm40*, *ppard*, *mfn2*, *fis1*, *opa1*, *ambra1*, *beclin*, *pink1*, *parkin*, *atg16l*, *pik3cd*, *nos3*, *sod1*, *sod2*, *lonp*, *hif-1*α). Each gene was compared between young (<40 years) and old (>65 years) healthy subjects. To evaluate a possible gender difference, all the analyses were then separately performed on females and males.

Regarding genes involved in mitobiogenesis (*pgc-1α*, *polγ*, *nrf1*, *tfam*, *twinkle*, *sirt1*, *sirt3*, *tomm40*, *ppard*), only the expression level of *pgc1α*, *polγ* and *tfam* were statistically different between young and old healthy subjects. In particular, the expression of *pgc1α* decreased in old healthy subjects (p=0.0002, X^2=14.173) compared to young healthy and, also analysing females and males separately, this difference between was maintained (p=0.0038, X^2=8.730 and p=0.0172, X^2=5.674, respectively; fig. 28).

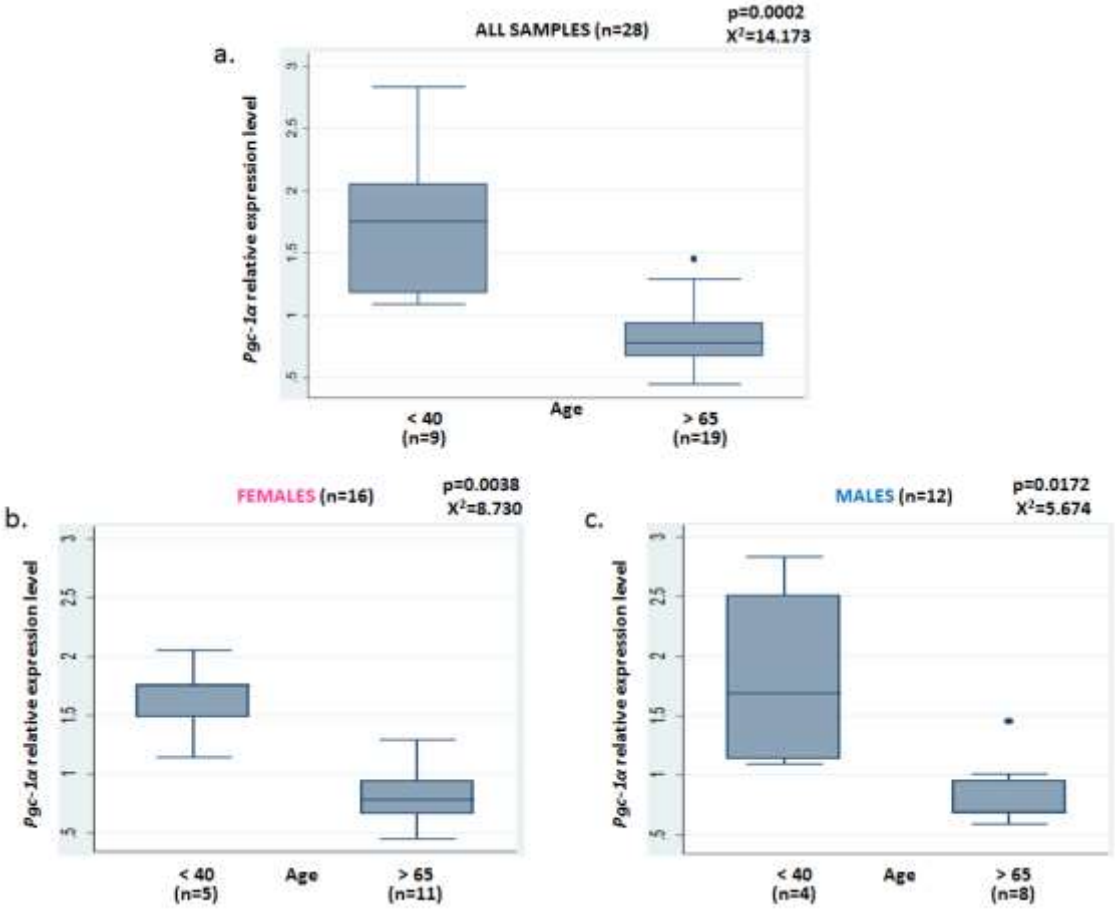

Figure 28: Analysis of expression level of *pgc-1α* in relation to age. To compare young (<40 years) and old (>65 years) subjects, Kruskal-Wallis test was applied. a.) In the total number of subjects (N=28) expression level of *pgc-1α* is significantly higher (p=0.0002; X^2=14.173) in young (N=9) with respect to old subjects (N=19). b.) In healthy females (N=16) expression level of *pgc-1α* is significantly higher (p=0.0038; X^2=8.730) in young (N=5) than in old subjects (N=11). c.) Also in healthy males (N=12), expression level of *pgc-1α* is significantly higher (p=0.0172; X^2=5.674) in young (N=4) than in old (N=5) subjects.

As can be seen in figure 29, *poly* expression level showed a significative decrease in elderly subjects compared to young when analysis was performed on all subjects (p=0.0067, X^2=9.03), however this difference was weakly maintained only in males (p=0.0485, X^2=5.69), when genders were considered singly.

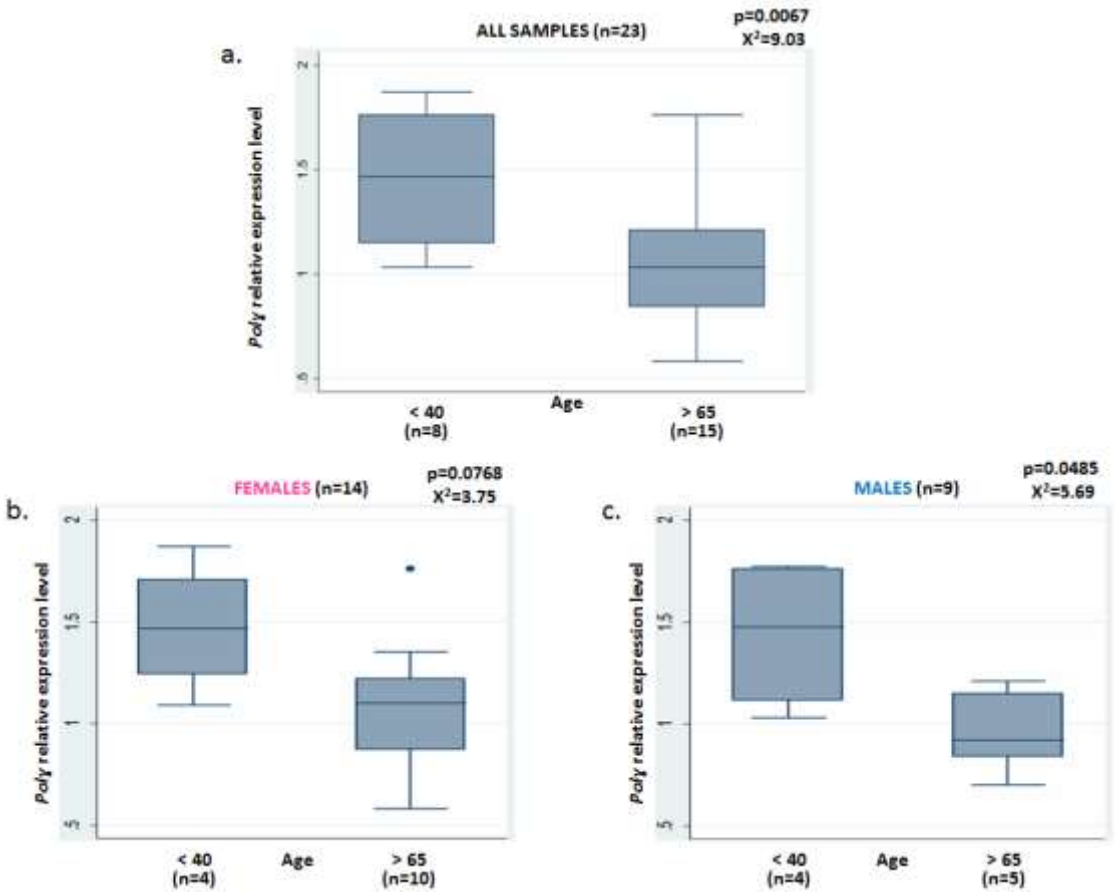

Figure 29: Analysis of expression level of *poly* in relation to age. To compare young (<40 years) and old (>65 years) subjects, Kruskal-Wallis test was applied. a.) In the total number of subjects (N=23) expression level of *poly* is significantly higher (p=0.0067; X^2=9.03) in young (N=8) with respect to old subjects (N=15). b.) In healthy females (N=12) expression level of *poly* does not change (p=0.0768; X^2=3.75) between young (N=4) and old subjects (N=10). c.) In healthy males (N=9), expression level of *poly* is significantly higher (p=0.0485; X^2=5.69) in young (N=4) than in old (N=5) subjects.

Tfam expression level displayed a statistically significant decrease in elderly subjects with respect to young individuals (p=0.0095, X^2=7.89) that was maintained in females (p=0.0155, X^2=7.94), but not in males (p=0.1650, X^2=2.21), as shown in fig. 30.

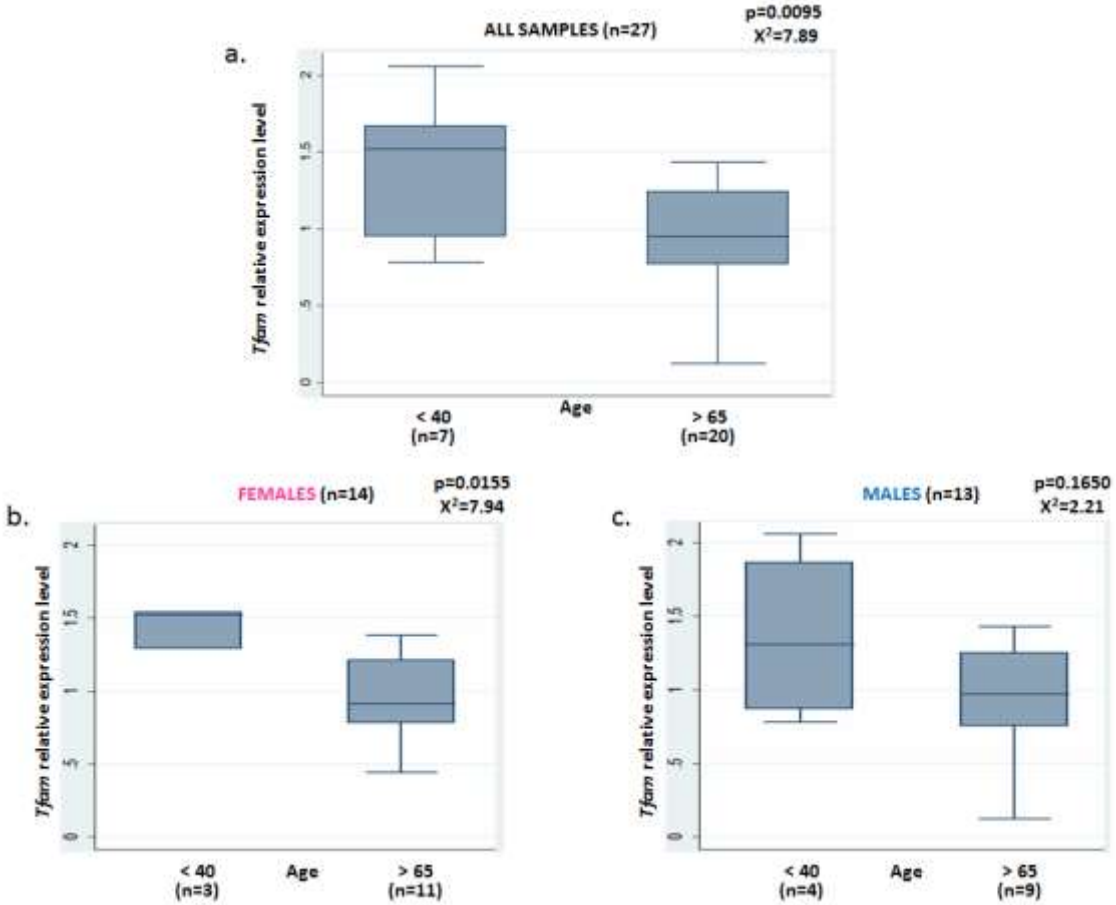

Figure 30: Analysis of expression level of *tfam* in relation to age. To compare young (<40 years) and old (>65 years) subjects, Kruskal-Wallis test was applied. a.) In the total number of subjects (N=27) expression level of *tfam* is significantly higher (p=0.0095; X^2=7.89) in young (N=7) with respect to old subjects (N=20). b.) In healthy females (N=14) expression level of *tfam* is significantly higher (p=0.0155; X^2=7.94) in young (N=3) than in old subjects (N=11). c.) In healthy males (N=13), expression level of *tfam* does not change (p=0.1650; X^2=2.21) in young (N=4) than in old (N=9) subjects.

Also some genes involved in mitophagy were found to be expressed at different level in healthy young and elderly subjects. These gene are *beclin*, *opa1* and *pik3cd*. The expression level of *beclin* was higher in young than in elderly (p=0.0065, X^2=8.82), but when looking at gender, the decrease with age in its expression level was significant only in females (p=0.0039, X^2=12.69) but not in males (p=0.3208, X^2=1.08; data shown in fig. 31).

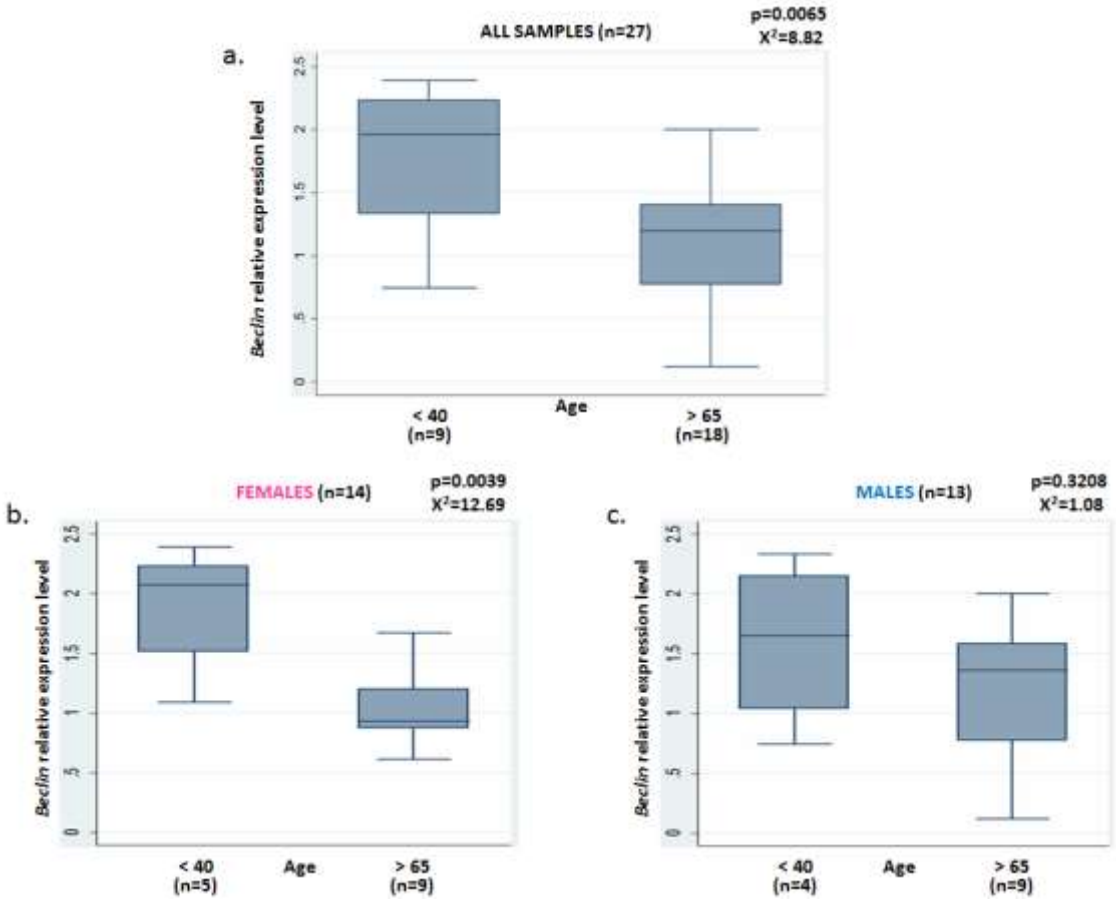

Figure 31: Analysis of expression level of *beclin* in relation to age. To compare young (<40 years) and old (>65 years) subjects, Kruskal-Wallis test was applied. a.) In the total number of subjects (N=27) expression level of *beclin* is significantly higher (p=0.0065; X^2=8.82) in young (N=9) with respect to old subjects (N=18). b.) In healthy females (N=14) expression level of *beclin* is significantly higher (p=0.0039; X^2=12.69) in young (N=5) than in old subjects (N=9). c.) In healthy males (N=13), expression level of *beclin* does not change (p=0.3208; X^2=1.08) in young (N=4) than in old (N=9) subjects.

Also for *opa1* and *pik3cd* the expression level was higher in healthy young subjects than in elderly (p=0.0236, X^2=2.264 and p=0.00164, X^2=2.389, respectively), nevertheless dissimilarly from *beclin*, this difference in the expression level was maintained its statistical significant in males but not in females (*opa1*: p=0.0308, X^2=2.160 and p=0.3952, X^2=0.850; *pik3cd*: p=0.0247, X^2=2.245, p=0.3603, X^2=0.915, respectively). Data relative to *opa1* and *pik3cd* are shown in figures 32 and 33 respectively.

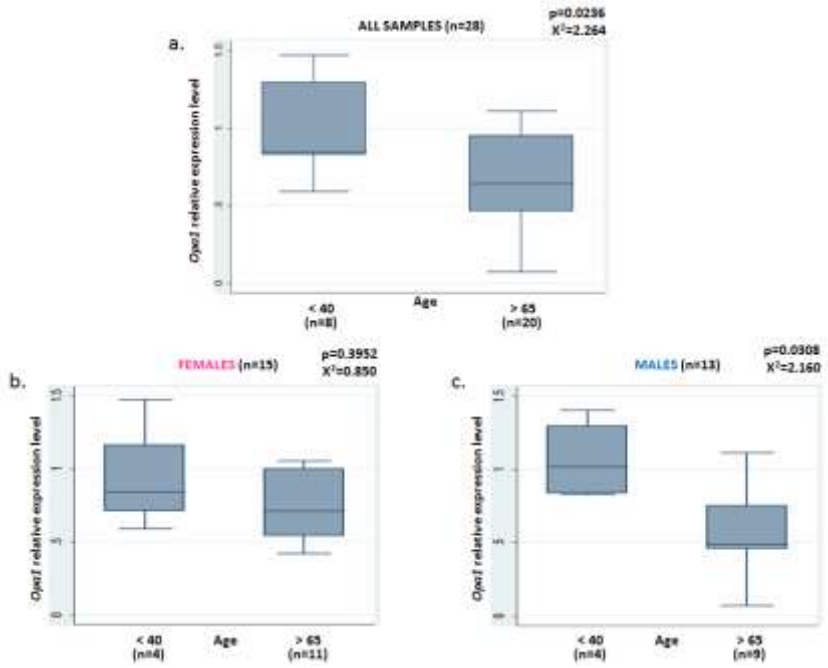

Figure 32: Analysis of expression level of *opa1* in relation to age. To compare young (<40 years) and old (>65 years) subjects, Kruskal-Wallis test was applied. a.) In the total number of subjects (N=28) expression level of *opa1* is significantly higher (p=0.0236; X^2=2.264) in young (N=8) with respect to old subjects (N=20). b.) In healthy females (N=15) expression level of *opa1* does not change (p=0.3952; X^2=0.850) between young (N=4) and old subjects (N=11). c.) In healthy males (N=13), expression level of *opa1* is significantly higher (p=0.0308; X^2=2.160) in young (N=4) with respect to old subjects (N=9).

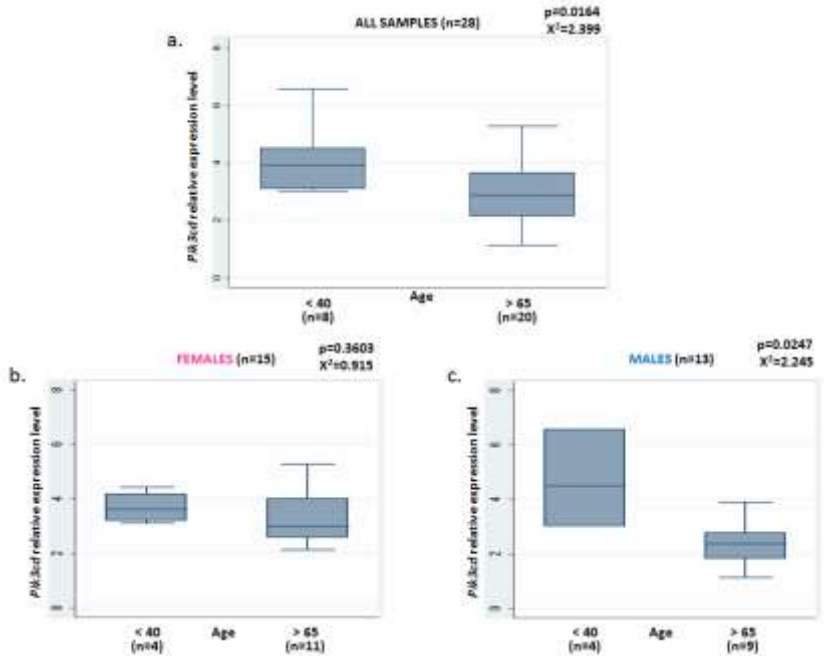

Figure 33: Analysis of expression level of *pik3cd* in relation to age. To compare young (<40 years) and old (>65 years) subjects, Kruskal-Wallis test was applied. a.) In the total number of subjects (N=28) expression level of *pik3cd* is significantly higher (p=0.0164; X^2=2.399) in young (N=8) with respect to old subjects (N=20). b.) In healthy females (N=15) expression level of *pik3cd* does not change (p=0.3603; X^2=0.915) between young (N=4) and old subjects (N=11). c.) In healthy males (N=13), expression level of *pik3cd* is significantly higher (p=0.0247; X^2=2.245) in young (N=4) with respect to old subjects (N=9).

Finally, as displayed in figure 34, the expression level of *nos3* was found significantly high in healthy young males compared to old males (p=0.0308, X^2=4.667), while no significative difference emerged in the total number of healthy subjects and in females (p=0.1710, X^2=1.874 and p=0.4243, X^2=0.638, respectively).

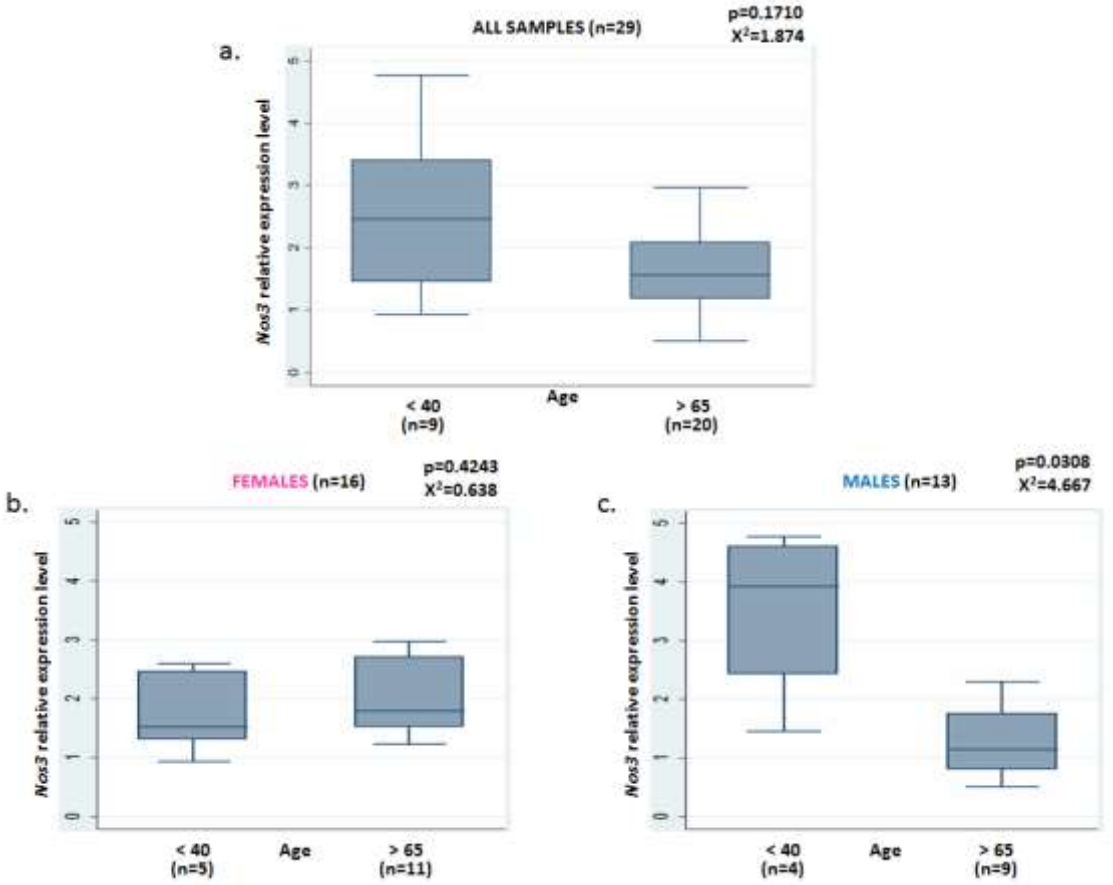

Figure 34: Analysis of expression level of *nos3* in relation to age. To compare young (<40 years) and old (>65 years) subjects, Kruskal-Wallis test was applied. a.) In the total number of subjects (N=29) expression level of *nos3* does not change (p=0.1710; X^2=1.874) between young (N=9) and old subjects (N=20). b.) In healthy females (N=16) expression level of *nos3* does not change (p=0.4243; X^2=0.638) between young (N=5) and old subjects (N=11). c.) Only in healthy males (N=13), expression level of *nos3* is significantly higher (p=0.0308; X^2=4.667) in young (N=4) with respect to old subjects (N=9).

Instead, any significant changes between the two age groups emerged in the expression level of genes involved in mitochondrial biogenesis (*nrf1*, *tomm40*, *sirt1*, *twinkle*, *sirt3*, *ppard*), mitochondrial dynamics (*mfn2*, *fis1*), mitophagy (*ambra1*, *pink1*, *parkin*, *atg16l*), protein quality control system (*lonp*), protection from ROS (*sod1* and *sod2*) and hypoxia (*hif-1*α), neither in the total number of subjects, nor in females and in males (data not shown).

4.2.2 LLMI patients

4.2.2.1 mtDNA copy number

As can be observed in figure 35, regression analysis of mtDNA copy number in *vastus lateralis* biopsies of LLMI in function of age showed a significative decrease in total number of subjects (p=0.0055, R^2=0.1497) and in males (p=0.0357, R^2=0.1588), but not in females (p=0.2071, R^2=0.0783).

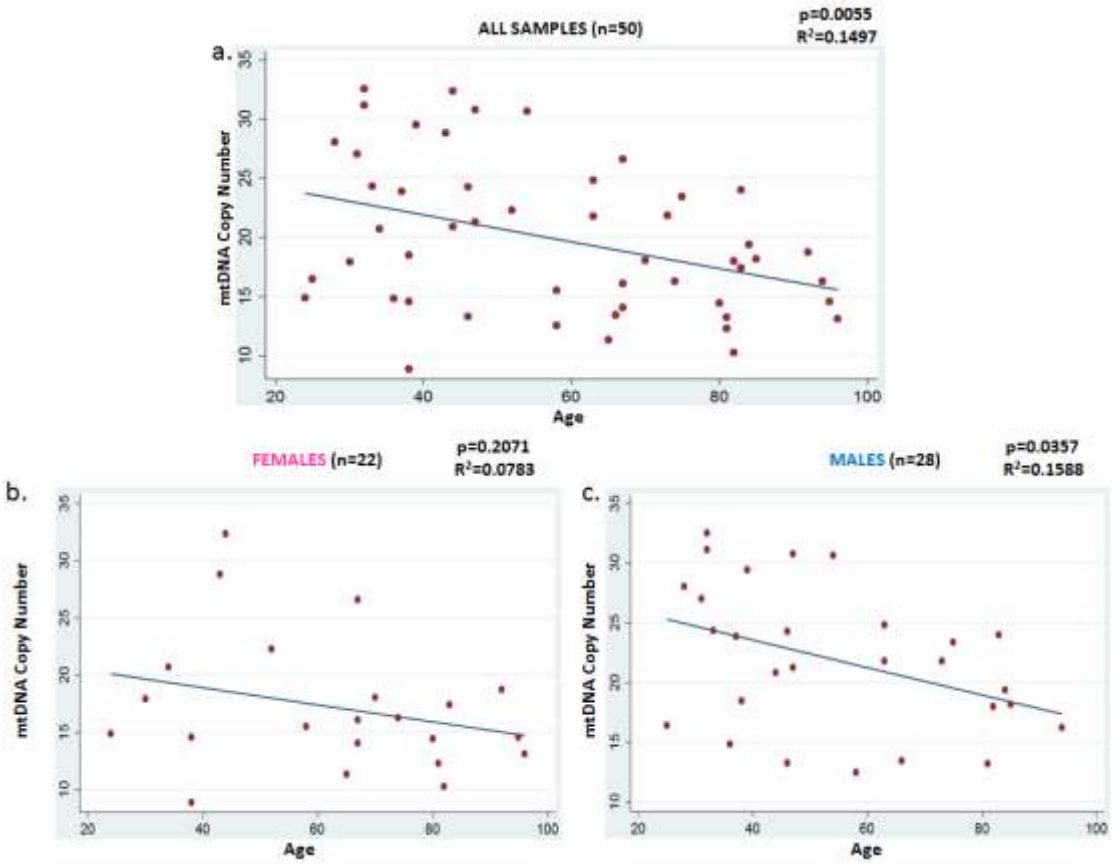

Figure 35: Regression analysis of mtDNA copy number as a function of age was performed in 50 DNA samples from muscle biopsies of LLMI patients. a.) In the total number of samples (N=50), mtDNA copy number significantly decreases with age (p=0.0055; R^2=0.1497). b.) In females (N=22) mtDNA copy number does not change with age (p=0.2072; R^2=0.0783). c.) In males (N=28) mtDNA copy number significantly decreases with age (p=0.0357; R^2=0.1588).

4.2.2.2 mtDNA deletion level

Figure 36 shows as a significative increment in mtDNA deletion level with age in patients males samples (p=0.0022, R^2=0.3086), while no significative difference were revealed either in total number of patients (p=0.5669, R^2=0.0070) and in females (p=0.2073, R^2=0.0823).

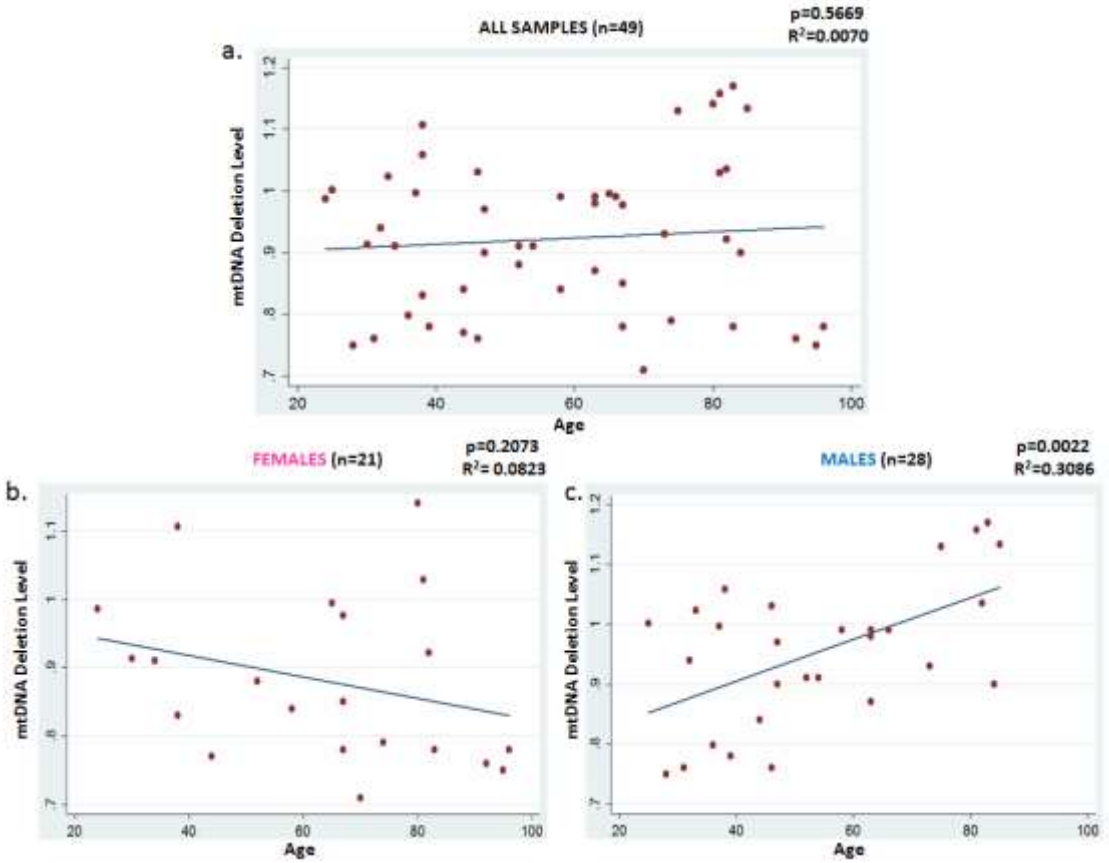

Figure 36: Regression analysis of mtDNA deletion level as a function of age. a.) In the total number of patients (N=49), mtDNA deletion level does not significantly change with age (p=0.5669; R^2=0.0070). b.) In females (N=21) mtDNA deletion level does not significantly change with age (p=0.2073; R^2=0.0823). c.) In males (N=28) mtDNA deletion level significantly increases with age (p=0.0022; R^2=0.3086).

4.2.2.3 mtDNA integrity

With age, in LLMI patients, there was a significative decrement in mtDNA integrity in all samples (p=0.0271, R^2=0.1039) and in males (p=0.0195, R^2=0.2072), but not in females (p=0.7088, R^2=0.0075), as shown in figure 37.

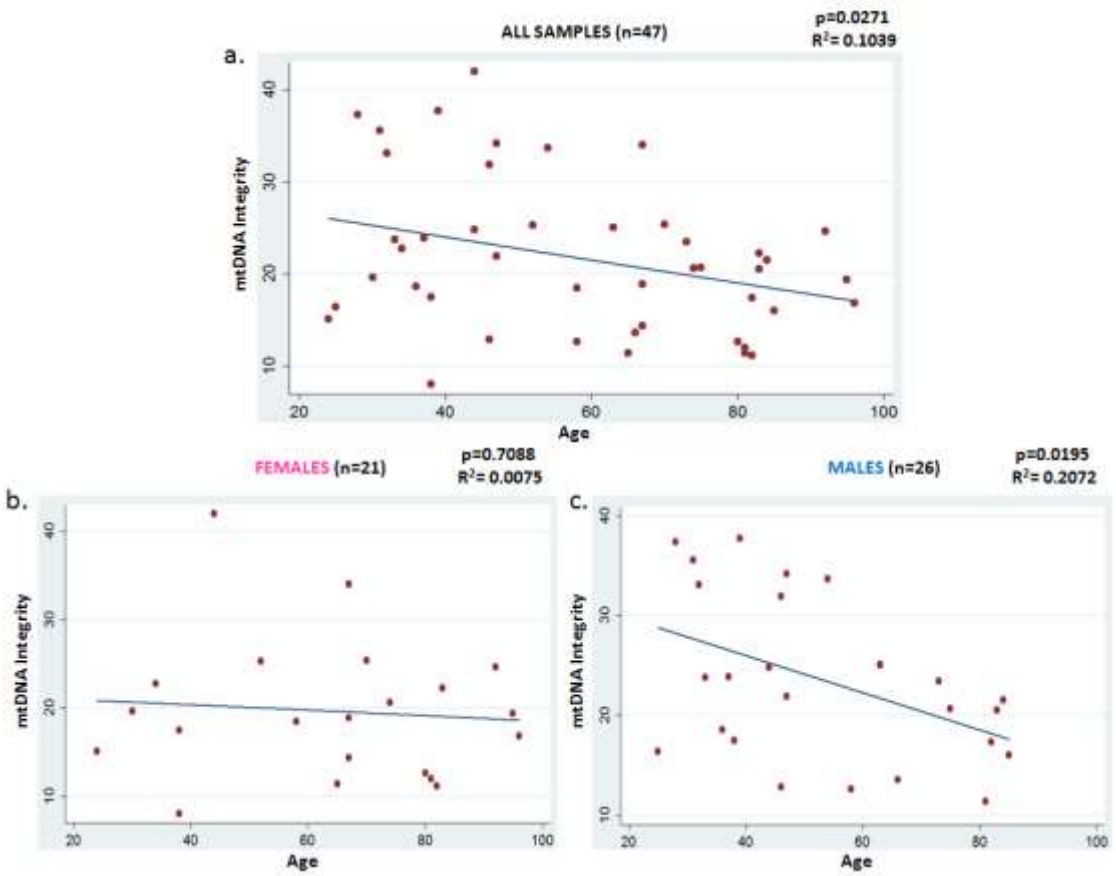

Figure 37: Regression analysis of mtDNA integrity as a function of age. a.) In the total number of patients (N=47), mtDNA integrity significantly decreases with age (p=0.0271; R^2=0.1039). b.) In females (N=21) mtDNA integrity does not significantly change with age (p=0.7088; R^2=0.0075). c.) In males (N=26) mtDNA integrity significantly increases with age (p=0.0195; R^2=0.2072).

4.2.2.4 Telomere length

Regression analysis of telomere length in function of age in DNA samples from LLMI patients biopsies did not underlie any statistical significant change, neither in total number of samples ($p=0.1528$, $R^2=0.0439$) nor in patients divided by gender ($p=0.8639$, $R^2=0.0017$ and $p=0.0649$, $R^2=0.1250$, for females and males, respectively) as figure 38 shows.

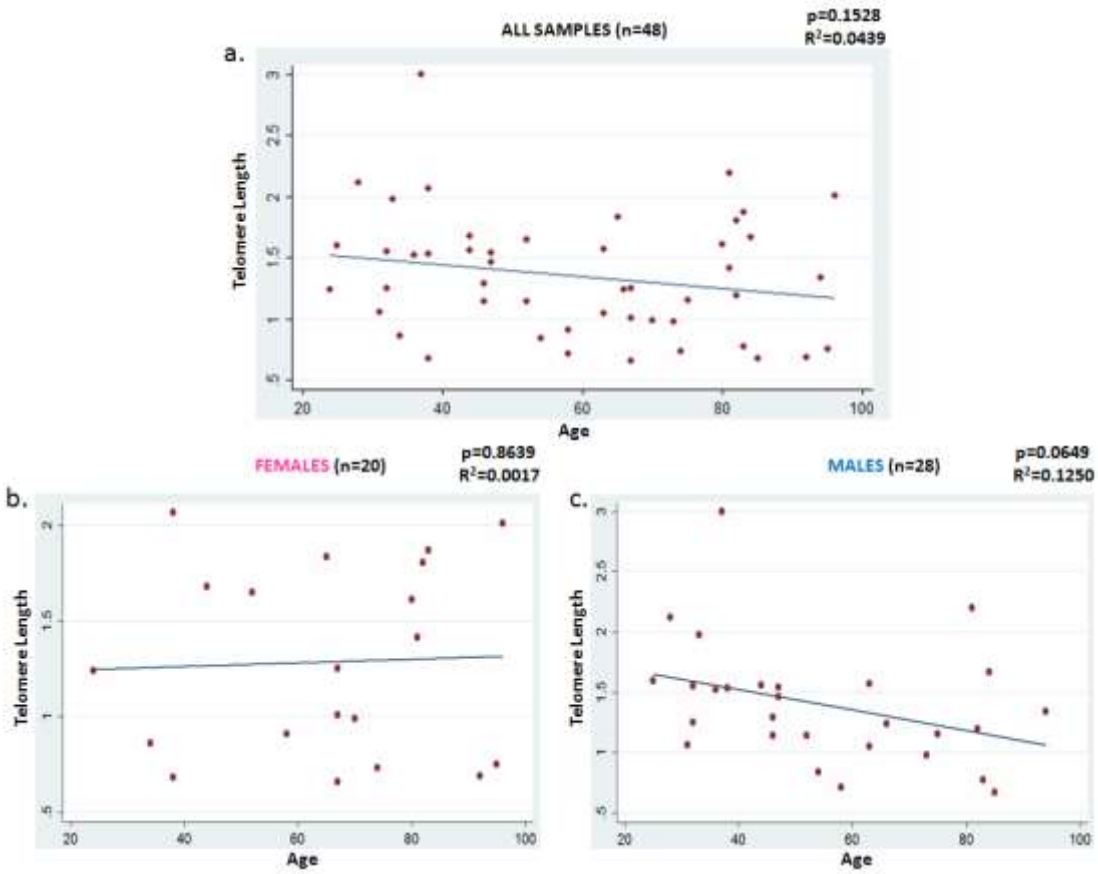

Figure 38: Regression analysis of telomere length as a function of age. a.) In the total number of patients (N=48), telomere length does not with age ($p=0.1528$; $R^2=0.0439$). b.) In females (N=20) telomere length does not with age ($p=0.8639$; $R^2=0.0017$). c.) In males (N=28) telomere length does not with age ($p=0.0649$; $R^2=0.1250$).

Also the correlation analysis between telomere length and mtDNA copy number, deletion level and integrity did not exhibit any significative association, also when analysis were performed by gender (data not shown).

4.2.2.5 Gene expression analysis

The gene expression analysis of LLMI patients muscle biopsies was conducted in a subgroup of samples at different age (13-94 years).

Regarding mitobiogenesis, among *pgc-1α*, *polγ*, *nrf1*, *tfam*, *twinkle*, *sirt1*, *sirt3*, *tomm40*, *ppard*, only *tfam* and *sirt1* showed statistically significant changes in expression level. In particular, the expression level of *tfam* significantly decreased with age only in females (p=0.0171, R^2=0.3894), but not in males (p=0.4460, R^2=0.0492) and in all samples (p=0.3117, R^2=0.0393), as displayed in figure 39.

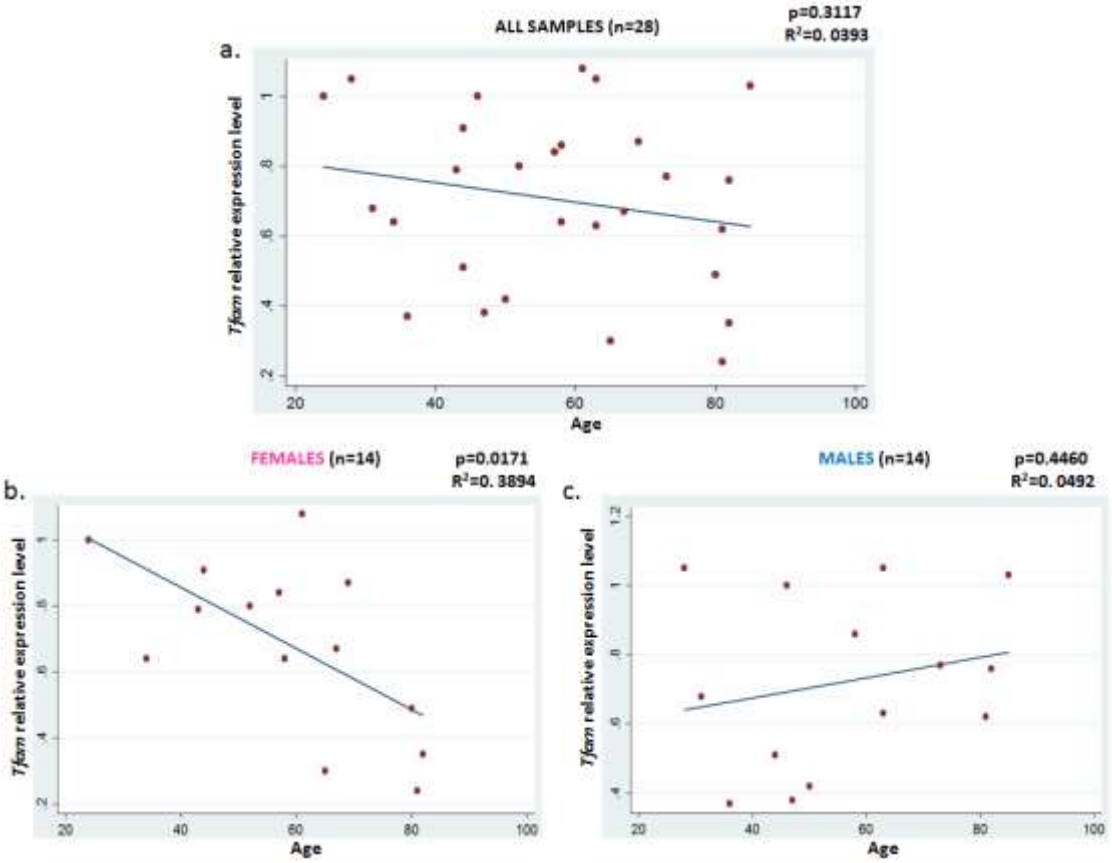

Figure 39: Regression analysis of expression level of *tfam* as a function of age. a.) In the total number of patients (N=28), expression level of *tfam* does not change with age (p=0.3117; R^2=0.0393). b.) In females (N=14) expression level of *tfam* significantly decreases with age (p=0.0171; R^2=0.3894). c.) In males (N=14) expression level of *tfam* does not change with age (p=0.4460; R^2=0.0492).

For *sirt1*, instead, there was a significative increment in the expression level of all samples (p=0.0353, R^2=0.1787; fig. 40a), that was completely lost when analysis was conducted by gender (for females: p=0.2367, R^2=0.1368; for males: p=0.1199, R^2=0.2054; figures 40b and 40c).

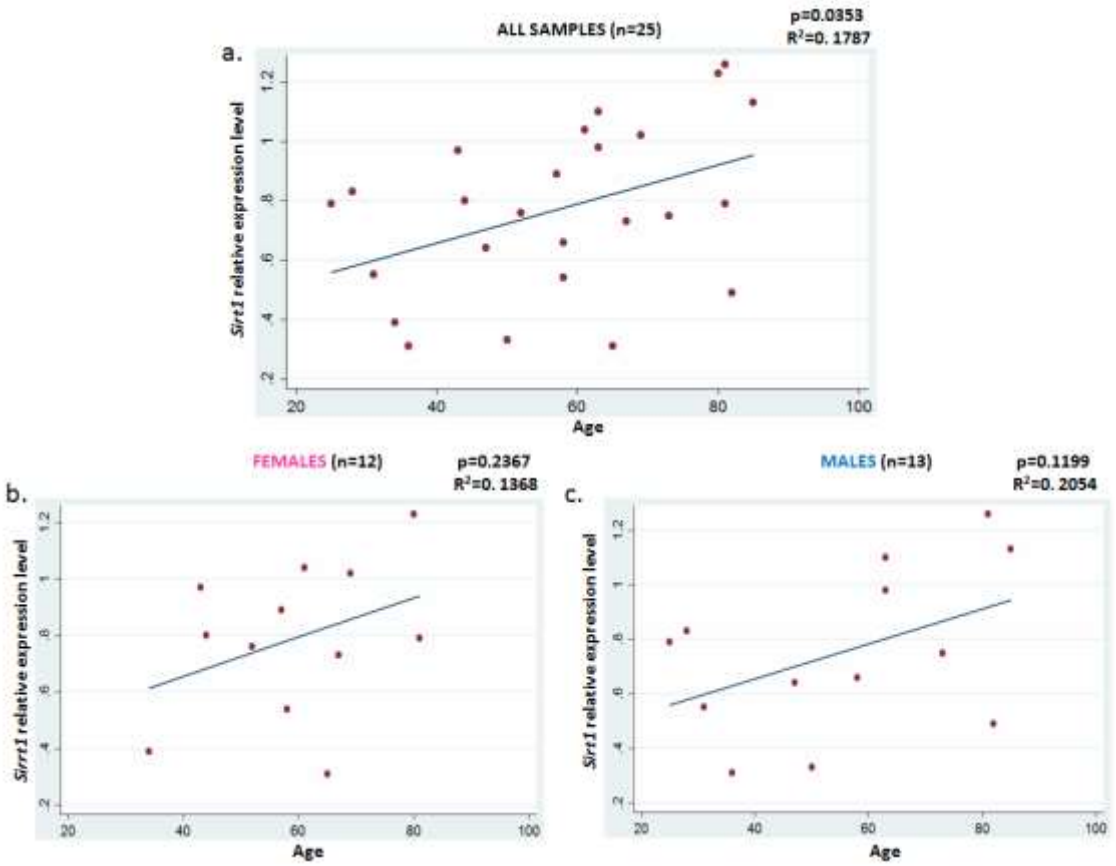

Figure 40: Regression analysis of expression level of *sirt1* as a function of age. a.) In the total number of patients (N=25), expression level of *sirt1* significantly increases with age (p=0.0353; R^2=0.1787). b.) In females (N=12) expression level of *sirt1* does not change with age (p=0.2367; R^2=0.1368). c.) In males (N=13) expression level of *sirt1* does not change with age (p=0.1199; R^2=0.2054).

From the regression analysis also emerged a significant decrease of the expression level of *beclin* with age in both total number of patients (p=0.0161, R^2=0.1964, figure 41a) and females (p=0.0282, R^2=0.3192), but not in males (p=0.3352, R^2=0.0775).

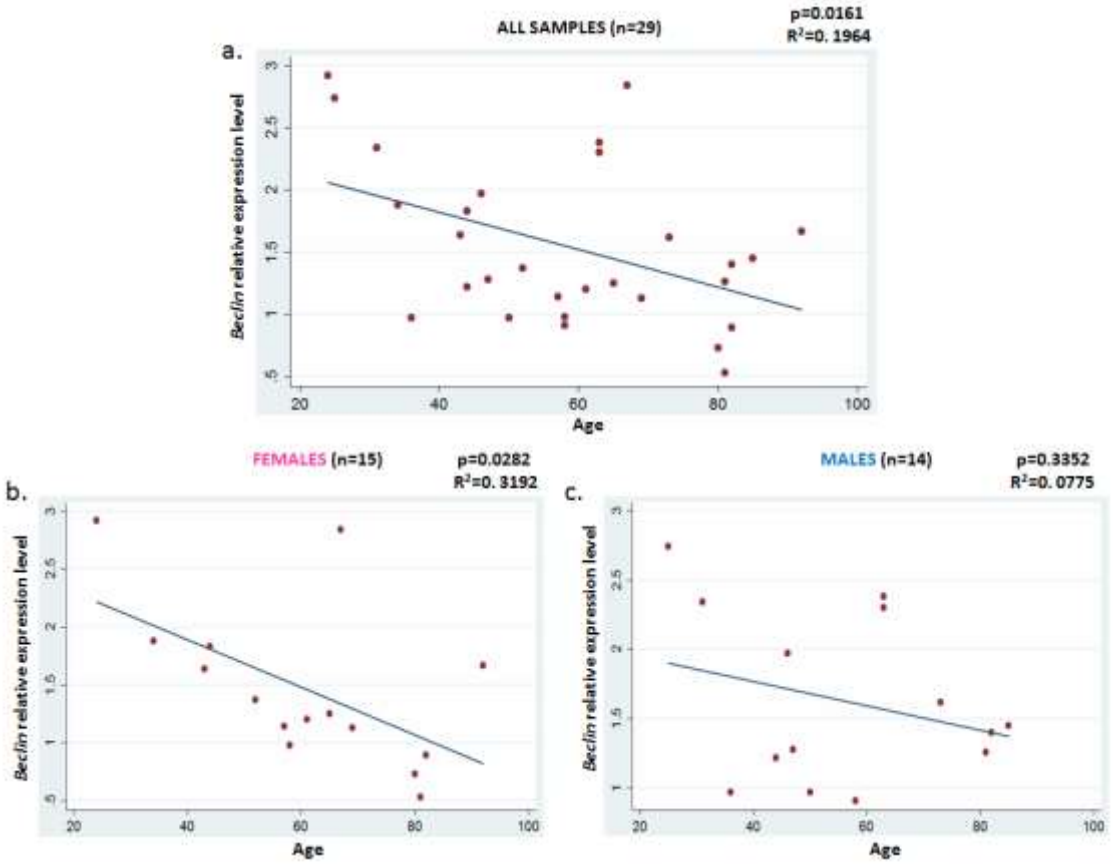

Figure 41: Regression analysis of expression level of *beclin* as a function of age. a.) In the total number of patients (N=29), expression level of *beclin* significantly decreases with age (p=0.0161; R^2=0.1964). b.) In females (N=15) expression level of *beclin* significantly decreases with age (p=0.0282; R^2=0.3192). c.) In males (N=14) expression level of *beclin* does not change with age (p=0.3352; R^2=0.0775).

Also *pink1*, another gene involved in mitophagy, showed a significant decrease with age in total number of samples (p=0.0179, R^2=0.1906, figure 42a), and like *beclin*, when analysis was performed by gender, the decrease was significative in females (p=0.0378, R^2=3121, figure 42b) but not in males (p=0.2553, R^2=0.0982, figure 42c).

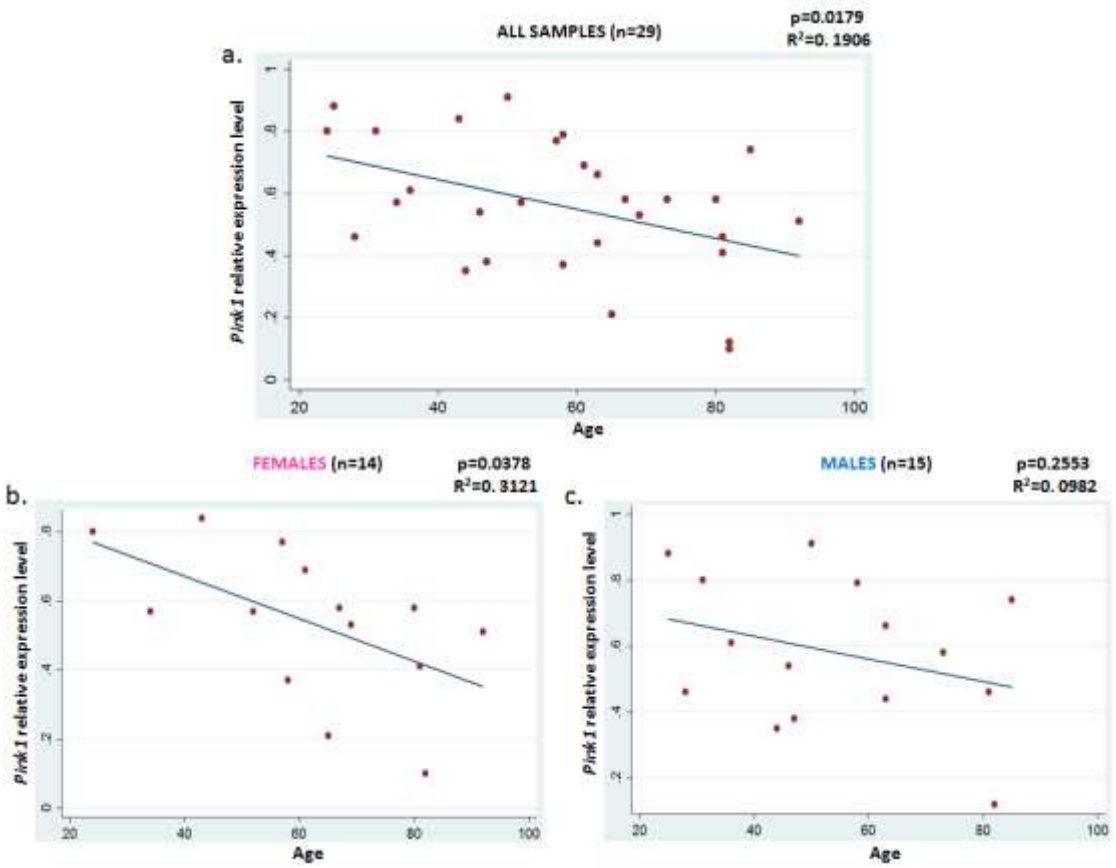

Figure 42: Regression analysis of expression level of *pink1* as a function of age. a.) In the total number of patients (N=29), expression level of *pink1* significantly decreases with age (p=0.0179; R^2=0.1906). b.) In females (N=14) expression level of *pink1* significantly decreases with age (p=0.0378; R^2=0.3121). c.) In males (N=15) expression level of *pink1n* does not change with age (p=0.2553; R^2=0.0982).

Another gene, codifying for superoxide dismutase 1 (*sod1*) displayed significant decrement in its expression level with age only in males (p=0.0078, R^2=0.4591, as shown in figure 43), but not in the total number of subjects and in females (p=0.0527, R^2=0.1275 and p=0.2970, R^2=0.0832, respectively; data not shown).

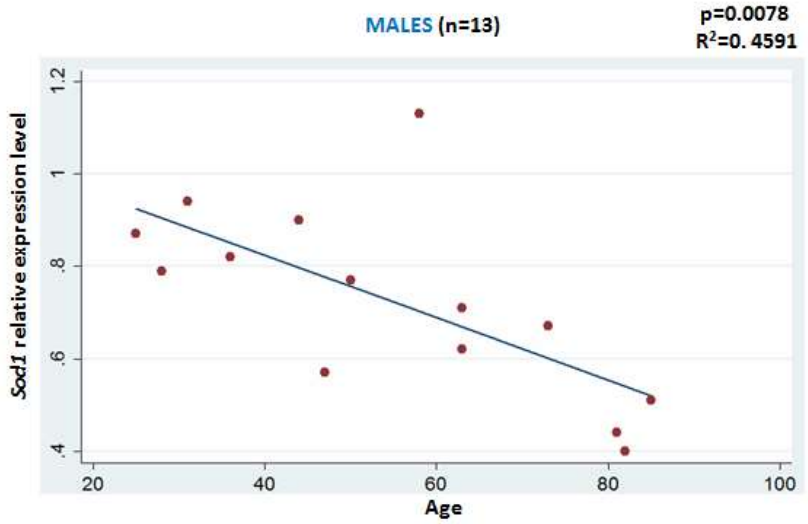

Figure 43: Regression analysis of expression level of *pink1* as a function of age in males (N=13). The expression level of *pink1n* significantly decreases with age (p=0.0078; R^2=0.4591).

Any significant difference with age emerged from analysis of the expression level of genes involved in mitochondrial biogenesis (*pgc1α*, *polγ*, *nrf1*, *tomm40*, *twinkle*, *sirt3*, *ppard*), mitochondrial dynamics (*mfn2*, *fis1*, *opa1*,), mitophagy (*ambra1*, *pik3cd*, *parkin*, *atg16l*), protein quality control system (*lonp*), protection from ROS (*sod2*), production of ROS (*nos3*) and hypoxia (*hif-1*α), neither in the total number of patients, nor in females and in males (data not shown).

4.3 Adipose Tissue

4.3.1 mtDNA copy number

mtDNA copy number was quantified in 19 DNA samples from adipose tissue biopsies, coming from LLMI patients biopsies.

Any statistically significant difference emerged from regression analysis of mtDNA copy number and age, both in the total number of samples (p=0.2854, R^2=0.0668) and by gender analysis (for females: p=0.4406, R^2=0.0871; for males: p=0.5385, R^2=0.0491), as displayed in figure 44.

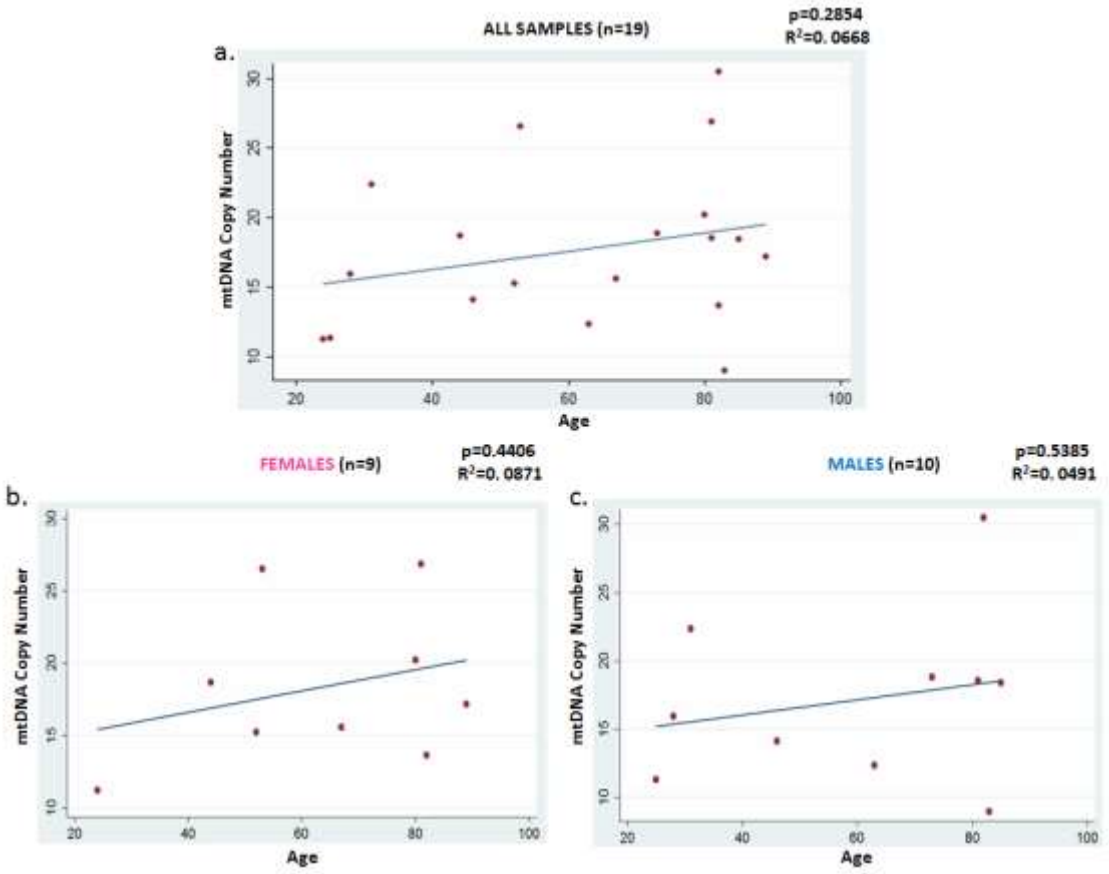

Figure 44: Regression analysis of mtDNA copy number as a function of age was performed in 19 DNA samples from adipose tissue biopsies. a.) In the total number of samples (N=19), mtDNA copy number does not change with age (p=0.2854; R^2=0.0668). b.) In females (N=9) mtDNA copy number does not change with age (p=0.4406; R^2=0.0871). c.) In males (N=10) mtDNA copy number integrity does not change with age (p=0.5385; R^2=0.0491).

4.3.2 mtDNA deletion level

As can be seen in figure 45, in adipose tissue no significative difference was found with age in mtDNA deletion level in all samples (p=0.4471, R^2=0.0344) and also in samples divided by gender (p=0.0537, R^2=0.4339; p=0.6240, R^2=0.0315, for females and males, respectively).

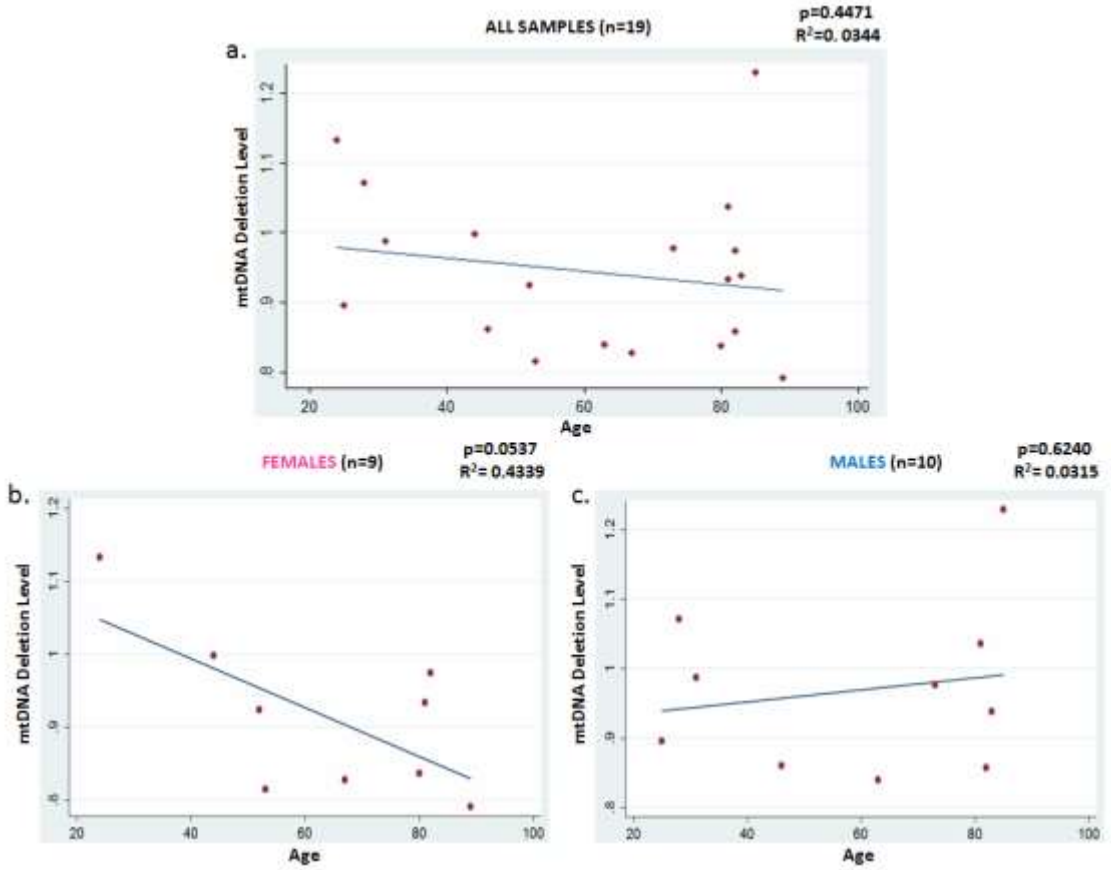

Figure 45: Regression analysis of mtDNA deletion level as a function of age was performed in 19 DNA samples from adipose tissue biopsies. a.) In the total number of samples (N=19), mtDNA deletion level does not change with age (p=0.4471; R^2=0.0344). b.) In females (N=9) mtDNA deletion level does not change with age (p=0.0537; R^2=0.4339). c.) In males (N=10) mtDNA deletion level integrity does not change with age (p=0.6240; R^2=0.0315).

4.3.3 mtDNA integrity

From regression analysis of mtDNA integrity with age in adipose tissue samples, no significative changes emerged both in total number of samples (p=0.2384, R^2=0.0807) and in samples divided by gender (for females: p=0.2984, R^2=0.1527; for males: p=0.6109, R^2=0.0338), as can be observed in figure 46.

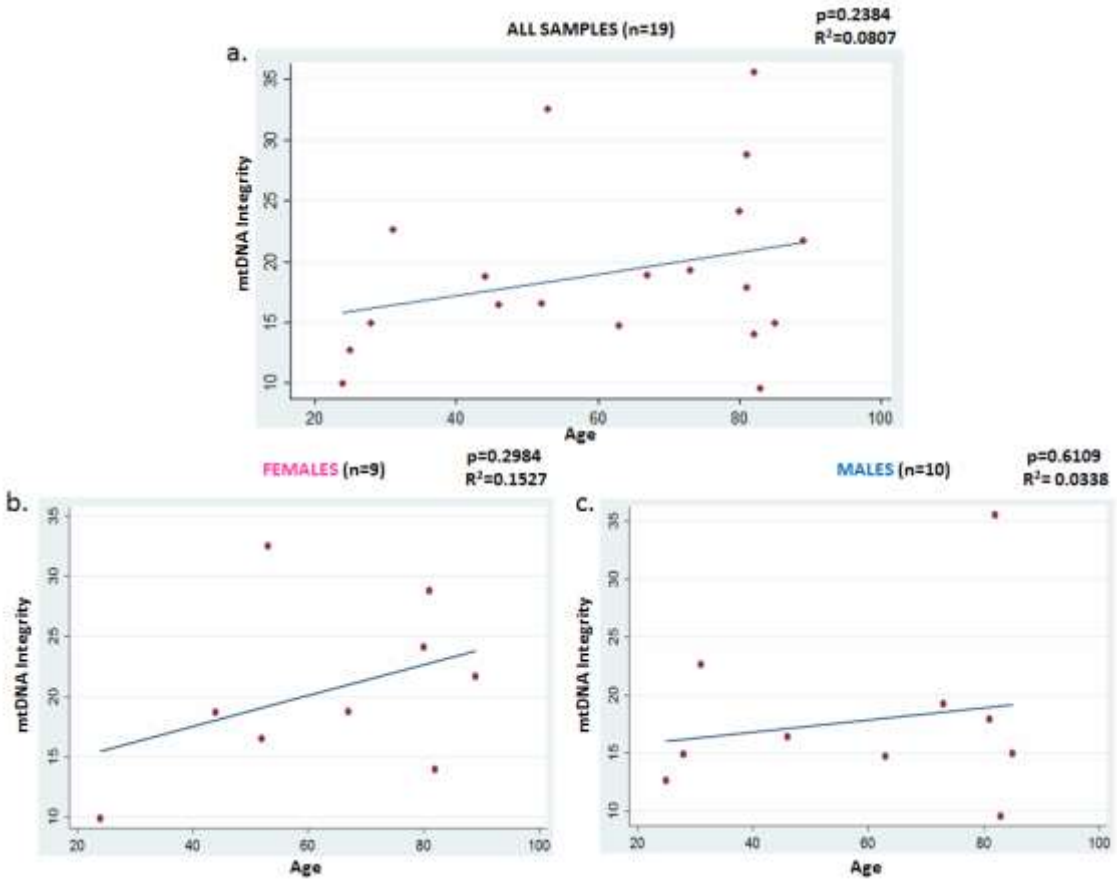

Figure 46: Regression analysis of mtDNA integrity as a function of age was performed in 19 DNA samples from adipose tissue biopsies. a.) In the total number of samples (N=19), mtDNA integrity does not change with age (p=0.2384; R^2=0.0807). b.) In females (N=9) mtDNA integrity does not change with age (p=0.2984; R^2=0.1527). c.) In males (N=10) mtDNA integrity does not change with age (p=0.6109; R^2=0.0338).

4.3.4 Telomere length

In DNA samples from adipose tissue was also analyzed telomere length. Also for this parameter, no significative difference was found with regression analysis with age in total samples (p=0.5888, R^2=0.0187) and both in females (p=0.4284, R^2=0.0917) and males (p=0.8622, R^2=0.0046) separately. These data can be seen in figure 47.

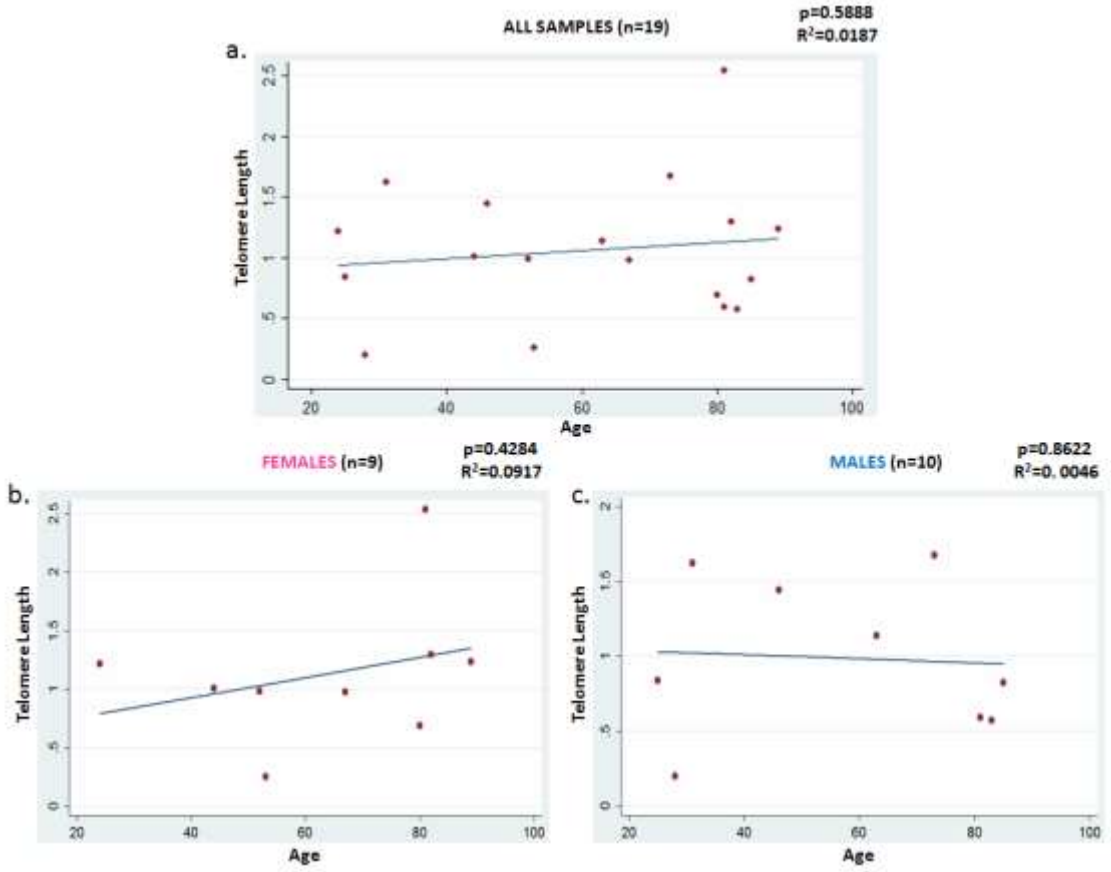

Figure 47: Regression analysis of telomere length as a function of age was performed in 19 DNA samples from adipose tissue biopsies. a.) In the total number of samples (N=19), telomere length does not change with age (p=0.5888; R^2=0.0187). b.) In females (N=9) telomere length does not change with age (p=0.4284; R^2=0.0917). c.) In males (N=10) telomere length does not change with age (p=0.6109; R^2=0.0046).

Subsequently, was investigated the relation between telomere length and mtDNA parameters in order to understand the possible relation of telomere shortening and mitochondrial dysfunction. Nevertheless the regression analysis did not highlight any statistically significant relation, neither in the total number of subjects nor in females or males (data not shown).

4.3.5 Gene expression analysis

To further characterise the involvement of mtDNA rearrangements during the aging of human adipose tissue, the relative expression of key genes for mitobiogenesis (*pgc-1α*, *polγ*, *nrf1*, *tfam*, *twinkle*, *sirt1*, *sirt3*, *tomm40*, *ppard*), for fusion and fission processes (*mfn2*, *fis1* and *opa1*), for mitophagy (*ambra1*, *beclin*, *pink1*, *parkin*, *atg16l* and *pik3cd*), for production of ROS (*nos3*), for protection from ROS (*sod1* and *sod2*), for the protein quality control system (*lonp*) and for hypoxia (*hif-1α*) studied in liver and muscle biopsies was evaluated in samples from adipose tissue.

Like for liver and muscle samples, also in this case the relative expression of each gene was considered as function of age first in the total number of samples and then separately on females and males.

For genes involved in mitobiogenesis (*pgc-1α*, *polγ*, *nrf1*, *tfam*, *twinkle*, *sirt1*, *sirt3*, *tomm40*, *ppard*), only for *twinkle* and for *nrf1* were found significative differences with age. However, for *twinkle* the statistical significant change in expression level was only marginal in the total number of subjects (p=0.0431, R^2=0.2318) and completely lost when data were analyzed by gender (for females: p=0.0607, R^2=0.4161; for males: p=0.1169, R^2=0.3135), as shown in figure 48.

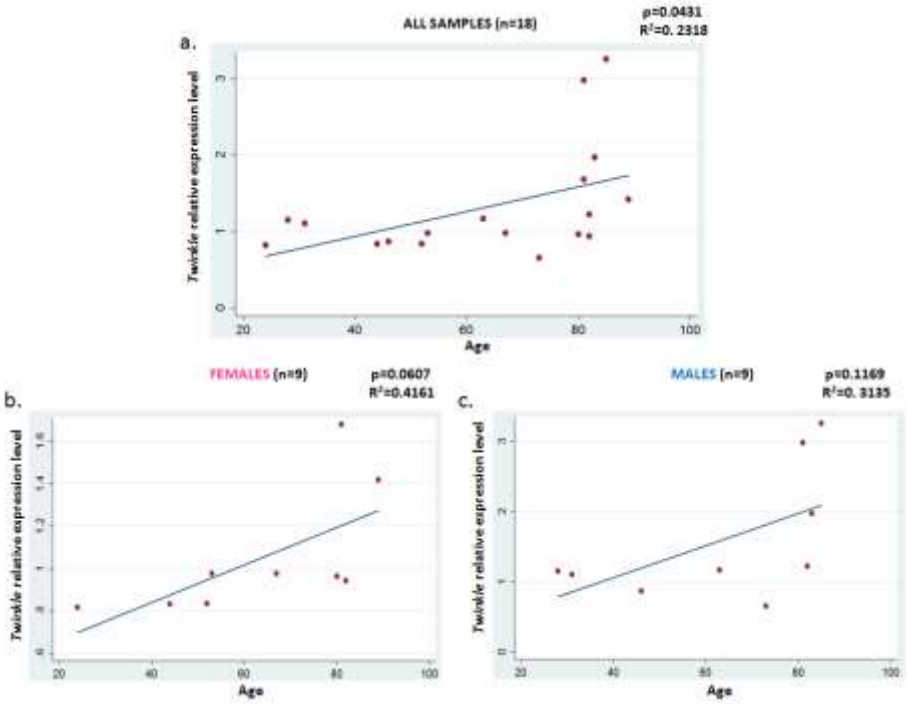

Figure 48: Regression analysis of expression level of *twinkle* as a function of age was performed in 18 cDNA samples from adipose tissue biopsies. a.) In the total number of samples (N=18), expression level of *twinkle* significantly decreases with age (p=0.0431; R^2=0.2318). b.) In females (N=9) expression level of *twinkle* does not change with age (p=0.0607; R^2=0.416). c.) In males (N=9) expression level of *twinkle* does not change with age (p=0.1169; R^2=0.3135).

Conversely for *nrf1*, significative increases were found in the total number of samples (p=0.0169, R^2=0.3248) and in females (p=0.0143, R^2=0.5999), but not in males, where no significative difference with age emerged (p=0.1730, R^2=0.2849), as can be seen in figure 49.

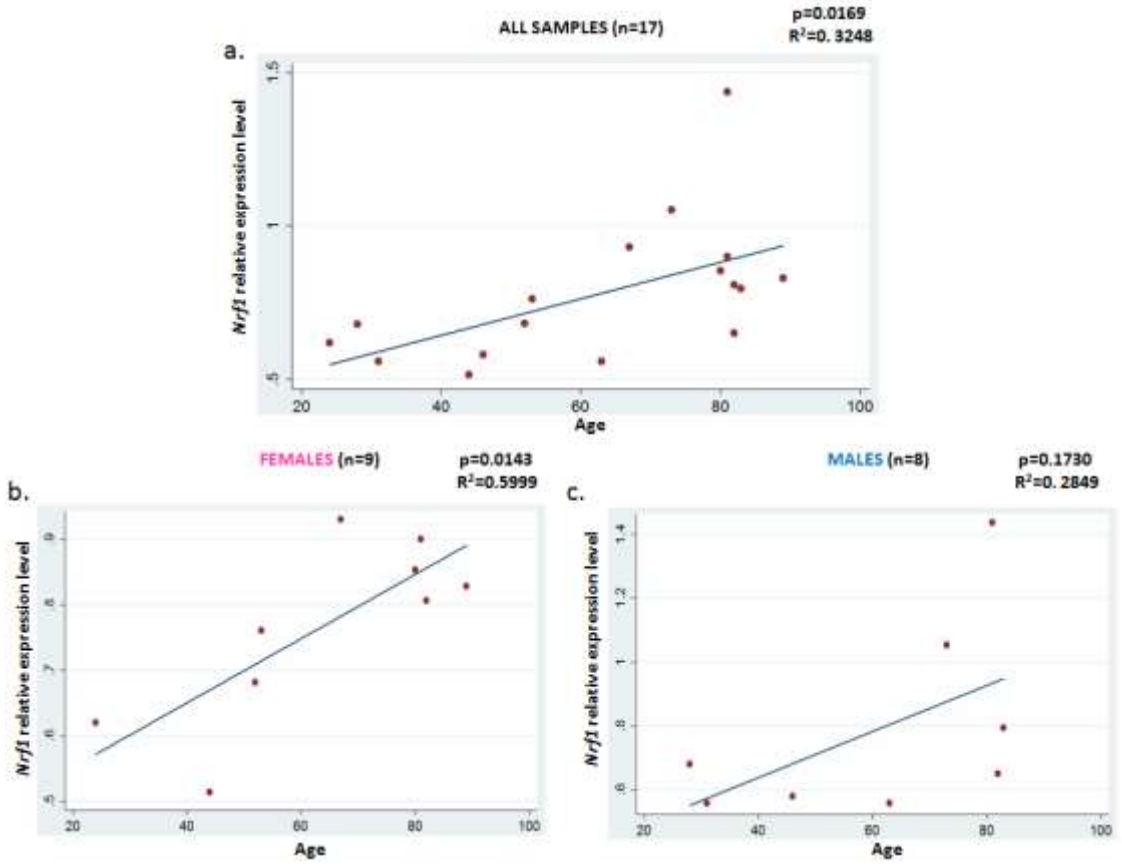

Figure49: Regression analysis of expression level of *nrf1* as a function of age was performed in 18 cDNA samples from adipose tissue biopsies. a.) In the total number of samples (N=18), expression level of *nrf1* significantly increases with age (p=0.0169; R^2=0.3248). b.) In females (N=9) expression level of *nrf1* significantly increases with age (p=0.0143; R^2=0.5999). c.) In males (N=9) expression level of *nrf1* does not change with age (p=0.1730; R^2=0.2849).

Regarding genes for mitophagy, significative increments with age were found in the expression level of *pink1* and *ambra*. In particular, for both these genes, the increment was significative in all samples (for *pink1*: p=0.0046, R^2=0.4045; for *ambra*: p=0.0306, R^2=0.2601) and in females (for *pink1*: p=0.0294, R^2=0.5154; for *ambra:* p=0.0386, R^2=0.4798), but not in males (for *pink1*: p=0.0638, R^2=0.4086; for *ambra:* p=0.3147, R^2=0.1435). Figure 50 shows data relative to *pink1*, while figure 51 shows those for *ambra*.

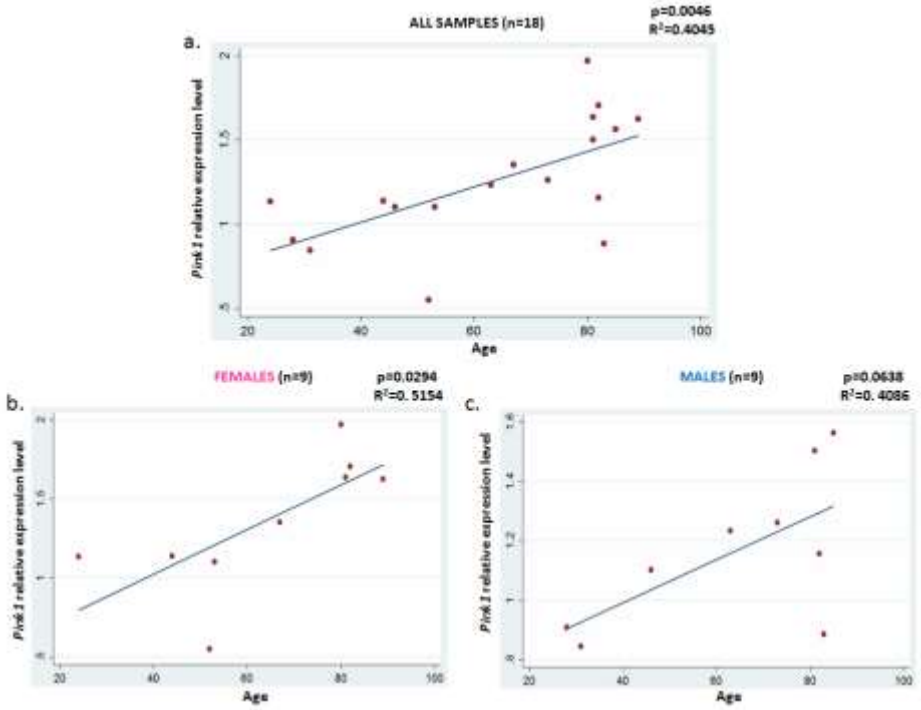

Figure50: Regression analysis of expression level of *pink1* as a function of age was performed in 18 cDNA samples from adipose tissue biopsies. a.) In the total number of samples (N=18), expression level of *pink1* significantly increases with age (p=0.0046; R^2=0.4045). b.) In females (N=9) expression level of *pink1* significantly increases with age (p=0.0294; R^2=0.5154). c.) In males (N=9) expression level of *pink1* does not change with age (p=0.0638; R^2=0.4086).

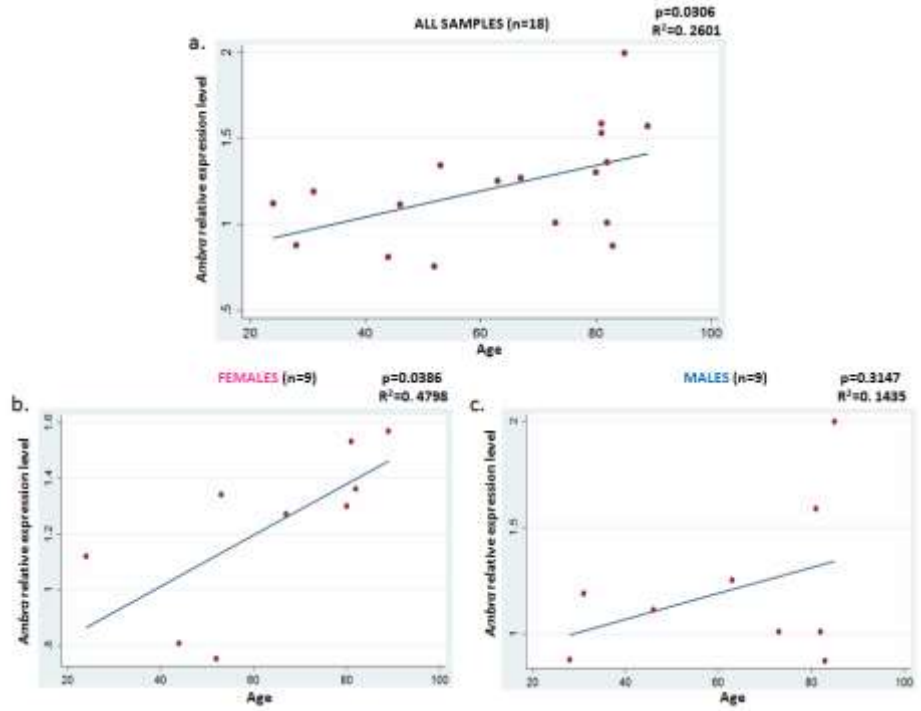

Figure51: Regression analysis of expression level of *ambra* as a function of age was performed in 18 cDNA samples from adipose tissue biopsies. a.) In the total number of samples (N=18), expression level of *ambra* significantly increases with age (p=0.0306; R^2=0.2601). b.) In females (N=9) expression level of *ambra* significantly increases with age (p=0.0386; R^2=0.4798). c.) In males (N=9) expression level of *ambra* does not change with age (p=0.3147; R^2=0.1435).

Figure 52 shows as also for *nos3*, a gene involved in the production of ROS, a significative increment with age was found in all samples and in females (p=0.0320, R^2=0.2565; p=0.0288, R^2=0.5180, respectively), but not in males (p=0.2736, R^2=0.1678).

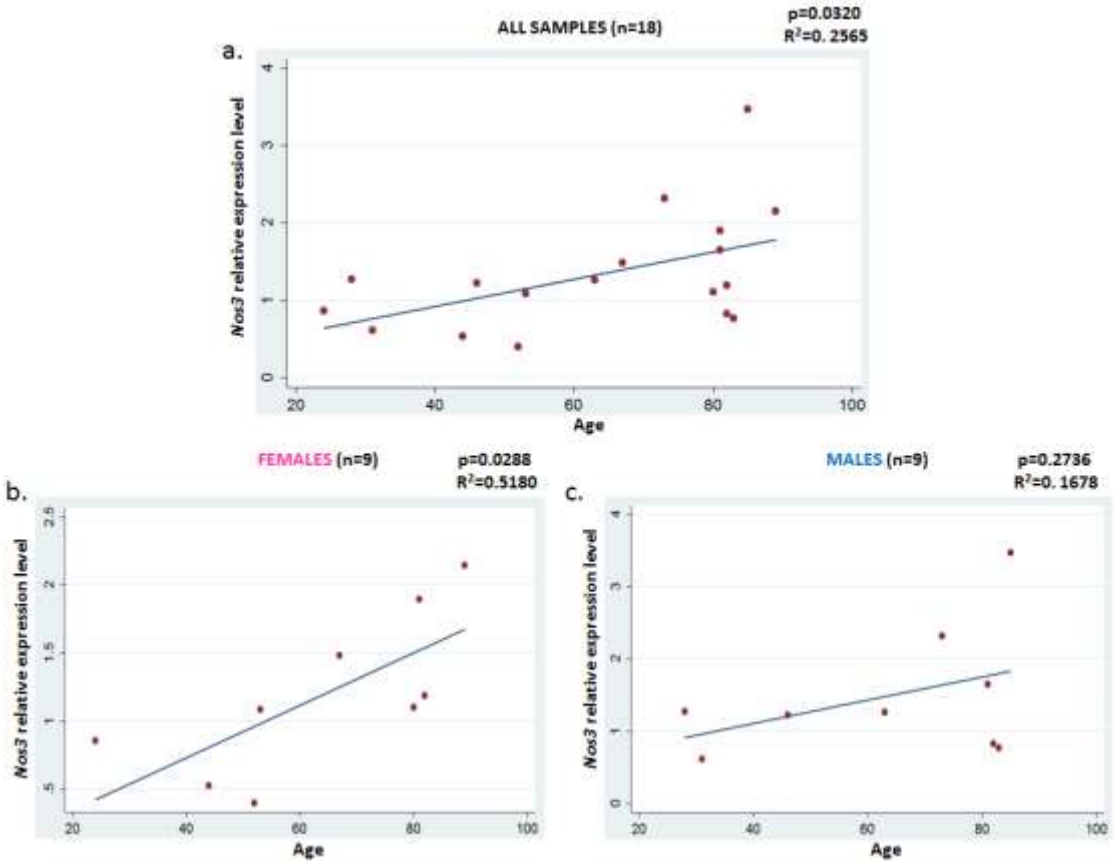

Figure52: Regression analysis of expression level of *nos3* as a function of age was performed in 18 cDNA samples from adipose tissue biopsies. a.) In the total number of samples (N=18), expression level of *nos3* significantly increases with age (p=0.0320; R^2=0.2565). b.) In females (N=9) expression level of *nos3* significantly increases with age (p=0.0288; R^2=0.5180). c.) In males (N=9) expression level of *nos3* does not change with age (p=0.2736; R^2=0.1678).

Finally, as shown in figure 53, the expression level of *sod1* was found significantly increased with age in the total number of subjects (p=0.0283, R^2=0.2665), but analyzing data by gender, no statistically significant differences were detected neither in females (p=0.1387, R^2=0.2851; data not shown) nor in males (p=0.1584, R^2=0.2626; data not shown).

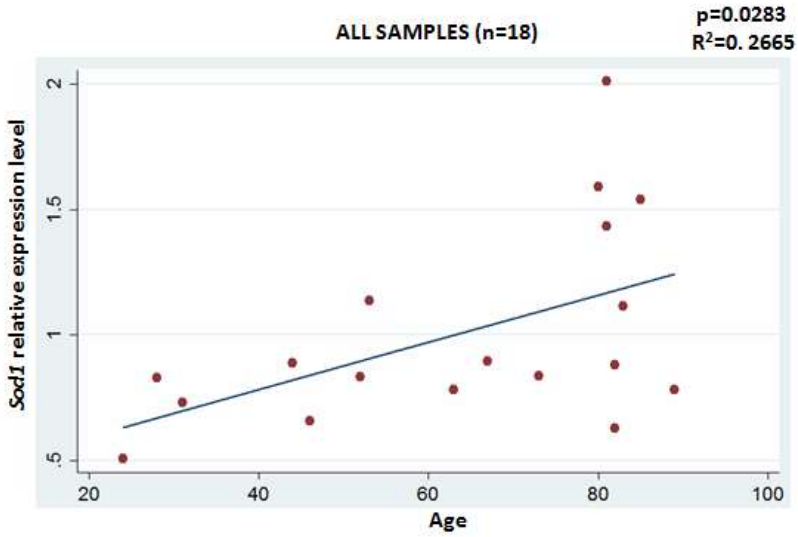

Figure53: Regression analysis of expression level of *sod1* as a function of age in all samples (N=18). The expression level of *sod1n* significantly decreases with age (p=0.0283; R^2=0.2665).

Any statistically significant difference neither in all samples nor in by gender analysis was found for gene involved in mitobiogenesis (*pgc1α*, *polγ*, *tfam*, *tomm40*, *sirt1*, *sirt3*, *ppard*), in mitochondrial dynamics (*mfn2*, *fis1*, *opa1*), in protein quality control system (*lonp*), in mitophagy (*beclin1*, *parkin*, *pik3cd* and *atg16l*), in protection from ROS (*sod2*) and finally in hypoxia (*hif-1α*). These data are not shown.

4.4 Tissue comparison

In order to evaluate possible differences between the studied tissues (liver, healthy muscle, LLMI patients muscles and adipose tissue), mtDNA copy number, deletion level, integrity and telomere length as well as gene expression of the examined nuclear genes were compared among tissues independently from age in the total number of samples and then in females and males separately. In table 17, are reported the assigned tissue index.

Tissue Index	Tissue	Number of samples (N)	Gender (N)	
			M	F
0	Liver	28	12	16
1	Healthy muscle	29	14	15
2	Patient muscle	30	15	15
3	Adipose tissue	19	10	9

Table 17: Tissue index assigned to every type of tissues samples and number of samples considered for each tissue.

4.4.1 mtDNA copy number

mtDNA copy number was found significantly different between the examined tissues. In particular, in livers samples, mtDNA copy number was significantly lower than in muscles, both healthy subjects and patients, and than in adipose tissue (fig. 54).

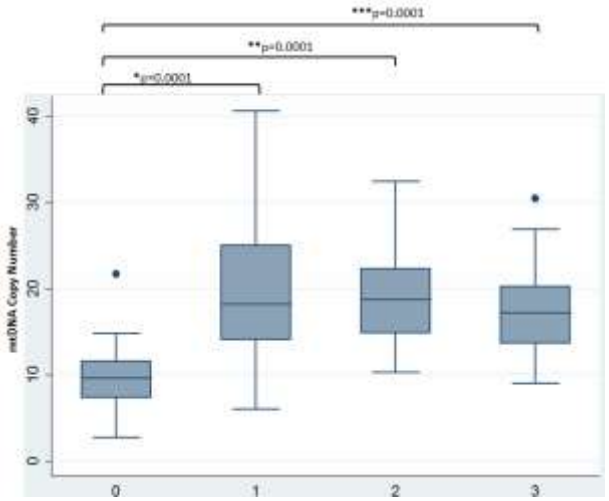

Figure 54: Comparison of mtDNA copy number among liver (0), muscle from healthy subjects (1), muscle from LLMI patients (2) and adipose tissue (3). To compare tissues, Kruskal-Wallis test was applied; mtDNA copy number is significantly lower in liver than in muscle from healthy subjects (p=0.0001), in muscle from LLMI patients (p=0.0001) and in adipose tissue (p=0.0001).

mtDNA copy number was found different between these tissues also when gender was considered separately: it was lower in livers samples than in others tissues both in females and in males, as shown in fig. 55.

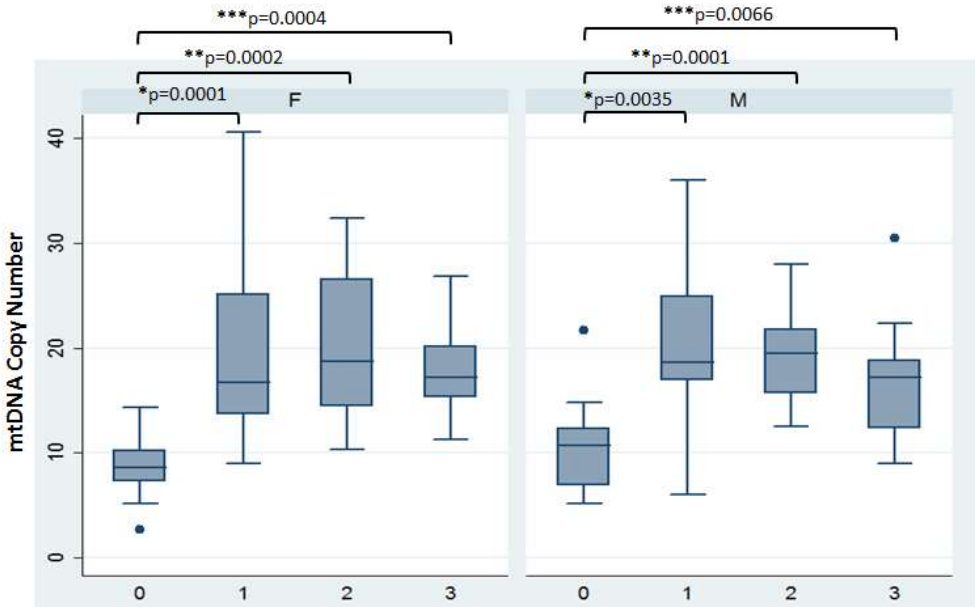

Figure 55: Comparison of mtDNA copy number among liver (0), muscle from healthy subjects (1), muscle from LLMI patients (2) and adipose tissue (3). To compare tissues, Kruskal-Wallis test was applied. In the left panel are represented females, whose mtDNA copy number is significantly lower in liver than in muscle from healthy subjects (p=0.0001), in muscle from LLMI patients (p=0.0002) and in adipose tissue (p=0.0004). In the right panel are represented males, whose mtDNA copy number is significantly lower in respect to muscle from healthy subjects (p=0.0035), to muscle from LLMI patients (p=0.0001) and to adipose tissue (p=0.0066).

4.4.2 mtDNA deletion level

As fig. 56 shows, no significative difference in mtDNA deletion level was found among liver, muscle and adipose tissue (p=0.3139), even when comparing tissues one to each other and considering genders separately.

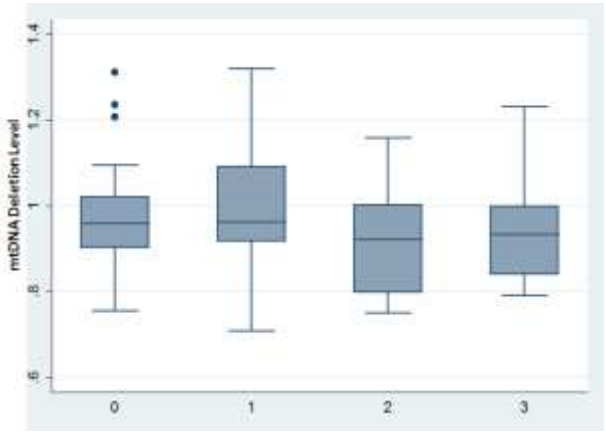

Figure 56: Comparison of mtDNA deletion level among liver (0), muscle from healthy subjects (1), muscle from LLMI patients (2) and adipose tissue (3). To compare tissues, Kruskal-Wallis test was applied; mtDNA deletion level does not differ among the tissues considered (p=0.3139).

4.4.3 mtDNA integrtiy

When investigating all samples and sample divided by gender, mtDNA integrity differenced in a significant way among tissues and in livers samples was significantly lower than in muscle and adipose tissues, both in the total number of samples and in samples divided by gender. Figure 57 and figure 58 illustrate these results.

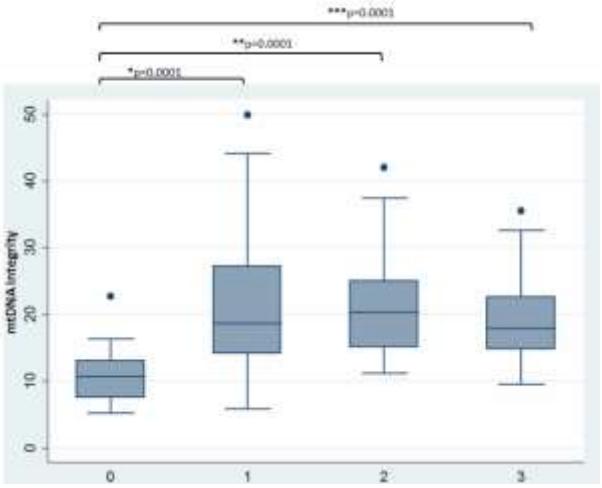

Figure 57: Comparison of mtDNA integrity among liver (0), muscle from healthy subjects (1), muscle from LLMI patients (2) and adipose tissue (3). To compare tissues, Kruskal-Wallis test was applied; mtDNA integrity is significantly lower in liver than in muscle from healthy subjects (p=0.0001), in muscle from LLMI patients (p=0.0001) and in adipose tissue (p=0.0001).

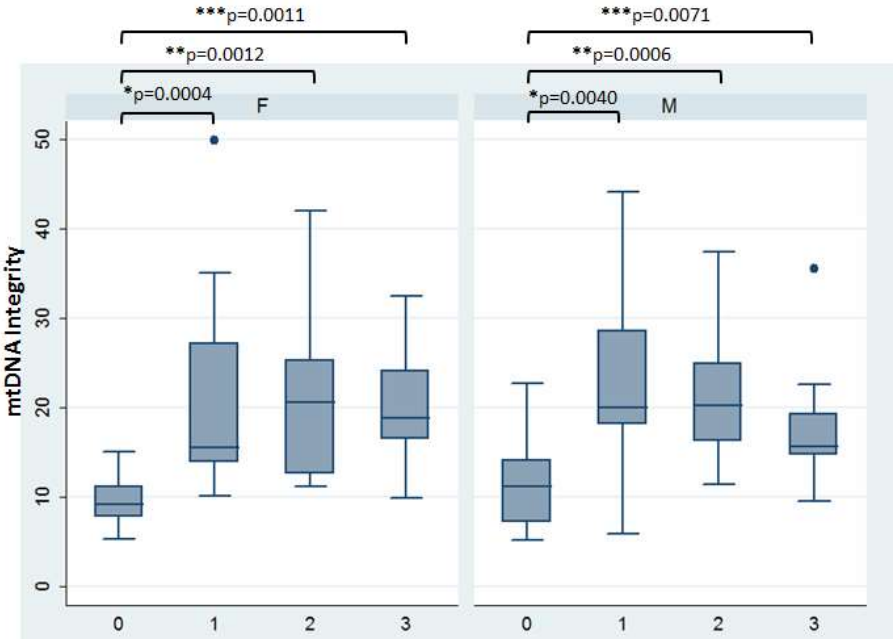

Figure 58: Comparison of mtDNA integrity among liver (0), muscle from healthy subjects (1), muscle from LLMI patients (2) and adipose tissue (3). To compare tissues, Kruskal-Wallis test was applied. In the left panel are represented females, whose mtDNA integrity is significantly lower in liver than in muscle from healthy subjects (p=0.0004), in muscle from LLMI patients (p=0.0012) and in adipose tissue (p=0.0011). In the right panel are represented males, whose mtDNA integrity is significantly lower in respect to muscle from healthy subjects (p=0.0040), to muscle from LLMI patients (p=0.0006) and to adipose tissue (p=0.0071).

4.4.4 Telomere length

Regarding telomere length, no significative differences were found among tissues (p=0.0620; fig. 59). However, when comparing tissue one to each other and considering genders separately, a significative difference between telomere length in liver and adipose tissue emerged: telomere length in females liver was significantly higher than in females adipose tissue, as shown in fig. 60.

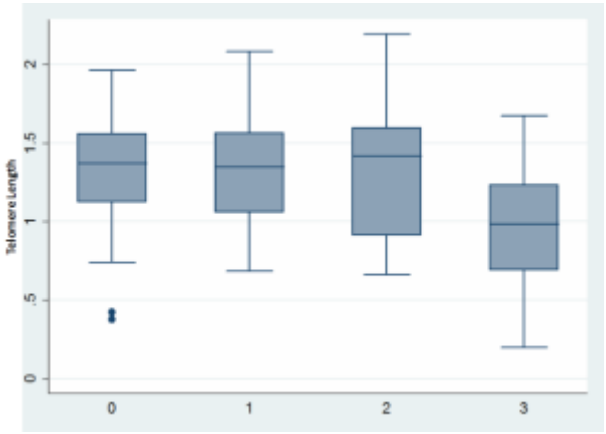

Figure 59: Comparison of telomere length among liver (0), muscle from healthy subjects (1), muscle from LLMI patients (2) and adipose tissue (3). To compare tissues, Kruskal-Wallis test was applied; telomere length level does not differ among the tissues considered (p=0.0620).

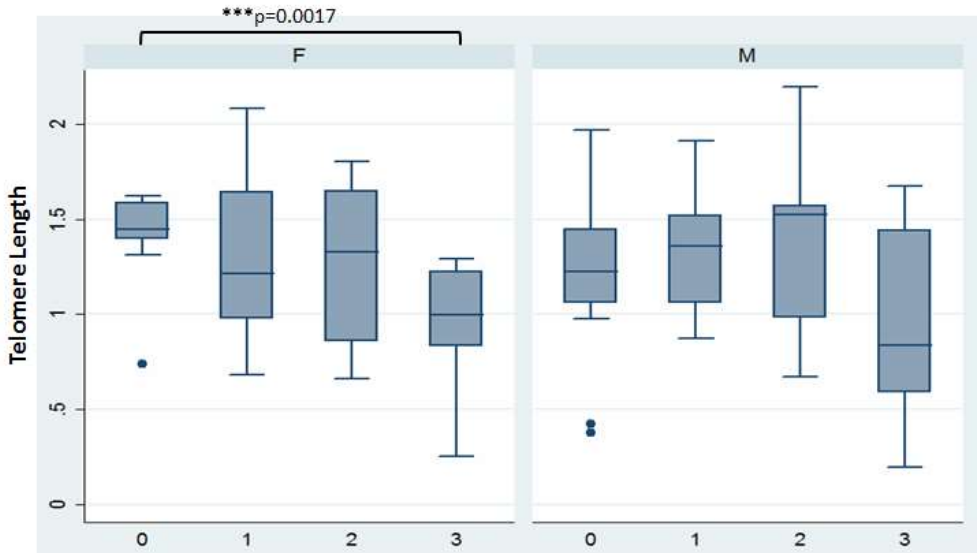

Figure 60: Comparison of telomere length among liver (0), muscle from healthy subjects (1), muscle from LLMI patients (2) and adipose tissue (3). To compare tissues, Kruskal-Wallis test was applied. In the left panel are represented females, whose telomere length is significantly higher in liver than in adipose tissue (p=0.0017). In the right panel are represented males, whose telomere length does not differ among the considered tissues.

4.4.5 Gene expression

The relative expression of the aforementioned nuclear mitochondrial-related genes has been also compared among liver, muscle (from healthy subjects and patients) and adipose tissue, to identify possible different mechanisms involved in mtDNA rearrangements. The analyses were conducted independently to age, first in the total number of subjects and then in females and males separately to evaluate a possible gender difference.

4.4.5.1 Pgc1-α

The expression level of *pgc1-α* was found significantly higher in muscle from healthy subjects than in liver and adipose tissue. Also the expression level of *pgc1-α* in muscle from LLMI patients significantly differed from those of liver and adipose tissue. However also between liver and adipose tissue the expression level of *pgc1-α* was significantly different, greater for the former than the latter, as shown in figure 61.

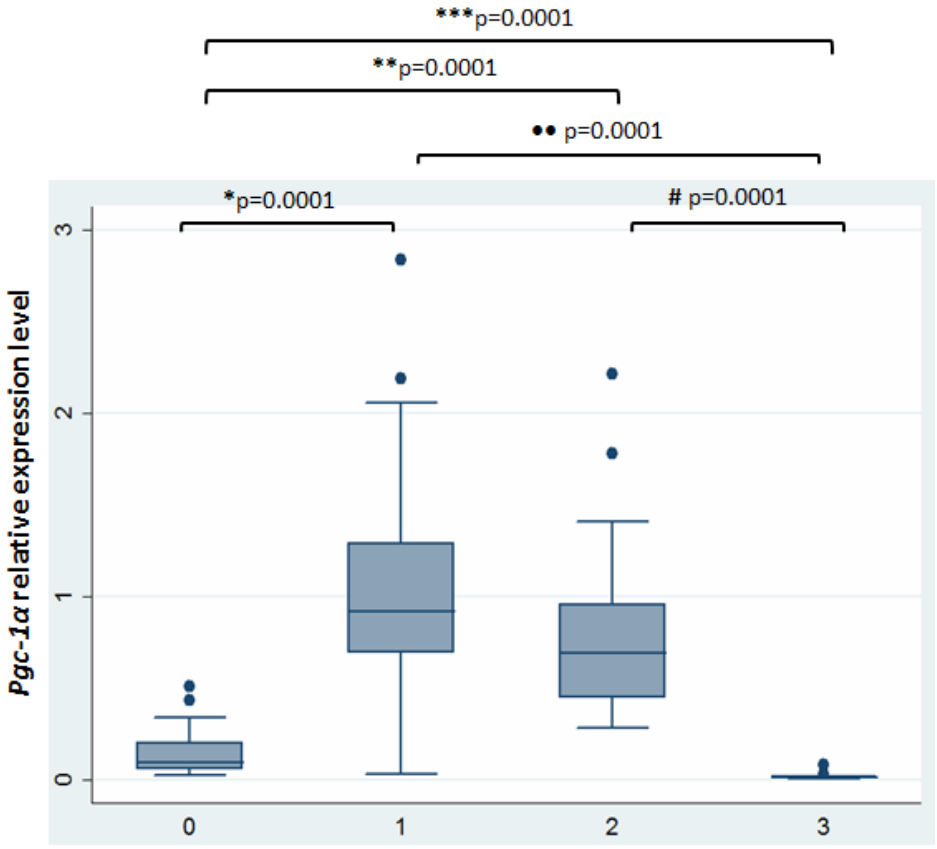

Figure 61: Comparison of *pgc-1α* relative expression level among liver (0), muscle from healthy subjects (1), muscle from LLMI patients (2) and adipose tissue (3). To compare tissues, Kruskal-Wallis test was applied; *pgc-1α* relative expression level is significantly lower in liver than in muscle from healthy subjects (p=0.0001), in muscle from LLMI patients (p=0.0001) and in adipose tissue (p=0.0001). *Pgc-1α* relative expression level is significantly different among adipose tissue and muscle from healthy subjects (p=0.0001) and from LLMI patients (p=0.0001).

When genders were considered separately, the different expression levels were maintained both in males and females, but in females, the *pgc1-α* expression level was different also between healthy subjects and LLMI patients muscles, as illustrated in figure 62.

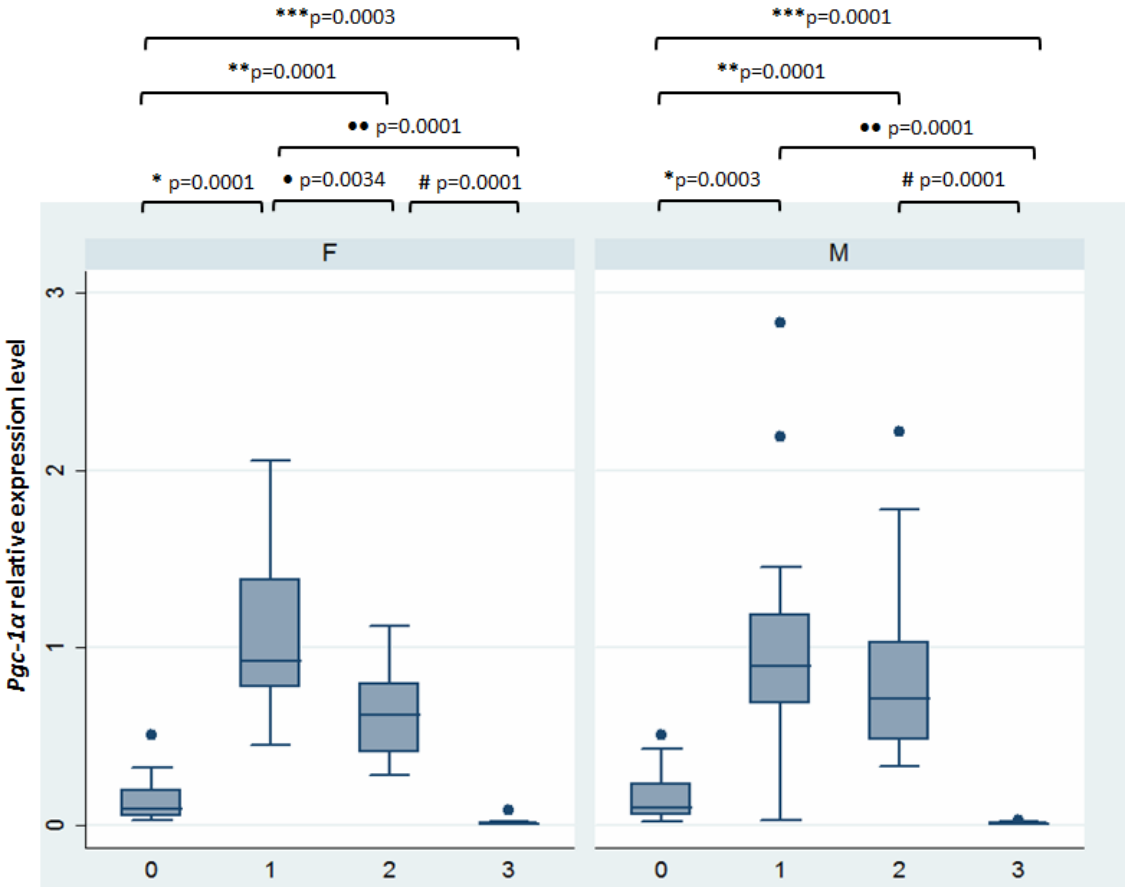

Figure 62: Comparison of *pgc-1α* relative expression level among liver (0), muscle from healthy subjects (1), muscle from LLMI patients (2) and adipose tissue (3). To compare tissues, Kruskal-Wallis test was applied. In the left panel are represented females: *pgc-1α* relative expression level is significantly different among liver and muscle, both from healthy subjects (p=0.0001) and from LLMI patients (p=0.0001), between liver and adipose tissue (p=0.0003), between muscle from healthy subjects and muscle from LLMI patients (p=0.0034), between muscle from healthy subjects and adipose tissue (p=0.0001) and finally between adipose tissue and muscle from LLMI patients (p=0.0001). In the right panel are represented males: *pgc-1α* relative expression level is significantly different among liver and muscle, both from healthy subjects (p=0.0003) and from LLMI patients (p=0.0001), between liver and adipose tissue (p=0.0001), and finally among adipose tissues and muscles, both from healthy subjects (p=0.0001) and from LLMI patients (p=0.0001).

4.4.5.2 Poly

Poly expression level was found significantly different between all tissues considered: it was higher in muscles from patients than in samples from healthy subjects muscle, from liver and from adipose tissue. However, in healthy subjects the expression level was greater than in liver and in adipose tissue and also between liver and adipose tissue the expression level of *poly* was significantly different, greater for the former and lower the latter. Data are presented in figure 63.

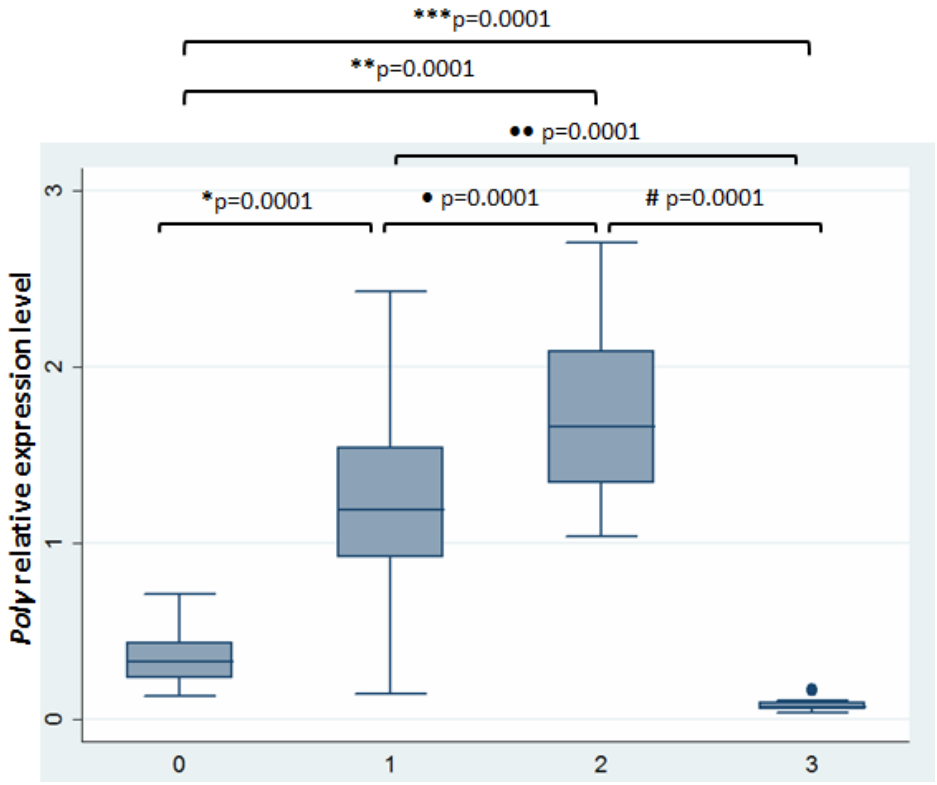

Figure 63: Comparison of *poly* relative expression level among liver (0), muscle from healthy subjects (1), muscle from LLMI patients (2) and adipose tissue (3). To compare tissues, Kruskal-Wallis test was applied; *poly* relative expression level is significantly lower in liver than in muscle from healthy subjects (p=0.0001), in muscle from LLMI patients (p=0.0001) and higher than in adipose tissue (p=0.0001). *Poly* relative expression level is significantly different between muscle from healthy subjects and LLMI patients (p=0.0001), between muscle from healthy subjects and adipose tissue (p=0.0001) and finally between muscle from LLMI patients and adipose tissue (p=0.0001).

When data were analyzed by gender, the difference in the expression level between muscles from healthy subjects and from patients was lost both in females and in males, while all the others significative differences between tissue were maintained (fig. 64).

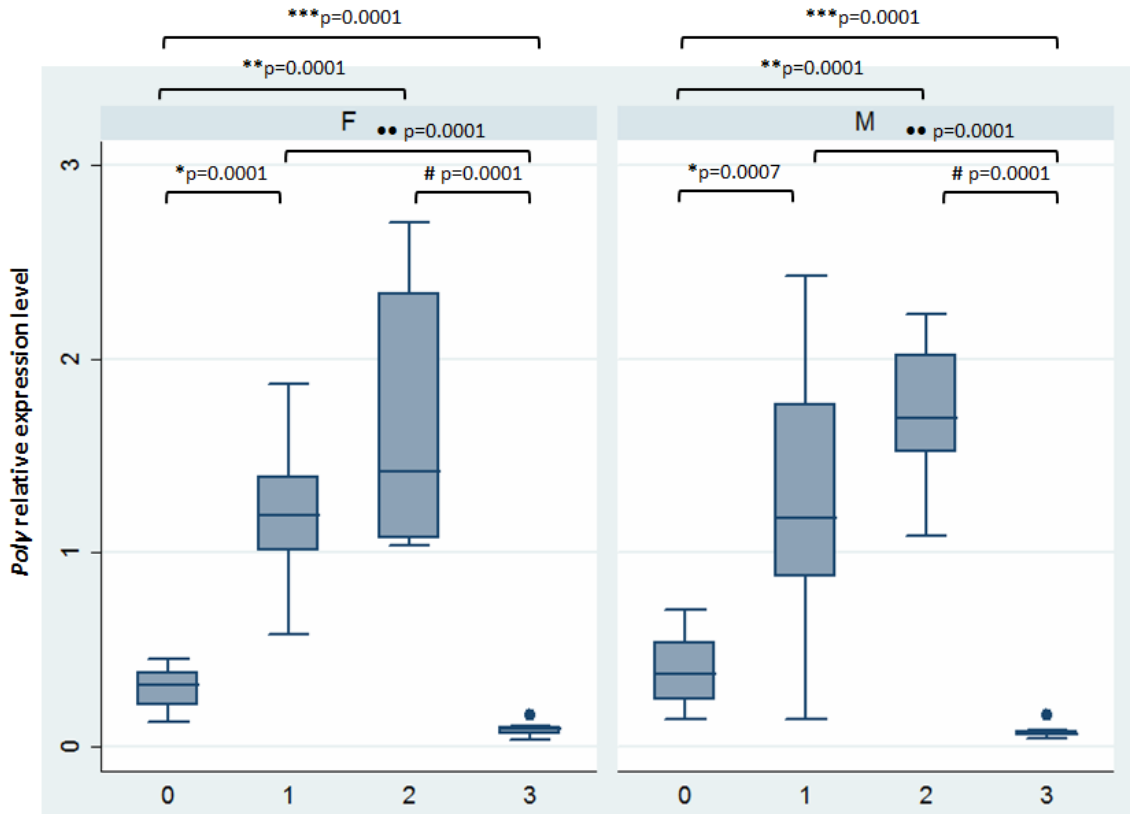

Figure 64: Comparison of *poly* relative expression level among liver (0), muscle from healthy subjects (1), muscle from LLMI patients (2) and adipose tissue (3). To compare tissues, Kruskal-Wallis test was applied. In the left panel are represented females: *poly* relative expression level is significantly different among liver and muscle, both from healthy subjects (p=0.0001) and from LLMI patients (p=0.0001), between liver and adipose tissue (p=0.0001), among adipose tissue and muscles, both from healthy subjects (p=0.0001) and from LLMI patients (p=0.0001). In the right panel are represented males: *poly* relative expression level is significantly different among liver and muscle, both from healthy subjects (p=0.0007) and from LLMI patients (p=0.0001), between liver and adipose tissue (p=0.0001), among adipose tissue and muscles, both from healthy subjects (p=0.0001) and from LLMI patients (p=0.0001).

4.4.5.3 Tfam

The expression level of *tfam* in livers was significantly the highest among tissues, following in order by the expression level of muscles from healthy subjects, that was higher than that from patients and that from adipose tissue. However, also LLMI patients had a higher *tfam* expression level than adipose tissue, whose expression level was significantly the lowest (fig. 65).

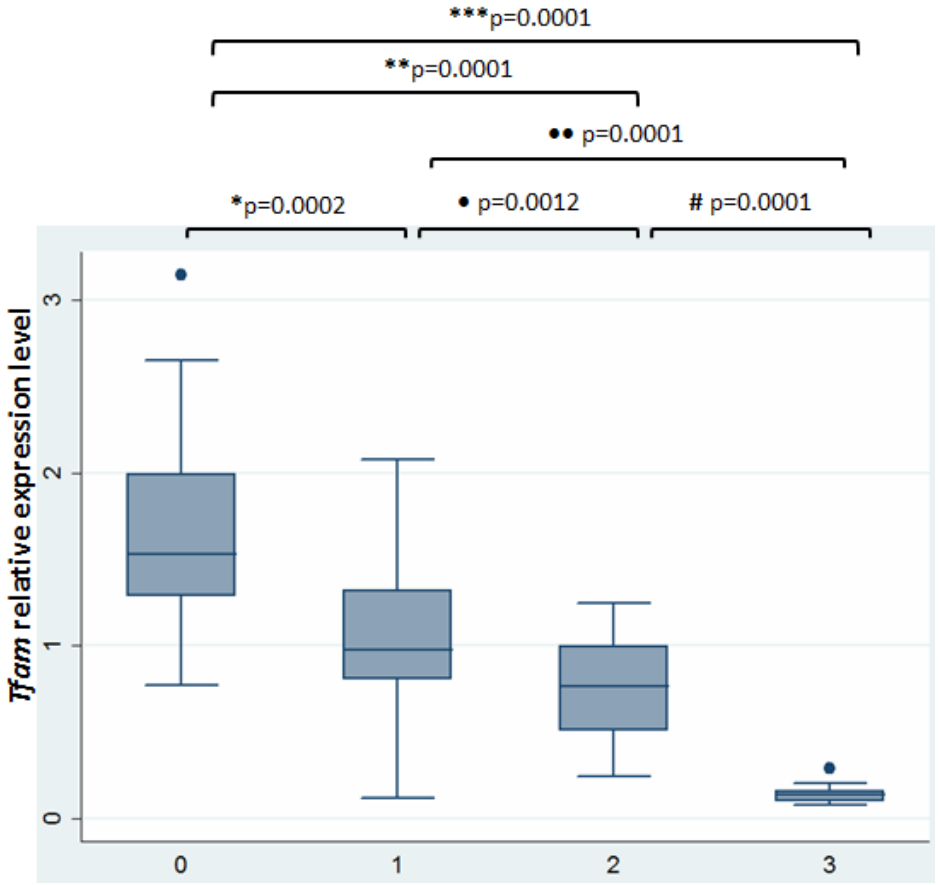

Figure 65: Comparison of *tfam* relative expression level among liver (0), muscle from healthy subjects (1), muscle from LLMI patients (2) and adipose tissue (3). To compare tissues, Kruskal-Wallis test was applied; *tfam* relative expression level is significantly higher in liver than in muscle from healthy subjects (p=0.0002), in muscle from LLMI patients (p=0.0001) and in adipose tissue (p=0.0001). *Tfam* relative expression level is significantly different between muscle from healthy subjects and LLMI patients (p=0.0012), between muscle from healthy subjects and adipose tissue (p=0.0001) and finally between muscle from LLMI patients and adipose tissue (p=0.0001).

Some differences were lost when data were analyzed by gender, as shown in fig. 66, in particular both in males and females the difference between the two group of muscles was no more significant and only in females the differences between liver and muscle from healthy subjects was not significant.

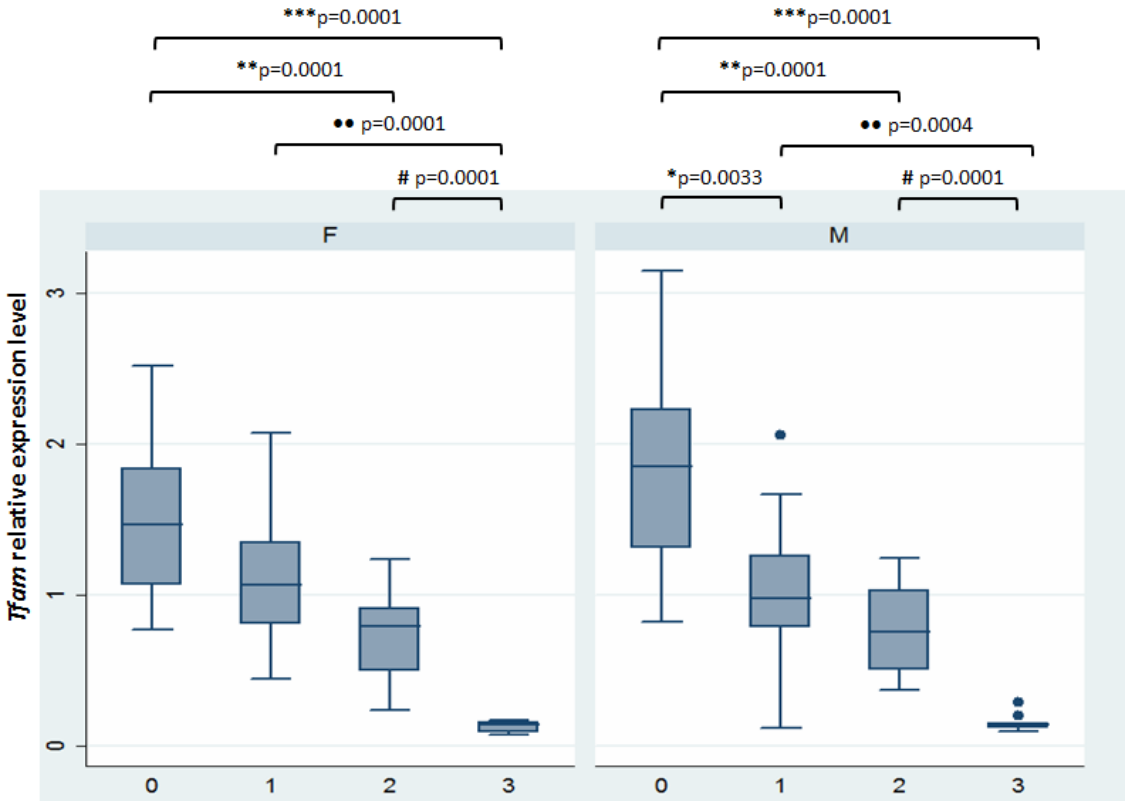

Figure 66: Comparison of *tfam* relative expression level among liver (0), muscle from healthy subjects (1), muscle from LLMI patients (2) and adipose tissue (3). To compare tissues, Kruskal-Wallis test was applied. In the left panel are represented females: *tfam* relative expression level is significantly different between liver and muscle from LLMI patients (p=0.0001), between liver and adipose tissue (p=0.0001), among adipose tissue and muscle, both from healthy subjects (p=0.0001) and from LLMI patients (p=0.0001). In the right panel are represented males: *tfam* relative expression level is significantly different among liver and muscle, both from healthy subjects (p=0.0033) and from LLMI patients (p=0.0001),between liver and adipose tissue (p=0.0001), among adipose tissue and muscles, both from healthy subjects (p=0.0004) and from LLMI patients (p=0.0001).

4.4.5.4 Nrf1

In healthy subjects muscles the expression level of *nrf1* was significantly greater than in patient muscles, in livers and in adipose tissues. Moreover, the differences in the expression level between LLMI patients, livers and adipose tissue were significative, as the difference between livers and adipose tissue (fig. 67).

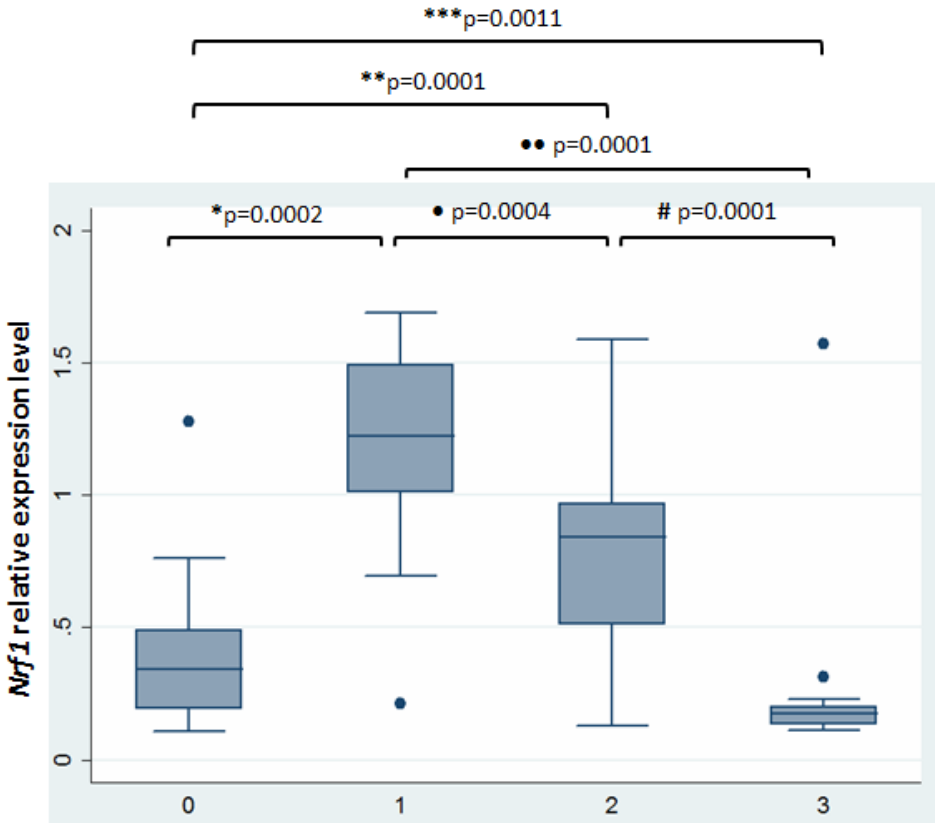

Figure 67: Comparison of *nrf1* relative expression level among liver (0), muscle from healthy subjects (1), muscle from LLMI patients (2) and adipose tissue (3). To compare tissues, Kruskal-Wallis test was applied; *nrf1* relative expression level is significantly different among liver and muscle, both from healthy subjects (p=0.0002) and from LLMI patients (p=0.0001) and between liver and adipose tissue (p=0.0011). *Nrf1* relative expression level is significantly different between muscle from healthy subjects and LLMI patients (p=0.0004), between muscle from healthy subjects and adipose tissue (p=0.0001) and finally between muscle LLMI patients and adipose tissue (p=0.0001).

Data analyzed by gender showed some differences between females and males. In particular, in females were lost the significative differences between healthy subjects and patient muscles, and among the expression level in livers and adipose tissues. Instead in males, only the difference in livers and adipose tissue *nfr1* expression level was not significative (fig. 68).

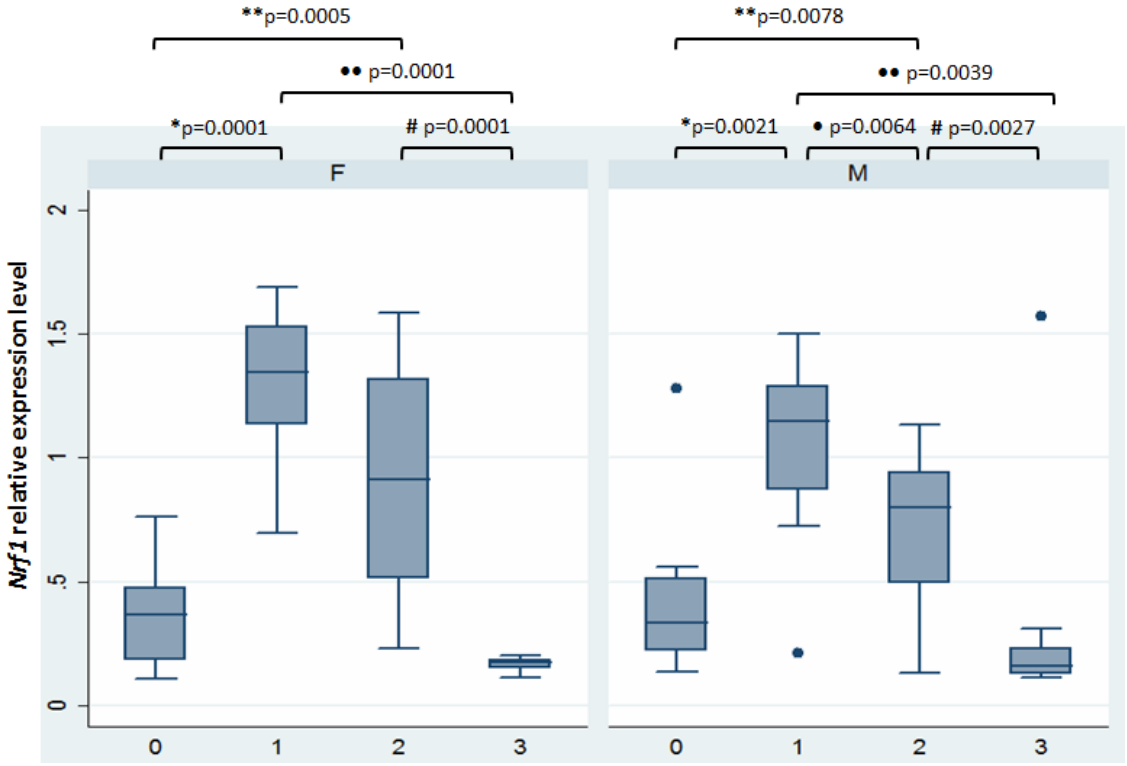

Figure 68: Comparison of *nrf1* relative expression level among liver (0), muscle from healthy subjects (1), muscle from LLMI patients (2) and adipose tissue (3). To compare tissues, Kruskal-Wallis test was applied. In the left panel are represented females: *nrf1* relative expression level is significantly different among liver and muscle, both from healthy subjects (p=0.0001) and from LLMI patients (p=0.0005) and among adipose tissues and muscles, both from healthy subjects (p=0.0001) and from LLMI patients (p=0.0001). In the right panel are represented males: *nrf1* relative expression level is significantly different among liver and muscle, both from healthy subjects (p=0.0021) and from LLMI patients (p=0.0078), between muscle from healthy subjects and muscle from LLMI patients (p=0.0064), among adipose tissue and muscles, both from healthy subjects (p=0.0039) and from LLMI patients (p=0.0027).

4.4.5.5 Twinkle

From the analysis of all samples, the expression level of *twinkle* was significantly different between livers and muscles (both healthy subjects and patients) and between adipose tissue and both groups of muscles, as illustrated in fig. 69.

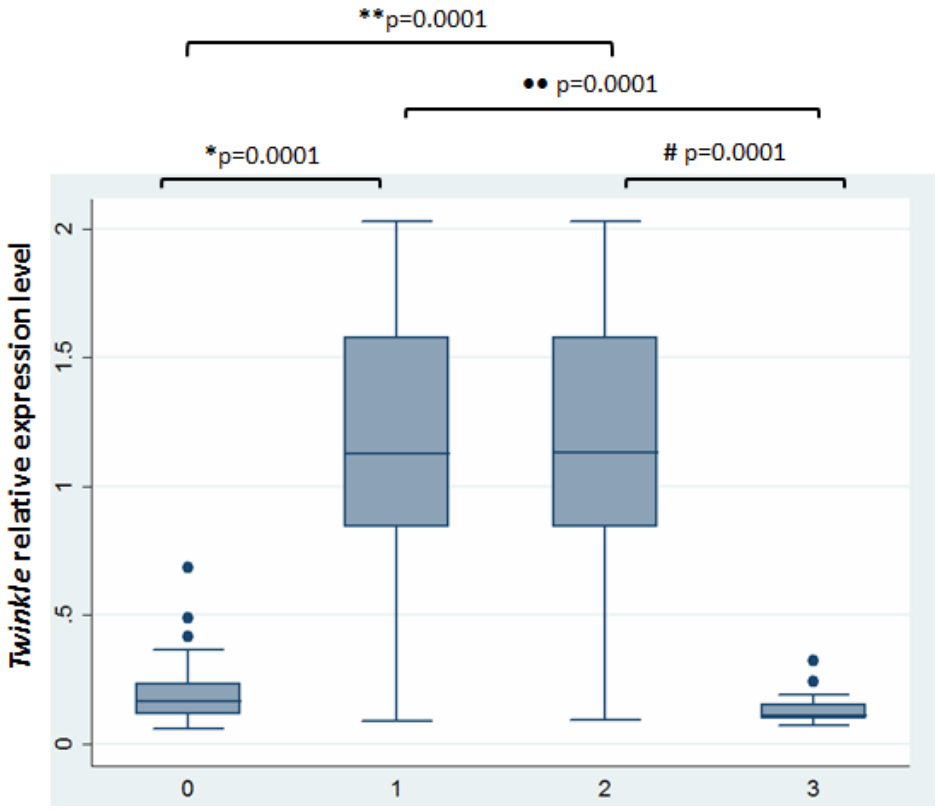

Figure 69: Comparison of *twinkle* relative expression level among liver (0), muscle from healthy subjects (1), muscle from LLMI patients (2) and adipose tissue (3). To compare tissues, Kruskal-Wallis test was applied; *twinkle* relative expression level is significantly different among liver and muscle, both from healthy subjects (p=0.0001) and from LLMI patients (p=0.0001), and among adipose tissue and muscles, both from healthy subjects (p=0.0001) and from LLMI patients (p=0.0001).

The same significant differences were found in females and males examined separately: the expression level of twinkle was lower in adipose tissues and in livers than in the groups of muscles, but no differences among livers and adipose tissues emerged. Figure 70 shows data relative to twinkle expression levels in females and males.

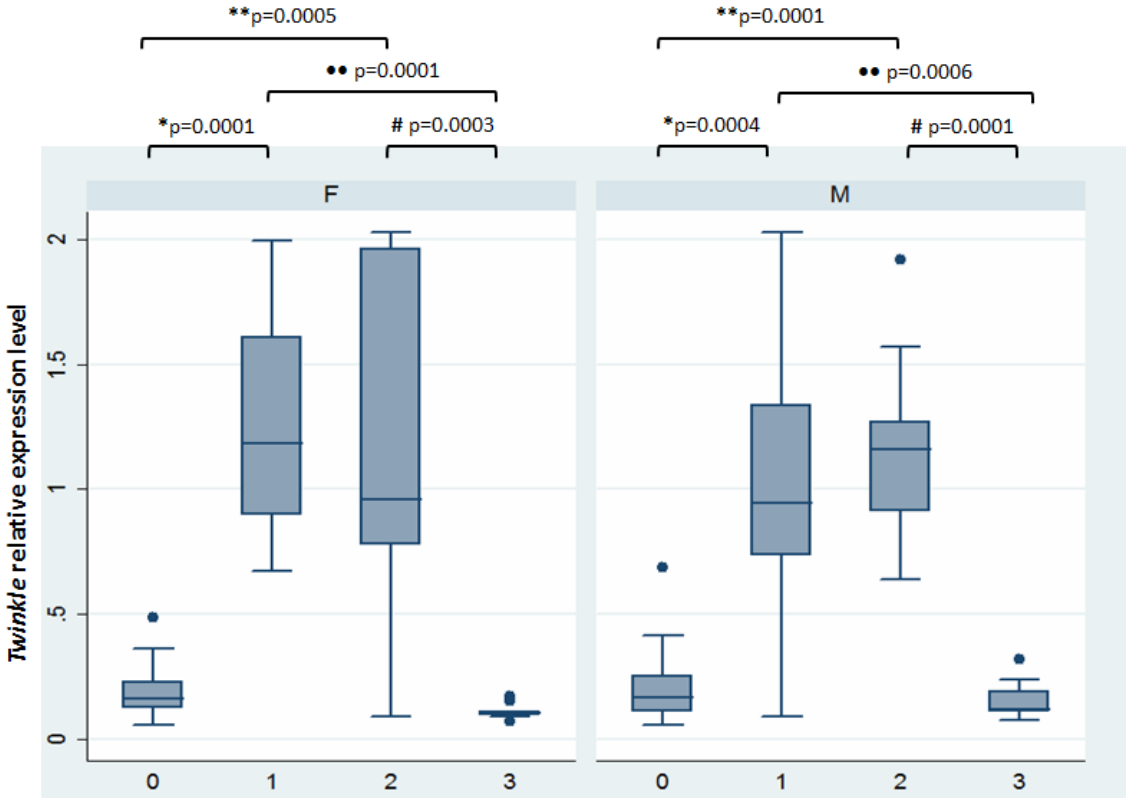

Figure 70: Comparison of *twinkle* relative expression level among liver (0), muscle from healthy subjects (1), muscle from LLMI patients (2) and adipose tissue (3). To compare tissues, Kruskal-Wallis test was applied. In the left panel are represented females: *twinkle* relative expression level is significantly different among liver and muscle, both from healthy subjects (p=0.0001) and from LLMI patients (p=0.0005) and among adipose tissue and muscles, both from healthy subjects (p=0.0001) and from LLMI patients (p=0.0003). In the right panel are represented males: *twinkle* relative expression level is significantly different among liver and muscle, both from healthy subjects (p=0.0004) and from LLMI patients (p=0.0001) and among adipose tissue and muscles, both from healthy subjects (p=0.0006) and from LLMI patients (p=0.0001).

4.4.5.6 Sirt1

As fig. 71 shows, the dissimilarities in *sirt1* expression level thought the investigated tissue were similar to those observed for *nrf1*: *sirt1* was highly expressed in muscle from healthy subjects than in muscles from LLMI patients, from livers and from adipose tissues. However, there was no significative difference in *sirt1* expression level between livers and LLMI patients, while both of their expression levels were significantly higher than that of adipose tissues.

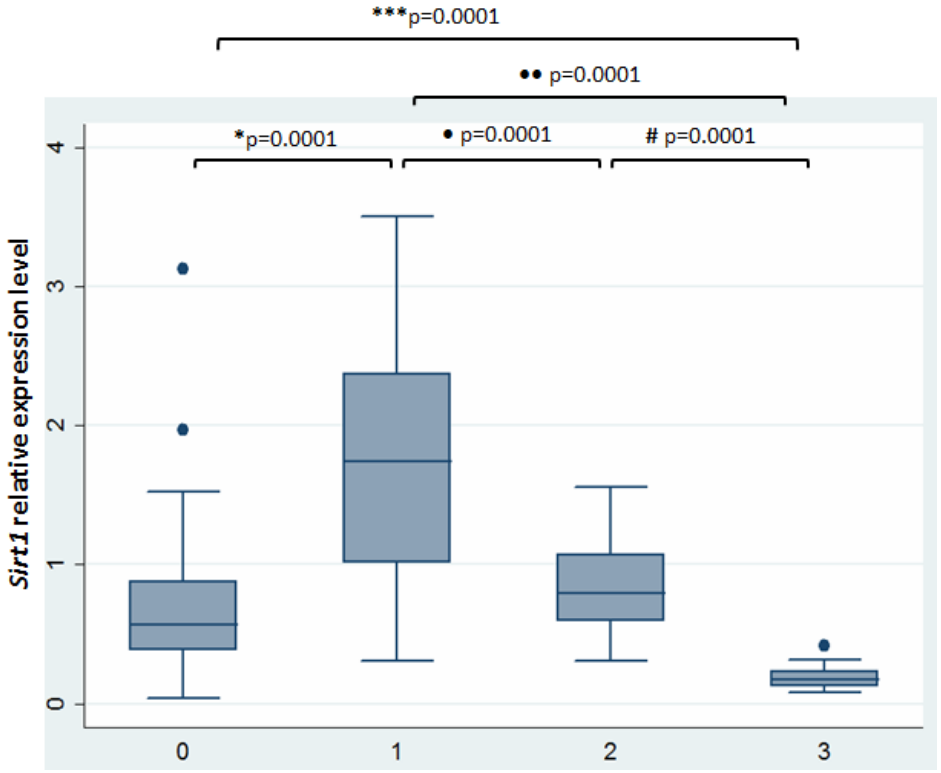

Figure 71: Comparison of *sirt1* relative expression level among liver (0), muscle from healthy subjects (1), muscle from LLMI patients (2) and adipose tissue (3). To compare tissues, Kruskal-Wallis test was applied; *sirt1* relative expression level is significantly different between liver and muscle from healthy subjects (p=0.0001), between liver and adipose tissue (p=0.0001), between muscle from healthy subjects and muscle from LLMI patients (p=0.0001), and among adipose tissues and muscles, both from healthy subjects (p=0.0001) and from LLMI patients (p=0.0001).

The same pattern of differences emerged when data were analyzed by gender, as shown in fig. 72.

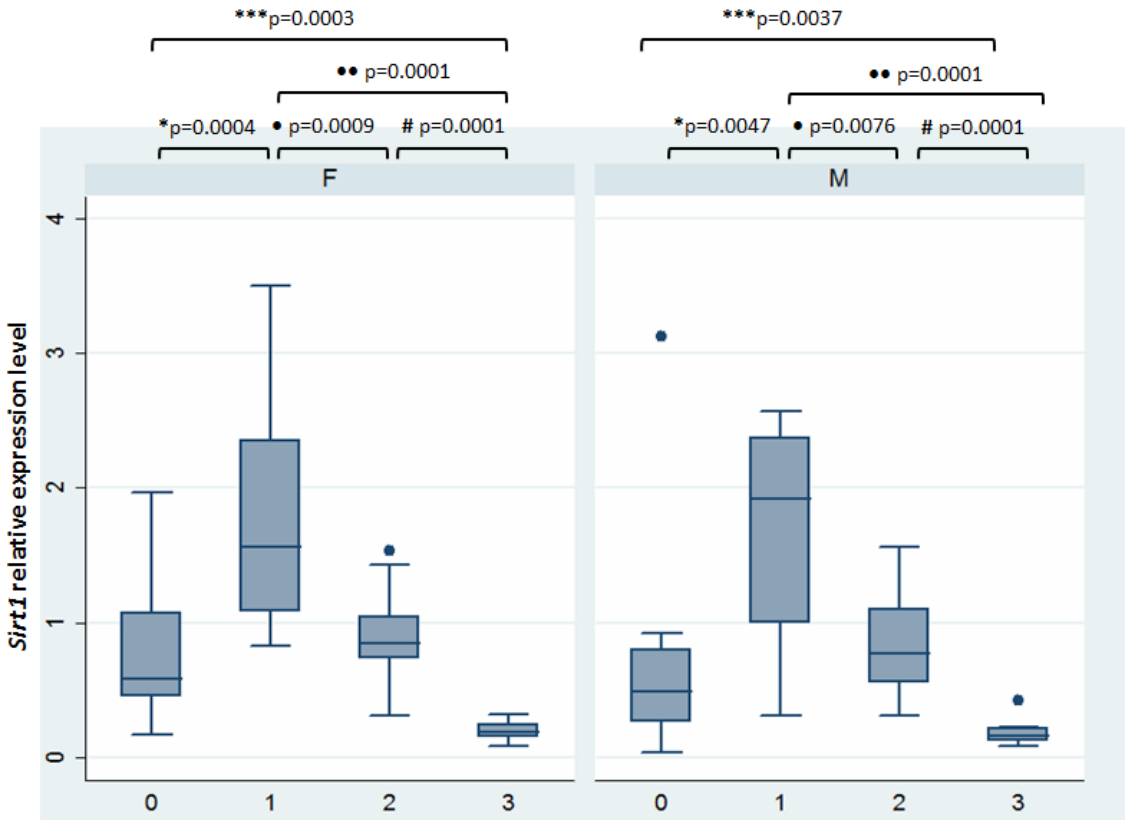

Figure 72: Comparison of *sirt1* relative expression level among liver (0), muscle from healthy subjects (1), muscle from LLMI patients (2) and adipose tissue (3). To compare tissues, Kruskal-Wallis test was applied. In the left panel are represented females: *sirt1* relative expression level is significantly different between liver and muscle from healthy subjects (p=0.0004) and between liver and adipose tissue (p=0.0003). Muscle from healthy subjects significantly differs to muscle from LLMI patients (p=0.0009), and finally significative differences exist among adipose tissue and muscles, both from healthy subjects (p=0.0001) and from LLMI patients (p=0.0001). In the right panel are represented males: *sirt1* relative expression level is significantly different between liver and muscle from healthy subjects (p=0.0047) and between liver and adipose tissue (p=0.0037). Muscle from healthy subjects significantly differs to muscles from LLMI patients (p=0.0076), and finally significative differences exist among adipose tissue and muscles, both from healthy subjects (p=0.0001) and from LLMI patients (p=0.0001).

4.4.5.7 Mfn2

Regarding the expression level of *mfn2*, it was found different between all the tissues considered: the expression levels of *mfn2* in livers was dissimilar from that of both the groups of muscle and from that of adipose tissue, that in turn was lower than that of muscles, that, finally, were different also among them (fig. 73).

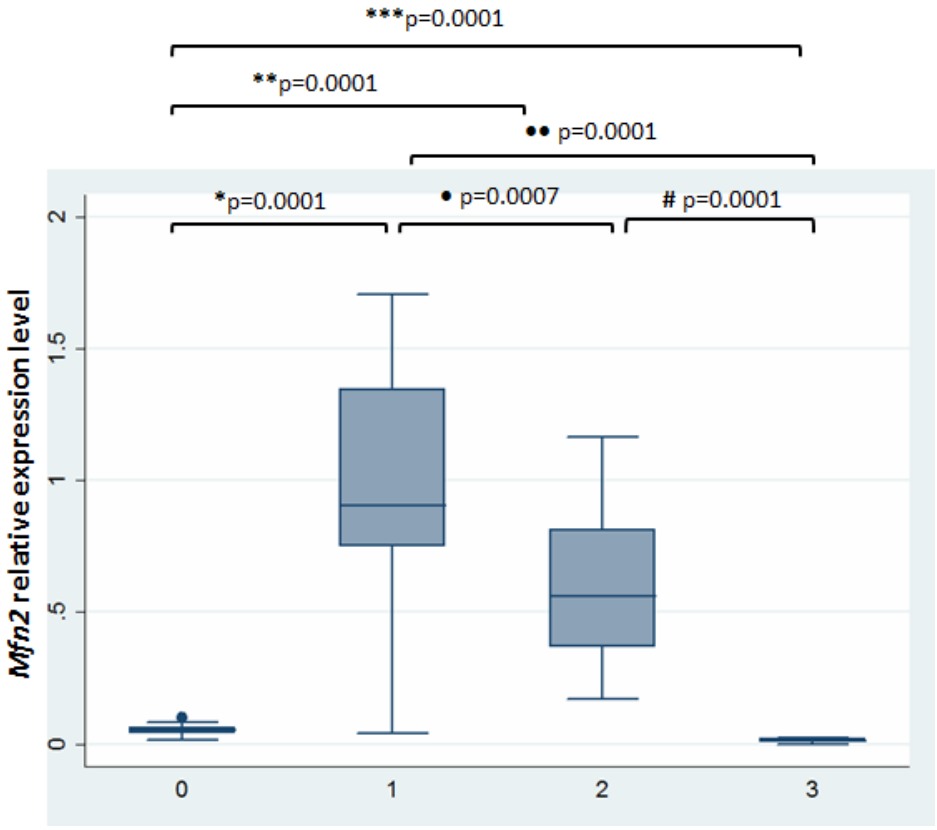

Figure 73: Comparison of *mfn2* relative expression level among liver (0), muscle from healthy subjects (1), muscle from LLMI patients (2) and adipose tissue (3). To compare tissues, Kruskal-Wallis test was applied; *mfn2* relative expression level is significantly different among liver and muscle, both from healthy subjects (p=0.0001) and from LLMI patients (p=0.0001) and between liver and adipose tissue (p=0.0001). *Mnf2* relative expression level is significantly different also between muscle from healthy subjects and from LLMI patients (p=0.0007), and among adipose tissue and muscles, both from healthy subjects (p=0.0001) and from LLMI patients (p=0.0001).

These divergences in the expression level of mfn2 were the same in females analyzed alone, whereas in males the difference between the two groups of muscles disappeared, as it can be seen in fig. 74.

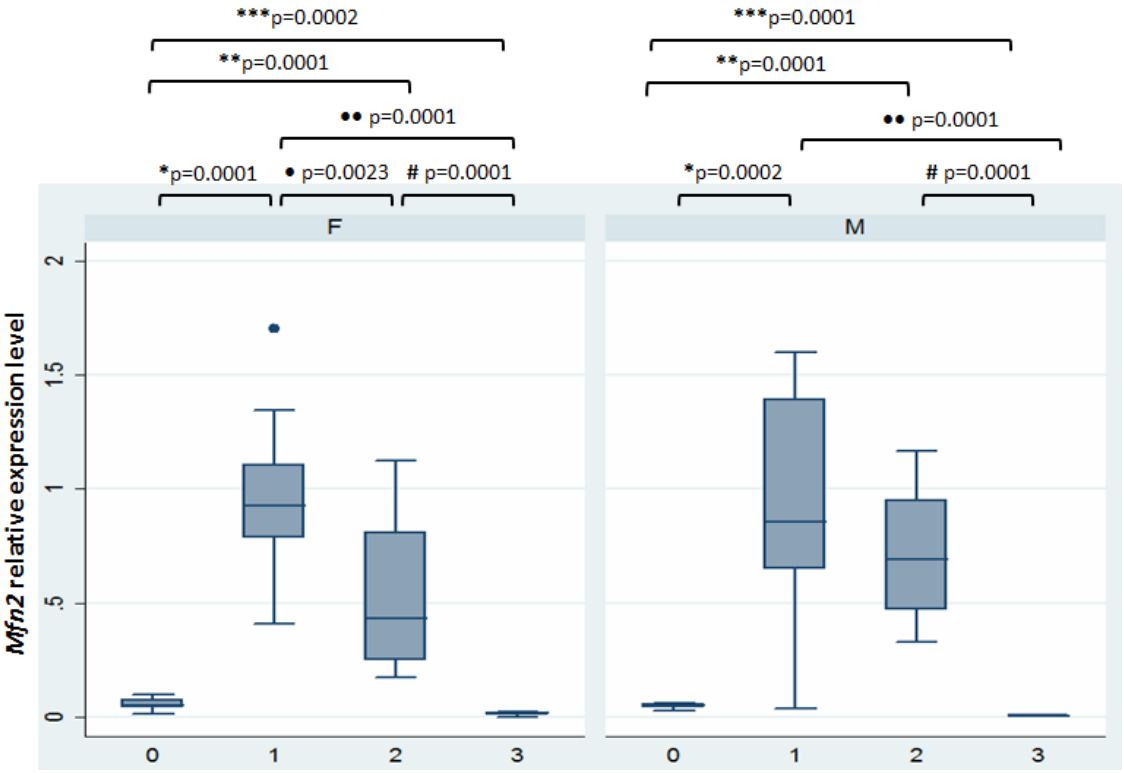

Figure 74: Comparison of *mfn2* relative expression level among liver (0), muscle from healthy subjects (1), muscle from LLMI patients (2) and adipose tissue (3). To compare tissues, Kruskal-Wallis test was applied. In the left panel are represented females: *mfn2* relative expression level is significantly different among liver and muscle, both from healthy subjects (p=0.0001) and from LLMI patients (p=0.0001), between liver and adipose tissue (p=0.0002), between muscle from healthy subjects and muscle from LLMI patients (p=0.0023), and finally among adipose tissue and muscles, both from healthy subjects (p=0.0001) and from LLMI patients (p=0.0001). In the right panel are represented males: *mfn2* relative expression level is significantly different among liver and muscle, both from healthy subjects (p=0.0002) and from LLMI patients (p=0.0001), between liver and adipose tissue (p=0.0001), and finally among adipose tissue and muscles, both from healthy subjects (p=0.0001) and from LLMI patients (p=0.0001).

4.4.5.8 Opa1

Opa1 expression level was higher in liver samples than in adipose tissue samples, that showed a lower expression level also compared to both groups of muscle samples (fig. 75).

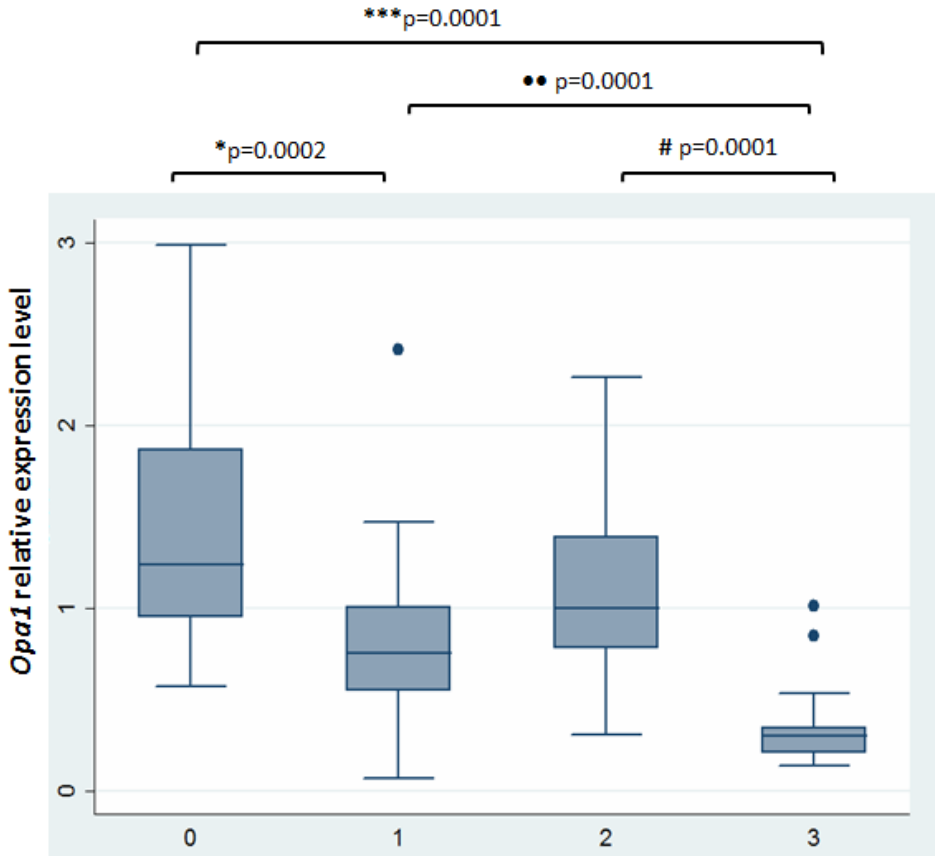

Figure 75: Comparison of *opa1* relative expression level among liver (0), muscle from healthy subjects (1), muscle from LLMI patients (2) and adipose tissue (3). To compare tissues, Kruskal-Wallis test was applied; *opa1* relative expression level is significantly different between liver and muscle from healthy subjects (p=0.0002), between liver and adipose tissue (p=0.0001), and among adipose tissue and muscles, both from healthy subjects (p=0.0001) and from LLMI patients (p=0.0001).

When genders were considered independently one to the other, a mismatched pattern of differences emerged, as shown in fig. 76. In more detail, in females, opa1 was significantly less expressed in adipose tissue with respect to liver and muscle. In males, instead, there were significative differences between the livers and the others tissues, and among the patients muscles and the adipose tissues.

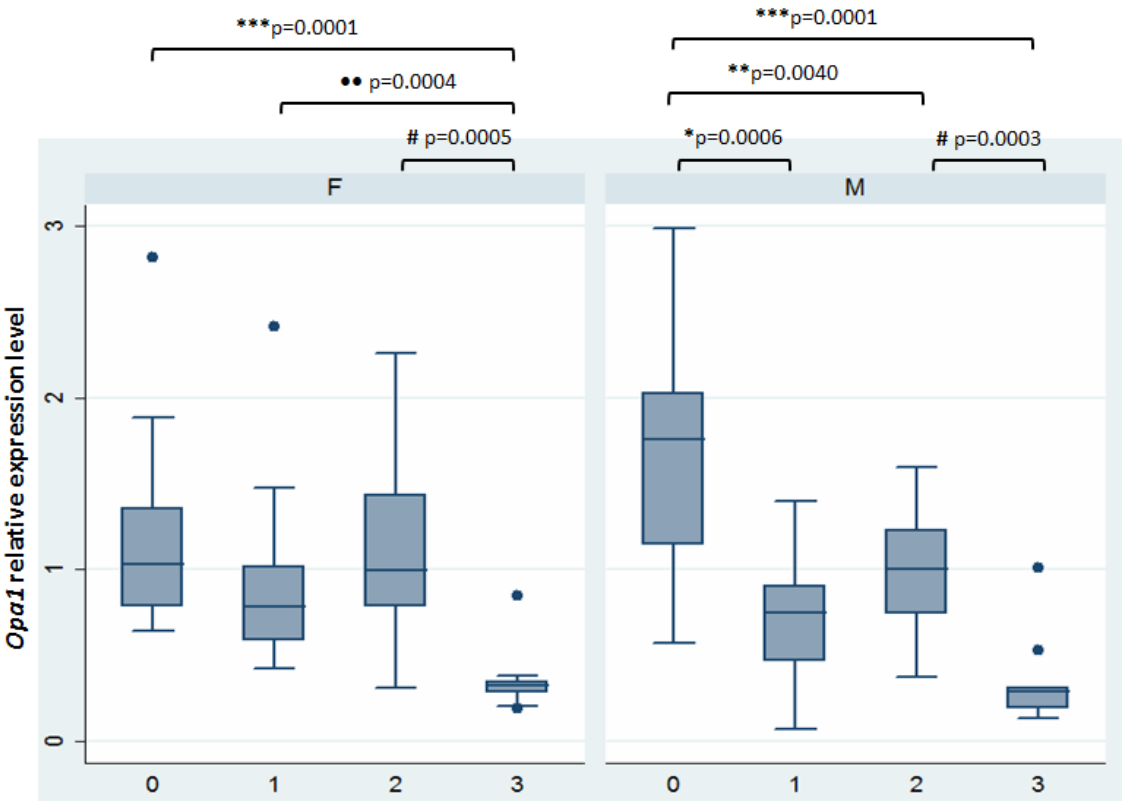

Figure 76: Comparison of *opa1* relative expression level among liver (0), muscle from healthy subjects (1), muscle from LLMI patients (2) and adipose tissue (3). To compare tissues, Kruskal-Wallis test was applied. In the left panel are represented females: *opa1*relative expression level is significantly different between adipose tissue and liver (p=0.0001) and among adipose tissue and muscles, both from healthy subjects (p=0.0004) and from LLMI patients (p=0.0005). In the right panel are represented males: *opa1* relative expression level is significantly different among liver and muscle, both from healthy subjects (p=0.0006) and from LLMI patients (p=0.0040), between liver and adipose tissue (p=0.0001), and finally between adipose tissue and muscle from LLMI patients (p=0.0003).

4.4.5.9 Fis1

Significative differences emerged in the expression level of *fis1*, in particular *fis1* was less expressed in liver and adipose tissue with respect to both the groups of muscles, nevertheless, the expression level of *fis1* in liver was higher than in adipose tissue, as can be seen in fig. 77.

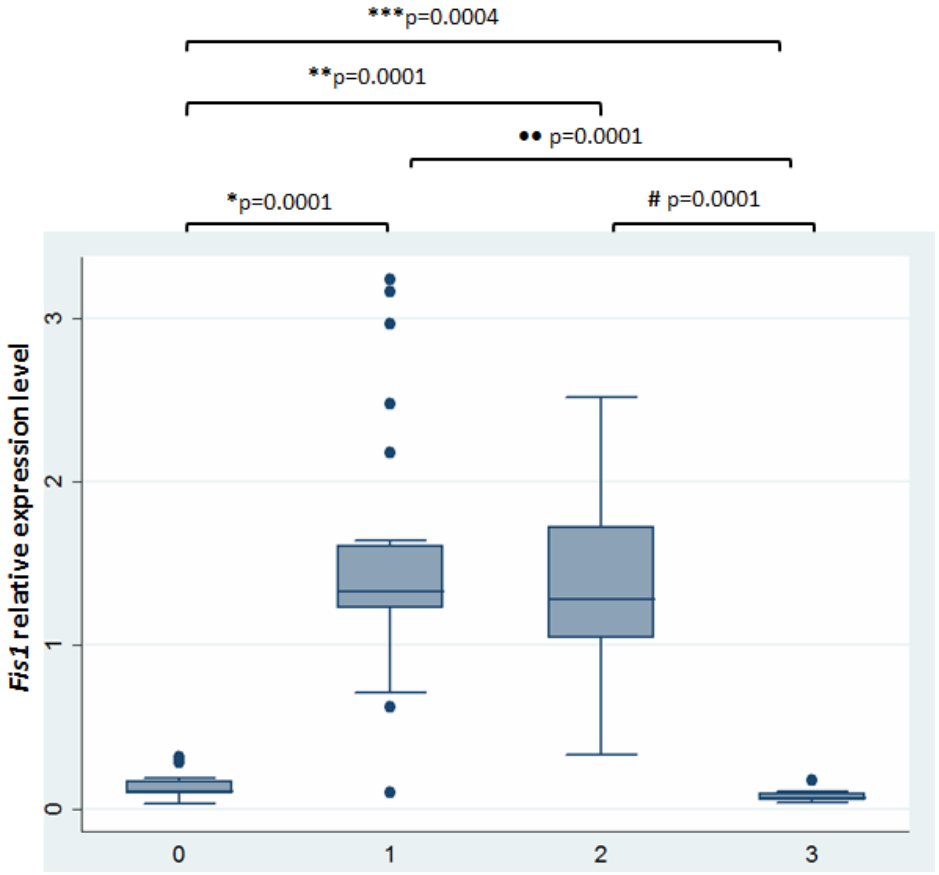

Figure 77: Comparison of *fis1* relative expression level among liver (0), muscle from healthy subjects (1), muscle from LLMI patients (2) and adipose tissue (3). To compare tissues, Kruskal-Wallis test was applied; *fis1* relative expression level is significantly different among liver and muscle, both from healthy subjects (p=0.0001) and from LLMI patients (p=0.0001) and between liver and adipose tissue (p=0.0004). *Fis1* relative expression level is also significantly different among adipose tissue and muscles, both from healthy subjects (p=0.0001) and from LLMI patients (p=0.0001).

The same differences emerged when data were analyzed by gender, but both in males and in females, the difference in *fis1* expression level between liver samples and adipose tissue samples was not still significant, whereas all the others differences were significantly maintained, as illustrated in fig. 78.

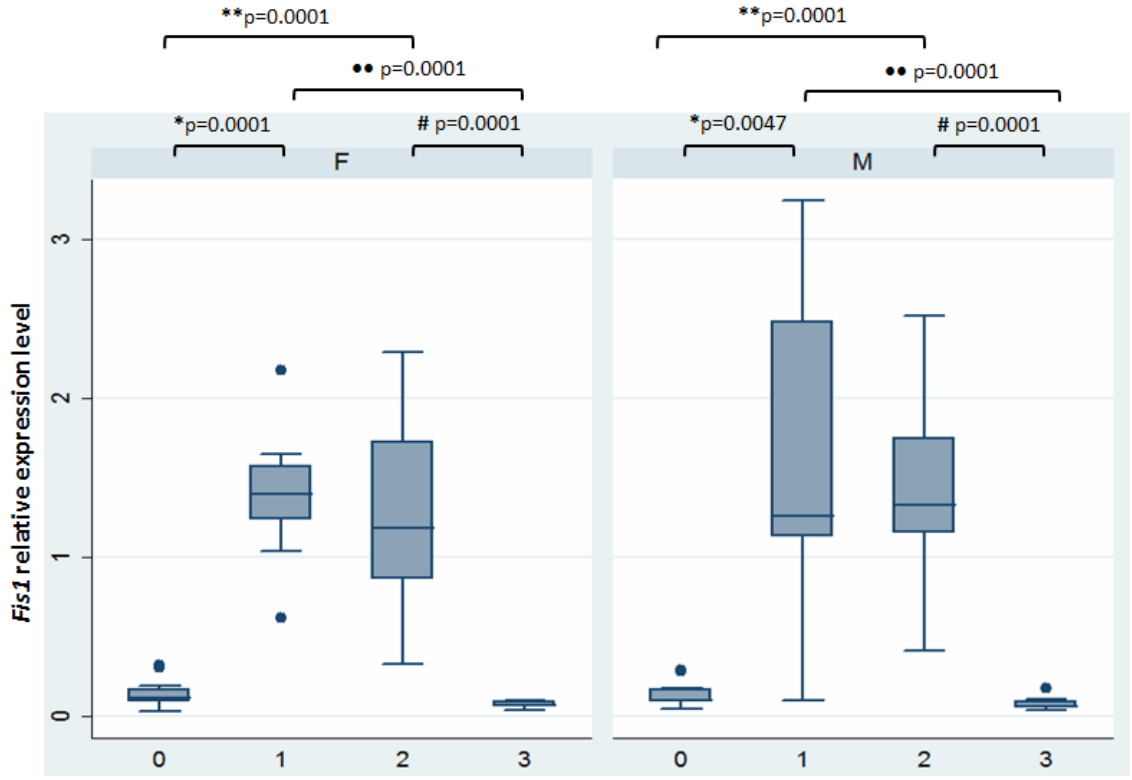

Figure 78: Comparison of *fis1* relative expression level among liver (0), muscle from healthy subjects (1), muscle from LLMI patients (2) and adipose tissue (3). To compare tissues, Kruskal-Wallis test was applied. In the left panel are represented females: *fis1* relative expression level is significantly different among liver and muscle, both from healthy subjects (p=0.0001) and from LLMI patients (p=0.0001) and among adipose tissue and muscles, both from healthy subjects (p=0.0001) and from LLMI patients (p=0.0003). In the right panel are represented males: *fis1* relative expression level is significantly different among liver and muscle, both from healthy subjects (p=0.0047) and from LLMI patients (p=0.0001) and among adipose tissue and muscles, both from healthy subjects (p=0.0001) and from LLMI patients (p=0.0001).

4.4.5.10 Pink1

Pink1 was less expressed in adipose tissue with respect to muscle and liver, but the liver expression level of *pink1* was lower than that of muscles from healthy subjects and patients (fig. 79).

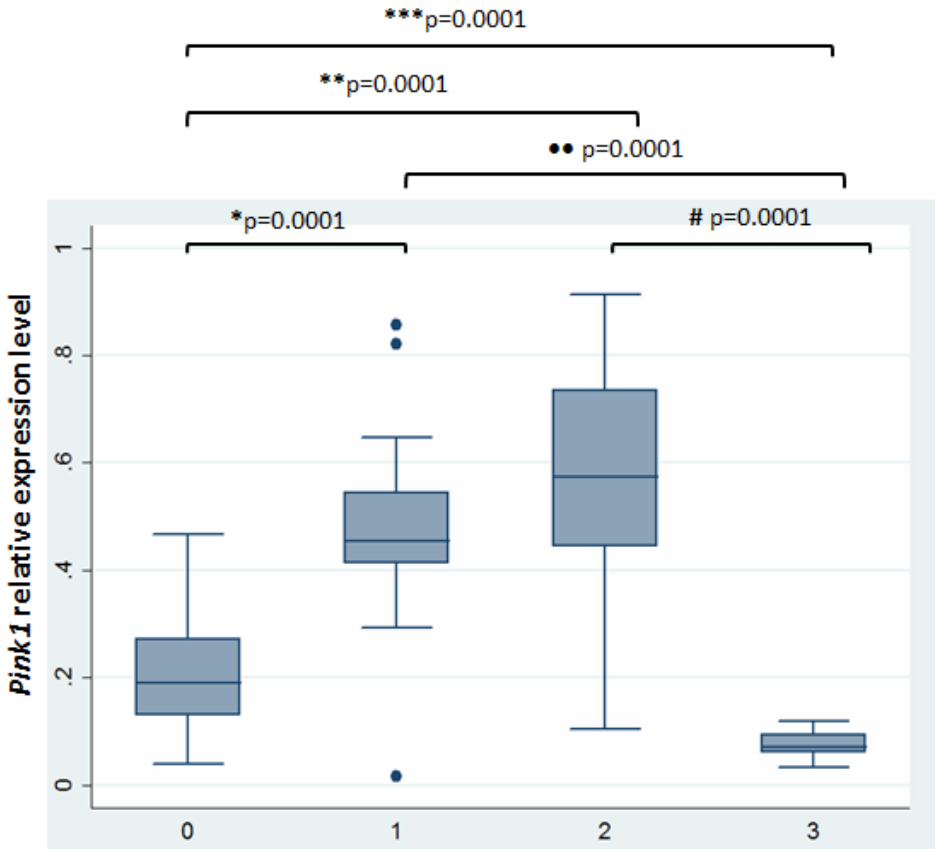

Figure 79: Comparison of *pink1* relative expression level among liver (0), muscle from healthy subjects (1), muscle from LLMI patients (2) and adipose tissue (3). To compare tissues, Kruskal-Wallis test was applied; *pink1* relative expression level is significantly different among liver and muscle, both from healthy subjects (p=0.0001) and from LLMI patients (p=0.0001) and between liver and adipose tissue (p=0.0001). *Pink1* relative expression level is also significantly different among adipose tissue and muscles, both from healthy subjects (p=0.0001) and from LLMI patients (p=0.0001).

If genders were considered separately, the differences in *pink1* expression levels among the 4 groups were maintained both for females and males were the same he same as those that emerged from the total samples, as shown in fig. 80.

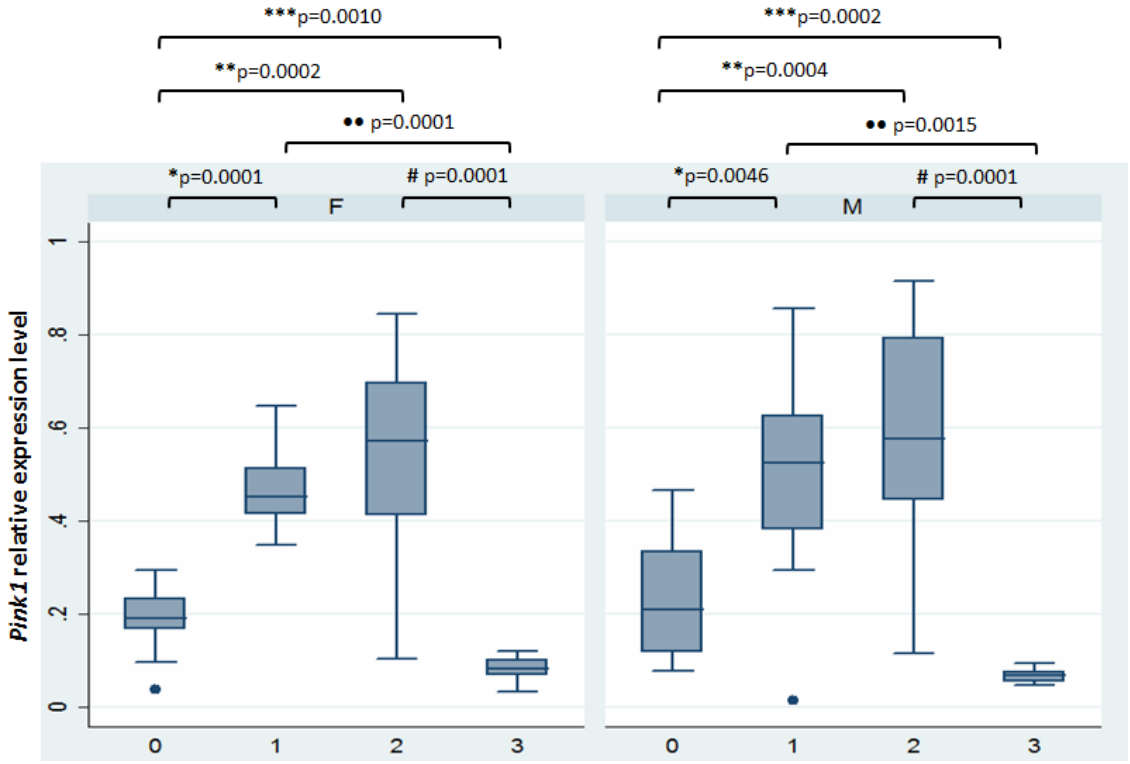

Figure 80: Comparison of *pink1* relative expression level among liver (0), muscle from healthy subjects (1), muscle from LLMI patients (2) and adipose tissue (3). To compare tissues, Kruskal-Wallis test was applied. In the left panel are represented females: *pink1* relative expression level is significantly different among liver and muscle, both from healthy subjects (p=0.0001) and from LLMI patients (p=0.0002), between liver and adipose tissue (p=0.0010), among adipose tissue and muscle, both from healthy subjects (p=0.0001) and from LLMI patients (p=0.0001). In the right panel are represented males: *pink1* relative expression level is significantly different among liver and muscle, both from healthy subjects (p=0.0046) and from LLMI patients (p=0.0004), between liver and adipose tissue (p=0.0002), among adipose tissue and muscle, both from healthy subjects (p=0.0015) and from LLMI patients (p=0.0001).

4.4.5.11 Beclin

Similarly to *poly*, *twinkle*, *fis1* and *pink1*, the expression level of *beclin* was lower in adipose tissue with respect to muscles and to livers, that in turn expressed less *beclin* compared to muscles from healthy subjects and patients. Data can be observed in fig. 81.

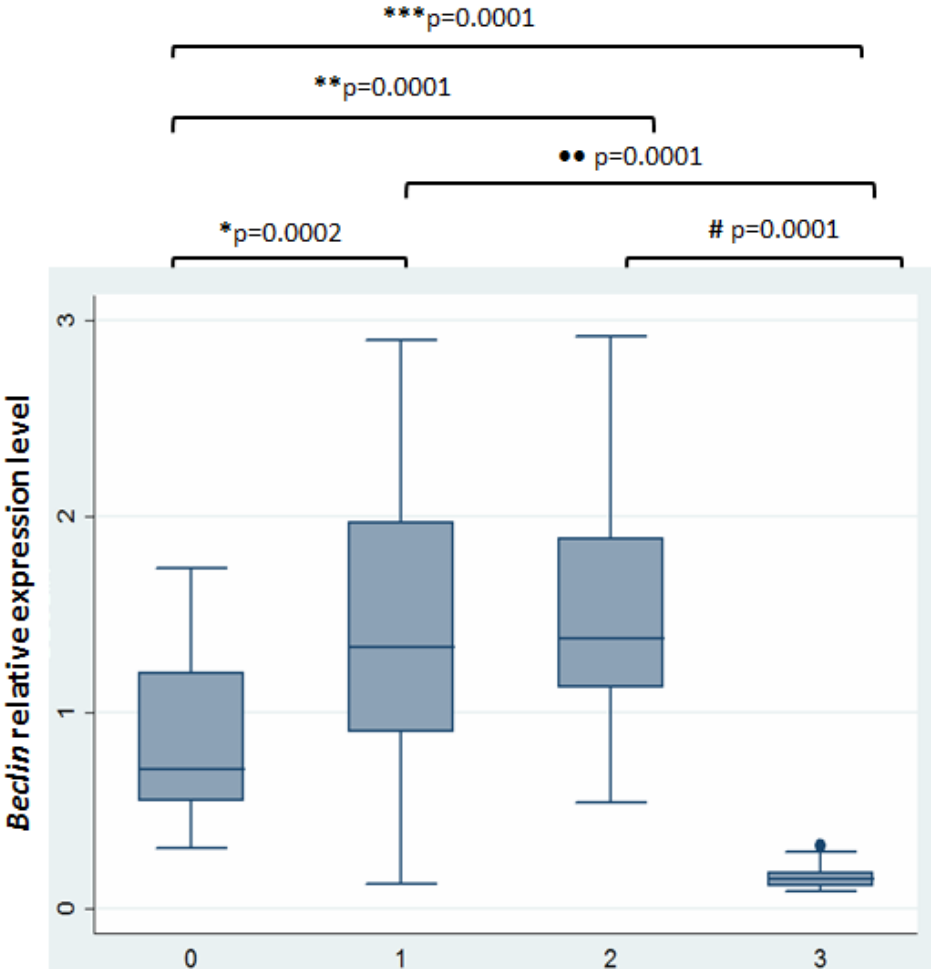

Figure 81: Comparison of *beclin* relative expression level among liver (0), muscle from healthy subjects (1), muscle from LLMI patients (2) and adipose tissue (3). To compare tissues, Kruskal-Wallis test was applied; *beclin* relative expression level is significantly different among liver and muscle, both from healthy subjects (p=0.0002) and from LLMI patients (p=0.0001) and between liver and adipose tissue (p=0.0001). *Beclin* relative expression level is also significantly different among adipose tissue and muscle, both from healthy subjects (p=0.0001) and from LLMI patients (p=0.0001).

For females, the pattern of differences between the tissues was maintained when they were investigated alone, for male, instead, the expression level of *beclin* in liver was not significantly different from the expression level of the muscles of healthy subjects, while all the others dissimilarities were still significative, fig. 82.

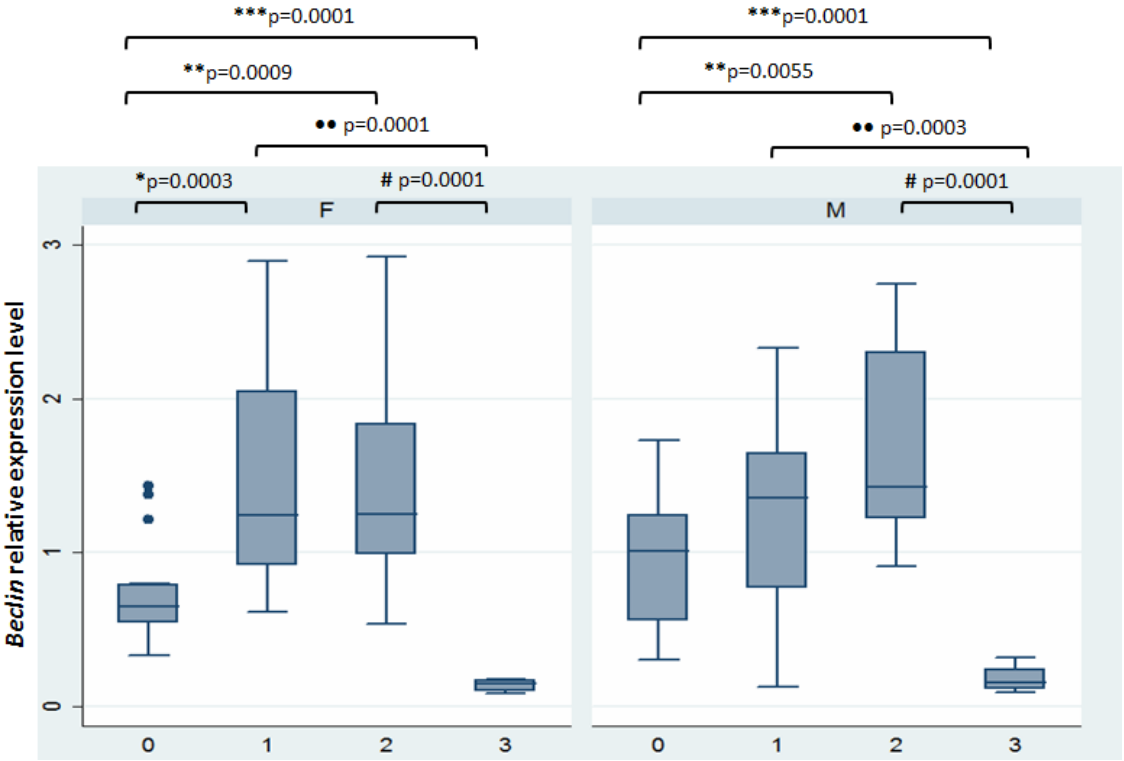

Figure 82: Comparison of *beclin* relative expression level among liver (0), muscle from healthy subjects (1), muscle from LLMI patients (2) and adipose tissue (3). To compare tissues, Kruskal-Wallis test was applied. In the left panel are represented females: *beclin* relative expression level is significantly different among liver and muscle, both from healthy subjects (p=0.0003) and from LLMI patients (p=0.0009), between liver and adipose tissue (p=0.0001), among adipose tissue and muscle, both from healthy subjects (p=0.0001) and from LLMI patients (p=0.0001). In the right panel are represented males: *beclin* relative expression level is significantly different between liver and muscle from LLMI patients (p=0.0055), between liver and adipose tissue (p=0.0001), among adipose tissue and muscle, both from healthy subjects (p=0.0003) and from LLMI patients (p=0.0001).

4.4.5.12 Ambra

Liver expressed less *ambra* than muscle (both from healthy subjects and from LLMI patients), but more than adipose tissue, that in turn, showed significant lower level of *ambra* than muscle, as showed in fig. 83.

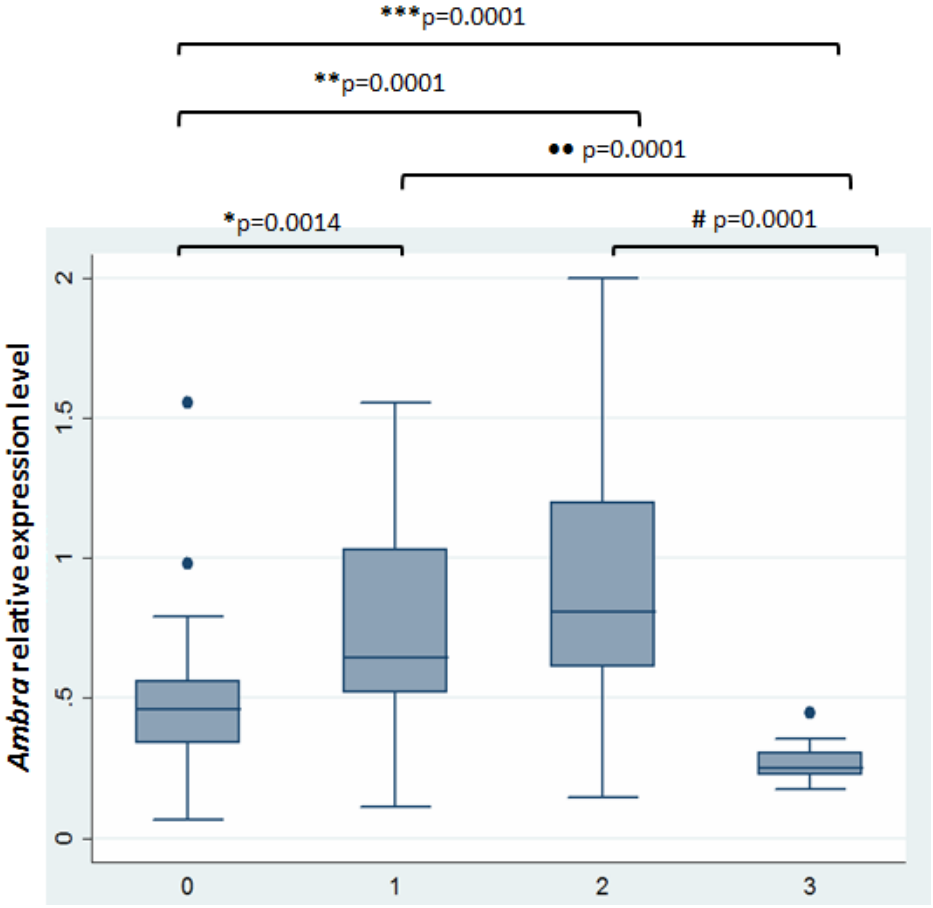

Figure 83: Comparison of *ambra* relative expression level among liver (0), muscle from healthy subjects (1), muscle from LLMI patients (2) and adipose tissue (3). To compare tissues, Kruskal-Wallis test was applied; *ambra* relative expression level is significantly different among liver and muscle, both from healthy subjects (p=0.0014) and from LLMI patients (p=0.0001) and between liver and adipose tissue (p=0.0001). *Ambra* relative expression level is also significantly different among adipose tissue and muscle, both from healthy subjects (p=0.0001) and from LLMI patients (p=0.0001).

In females, *ambra* expression levels were significative different between liver and muscle and between adipose tissue and muscle, but not between liver and adipose tissues, whereas in males, *ambra* expression level was significantly dissimilar between adipose tissue compared to liver and to muscle, but liver differed only to muscle from patients and not from healthy subjects (fig. 84).

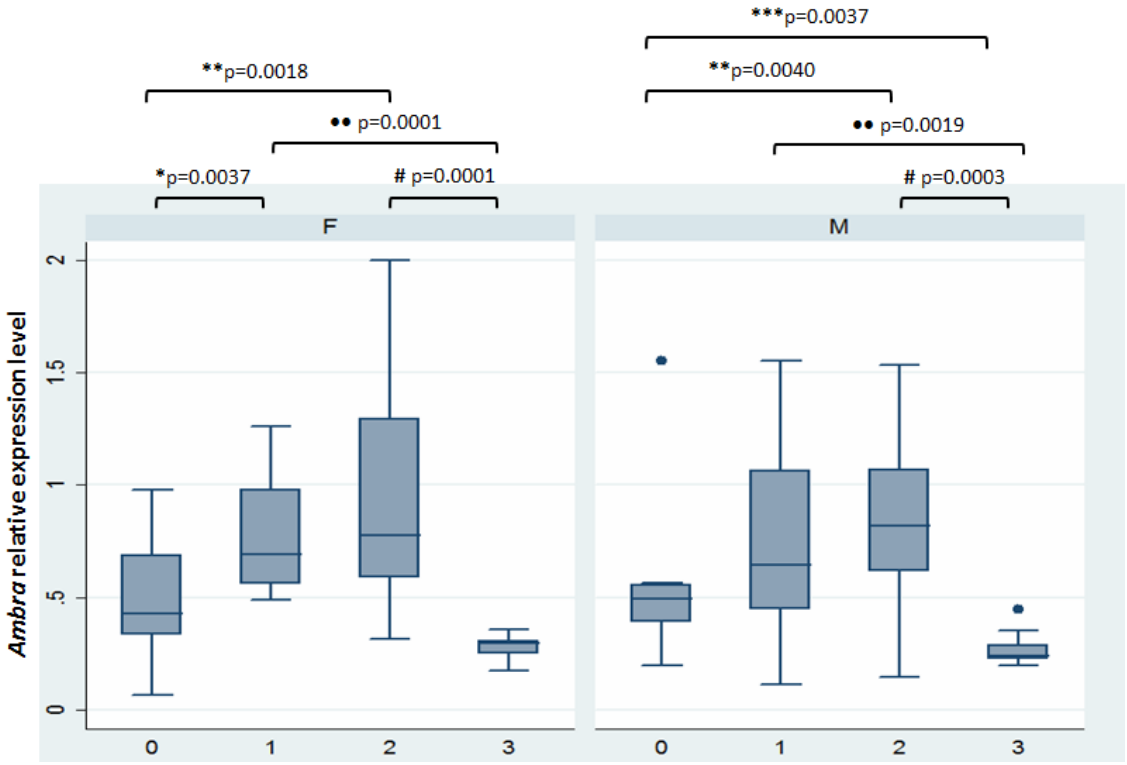

Figure 84: Comparison of *ambra* relative expression level among liver (0), muscle from healthy subjects (1), muscle from LLMI patients (2) and adipose tissue (3). To compare tissues, Kruskal-Wallis test was applied. In the left panel are represented females: *ambra* relative expression level is significantly different among liver and muscle, both from healthy subjects (p=0.0037) and from LLMI patients (p=0.0018), and among adipose tissue and muscle, both from healthy subjects (p=0.0001) and from LLMI patients (p=0.0001). In the right panel are represented males: *ambra* relative expression level is significantly different between liver and muscle from LLMI patients (p=0.0040), between liver and adipose tissue (p=0.0037), and finally among adipose tissue and muscle, both from healthy subjects (p=0.0019) and from LLMI patients (p=0.0003).

4.4.5.13 Pik3cd

In the expression level of pik3cd, some differences between tissues were found: muscles from LLMI patients showed lower expression levels with respect to muscles from healthy subjects, adipose tissues and livers, as shown in figure 85. These differences were completely lost when data were analyzed by gender (data not shown).

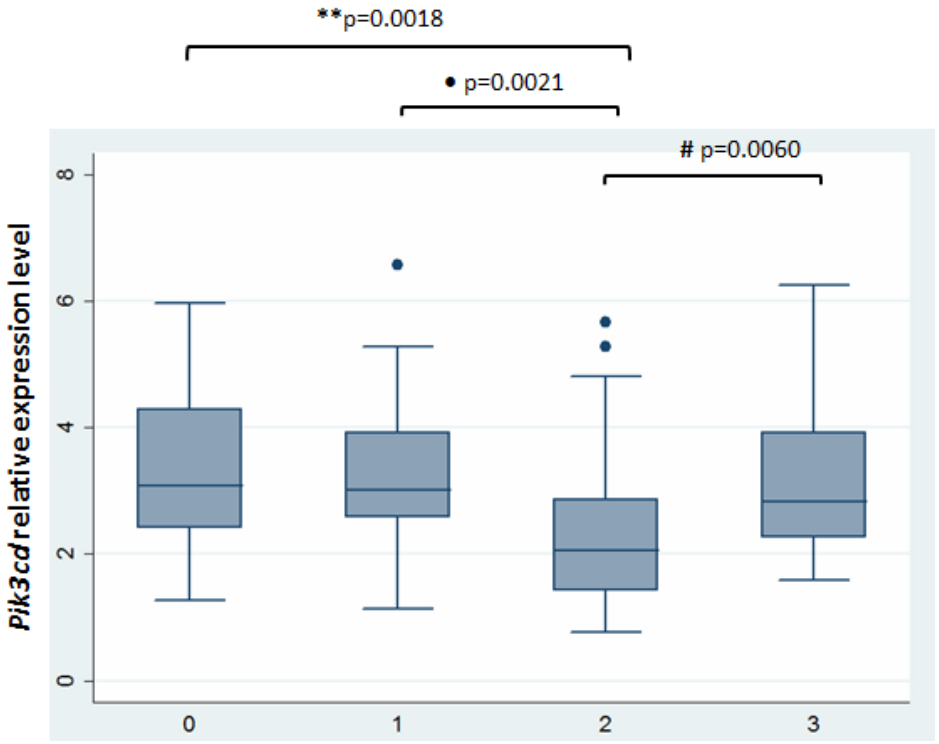

Figure 85: Comparison of *pik3cd* relative expression level among liver (0), muscle from healthy subjects (1), muscle from LLMI patients (2) and adipose tissue (3). To compare tissues, Kruskal-Wallis test was applied; *pik3cd* relative expression level is significantly different between liver and muscle from LLMI patients (p=0.0018), between muscles from healthy subjects and from LLMI patients (p=0.0021) and between adipose tissue and muscle and from LLMI patients (p=0.0060).

4.4.5.14 Lonp

A significative difference emerged between the expression level of *lonp* in liver and in muscle (for both the group of muscles considered), as well as for adipose tissue. Instead, no significative difference emerged between adipose tissue and liver.

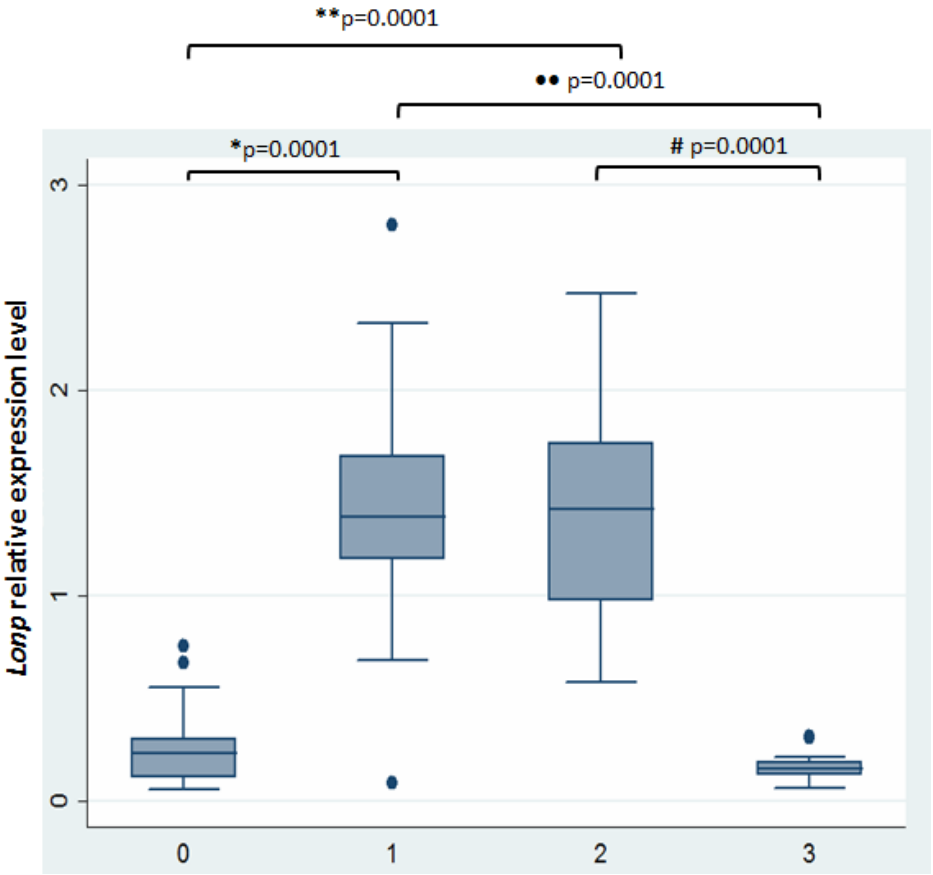

Figure 86: Comparison of *lonp* relative expression level among liver (0), muscle from healthy subjects (1), muscle from LLMI patients (2) and adipose tissue (3). To compare tissues, Kruskal-Wallis test was applied; *lonp* relative expression level is significantly different among liver and muscle, both from healthy subjects (p=0.0001) and from LLMI patients (p=0.0001). *Lonp* relative expression level is also significantly different among adipose tissue and muscle, both from healthy subjects (p=0.0001) and from LLMI patients (p=0.0001).

The same results emerged when gender were considered separately, as can be observed in figure 87.

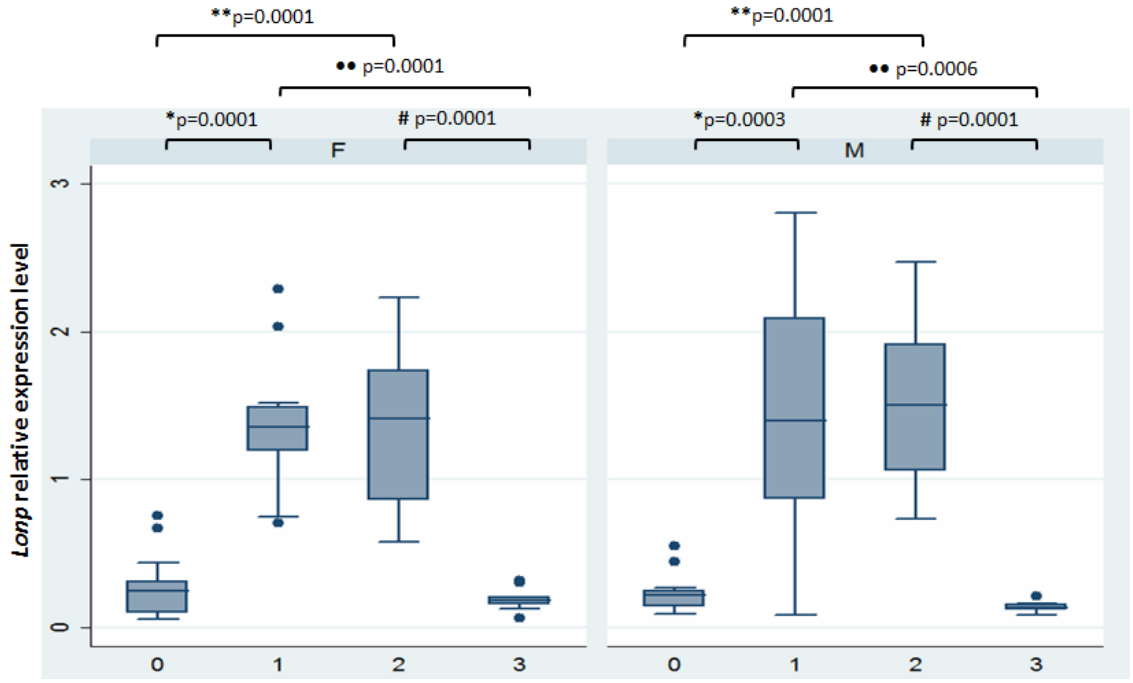

Figure 87: Comparison of *lonp* relative expression level among liver (0), muscle from healthy subjects (1), muscle from LLMI patients (2) and adipose tissue (3). To compare tissues, Kruskal-Wallis test was applied. In the left panel are represented females: *lonp* relative expression level is significantly different among liver and muscle, both from healthy subjects (p=0.0001) and from LLMI patients (p=0.0001) and among adipose tissue and muscle, both from healthy subjects (p=0.0001) and from LLMI patients (p=0.0003). In the right panel are represented males: *lonp* relative expression level is significantly different among liver and muscle, both from healthy subjects (p=0.0003) and from LLMI patients (p=0.0001) and among adipose tissue and muscle, both from healthy subjects (p=0.0006) and from LLMI patients (p=0.0001).

4.4.5.15 Nos3

A significative difference emerged in the expression level of *nos3* between muscles from healthy subjects and from patients. The expression level of *nos3* was higher in the former also than liver and adipose tissue, as can be seen in figure 88.

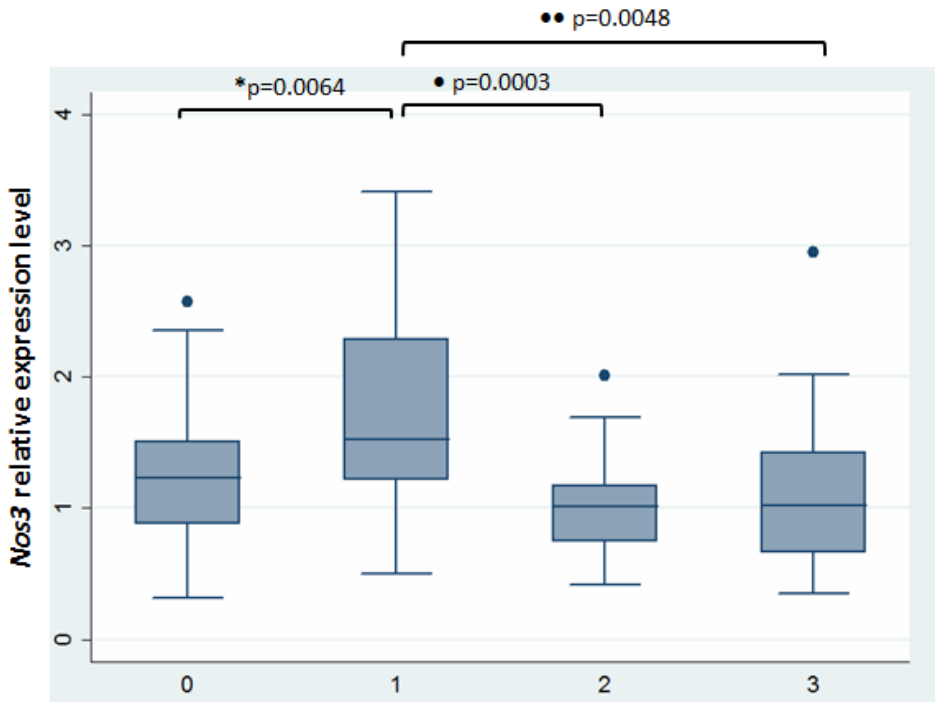

Figure 88: Comparison of *nos3* relative expression level among liver (0), muscle from healthy subjects (1), muscle from LLMI patients (2) and adipose tissue (3). To compare tissues, Kruskal-Wallis test was applied; *nos3* relative expression level is significantly different between muscle from healthy subjects and from LLMI patients (p=0.0003), and between muscle from healthy subjects and liver (p=0.0064). *Nos3* relative expression level is also significantly different between adipose tissue and muscle from healthy subjects (p=0.0048).

When data were divided and analyzed by gender, these differences were still found significant in females, but not in males, that did not show any significant difference in the expression level of *nos3* between the investigated tissues.

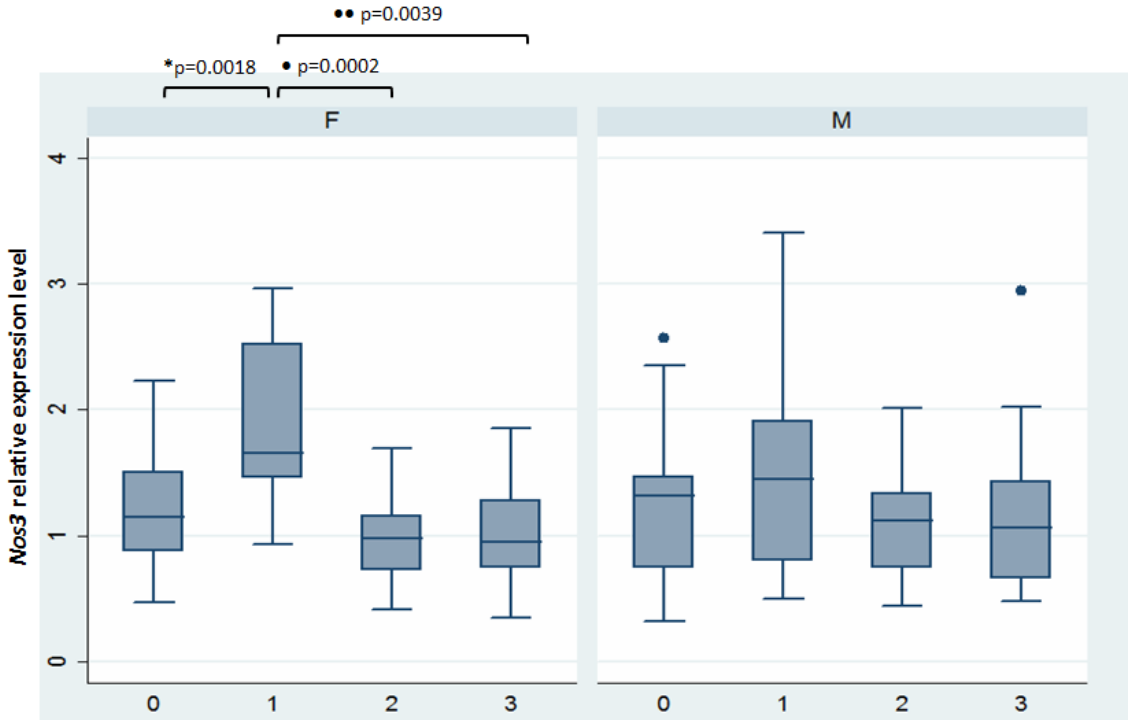

Figure 89: Comparison of *nos3* relative expression level among liver (0), muscle from healthy subjects (1), muscle from LLMI patients (2) and adipose tissue (3). To compare tissues, Kruskal-Wallis test was applied. In the left panel are represented females: *nos3* relative expression level is significantly different between muscle from healthy subjects and from LLMI patients (p=0.0002), between muscle from healthy subjects and liver (p=0.0018) and finally between muscle from healthy subjects and adipose tissue (p=0.0039). In the right panel are represented males: *nos3* relative expression level is not significantly different among the 4 types of tissue.

4.4.5.16 Sod1

The significant differences in the expression level of *sod1* were found between liver and muscles, both from healthy subjects and from LLMI patients, and between adipose tissues and muscles, also in this case for both the groups of muscles.

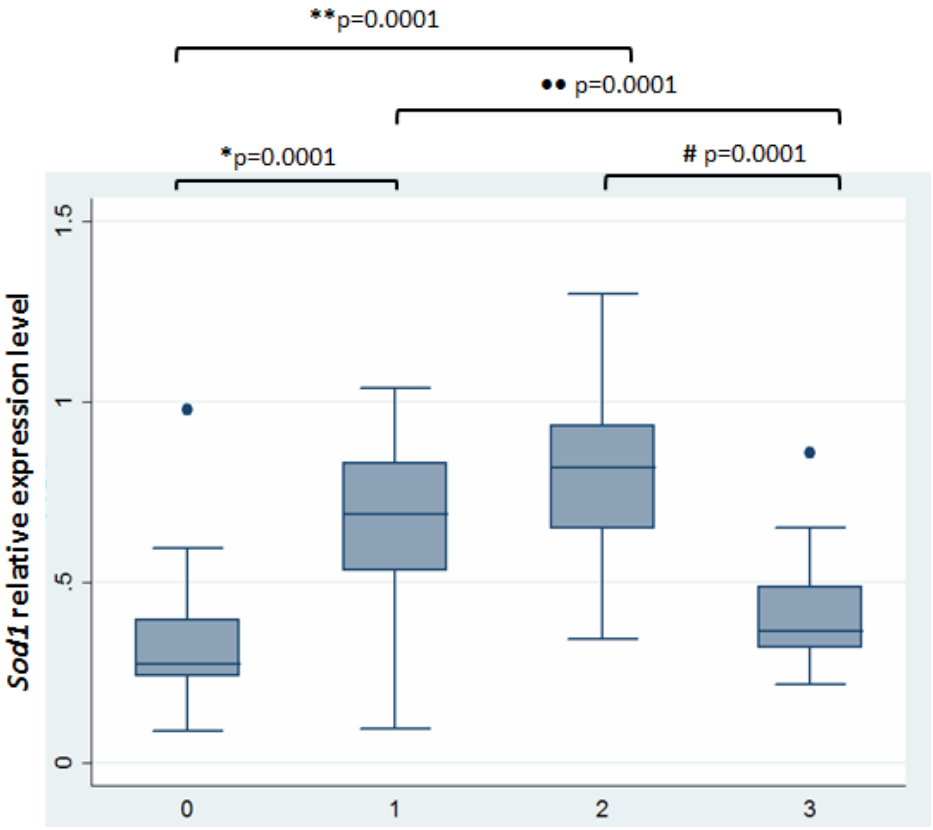

Figure 90: Comparison of *sod1* relative expression level among liver (0), muscle from healthy subjects (1), muscle from LLMI patients (2) and adipose tissue (3). To compare tissues, Kruskal-Wallis test was applied; *sod1* relative expression level is significantly different among liver and muscle, both from healthy subjects (p=0.0001) and from LLMI patients (p=0.0001). *Sod1* relative expression level is also significantly different among adipose tissue and muscle, both from healthy subjects (p=0.0001) and from LLMI patients (p=0.0001).

Regarding the analysis by gender, some differences between females and males emerged. In particular, for females the same dissimilarities, showed in the total number of samples, were still significant, whereas for males, only the differences between liver and muscles from LLMI patients and between the latter and adipose tissue were still significantly diverse when data were divided, as demonstrated in figure 91.

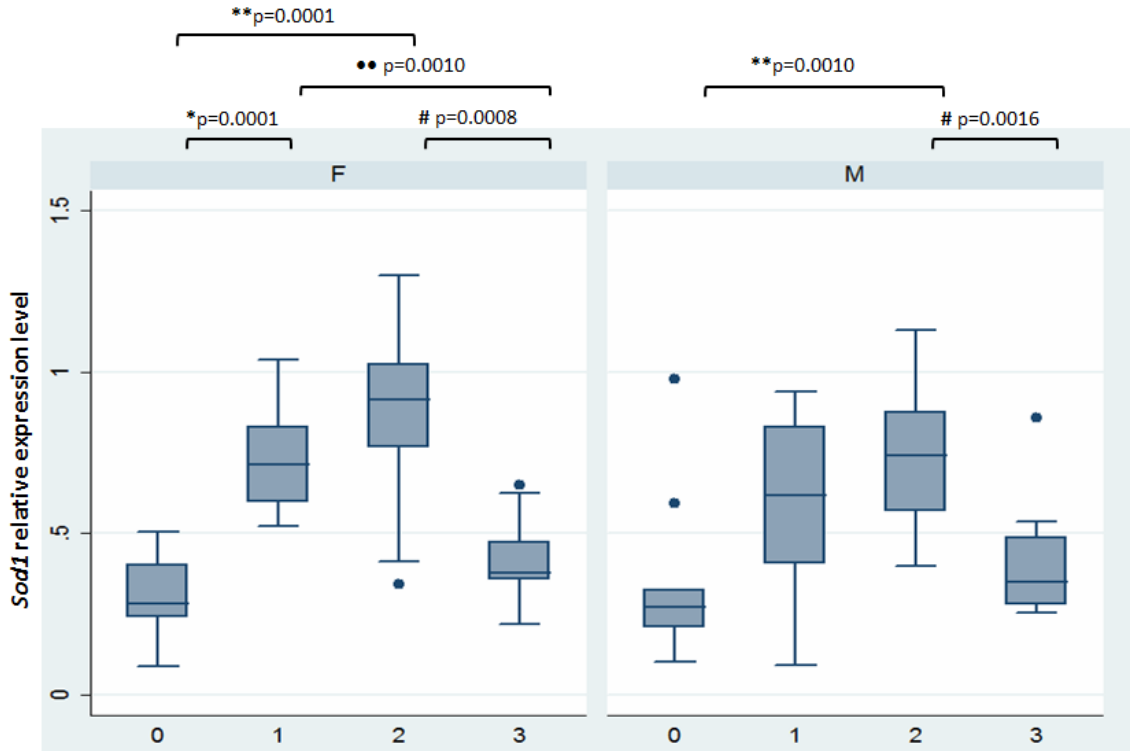

Figure 91: Comparison of *sod1* relative expression level among liver (0), muscle from healthy subjects (1), muscle from LLMI patients (2) and adipose tissue (3). To compare tissues, Kruskal-Wallis test was applied. In the left panel are represented females: *sod1* relative expression level is significantly different among liver and muscle, both from healthy subjects (p=0.0001) and from LLMI patients (p=0.0001) and among adipose tissue and muscle, both from healthy subjects (p=0.0010) and from LLMI patients (p=0.0008). In the right panel are represented males: *sod1* relative expression level is significantly different between liver and muscle from LLMI patients (p=0.0010) and between adipose tissue and muscle from LLMI patients (p=0.0016).

5 Discussion

Human aging is a highly complex process, comprising multiple mechanisms at different levels (Kirkwood, 2005). A general characteristic of aging is the systemic, chronic and low grade inflammation described as “inflamm-aging” (Franceschi et al., 2000), provoked by the persistence of inflammatory stimuli in answer to continuous antigenic load and stress (Morrissette-Thomas et al., 2014) and to the related accumulation of damaged macromolecules and cells (self-debris) (Franceschi and Campisi, 2014). Damage to biomolecules and to cellular components can be due to the excessive production of highly toxic reactive oxygen species (ROS), concept at the basis of the mitochondrial theory of aging, since mitochondria are the major intracellular producers of ROS (Chistiakov et al., 2014). This theory explains how a high ROS production leads to mtDNA mutations and deletions and thus to a decline in mitochondrial function with age (Harman, 1956). Moreover, as deleted mtDNA molecules increase in number, the level of ROS production becomes greater, inducing a vicious circle that enhances mitochondrial damages and eventually cell dysfunction (Wallace 2005). This phenomenon is more severe in post-mitotic tissues where the energy demand is particularly higher and the capability to eliminate damaged organelles progressively wanes (Salvioli et al., 2008). Data from literature suggest that metabolic or pathophysiological tissue properties may outline deletion specific fingerprints, basing on different mitotic activities, varied metabolic rates or exposure to specific genotoxins. Nevertheless, the tissue specific generation of deletions can be due also by tissue specific nuclear genes expression and nucleo-mitochondrial interactions (Meissner et al., 2006).

Moreover, in order to warrant oxidative capacity and cell survival it is therefore mandatory to maintain a sufficient number of intact mtDNA copies (Ylikallio et al., 2010), as well as the integrity of mitochondrial function, activity and appropriate morphology (Michel et al., 2012).

Therefore, since in literature are present contrasting data regarding mtDNA rearrangements in different tissues, furthermore coming in a large part from model animals, and as less is known about the mechanisms that lead to tissue specific presence of mtDNA rearrangements, we focused our attention on three different human tissues. Thus, in our work we study mtDNA copy number, deletion level and integrity, as well as telomere length and the expression level of several genes involved in mitochondrial biogenesis, dynamics, protein degradation and mitophagy in order to understand if they are involved during aging of human liver, *vastus lateralis* skeletal muscle and adipose tissue.

However, to explain better our observations, data are discussed in four section: one for liver, one for skeletal muscle, one for adipose tissue and one dedicated to the comparison of the three different tissues.

5.1 Liver

In liver, what emerge from our data is that there is an increase in mtDNA copy number with age in human livers, while there is any change in mtDNA deletion level. However, when mtDNA deletion levels and copy number were examined together, independently of age, we found a strong correlation, from which results that as mtDNA copy number increases, mtDNA deletion level decreases. We called this ratio "mtDNA integrity", representing the number of deleted molecules on the total number of mtDNA molecules presents in mitochondria and we found that it just slightly decreases with age. Therefore this data could suggest that deleted mtDNA copies has a replicative advantage compared to intact mtDNA copies (Wallace, 1989), but the increase in mtDNA copy number is likely a compensatory mechanism for defective mitochondria bearing mutated mtDNA. These data, in fact, are consistent with the previous study of Masuyama and colleagues on murine animal model in which they found an increase in mtDNA copy number during aging in several tissues of mice at different ages (Masuyama et al., 2005).

Telomere length was also investigated in our liver samples and as expected there is a significant telomere shortening during the aging of human liver. Besides, in 2011 Sahin and colleagues published a work in which they observed an association between telomere shortening and mitochondrial dysfunction, with a diminished expression of *pgc-1α*, that is a master regulator of mitochondrial biogenesis (Sahin et al., 2011).

Interestingly, our data show how telomere attrition in liver is associated with an increase in mtDNA copy number and with a decrease in mtDNA deletion level and mtDNA integrity. As telomere shortening is a well-known marker of aging, we could hypothesize that liver mtDNA integrity is not preserved during aging, likely due to the activation of a compensatory mechanism regulating mtDNA copy number, that in turn increases to prevent a consecutive accumulation of deleted mtDNA molecules.

This hypothesis is also sustained by the results coming from our gene expression analyses. In fact, we also analyzed the expression levels of some nuclear genes involved in several mitochondrial pathways, such as mitochondrial biogenesis (*pgc-1α*, *polγ*, *nrf1*, *tfam*, *twinkle*, *sirt1*, *sirt3*, *tomm40* and *ppard*), fusion and fission processes (*mfn2*, *fis1* and *opa1*), mitophagy

(*ambra1*, *beclin*, *pink1*, *parkin*, *atg16l* and *pik3cd*), production of ROS (*nos3*), protection from ROS (*sod1* and *sod2*), protein quality control system (*lonp*) and finally hypoxia (*hif-1*α), discovering that in all liver samples the expression level of some of these genes changes with age. In particular we observed an increment in the expression level of *nrf1*, that is involved in mitobiogenesis, of *mfn2* and *fis1*, which are responsible for mitochondrial dynamism processes, and of *lonp*, than encodes for a mitochondrial protease. Therefore, the pathways that seem to be involved in the aging of human liver are those affected in mitochondrial quality control, which implies also a tight control of mtDNA copy number. Data from literature suggest the existence of a still unknown sensor of a lower or a higher threshold of mtDNA copy number leading to the activation of the replication machinery (biogenesis and fusion process) or of the degradation machinery (fission process and mitophagy) of mtDNA, respectively (Michel et al., 2012), as we can see in our samples. Moreover, Lon protease contributes to degradation of short-lived, misfolded or damaged proteins in mitochondria and is regulated by transcription factors associated to mitochondrial biogenesis and oxidative stress (Ngo et al, 2013).

What we can suppose is that during aging of human liver, a reduction, however small, of mtDNA integrity leads to increased expression of genes involved in the regulation of mtDNA copy number, that in turn increase as to compensate the damage.

Therefore, even if our data on telomere shortening could indicate that liver ages, our data on mtDNA rearrangements suggest that they seem not to impinge upon macroscopic organ defects. In closing, it is worth noting that livers in this thesis are considered suitable for transplantation including that from very old donors, which are grafted in younger subjects with a successful outcome (Grazi et al., 2001; Cescon et al., 2003; Cescon et al., 2008).

5.1.1 Gender difference in human liver aging

Observing our data more deeply, a gender difference emerged, leading us to hypothesize that what we see in a global vision of liver is actually due to molecular mechanisms, which could act in a different way in females and males.

In particular, in males mtDNA copy number increases with age, also in relation with telomere attrition. However, the increased expression level of *nrf1* and *lonp* suggest that the mechanisms involved in the “compensatory pathway” are mitochondrial biogenesis and the protein quality control system, without changes in mitochondrial dynamics. Nevertheless, these mechanisms are still sufficient to maintain regulated mtDNA rearrangements, without impairment of mitochondrial functions.

Instead, in liver biopsies from female's donors we did not find any change in mtDNA rearrangements during aging, as well as any association with telomere shortening, that instead increases with age. Also the expression level of *nrf1*, *fis1* (that instead do not change in males) and *lonp* increases with age in females, suggesting that the involvement of fission process added to mitochondrial biogenesis and the protein quality control system allows mtDNA copy number to be highly regulated and to avoid mtDNA rearrangements. This is supported by literature data reporting that, promoting mitochondrial fission, mitochondrial dysfunction partially reverts (Liu et al., 2011), since mitochondrial quality and integrity are maintained selecting dysfunctional mitochondria (Chistiakov et al., 2014).

At the end, either for males and females, the increase of expression level of *lonp* could have a beneficial effect, seeing that conversely in rat the age-related downregulation of Lon protease has detrimental effect, not allowing the degradation of oxidized proteins (Ngo et al.,2013). Moreover, from these data come out that the expression level of *lonp* and *nrf1* increase with age and this is particularly important since the protein encoded by *nrf1* gene is critical to expression of genes encoding proteasomal subunit (Oh et al., 2013), while *lonp* encodes the main mitochondrial protease. Thus, these data fit perfectly with data of Bellavista and colleagues coming out from experiments performed on the same liver biopsies that show how efficient proteostasis and proteasome are maintained with age (Bellavista et al., 2014).

5.2 Skeletal muscle

The progressive and age-associated decline in skeletal muscle mass, strength and function was defined by Roseberg as sarcopenia (Roseberg, 1989), and its leads to reduced endurance capacity and increased muscle fatigability, that in turn may contribute to increase frailty and greater risk of falls (Cruz-Jentoft, 2010; Fielding et al., 2011).

Since skeletal muscle is one of the tissue with high energy demand and mitochondria carry out pivotal functions in the context of energy provision, many studies focus on the role of mitochondria in sarcopenia, suggesting that mtDNA rearrangements are one of the major causes. Nevertheless, literature data about this topic are often controversial (Peterson et al., 2012; Johnson et al., 2013).

Thus, in our study we focused on the analysis of mtDNA rearrangements in order to better characterize and understand the involvement of the mitochondrion in skeletal muscle aging and sarcopenia. To reach this goal, we studied mtDNA copy number, deletion level and integrity, as well as telomere shortening and the expression level of several nuclear genes, in

vastus lateralis biopsies from two different groups of subjects at different ages: healthy subjects and lower limb mobility impairment (LLMI) patients.

5.2.1 Healthy subjects

Consistently with the work of Welle and colleagues (Welle et al., 2003), our data from the group of healthy subjects suggest that mtDNA copy number decreases with age, even if in a barely significant way, while no significative change emerges in mtDNA deletion level. Moreover, during physiological aging of human skeletal muscle, mtDNA integrity shows a marked reduction with age. This decline of mtDNA integrity with age is consistent with literature data, which report an increase in mutation and oxidative damages on mtDNA with age (Kazachkova et al., 2013). Indeed, with advancing age there is a well established decline in mitochondrial activity, due to mtDNA damage caused by an increase in ROS production and to the mtDNA proximity to the source of ROS, in addition to its lack of introns and its weak DNA repair systems. These lacks can facilitate the accumulation of mtDNA mutation and rearrangements, that could be provoked during mtDNA replication, but, above all, can occur in genes coding for ETC subunits or at control sites. In this way, a sort of damage-propagating loop is generated, further worsening mitochondrial activity and enhancing ROS production. Thereby mtDNA rearrangements have been associated to muscle mass loss, weakness and sarcopenia (Johnson et al., 2013).

Besides mtDNA rearrangements, also telomere length has been investigated in our *vastus lateralis* muscle biopsies from healthy subjects, as the majority of the literature data consider this parameter as a biomarker of aging and longevity, reporting a decrease in telomere length with age. However, we did not find any significative change in telomere length in healthy skeletal muscle, like reported by the study of Ponsot and colleagues in 2008 (Ponsot et al., 2008). In addition to this, we did not find significant relations among mtDNA rearrangements and telomere shortening, suggesting us that the relation is not direct and other mechanisms could affect mitochondrial dysfunction.

To characterize more deeply the involvement of mitochondria and mtDNA rearrangements in the aging of human skeletal muscle, the relative expression level of genes involved in mitobiogenesis (*pgc-1α*, *polγ*, *nrf1*, *tfam*, *twinkle*, *sirt1*, *sirt3*, *tomm40* and *ppard*), fusion and fission processes (*mfn2*, *fis1* and *opa1*), mitophagy (*ambra1*, *beclin*, *pink1*, *parkin*, *atg16l* and *pik3cd*), production of ROS (*nos3*), protection from ROS (*sod1* and *sod2*), protein quality control system (*lonp*) and finally hypoxia (*hif-1*α), was also evaluated. What we observed is a general decrease in the expression level of *pgc-1α*, *polγ*, *tfam*, *opa1*, *beclin* and *pik3cd*, that

suggest how, during the physiological aging of skeletal muscle, some mechanisms can be impaired.

In particular, these data are consistent with that present in literature, reporting a decline in mitochondrial activity and dynamics with aging, due to accumulation of mtDNA damages and ROS overproduction. Specifically, the majority of studies performed on both skeletal muscle in humans and rodents report a decrease in mitochondrial biogenesis with reduction of *pgc-1α* and *tfam* expression level (Ling et al., 2004; Lanza et al., 2008; Safdar et al., 2010; Koltai et al., 2012). Moreover, also the downregulation of fusion process has been detected in muscle of subjects affected by type-2-diabetes and obesity, which are associated with accelerated development and/or progression of sarcopenia. In particular, depletion of opa1, that is a mitochondrial fusion factor, disintegrates the mitochondrial network and sensitizes cultured cell to apoptosis (Marzetti et al, 2013). Finally, also mitophagy has been reported to decline with age with consequent accumulation of dysfunctional mitochondrial and oxidative damage that may contribute to muscle loss and sarcopenia (Peterson et al., 2012; Johnson et al., 2013; Marzetti et al., 2013).

Hence, our results are in accordance with mitochondrial data present in literature, suggesting that during physiological aging, skeletal muscle is affected by mitochondrial DNA rearrangements which are due to the reduction of mitochondrial biogenesis and to the impairment of the fusion and autophagy processes.

5.2.1.1 Gender difference in aging of skeletal muscle from healthy subjects

As for the liver, also in the case of skeletal muscle *vastus lateralis*, a gender difference emerges during aging, regarding mtDNA modifications and above all the expression level of the considered genes.

In particular, in males mtDNA integrity decreases with age, as well as the expression level of *pgc-1α*, *polγ*, *opa1*, *pik3cd* and *nos3*. These data lead us to speculate that the diminished expression of some of the pivotal factor of mitochondrial biogenesis, fusion and mitophagy is rather as a deficiency in the activation of a compensatory mechanism, which leads to the establishment of the damage-propagating loop at the basis of mitochondrial dysfunction and, likely, of sarcopenia.

This is enhanced in females samples, where the reduction in the expression level of *pgc-1α*, *tfam*, and *beclin* is sufficient to induce not only a decrease in mtDNA integrity, but also a light increase in mtDNA deletion, as to indicate that are precisely mitochondrial biogenesis and autophagy the key processes to the maintenance of mitochondrial function.

Even if the actors that change with age are different between females and males, our data are consistent with those present in literature, where several studies report how, mitochondrial density decline gradually during skeletal muscle aging, due to an age-dependent reduction of *pgc-1α* and thus of mitochondrial biogenesis (Wenz et al., 2009). Moreover, it is reported that also mitophagy declines with aging, leading to an accumulation of aberrant mitochondria (Mammuccari and Rizzuto, 2010), how happens in our samples.

5.2.2 LLMI patients

During muscle disuse due to lower limb mobility impairment, the scenario is quite similar to that of physiological aging: mtDNA copy number and mtDNA integrity markedly decrease with age, while no changes emerge in mtDNA deletion level.

Also for telomere length, we found that there are no changes with age and any direct relation among telomere shortening and mtDNA rearrangements is present, even if mitochondria are the most important source of ROS and a connection between the role of mitochondria and oxidative stress in telomere-driven replicative senescence has been proposed (von Zglinicki et al., 2001; Saretzki and von Zglinicki, 2002; Passos et al., 2007; Ahmend et al., 2008; Sahin and DePinho, 2012).

The gene expression analysis, instead, shows how different mechanisms are involved in the pathological aging process of skeletal muscle. In particular, in this group there is an increase in *sirt1* expression level, that could be related to an increase in mitochondrial biogenesis, since sirt1 promoted the deacetylation of *pgc-1α*, leading to its activation (Houtkooper et al., 2012). However we conversely observed a decrease in mtDNA copy number, as to indicate that the increment in *sirt1* is not sufficient to deacetylate enough *pgc-1α*, inducing mitobiogenesis. Moreover, there is a decrease in the expression level of *beclin*, *pink1* and *sod1*, as to indicate that also in the case of muscle disuse, aging is driven by deregulated mitophagy, in addition to a reduced capacity to contrast ROS production. As for the reduction in mitophagy activation, also the diminished expression level of *sod1* is in agreement with what reported in literature, since Watanabe described how *sod1*$^{-/-}$ mice showed significant age-dependent decrease in the whole hind limb muscle mass, inducing skeletal muscle atrophy (Watanabe et al., 2014).

5.2.2.1 Gender difference in aging of skeletal muscle from LLMI patients

How expected, also in the case of muscle atrophy due to hospitalization, a gender difference emerged, either for mtDNA rearrangements and genes expression level.

In particular, in males mtDNA copy number and integrity decrease with age, while the mtDNA deletion level increases. This is accompanied by a diminution of the expression level of *sod1*,

that is one of the main antioxidant enzymes present in cells. The *sod1* deficiency in muscle was previously demonstrated as responsible of the $O_2^{\bullet -}$ intracellular enhancement that leads to increased oxidative damage and induces aberrant mitochondria with lower ATP production (Watanabe et al., 2014). Therefore these data lead us to suppose that the diminished mtDNA copy number, in addition to the increment of mtDNA deletion level, is due to the decrease expression level of *sod1* without the activation of any compensatory mechanism.

What happens in females is different, since there is a reduction in the expression level of *tfam*, *pink1* and *beclin* without any changes in mtDNA copy number, deletion level and integrity. Some years ago, Dagda and colleagues observed that a loss of regulation of mitophagy, with a consecutive increase of this process, results in increased mtDNA degradation, that has been implicated in human disease such as Parkinson's disease (Dagda et al., 2008). Hence, it is plausible that to maintain the present complete mtDNA molecules, without new mitochondrial biogenesis, that it is also diminished, also mitophagy is kept to low levels, in order to escape the degradation of intact mtDNA.

5.3 Adipose tissue

Even if the importance of white adipose tissue (WAT) is increasing more and more as an endocrine organ responsible for energy intake, energy expenditure, and insulin resistance, literature data about WAT mitochondria in aging are still poor of evidences. It is known that with age, white adipocytes reduce their mitochondrial content (Kusminski and Scherer, 2012), and that a decreased expression of key regulators of mitochondrial biogenesis have been described in type-2-diabetes patients (van Tienen et al., 2010), which, as age-related disease, could indicate what happen in a harmful aging process. Hence, what emerge from our data is quite new but at the same time, controversial in respect to literature. Indeed, mtDNA copy number, deletion level and integrity did not show any change with age in our samples.

What is known in literature regarding the telomere shortening in adipose tissue is that it is significantly associated with hypertrophy adipocytes, low circulating adiponectin levels and impaired glucose and lipid metabolism in individual either with obesity and type-2-diabetis. Moreover, in subcutaneous adipose tissue, telomere length is negatively associated with age (Lakowa et al, 2015). However, in our samples telomere length did not vary with age, probably because, as suggested by Spalding and colleagues, mature adipocytes have relatively low renewal rate and it is known that telomere shorten when cell proliferate (Spalding et al.,

2008). Additionally, we did not find any relation between telomere length and mtDNA parameters.

However, different variations in genes expression level were found in our samples. In particular, among the genes considered, we detected an increase in *twinkle*, *nrf1*, *pink1*, *ambra*, *nos3* and *sod1* expression level. Since little is known about the regulation of mitochondrial processes in adipose tissues, from these data we can speculate that, like in liver, the increased expression of these genes is like a sort of activation of a compensatory mechanism which lead at the end to the lack of changes in mtDNA copy number, deletion level and integrity.

Though, based on a study of van Tienen and colleagues where it is showed how in mouse 3T3-L1 cultured cells overexpression of *nrf1* can induce directly inflammation in adipocytes (van Tienen et al., 2010), another speculation is plausible. From literature, in fact, it is known that WAT is one of the most important players in the establishment of metaflammation (Gregor and Hotamisligil, 2011), and that the latter contributes to the systemic phenomenon of inflammaging (Cevenini et al., 2013). Thus we could hypothesize that, with age, the increased expression of *nrf1* causes an augmented release of inflammatory mediators and, in this way, an elevated *nos3* expression and ROS production, which in turn could raise the expression level of those genes involved in the mitochondrial quality control and ROS scavenger processes.

Besides, this seems to happen only in females, since in males there are no changes either in mtDNA rearrangements or in gene expression level. Probably this gender difference is caused by the different metabolic function of adipose tissue in women with respect to men, in addition to a dissimilar distribution. In particular, women have higher subcutaneous adipose tissue compared to men, which instead have high level of visceral adipose tissue. This difference is related to the influence of sex hormones, but also to the diverse function of subcutaneous adipose tissue in women, which is important to support lactation, and the visceral adipose tissue in males, that serves as readily mobilizable deposition to facilitate rapid burst of energy (Palmer and Clegg, 2015).

5.4 Tissue comparison

As aging is tissue specific, also mitochondrial respiration capacity and mtDNA copy number are not random, but rather specific to tissue type and to developmental stage (Clay Montier, 2009). In 1988, Robin and Wong observed that the numbers of mitochondria vary among different cell types and that the amount of mtDNA per mitochondrion is constant in all cell

types, measuring both the virtual mitochondrial number and the mtDNA amount per mitochondrion in different cell types (Robin and Wong, 1988). Later, several studies were performed both in human and in animal model to assess the mtDNA abundance in terminally differentiated tissues, such as brain, skeletal muscle and heart, in relation to age (Herbert et al., 2011).

In our work, we had the possibility to compare mtDNA copy number, deletion level and integrity, as well as telomere length and the expression level of nuclear genes involved in mitochondrial pathways among three different human tissues, independently of age. What emerge by our data is that no differences appear in telomere length and mtDNA deletion level among the three tissues, but in liver mtDNA copy number and integrity are lower than in skeletal muscle and adipose tissue. These data are consistent with the recent work of D'Erchia and colleagues, which measured mtDNA copy number in six human tissue types (brain, lung, kidney, liver, heart and skeletal muscle) from three unrelated individuals, founding that in heart and skeletal muscle mtDNA copy number is higher than in liver (D'Erchia et al., 2015).

Moreover, in our case, it is to underlie that nevertheless liver has the lowest mtDNA copy number and mtDNA integrity, it has the highest expression level of *tfam* and *opa1*, that are genes involved in mitochondrial biogenesis and fusion process. It is to note that mitochondrial biogenesis and fusion process can affect directly mtDNA copy number, suggesting that they are involved in cellular adaptation to environmental stimuli and in physiological activity. Also the expression level of *pik3cd* is different among the considered tissues, as to indicate that also autophagy is tissue-specifically regulated. Instead, all the other genes (*pgc-1α*, *polγ*, *nrf1*, *twinkle*, *sirt1*, *mfn2*, *fis1*, *pink1*, *beclin*, *ambra*, *lonp*, *nos3* and *sod1*) are more expressed in skeletal muscle than in liver and adipose tissue. These data of gene expression, together with the high amount of mtDNA in skeletal muscle, are in agreement with those of D'Erchia and colleagues, that measured also the respiratory capacity of the tissues considered, founding that skeletal muscle and heart have the highest one (D'Erchia et al., 2015).

Thus, even if we are only at the beginning of a comprehensive and age-independent vision of tissue-related variability in mtDNA, from this comparison is quite clear that mtDNA copy number and integrity as well as the expression level of nuclear genes involved in mitochondrial pathways are strictly linked to metabolic and bioenergetics tissue demands.

6 Conclusions

The involvement of mitochondria and mtDNA rearrangements in human aging is still an open and debated issue, which is based on controversial data from different groups. The results presented in this thesis represent a first attempt to study the involvement of mitochondrial rearrangements, intended as mtDNA copy number, deletion level and integrity, from a tissue-specific point of view, studying three different human tissues: liver, skeletal muscle and adipose tissue.

From the results obtained in this study on biopsies of liver, we can presume that the decrease in mtDNA integrity is accompanied with an increase in mtDNA copy number, suggesting the existence of a "compensatory mechanism" that it is able to maintain the functionality of liver. The gene expression analysis, in fact, revealed that with age there is an increase in the expression level of those nuclear genes involved in mitochondrial biogenesis, mitochondrial dynamic processes and mitochondrial protein quality control system, suggesting that these mechanisms represent the "compensatory pathway" activated in liver aging. Supporting this hypothesis, it is to be considered that the biopsies utilized in this study were taken from organs considered suitable for transplantation and liver from very old donors were grafted in younger subjects with a successful outcome.

Different is the case of *vastus lateralis* muscle of which we had two groups of subjects at different ages, healthy subjects and patients with muscle disuse due to hip osteoarthritis (leading to hip replacement). Effectively from the muscle results we can conclude that, since mtDNA integrity and copy number decrease with age both in healthy subjects and in patients, during muscle aging any "compensatory pathway" is activated, leading to the well-known phenomenon of sarcopenia. Indeed, conversely from the liver, the gene expression analysis shows a reduced level of the genes involved in mitochondrial biogenesis and autophagy.

We also studied white adipose tissue coming from the same subjects with muscle disuse, knowing that during aging there is an accumulation of inter-muscular adipose tissue. From literature less is known about the aging of this tissue, but it is known that it contributes to the metaflammation process and, in this way, to the more complex phenomenon of inflammaging. Our data suggest us that mtDNA rearrangements in adipose tissue do not incur in changes with advancing age, but from the results of the gene expression analysis, we can deduce two different hypotheses. The former is that the increased expression of the genes considered represent, like for liver, the activation of the compensatory mechanism that allows any mitochondrial changes. Instead the latter is that the increased expression of the genes

considered could be due to the involvement of the chronic, low grade inflammatory response that is common in human aging.

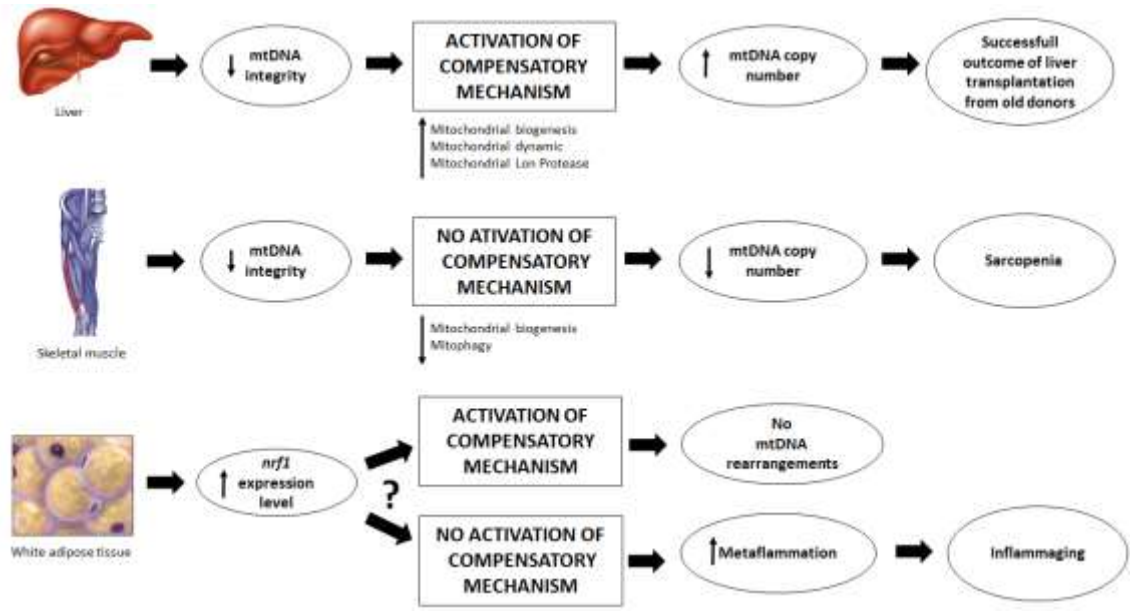

Figure 92: mtDNA rearrangements during aging of three different human tissues, such as liver, skeletal muscle and white adipose tissue. In the circular boxes there are observed data, whereas in rectangular boxes there are our hypotheses.

We analyzed also the telomere length in these different tissues, as in literature it is reported as a good marker of aging. However, while in liver there was a significantly decrease in telomere length with advancing age, no changes were observed in skeletal muscle and adipose tissue. These results lead us to conclude that, as proposed by Martin-Ruiz and colleagues, telomere length is more a risk indicator than a marker of aging (Martin-Ruiz et al., 2014) and that, as for mtDNA rearrangements, also the telomere length is tissue specific.

Since we started this work in order to study the tissue specificity of mtDNA rearrangements, we finally compared the mtDNA copy number, deletion level and integrity, as well as the gene expression levels among the different tissues, independently from age. From the comparison results we can conclude that metabolic and bioenergetics tissue demands are fundamental aspects regulating mitochondrial functionality and activity.

What is extremely peculiar in our work is that for all tissues a markedly gender difference appears either in mtDNA rearrangements or in gene expression levels. As far as we know, literature reports studies performed in humans and animal models without any particular attention to gender. Thus this thesis can be the starting point to study how mtDNA rearrangements differently affect aging in males and females.

7 Bibliography

1. Ahmed S, Passos JF, Birket MJ, Beckmann T, Brings S, Peters H, Birch-Machin MA, von Zglinicki T, Saretzki G, Telomerase does not counteract telomere shortening but protects mitochondrial function under oxidative stress. J. Cell. Sci. 2008 Apr 1; 121(Pt 7):1046-53. doi: 10.1242/jcs.019372.

2. Anderson S, Bankier AT, Barrel BG, De Brujin MH, Coulson AR, Drouin J, Eperon IC, Nierlich DP, Roe BA, Sanger F, Schreier PH, Smith AJ, Staden R, Young IG, Sequence and organization of the human mitochondrial genome. Nature. 1981 Apr 9; 290(5806):457-65.

3. Ashar FN, Moes A, Moore AZ, Grove ML, Chaves PHM, Coresh J, Newman AB, Matteini AM, Bandeen-Roche K, Boerwinkle E, Walston JD, Arking DE, Association of mitochondrial DNA levels with frailty and all-cause mortality. J Mol Med (Berl). 2014 Dec 4.

4. Attardi G, Schatz G, Biogenesis of mitochondria. Annu. Rev. Biol. 1988; 4:289-333.

5. Bai RK, Perng CL; Hsu CH, Wong LJC, Quantitative PCR analysis of mitochondrial DNA content in patients with mitochondrial disease, 2004. Ann. N. Y. Acad. Sci. 1011, 304-309.

6. Bakala H, Delaval E, Hamelin M, Bismuth J, Borot-Laloi C, Croman B, Friguet B, Changes in rat liver mitochondria with aging. Lon protease-like reactivity and N(epsilon)-carboxymethyllysine accumulation in the matrix. Eur J Biochem. 2003 May; 270(10):2295-302.

7. Barazzoni R, Short KR, Nair KS, Effects of Aging on Mitochondrial DNA Copy Number and Cytochrome *c* Oxidase Gene Expression in Rat Skeletal Muscle, Liver, and Heart. J Biol Chem. 2000 Feb 4; 275(5):3343-7.

8. Bellavista E, Martucci M, Vasuri F, Santoro A, Mishto M, Kloss A, Capizzi E, Degiovanni A, Lanzarini C, Remondini D, Dazzi A, Pellegrini S, Cescon M, Capri M, Salvioli S, D'Errico-Grigioni A, Dahlmann B, Grazi GL, Franceschi C, Lifelong maintenance of composition, function and cellular/subcellular distribution of proteasomes in human liver. Mech Ageing Dev. 2014 Oct 1; 141-142C:26-34.

9. Bizeau ME, Willist WT, Hazel JR, Differential responses to endurance training in subsarcolemmal an intermyofibrillar mitochondria. J Appl Physiol (1985). 1998 Oct; 85(4):1279-84.

10. Bota DA, Ngo JK, Davies KJ, Downregulation of the human Lon protease impairs mitochondrial structure and function and causes cell death. Free Radical Biology and Medicine. 2005; 38:665-667.

11. Brunk UT, Terman A, Lipofuscin: mechanisms of age-related accumulation and influence on cell function. Free Radic Biol Med. 2002 Sep 1; 33(5):611-9.

12. Bulteau AL, Szweda LI, Friguet B, Mitochondrial protein oxidation and degradation in response to oxidative stress and aging. Exp. Gerontol. 2006; 41:653-657.

13. Carlsson LM, Jonsson J, Edlund T, Marklund SL, Mice lacking extracellular superoxide dismutase are more sensitive to hyperoxia. Proc Natl Acad Sci U S A. 1995 Jul 3; 92(14):6264-8.

14. Castro Mdel R, Suarez E, Kraiselburd E, isidro A, Paz J, Ferder l, Ayala-Torres S, Aging increases mitochondrial DNA damage and oxidative stress in liver of rhesus monkeys. Exp Gerontol. 2012 Jan; 47(1):29-37. Epub 2011 Oct 12.

15. Cescon M, Grazi GL, Ercolani G, Nardo B, Ravaioli M, Gardini A, Cavallari A, Long-term survival of recipients of liver grafts from donors older than 80 years: is it achievable? Liver Transpl. 2003 Nov;9(11):1174-80.

16. Cescon M, Grazi GL, Cucchetti A, Ravaioli M, Ercolani G, Vivarelli M, D'Errico A, Del Gaudio M, Pinna AD. Improving the outcome of liver transplantation with very old donors with updated selection and management criteria. Liver Transpl. 2008 May;14(5):672-9. doi: 10.1002/lt.21433.

17. Cevenini E, Invidia L, Lescai F, Salvioli S, Tieri P, Castellani G, Franceschi C, Human models of aging and longevity. Expert Opin Biol Ther. 2008; 8(9):1393-405.

18. Cevenini E, Monti D, Franceschi C, Inflamm-ageing. Curr Opin Clin Nutr Metab Care. 2013 Jan; 16(1):14-20. doi: 10.1097/MCO.0b013e32835ada13.

19. Chistiakov DA, Sobenin IA, Revin VV, Orekhov AN, Bobryshev YV, Mitochondrial Aging and Age-Related Dysfunction of Mitochondria. Biomed Res Int. 2014; 2014:238463. doi: 10.1155/2014/238463. Epub 2014 Apr 10.

20. Clay Montier LL, Deng JJ, Bai Y, Number matters: control of mammalian mitochondrial DNA copy number. J Genet Genomics. 2009 Mar; 36(3):125-31. doi: 10.1016/S1673-8527(08)60099-5.

21. Cogswell AM, Stevens RJ, Hood DA, Properties of skeletal muscle mitochondria isolated from subsarcolemmal and intermyofibrillar regions. Am J Physiol. 1993 Feb;264(2 Pt 1):C383-9.

22. Conboy IM, Conboy MJ, Wagers AJ, Girma ER, Weissman IL, Rando TA, Rejuvenation of aged progenitor cells by exposure to a young systemic environment. Nature, 433 (7027) 2005; 760‑764.

23. Cong HY, Wright WE, Shay JW, Human telomerase and its regulation. Microbiol. Mol. Biol. Rev. 2002 September; 66(3):407-25.

24. Copeland WC, Longley MJ, Mitochondrial genome maintenance in health and disease. DNA Repair (Amst). 2014 Jul; 19:190-8. doi: 10.1016/j.dnarep.2014.03.010. E Epub 2014 Apr 26

25. Cortopassi GA, Shibata D, Soong NW, Arnheim N, A pattern of accumulation of a somatic deletion of mitochondrial DNA in aging human tissues. Proc Natl Acad Sci U S A. 1992 Aug 15; 89(16):7370-4.

26. Cruz-Jentoft AJ, Baeyens JP, Bauer JM, Boirie Y, Caderholm T, Landi F, Martin FC, Michel JP, Rolland Y, Schneider SM, Topinková E, Vanderwoulde M, Zamboni M, Sarcopenia: European consensus on definition and diagnosis: Report of the European Working Group on Sarcopenia in Older People. Age Ageing. 2010 Jul;39(4):412-23. doi: 10.1093/ageing/afq034. Epub 2010 Apr 13.

27. Cui H, Kong Y, Zhang H, Oxidative stress, mitochondrial dysfunction, and aging. J Signal Transduct. 2012; 2012:646354. doi: 10.1155/2012/646354. Epub 2011 Oct 2.

28. D'Erchia AM, Atlante A, Gadaleta G, Pavesi G, Chiara M, De Virgilio C, Manzari C, Mastropasqua F, Prazzoli GM, Picardi E, Gissi C, Horner D, Reyes A, Sbisà E, Tullo A, Pesole G, Tissue-specific mtDNA abudance from exome data and its correlation with mitochondrial transcription, mass and respiratory activity. Mitochondrion. 2015; 20:13-21.

29. Dagda RK, Zhu J, Kulich SM, Chu CT, Mitochondrially localized ERK2 regulates mitophagy and autophagic cell stress: implication for Parkinson's disease. Autpophagy. 2008; 4:770-782.

30. Dato S, Crocco P, D'Aquila P, de Rango F, Bellizzi D, Rose G, Passarino G, Exploring the role of genetic variability and lifestyle in oxidative stress response for healty aging and longevity. Int. J. Mol. Sci. 2013, 14, 16443-16472. doi: 10.3390/ijms140816443.

31. Desler C, Rasmussen LJ, Mitochondria in biology and medicine – 2012. Mitochondrion. 2012 Jul;12(4):472-6. doi: 10.1016/j.mito.2012.06.008. Epub 2012 Jun 30.

32. Fantuzzi G, Adipose tissue, adipokines, and inflammation. J Allergy Clin Immunol. 2005 May; 115(5):911-9; quiz 920.

33. Fielding RA, Vellas B, Evans WJ, Bhasin S, Morley JE, Newman AB, Abellan van Kan G, Andrieu S, Bauer J, Breuille D, Cederholm T, Chandler J, De Meynard C, Donini L, Harris T, Kannt A, Keime Guibert F, Onder G, Papanicolaou D, Rolland Y, Rooks D, Sieber C, Souhami E, Verlaan S, Zamboni M, Sarcopenia: an undiagnosed condition in older adults. Current consensus definition: prevalence, etiology, and consequences. International working group on sarcopenia. 2011. J. Am. Med. Dir. Assoc.;12(4):249-56. doi: 10.1016/j.jamda.2011.01.003.

34. Frahm T, Mohamed SA, Bruse P, Gemünd C, Oehmichen M, Meissner C, Lack of age-related increase of mitochondrial DNA amount in brain, skeletal muscle and human heart. Mech Ageing Dev. 2005 Nov; 126(11):1192-200.

35. Franceschi C, Bonafè M, Valensin S, Olivieri F, De Luca M, Ottaviani E, De Benedictis G, Inflamm-aging. An evolutionary perspective on immunoscenescence. Ann N Y Acad Sci. 2000 Jun; 908:244-54.

36. Franceschi C, Campisi J, Chronic Inflammation (Inflammaging) and Its Potential Contribution to Age-Associated Diseases. J Gerontol A Biol Sci Med Sci. 2014 Jun; 69 Suppl 1:S4-9. doi: 10.1093/gerona/glu057.

37. Gopinath SD, Rando TA, Stem cell review series: aging of the skeletal muscle stem cell niche. Aging Cell. 2008 Aug;7(4):590-8. doi: 10.1111/j.1474-9726.2008.00399.x. Epub 2008 Jun 28.

38. Grazi GL, Cescon M, Ravaioli M, Ercolani G, Pierangeli F, D'Errico A, Ridolfi L, Cavallari A, Mazziotti A, A revised consideration on the use of very aged donors for liver transplantation. Am J Transplant. 2001 May; 1(1):61-8.

39. Gredilla R, Bohr VA, Stevnsner T, Mitochondrial DNA repair and association with aging--an update. Exp Gerontol. 2010 Aug; 45(7-8):478-88. doi: 10.1016/j.exger.2010.01.017. Epub 2010 Jan 22.

40. Green DR, Galluzzi L, Kroemer G, Mitochondria and the autophagy-inflammation-cell death axis in organismal aging. Science. 2011 Aug 26; 333(6046):1109-12. doi: 10.1126/science.1201940.

41. Gregor MF, Hotamisligil GS, Inflammatory mechanisms in obesity. Annu Rev Immunol. 2011; 29:415-45. doi: 10.1146/annurev-immunol-031210-101322.

42. Gomes LC, Scorrano L, Mitochondrial morphology in mitophagy and macroautophagy. Biochim Biophys Acta. 2013 Jan;1833(1):205-12. doi: 10.1016/j.bbamcr.2012.02.012. Epub 2012 Mar 1.

43. Gurd BJ, Deacetylation of PGC-1α by SIRT1: importance of skeletal muscle function and exercise-induced mitochondrial biogenesis. Appl. Physiol. Nutr. Metab. 2011; 36:589-597.

44. Jackson AS, Janssen I, Sui X, Church TS, Blair SN, Longitudinal changes in body composition associated with healthy ageing: men, aged 20-96 years. Br J Nutr. 2012 Apr;107(7):1085-91. doi: 10.1017/S0007114511003886. Epub 2011 Aug 3

45. Johnson ML, Robinson MM, Nair KS, Skeletal muscle aging and the mitochondrion. Trends Endocrinol Metab. 2013 May; 24(5):247-56. doi: 10.1016/j.tem.2012.12.003. Epub 2013 Feb 1.

46. Kasamatsu H, Vinograd J, Replication of circular DNA in eukaryotic cell. Annu. Rev. Biochem. 43(1974)695-719.

47. Kasamatsu H, Vinograd J, Unidirectionality of replication in mouse mitochondrial DNA. Nat. New. Biol. 1973; 241(108):103-5, Jan 24.

48. Kato T, The other forgotten genome: mitochondrial DNA and mental disorders. Mol. Psyhiatry. 2001 Nov; 6(6):625-33.

49. Kazachkova N, Ramos A, Santos C, Lima M, Mitochondrial DNA Damage Patterns and Aging: Revisiting the Evidence for Humans and Mice. Aging Dis. 2013 Sep 24; 4(6):337-50. doi: 10.14336/AD.2013.0400337.

50. Kennedy BK, Berger SL, Brunet A, Campisi J, Cuervo AM, Epel ES, Franceschi C, Lithgow GJ, Morimoto RI, Pessin JE, Rando TA, Richardson A, Schadt EE, Wyss-Coray T, Sierra F,

Geroscience: Linking Aging to Chronic Disease. Cell. 2014 Nov 6; 159(4):709-13. doi: 10.1016/j.cell.2014.10.039.

51. Kirkwood TBL, Understanding the Odd Science of Aging. Cell. 2005 Feb 25; Vol. 120, 437-447. doi: 10.1016/j.cell.2005.01.027.

52. Klionsky DJ, Autophagy: from phenomenology to mlecula understanding in less than a decade. Nat. Rev. Mol. Cell. Biol. 2007; 8:931-937.

53. Koltai E, Hart N, Taylor AW, Goto S, Ngo JK, Davies KJ, Radak Z, Age-associated declines in mitochondrial biogenesis and protein quality control factors are minimized by exercise training. Am. J. Physiol. Regul. Integr. Comp. Physiol. 303(2):R127-34, 2012 Jul 15;. doi: 10.1152/ajpregu.00337.2011.

54. Kovalenko SA, Kopsidas G, Kelso J, Rosenfeldt F, Linnane AW, Tissue-specific Distribution of Multiple Mitochondrial DNA Rearrangements during Human Aging. Ann N Y Acad Sci. 1998 Nov 20; 854:171-81.

55. Krishnan KJ, Reeve AJ, Samuels DC, Chinnery PF, Blackwood JK, Taylor RW, Wanrooij S, Spelbrink JN, Lightowelers RN, Turnbull DM, What cause mitochondrial DNA deletions in human cells? Nat Genet. 2008 Mar; 40(3):275-9. doi: 10.1038/ng.f.94.

56. Halliwell B, Reactive oxygen species in living systems: source, biochemistry, and role in human disease. Am J Med. 1991 Sep 30; 91(3C):14S-22S.

57. Harman D, Aging: a theory based on free radical and radiation chemistry. J Gerontol. 1956 Jul; 11(3):298-300.

58. Hayflick L, How and why we age. Exp. Gerontol. 1998 Nov-Dec; 33(7-8):639-53.

59. Hayflick L, Moorhead PS, The serial cultivation of human diploid cell strains. Exp. Cell. Res. 1961; 25:585-621.

60. Hebert SL, Lanza IR, Nair KS, Mitochondrial DNA alterations and Reduced Mitochondrial Function in Aging. Mech Ageing Dev. 2010 Jul-Aug; 131(7-8):451-62. doi: 10.1016/j.mad.2010.03.007. Epub 2010 Mar 20.

61. Hoare M, Das T, Alexander G, Ageing, telomeres, senescence, and liver injury. J Hepatol. 2010 Nov; 53(5):950-61. doi: 10.1016/j.jhep.2010.06.009. Epub 2010 Jul 24.

62. Holt IJ, Lorimer HE, Jacobs HT, Coupled leading- and lagging-strand synthesis of mammalian mitochondrial DNA. Cell. 2000; 100(5):515-24, Mar 3.

63. Holt IJ, Reyes A, Human mitochondrial DNA replication. Cold. Spring. Harb. Perspect. Biol. 2012; 4(12). pii: a012971, Dec 1. doi: 10.1101/cshperspect.a012971.

64. Houtkooper RH, Pirinen E, Auwerx J, Sirtuins as regulators of metabolism and healthspan. Nat Rev Mol Cell Biol. 2012 Mar 7;13(4):225-38. doi: 10.1038/nrm3293.

65. Howcroft TK, Campisi J, Louis GB, Smith MT, Wise B, Wyss-Coray T, Augustine AD, McElhaney JE, Kohanski R, Sierra F, The role of inflammation in age-related disease. Aging (Albany NY). 2013 Jan; 5(1):84-93.

66. Lakowa N, Trieu N, Flehmig G, Lohmann T, Schön MR, Dietrich A, Helge Zeplin P, Langer S, Stumvoll M, Blüher M, Klöting N, Telomere length differences between subcutaneous and visceral adipose tissue in humans. Biochem Biophys Res Commun. 2015 Jan 13. pii: S0006-291X(15)00027-3. doi: 10.1016/j.bbrc.2014.12.122.

67. Lanza IR, Nair KS, Muscle mitochondrial changes with aging and exercise. Am. J. Clin. Nutr.; 2009; 89(1):467S-71S. doi: 10.3945/ajcn.2008.26717D.

68. Lee HC, Lu CY, Fahn HJ, Wei YH, Aging- and smoking- associated alteration in the relative content of mitochondrial DNA in human lung, 1998. FEBS Lett. 441,292-296.

69. Li Y, Huang TT, Carlson EJ, Melov S, Ursell PC, Olson JL, Noble LJ, Yoshimura MP, Berger C, Chan PH, Wallace DC, Epstein CJ, Dilated cardiomyopathy and neonatal lethality in mutant mice lacking manganese superoxide dismutase. Nat Genet. 1995 Dec;11(4):376-81.

70. Ling C, Poulsen P, Carlsson E, Ridderstråle M, Almgren P, Wojtaszewski J, Beck-Nielsen H, Groop L, Vaag A, Multiple environmental and genetic factors influence skeletal muscle PGC-1alpha and PGC-1beta gene expression in twins. J Clin Invest.; 2004; 114(10):1518-26.

71. Liu W, Acin-Perez R, Geghman KD, Manfredi G, Lu B, Li C, Pink1 regulates the oxidative phosphorylation machinery via mitochondrial fission. Proc. Natl. Acad. Sci. U.S.A. 108 (2011) 12920-12924.

72. López-Llunch G, irusta PM, Navas P, de Cabo R, Mitochondrial biogenesis and healthy aging. Exp. Gerontol. 2008 September; 43 (9):813-819.

73. López-Otín C, Blasco MA, Partridge L, Serrano M, Kroemer G, The hallmarks of aging. Cell. 2013 Jun 6; 153(6):1194-217. doi: 10.1016/j.cell.2013.05.039.

74. Manneschi L, Federico A, Polarographic analyses of subsarcolemmal and intermyofibrillar mitochondria from rat skeletal and cardiac muscle. J Neurol Sci. 1995 Feb;128(2):151-6.

75. Marcus RL, Addison O, Dibble LE, Foreman KB, Morrell G, Lastayo P, Intramuscular adipose tissue, sarcopenia, and mobility function in older individuals. J Aging Res. 2012; 2012:629637. doi: 10.1155/2012/629637. Epub 2012 Feb 6.

76. Martin-Ruiz CM, Baird D, Roger L, Boukamp P, Krunic D, Cawthon R, Dokter MM, van der Harst P, Bekaert S, de Meyer T, Roos G, Svenso U, Codd V, Samani NJ, McGlynn L, Shiels PG, Pooley KA, Dunning AM, Cooper R, Wong A, Kingston A, von Zglinicki T, Reproducinility of telomere length assessment: an international collaborative study. Int J Epidemiol. 2014 Sep 19. pii: dyu191.

77. Marzetti E, Calvani R, Cesari M, Buford TW, Lorenzi M, Behnke BJ, Leeuwenrburgh C, Mitochondrial dysfunction and sarcopenia of aging: from signaling pathways to clinical trials. Int J Biochem Cell Biol. 2013 Oct; 45(10):2288-301. doi: 10.1016/j.biocel.2013.06.024.

78. Masiero E, Sandri M, Autophagy inhibition induces atrophy and myopathy in adult skeletal muscles. Autophagy. 2010 Feb; 6(2):307-9. Epub 2010 Feb 6.

79. Masuyama m, Iida R, Takatsuka H, Yasuda T, Matsuki T, Quantitative change in mitochondrial DNA content mouse tissues during aging, Biochim Biophys Acta. 2005 May 25; 1723(1-3):302-8. Epub 2005 Mar 17.

80. McKinney EA, Oliveira MT, Replicating animal mitochondrial DNA. Genetics and Molecular Biology. 2013; 36, 3, 308-315.

81. Meissner C, Bruse P, Oehmichen M, Tissue-specific deletion patterns of the mitochondrial genome with advancing age. Exp. Gerontol. 2006, 41, 518-524.

82. Michel S, Wanet A, De Pauw A, Rommelaere G, Arnould T, Renard P, Crosstalk Between Mitochondrial (dys)Function and Mitochondrial Abundance. J Cell Physiol. 2012 Jun;227(6):2297-310. doi: 10.1002/jcp.23021.

83. Mishra P, Chan DC, Mitochondrial dynamics and inheritance during cell division, development and disease. Nat Rev Mol Cell Biol. 2014 Oct;15(10):634-46. doi: 10.1038/nrm3877. Epub 2014 Sep 17.

84. Mitchell JR, Wood E, Collins K, A telomerase component is defective in the human dyskeratosis congenita. Nature. 1999 Dec 2; 402(6761):551-5.

85. Montero-Fernández N, Serra-Rexach JA, Role of exercise on sarcopenia in the elderly. Eur J Phys Rehabil Med. 2013 Feb; 49(1):131-43.

86. Morrisette-Thomas V, Cohen AA, Fülöp T, Riesco E, Legault V, Li Q, Milot E, Dusseault-Bélanger F, Ferrucci L, Inflamm-aging does not simply reflect increases in pro-inflammatory markers. Mech Ageing Dev. 2014 Jul; 139:49-57. doi: 10.1016/j.mad.2014.06.005. Epub 2014 Jul 8.

87. Müller-Höcker J, Aust D, Rohrbach H, Napiwotzky J, Reith A, Link TA, Seibel P, Hölzel D, Kadenbach B, Defects of the respiratory chain in the normal human liver and in cirrhosis during aging. Hepatology. 1997 Sep; 26(3):709-19.

88. Navarro A, Sánchez Del Pino MJ, Gómez C, Peralta JL, Boveris A, Behavioral dysfunction, brain oxidative stress, and impaired mitochondrial electron transfer in aging mice. Am J Physiol Regul Integr Comp Physiol. 2002 Apr; 282(4):R985-92.

89. Ngo JK, Pomatto LCD, Davies KJA, Upregulation of the mitochondrial Lon Protease allows adaptation to acute oxidative stress but dysregulation is associated with chronic stress, disease, ad aging. Redox Biol. 2013 Feb 9;1(1):258-64. doi: 10.1016/j.redox.2013.01.015.

90. Nilwik R, Snijders T, Leenders M, Groen BB, van Kranenburg J, Verdijk LB, van Loon LJ, The decline in skeletal muscle mass with aging is mainly attributed to a reduction in type II muscle fiber size. Exp Gerontol. 2013 May; 48(5):492-8. doi: 10.1016/j.exger.2013.02.012. Epub 2013 Feb 17.

91. Noack H, Bednarek T, Heidler J, Ladig R, Holtz J, Szibor M, TFAM-dependent and independent dynamics of mtDNA levels in C2C12 myoblast caused by redox stress. Biochim. Bhophys. Acta. 2006; 1760:141-150.

92. Oesebrug H, de Boer RA, van Glist WH, van der Harst P, Telomere biology in healthy aging and disease. Pflugers. Arch. 2010 January; 459(2):259-68.

93. Okamoto K, Kondo-Okamoto N, Mitochondria and autophagy: critical interplay between the two homeostats. Biochim Biophys Acta. 2012 May;1820(5):595-600. doi: 10.1016/j.bbagen.2011.08.001. Epub 2011 Aug 7.

94. Osiewacz HD, Bernhardt D, Mitochondrial quality control: impact on aging and life span life span - a mini-review. Gerontology. 2013; 59(5):413-20. doi: 10.1159/000348662. Epub 2013 Apr 18.

95. Ostan R, Bucci L, Capri M, Salvioli S, Scurti M, Pini E, Monti D, Franceschi C. Immunosenescence and immunogenetics of human longevity. Neuroimmunomodulation. 2008;15(4-6):224-40. doi: 10.1159/000156466. Epub 2008 Nov 26.

96. Palmer BF, Clegg DJ, The sexual dimorphism of obesity. Mol Cell Endocrinol. 2015 Jan 8;402C:113-119. doi: 10.1016/j.mce.2014.11.029.

97. Passos JF, Saretzki G, Ahmed S, Nelson G, Richter T, Peters H, Wappler I, Birket MJ, Harold G, Schaeuble K, Birch-Machin MA, Kirkwood TB, von Zglinicki T, Mitochondrial dysfunction accounts for the stochastic heterogeneity in telomere-dependent senescence. PLoS Biol. 2007; 5(5):e110.

98. Payne BA, Wilson IJ, Hateley CA, Horvath R, Santibanez-Koref M, Samuels DC, Price DA, Chinnery PF, Mitochondrial aging is accelerated by anti-retroviral therapy through the clonal expansion of mtDNA mutations. Nat Genet. 2011 Jun 26;43(8):806-10. doi: 10.1038/ng.863.

99. Plaff MW, A new mathematical model for relative quantification in real-time RT-PCR. Nucleic Acids Res. 2001 May 1; 29(9):e45.

100. Pesce V, Cormio A, Fracasso F, Vecchiet J, Felzani G, Lezza AMS, Cantatore P, Gadaleta MN, Age-related mitochondrial genotypic and phenotypic alterations in human skeletal muscle, Free Radic Biol Med. 2001 Jun 1; 30(11):1223-33.

101. Peterson CM, Johannsen DL, Ravussin E, Skeletal muscle mitochondria and aging: a review. 2012. J. Aging. Res. 2012:194821. doi: 10.1155/2012/194821.

102. Picard M, White K, Turnbull DM, Mitochondrial morphology, topology, and membrane interactions in skeletal muscle: a quantitative three-dimensional electron microscopy study. J Appl Physiol (1985). 2013 Jan 15; 114(2):161-71. doi: 10.1152/japplphysiol.01096.2012. Epub 2012 Oct 25.

103. Ponsot E, Lexell J, Kadi F, Skeletal muscle telomere length is not impaired in healthy physically active old women and men. Muscle Nerve. 2008; 37(4):467-72. doi: 10.1002/mus.20964.

104. Reaume AG, Elliott JL, Hoffman EK, Kowall NW, Ferrante RJ, Siwek DF, Wilcox HM, Flood DG, Beal MF, Brown RH Jr, Scott RW, Snider WD, Motor neurons in Cu/Zn superoxide dismutase-deficient mice develop normally but exhibit enhanced cell death after axonal injury. Nat Genet. 1996 May;13(1):43-7.

105. Robin ED, Wong R, Mitochondrial DNA molecules and virtual number of mitochondria per cell in mammalian cells. J. Cell. Physiol. 136 (1988) 507-513.

106. Romanello V, Sandri M, Mitochondrial biogenesis and fragmentation as regulators of protein degradation in striated muscles. J Mol Cell Cardiol. 2013 Feb; 55:64-72. doi: 10.1016/j.yjmcc.2012.08.001. Epub 2012 Aug 10.

107. Roserberg IH, Summary comments. Am J Clin Nutr 1989; 50:1231-3.

108. Safdar A, Hamadeh MJ, Kaczor JJ, Raha S, Debeer J, Tarnopolsky MA, Aberrant mitochondrial homeostasis in the skeletal muscle of sedentary older adults. PLoS One. 5(5):e10778, 2010 May 24. doi: 10.1371/journal.pone.0010778.

109. Sahin E, Colla S, Liesa M, Moslehi J, Müller FL, Guo M, Cooper M, Kotton D, Fabian AJ, Walkey C, Maser RS, Tonon G, Foerster F, Xiong R, Wang YA, Shukla SA, Jaskelioff M, Martin ES, Heffernan TP, Protopopov A, Ivanova E, Mahoney JE, Kost-Alimova M, Perry SR, Bronson R, Liao R, Mulligan R, Shirihai OS, Chin L, DePinho RA, Telomere dysfunction induces metabolic and mitochondrial compromise. Nature. 2011 Feb 17; 470 (7334):359-65. doi: 10.1038/nature09787. Epub 2011 Feb 9.

110. Sahin E, DePinho RA, Linking functional decline of telomeres, mitochondria and stem cells during ageing. Nature. 2010 Mar 25;464(7288):520-8. doi: 10.1038/nature08982.

111. Sahin E, DePinho RA, Axis of ageing: telomeres, p53 and mitochondria. Nat Rev Mol Cell Biol. 2012 May 16;13(6):397-404. doi: 10.1038/nrm3352.

112. Salvioli S, Capri M, Tieri P, Loroni J, Barbi C, Invidia L, Altilia S, Santoro A, Pirazzini C, Pierini M, Bellavista E, Alberghina L, Franceschi C, Different types of cell death in organismal aging and longevity: state of the art and possible systems biology approach. Curr Pharm Des. 2008; 14(3):226-36.

113. Sandri M, Signaling in muscle atrophy and hypertrophy. Physiology (Bethesda) 2008, 23:160-70.

114. Saretzki G, Von Zglinicki T, Replicative aging, telomeres, and oxidative stress. Ann N.Y. Acad. Sci. 2002; 959:24-9.

115. Scheurmann J, Treiber N, Weber C, Renkl AC, Frenzel D, Trenz-Buback F, Rueß A, Schulz G, Scharffetter-Kochanek K, Weiss JM, Mice with heterozygous deficiency of manganese superoxide dismutase (SOD2) have skin immune system with features of “inflamm-aging”. Arch. Dermatol. Res. 2014; 306:143-155.

116. Schmucker DL, Hepatocyte fine structure during maturation and senescence. J Electron Microsc Tech. 1990 Feb; 14(2):106-25.

117. Schmucker Dl, Sachs H, Quantifying dense bodies and lipofuscin during aging: a morphologist's perspective. Arch Gerontol Geriatr. 2002 May-Jun;34(3):249-61.

118. Schmucker DL, Sanchez H, Liver regeneration and aging: a current perspective. Curr Gerontol Geriatr Res. 2011; 2011:526379. doi: 10.1155/2011/526379. Epub 2011 Sep 8.

119. Schon EA, DiMauro S, Hirano M, Human mitochondrial DNA: roles of inherited and somatic mutations. Nat Rev Genet. 2012 Dec; 13(12):878-90. doi: 10.1038/nrg3275.

120. Shepard TH, Muffley LA, Smith LT, Ultrastructural study of mitochondria and their cristae in embryonic rats and primate (*N. nemistrina*). Anat. Rec. 1998; 252:383-392.

121. Shokolenko IN, Wilson GL, Alexeyev MF, Aging: A mitochondrial DNA perspective, critical analysis and an update. World J Exp Med. 2014 Nov 20; 4(4):46-57. eCollection 2014.

122. Spalding KL, Arner E, Westermark PO, Bernard S, Buchholz BA, Bergmann O, Blomqvist L, Hoffstedt J, Näslund E, Britton T, Concha H, Hassan M, Rydén M, Frisén J, Arner P, Dynamics of fat cell turnover in humans. Nature 453 (2008) 783-787.

123. St John JC, Transmission, inheritance and replication of mitochondrial DNA in mammals: implications for reproductive processes and infertility. Cell Tissue Res. 2012 Sep;349(3):795-808. doi: 10.1007/s00441-012-1444-2. Epub 2012 Jun 14.

124. Starr ME, Hu Y, Stromberg AJ, Carmical JR, Wood TG, Evers BM, Saito H, Gene expression profile of mouse white adipose tissue during inflammatory stress: age-dependent upregulation of major procoagulant factors. Aging Cell. 2013 Apr; 12(2):194-206. doi: 10.1111/acel.12040. Epub 2013 Jan 30.

125. Stewart JA, Chaiken MF, Wang F, Price CM, Maintaining the end: roles of telomere proteins in end-protection, telomere replication and length regulation. Mutat Res. 2012 Feb 1; 730(1-2):12-9. doi: 10.1016/j.mrfmmm.2011.08.011.

126. Taanman JW, The mitochondrial genome: structure, transcription, translation and replication. Biochim Biophys Acta. 1999 Feb 9; 1410(2):103-23.

127. van Tienen FH, Lindsey PJ, van der Kallen CJ, Smeets HJ, Prolonged Nrf1 Overexpression Triggers Adipocytes Inflammation and Insulin Resistance. 2010 J Cell Biochem. 2010 Dec 15;111(6):1575-85. doi: 10.1002/jcb.22889.

128. Trayhurn P, Wood IS, Adipokines: inflammation and the pleiotropic role of white adipose tissue, British Journal of Nutrition (2004), 92, 347–355.

129. Trifunovic A, Larsson NG, Mitochondrial dysfunction as a cause of aging. J Intern Med. 2008 Feb;263(2):167-78. doi: 10.1111/j.1365-2796.2007.01905.x.

130. Trifunovic A, Wredenberg A, Falkenberg M, Spelbrink JN, Rovio AT, Bruder CE, Bohlooly-Y M, Gidlöf S, Oldfors A, Wibom R, Törnell J, Jacobs HT, Larsson NG, Premature ageing in mice expressing defective mitochondrial DNA polymerase. Nature 2004; 429- 417-23.

131. Verdijk LB, Koopman R, Schaart G, Meijer K, Savelberg HH, van Loon LJ, Satellite cell content is specifically reduced in type II skeletal muscle fibers in the elderly. Am J Physiol Endocrinol Metab. 2007 Jan;292(1):E151-7. Epub 2006 Aug 22.

132. Viña J, Gomez-Cabrera MC, Borras C, Froio T, Sanchis-Gomar F, Martinez-Bello VE, Pallardo FV, Mitochondrial biogenesis in exercise and ageing. Adv Drug Deliv Rev. 2009 Nov 30;61(14):1369-74. doi: 10.1016/j.addr.2009.06.006. Epub 2009 Aug 27.

133. Vitale G, Salvioli S, Franceschi C.Oxidative stress and the ageing endocrine system. Nat Rev Endocrinol 2013 Apr; 9(4):228-4. doi: 10.1038/nrendo.2013.29. Epub 2013 Feb 26.

134. von Zglinicki T, Bürkle A, Kirkwood TB, Stress, DNA damage and ageing -- an integrative approach. Exp. Gerontol. 2001; 36(7):1049-62.

135. Wallace DC, Mitochondrial DNA mutations and neuromuscular disease. Trends Genet. 1989 Jan;5(1):9-13.

136. Wanagat J, Ahmadieh N, Bielas JH, Ericson NG, Van Remmen HV, Skeletal muscle mitochondrial DNA deletions are not increased in CuZn-superoxide dismutase deficient mice. Exp. Gerontol. 2015; 61:15-19.

137. Watanabe K, Shibuya S, Ozawa Y, Nojiri H, Izuo N, Yokote K, Shimizu T, Superoxide Dismutase 1 Loss Disturbs Intracellular Redox Signaling, Resulting in Global Age-Related Pathological Changes. Biomed Res Int. 2014;2014:140165. doi: 10.1155/2014/140165. Epub 2014 Sep 8.

138. Welle S, Bhatt K, Shah B, Needler N, Delehanty JM, Thorton CA, Reduced amount of mitochondrial DNA in aged human muscle, J Appl Physiol (1985). 2003 Apr; 94(4):1479-84. Epub 2002 Dec 20.

139. Wenz T, Rossi SG, Rotundo RL, Spiegelman BM, Moares CT, Increased muscle PGC-1α expression protects from sarcopenia and metabolic disease during aging. Proc Natl Acad Sci U S A. 2009 Dec 1;106(48):20405-10. doi: 10.1073/pnas.0911570106. Epub 2009 Nov 16.

140. Ylikallio E, Tyynismaa H, Tsutsui H, Ide T, Suomalainen A, High mitochondrial DNA copy number has detrimental effects in mice. Hum Mol Genet. 2010 Jul 1; 19(13):2695-705.

141. Zhang C, Bills M, Quigley A, Maxwell RJ, Linnane AW, Nagley P, Varied Prevalanced of Age-Associated Mitochondrial DNA Deletions in Different Species and Tissues: A Comparison between Human and Rat, Biochem Biophys Res Commun. 1997 Jan 23; 230(3):630-5.

142. Zhang H, Singh KK, Global genetic determinants of mitochondrial DNA copy number. PLoS One. 2014 Aug 29;9(8):e105242. doi: 10.1371/journal.pone.0105242. eCollection 2014.

143. Ziegler DV, Wiley CD, Velarde MC, Mitochondrial effectors of cellular senescence: beyond the free radical theory of aging. 2014 Nov 14, Aging Cell. doi: 10.1111/acel.12287.

144. Zorzano A, Liesa M, Sebastián D, Segalés J, Palacín M, Mitochondrial fusion proteins: dual regulators of morphology and metabolism. Semin Cell Dev Biol. 2010 Aug;21(6):566-74. doi: 10.1016/j.semcdb.2010.01.002. Epub 2010 Jan 15.

7.1 Books

1. Lehninger AL, Nelson DL, Cox MM, Lehninger Principles of Biochemistry, Ed. Freeman W. H. & Company, 4th edition, 2004.
2. Mathews CK, Van Holde KE, Ahren KG, Biochimica, Ed. CEA MIlano, 4° edizione, 2004.
3. Martini FH, Timmons MJ, Tallitsch RB, Anatomia umana. EdiSES. 2008.

7.2 Web sites

1. http://thewellnessdigest.com
2. http://www.sccollege.edu
3. http://en.wikipedia.org

4. http://http://mjlightfoot.edublogs.org/
5. http://www.ncbi.nlm.nih.gov/pubmedhealth
6. http://cnx.org/content/col11496/1.6/

8 Ringraziamenti

Arrivata al termine del mio progetto di dottorato voglio ringraziare le persone che hanno contribuito e mi hanno permesso di raggiungere questo traguardo.

Innanzitutto il Chiar.mo prof. Claudio Franceschi, che accogliendomi nel suo laboratorio 3 anni fa, mi ha dato la possibilità di studiare quei magnifici organelli che sono "la centrale energetica" della cellula, i mitocondri. La sua passione per il sapere scientifico e il suo entusiasmo per tutto ciò che riguarda l'uomo mi hanno arricchita non solo professionalmente, ma anche umanamente, insegnandomi qualcosa che va oltre allo studio e che non dimenticherò mai.

Vorrei poi ringraziare il prof. Stefano Salvioli e la dott.ssa Miriam Capri, che mi hanno accompagnato più da vicino in questo percorso, discutendo con me dei dati, cercando di risolvere dubbi e aiutandomi a sviluppare quello spirito critico che è fondamentale per chi fa ricerca.

Un sentito ringraziamento va al dott. Gianluca Grazi, coordinatore del progetto MIUR-PRIN 2008, e al dott. Matteo Cescon, Ospedale Sant'Orsola-Malpighi , Bologna (Italia), che hanno fornito i campioni di fegato utilizzati in questo lavoro, e alla prof.ssa Gillian Butler-Browne, coordinatrice del progetto European Project MYOAGE, che insieme al prof. Ermanno Martucci e al dott. Giovanni Trisolino, Istituto Ortopedico Rizzoli, Bologna (Italia), al prof. Enn Seppet, Centre of Molecular and Clinical Medicine, Univeristy of Tartu (Estonia) e alla prof.ssa Andrea Mayer, Department of Gerontology and Geriatrics, Leiden University (Netherlands) hanno fornito i campioni di muscolo e tessuto adiposo che ho usato in questa tesi.

Un grazie carico di affetto va, infine, alla dott.ssa Aurelia Santoro, che nel corso di questi anni ha avuto fiducia in me e, soprattutto, mi ha dedicato il suo tempo e la sua pazienza, oltre che tutta la sua esperienza, risultando essere un'ottima tutor, scientifica e non.

Grazie di cuore a tutti!!